The University of Nottingham

UNITED KINGDOM · CHINA · MALAYSIA

School of Medicine

Development of a Cell-seeded Construct for Osteochondral Modelling and Repair

Alexander A. Popov, MSc

September 2015

Thesis submitted to the University of Nottingham for the degree of Doctor of Philosophy

Abstract

Regenerative therapeutic solutions are required to address the increasing prevalence of bone and cartilage diseases within the population. Limitations of existing treatments, such as bone graft reconstructions or biomaterial implants, suggest that osteochondral tissue constructs with the ability to support differentiation of mesenchymal stem cells into both osteoblast and chondrocyte lineages is desirable. To date, tissue-engineering approaches have focused on developing individual scaffolds for each osteochondral lineage. Constructs are combined once tissues have developed sufficiently. Unfortunately, delamination often occurs under normal physiological loading and implants fail.

The overall aim of this research project was to develop a scaffold made from a single material with the capacity to maintain osteogenic and chondrogenic cells. In this manner, it was intended to overcome issues arising from delamination and the divergent differentiation requirements for each lineage by providing scaffolds with spatially resolved environments, each supportive of one of osteochondral cell lineages.

The work reported here describes a novel method to produce porous chitosan scaffolds with large pore regions (300-425 μm) to promote the osteogenic differentiation of mesenchymal stem cells, and smaller pores (180-300 μm) to encourage chondrogenesis. Porogen properties and cross-linker optimisation were fundamental for the production of a bi-layered chitosan scaffolds containing two distinct pore sizes, successfully achieved in the current project.

The architecture of the chitosan scaffolds also permitted the development of a culture medium that could activate simultaneous osteogenic and chondrogenic differentiation in mesenchymal stem cells. More specifically, it was determined that 5-day transient serum treatments with fetal calf serum or human serum, allowed bone and cartilage development.

Finally, a perfusion bioreactor system was used to confirm the biocompatibility and osteochondral differentiation potential of the bi-layered chitosan scaffolds.

Acknowledgements

Firstly, I would like to my thank my PhD supervisors Dr Virginie Sottile, Prof. David Grant and Dr Colin Scotchford for their patience, guidance and support during the whole project. Additionally, thanks go to Prof. George Roberts for his continuous advice and expertise on chitosan chemistry.

Further acknowledgements go to Dr Martin Corfield (MicroCT in Tower Block), and Dr Bettina Wolf and Dr Guy Channell (Rheology at Sutton Bonington Campus) for their valuable technical guidance.

I would also like to recognise all my friends at Nottingham for making my PhD more enjoyable, especially James Crutchley, Lazaros Fotopoulos and Jamie Patient.

Finally, special thanks goes to my family for their continuous encouragement and motivation in everything I do.

Table of Contents

Abbreviations

μ-CT	Micro-computed tomography
β-TCP	β-tricalcium phosphate
ALP	Alkaline phosphatase
BMP	Bone morphogenic protein
BSA	Bovine serum albumin
cDNA	Complimentary DNA
CHO	Chondrogenic culture medium
DMEM	Dulbecco's modified eagle medium
DMMB	1,9-dimethylmethylene blue
DMSO	Dimethyl sulfoxide
DNA	Deoxyribonucleic acids
dNTP	Deoxynucleotide triphosphate
ECM	Extracellular matrix
EDTA	Ethylenediaminetetraacetic acid
ELISA	Enzyme-linked immunosorbent assay
FCS	Fetal calf serum
FGF	Fibroblast growth factor
FTIR	Fourier transform infrared spectroscopy
GAG	Glycosaminoglycan
GFP	Green fluorescent protein
HA	Hydroxyapatite
HEK	Human embryonic kidney cells
HS	Human serum
HBSS	Hank's balanced salt solution
IMS	Industrial methylated spirit
MSC	Mesenchymal stem cell
NEAA	Non-essential amino acids
$NaBH_4$	Sodium borohydride
OC	Osteocalcin
OP	Osteopontin
OS	Osteogenic culture medium

OST-CHO	Combined osteogenic and chondrogenic culture medium
PBS	Phosphate buffer saline
PCL	Polycaprolactone
PCR	Polymerase chain reaction
PEEK	Polyetheretherketone
PFA	Paraformaldehyde
PG	Proteoglycan
PGA	Polyglycolic acid
PHBV	Poly(3-hydroxybutyrate-co-3-hydroxyvalerate)
PLA	Polylactic acid
PLGA	Poly(lactic-co-glycolic) acid
PVA	Polyvinyl alcohol
RGD	Arginine-glycine-aspartic acid
RNA	Ribonucleic acid
RT-PCR	Reverse transcription polymerase chain reaction
RUNX2	Run-related transcription factor-2
SC	Standard culture medium
SDW	Sterile distilled water
SEM	Scanning electron microscopy
SOX9	SRY (sex determining region Y)-box 9
TCP	Tissue culture plastic
TGF-β	Transforming growth factor-β
UV	Ultraviolet
VEGF	Vascular endothelial growth factor

1. Introduction

1.1 Osteochondral Defects

Regenerative therapeutic solutions are required to address the increasing prevalence of bone and cartilage diseases, such as osteoarthritis within the population. In the natural joint, articular cartilage plays an important role in protecting the subchondral bone from high stresses, as well as reducing contact pressure and allowing low-friction movements (Iozzo, 1998; Steele et al, 2014). Both the articular cartilage and the underlying subchondral bone are often subjected to structural damage as a result of trauma and disease, leading to severe pain, joint deformity and loss of motion (Swieszkowski et al, 2007; Tampieri et al, 2011).

In the next two decades, a 500% increase in the number of joint-related injuries is predicted in the United States (Iorio et al, 2008). In the UK, osteoarthritis is a leading cause of disability affecting 8.75 million people. This figure is estimated to double to 17 million by 2030 (Arthritis Research UK, 2015). This is primarily a consequence of more active lifestyles and improved healthcare, allowing people to live longer. Unfortunately, one in 10 of these joint injuries require surgery and total knee replacement. Due to the avascular nature of cartilage, and its limited capacity for self-repair, there is demand for bioengineered solutions.

Existing treatments such as biomaterial implants, demonstrate critical limitations – predominantly poor durability. These restraints necessitate follow-up surgery at least every 20 years. Furthermore, the indirect costs associated with osteoarthritis (£3.6 billion) are a burden to the UK economy from the days lost from work and the increased demand of welfare and social care (Conaghan et al, 2015). A significant treatment gap lies between the onset of osteoarthritis pain, managed conservatively through treatments such as non steroidal anti-inflammatory drugs and topical ointments, and the delayed surgical intervention of the disease at its end stage when cartilage degeneration, pain and immobility, are severe enough to justify total knee replacement.

An alternative therapy is to use osteochondral grafts or constructs. These consist of a cartilaginous layer with underlying calcified tissue, representing cartilage and bone respectively. However, layers in such constructs often delaminate when subjected to the mechanics and stresses of the body (Martin et al, 2007).

A solution would be to use tissue engineering to develop an osteochondral tissue construct (scaffold) with the ability to support the differentiation of mesenchymal stem cells (MSCs) into both osteoblast and chondrocyte lineages. Through using a single scaffold that can support the differentiation of MSCs for both tissue layers, the complications of delamination can be overcome (Cengiz et al, 2014; France et al, 2012). In addition to providing a potential regenerative therapy for minor joint damage, the osteochondral constructs can be applied as models of the basic articulate surface and used to test additional regenerative therapies and drugs.

1.2 General Project Aims

The overarching goal of this research is to develop a novel tissue engineered construct that closely represents the fundamental bone and cartilage interface in human joints – a new platform to progress the development of reliable, scalable and cost-effective regenerative therapies for joint injuries and defects. The research aims to overcome issues arising from scaffold delamination by providing scaffolds with spatially resolved environments, each supportive of one of the two principal cell lineages in the human joint. Furthermore, the project also aims to cellularise these graded scaffolds with a single cell source, and culture them in medium containing both osteogenic and chondrogenic factors to promote *in situ* differentiation in the 3D scaffold through the use of a perfusion bioreactor system.

1.3 Experimental Objectives

The experimental objectives of this project were to:

1. Develop a culture medium with the ability to support both osteogenic and chondrogenic differentiation of mesenchymal stem cells *in vitro*.

2. Explore the potential of fetal calf serum (FCS), human serum (HS) and transient-serum regimes for stem cell differentiation.

3. Assess the contents of FCS and HS using biochemical analysis to improve understanding of the osteochondral differentiation process.

4. Develop a robust fabrication method for a scaffold exhibiting pore sizes from 300-425 μm to 180-300 μm to represent the graded structure of the joint.

5. Consider the effects of porogen type on scaffold characteristics.

6. Investigate alternative cross-linking agents to glutaraldehyde.

7. Characterise pore structure, mechanics and biodegradation in the scaffolds developed.

8. Improve cell seeding and establish the biocompatibility of the scaffolds.

9. Determine whether human mesenchymal stem cells can be differentiated into osteogenic and chondrogenic lineages via the control of scaffold architecture and a perfusion bioreactor system.

2. Literature Review

This chapter provides a background to the relevant literature necessary to understand how osteochondral constructs are designed and produced. Focus is applied on bone and cartilage tissues, mesenchymal stem cells, current osteochondral defect repair solutions, chitosan scaffolds and the importance of bioreactors in tissue engineering. Each section is summarised below:

- Section 2.1 outlines the literature behind *in vivo* bone structure and development, repair and the mechanical properties of the skeletal system.
- Section 2.2 reviews cartilage structure and development.
- Section 2.3 explores the characteristics of mesenchymal stem cells (MSCs), and their differentiation potential into osteogenic and chondrogenic lineages.
- Section 2.4 explains first and second generation tissue-engineering approaches, with particular focus on the development of osteochondral constructs.
- Sections 2.5 focuses on chitosan production and the benefits of using this polymer in regenerative applications.
- Section 2.6 is an overview of the different types of bioreactors available, and the critical requirements for successful bioreactor design.
- Section 2.7 is a summary of the literature review. This part is intended to define the aims and objectives of this project.

2.1 Bone Anatomy and Development

Bone is the principal tissue in the skeletal system and functions to provide structural support. Furthermore, bone can be divided into two distinct subgroups, cancellous bone (also know as trabecular or spongy) and cortical (compact) (Marotti et al, 1985). Bone types can be further characterised into woven or lamellar bone.

Cancellous bones have relatively low mineral content (5-10%) (Kozielski et al, 2011) and can be identified in vertebrae and at the ends of long bones. In contrast, cortical bone is heavily mineralised and present in the channels of long bones (Hangartner & Gilsanz, 1996).

Woven bone is established during the development of the skeletal system and also located at joint surfaces in adults (Turner et al, 1994). This subtype of bone lacks collagen and osteocyte organisation due to its rapid production rate (Su et al, 2003). Weeks after initial production, woven bones are restructured into organised lamellar bone.

The main components of bone are calcium phosphate with Type I and V Collagen, and water. Cell numbers are very sparse within the skeletal tissue, and composition varies significantly with age, diet and health (Marshall et al, 1996).

2.1.1 Bone Structure

The structural anatomy of long bones consists of diaphysis, metaphysis and epiphysis (Clarke, 2008). More specifically, long bones have a tubular shaft (diaphysis), comprising of compact bone surrounding a connective tissue membrane, known as the endosteum (Figure 2.1). In adults, this medullary cavity contains yellow bone marrow (Kojimoto et al, 1988). The epiphyses are located at the end of long bones. They consist of cancellous bone covered by a layer of cortical bone. The epiphyseal line or metaphysis interconnects the diaphysis and epiphyses. Finally, a layer of vascular connective tissue covers the external surfaces of bones, and this is referred to as the periosteum (Yoshimura et al, 2007). The outer surfaces of epiphyses are covered by articular cartilage instead of periosteum.

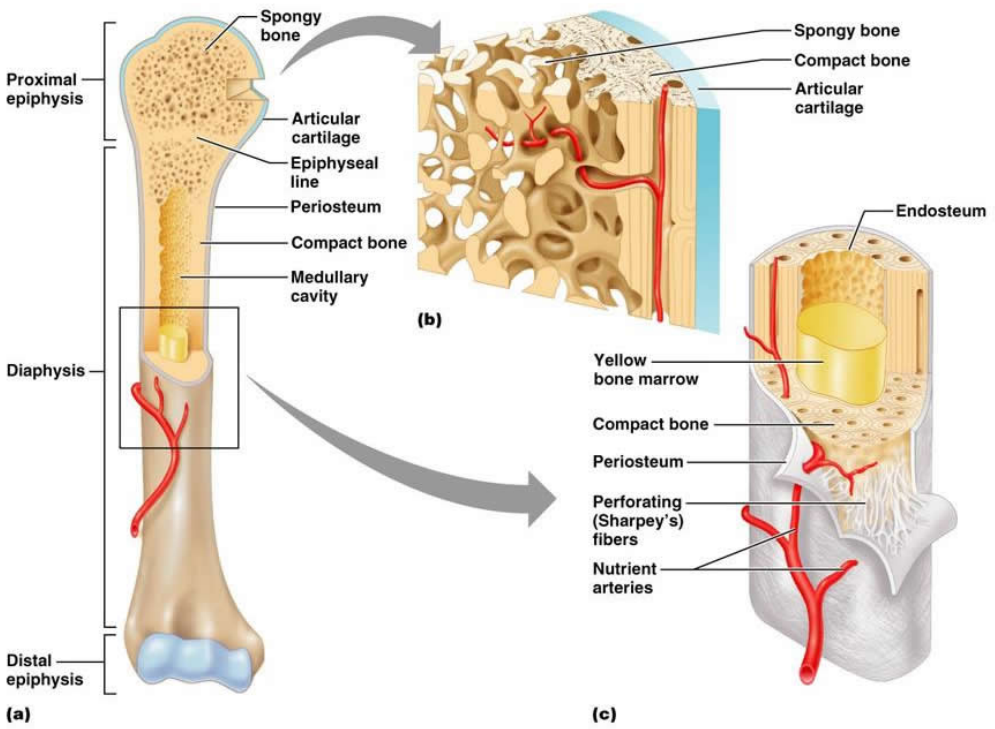

Figure 2.1 Anatomical structures of long bones. (A) The structure of long bones consists of diaphysis, metaphysis and epiphyses. (B) The epiphyses consist of cancellous/ spongy bone covered by layers of cortical/ compact bone and articular cartilage. (C) The tubular diaphysis is made of compact bone surrounding a connective tissue membrane, known as the endosteum. This membrane is filled with yellow bone marrow. Image taken from: http://classes.midlandstech.edu/carterp/Courses/bio210/chap06/lecture1.html

2.1.2 Bone Composition

Bone matrix is composed of around 70% inorganic mineral and 30% organic matrix and cells (Owen et al, 1990). The inorganic matrix consists of hydroxyapatite crystals, a mineral salt that is largely calcium phosphate, which accounts for the hardness of bone. The organic matrix is predominantly made of Type I Collagen, but also contains cells (osteoblasts, osteocytes, and osteoclasts). These organic components contribute to the flexibility and tensile strength of bone. During bone development, osteoblasts produce collagen fibres that are woven into sheet to enhance bone stiffness (Williams et al, 2005). Furthermore, osteoblasts have been confirmed to produce other proteins, proteoglycans and factors, which regulate the composition of bone. Proteins, such as osteocalcin, inhibit osteoblast activity and promote mineral maturation (Ducy et al, 1996).

2.1.3 Bone Development

Bone development can be divided into two different subtypes, depending on the location and type of bone being produced. During endochondral ossification, articular cartilage is replaced by bone, to form all bones below the cranium except for clavicles (collarbones) (Day et al, 2005). The cranial bones and collarbones develop through the intramembranous ossification of fibrous connective tissue membranes. In this section, both types of bone formation will be covered in more detail.

2.1.3.1 Cell Types

Bone is living matter, which is continuously remodelled by native cells. The main cell types in bone are osteoblasts, which maintain a mineralised extracellular matrix (ECM) via synthesis of dense, cross-linked collagens, as well as other proteins including osteocalcin and osteopontin (Engler et al, 2006). Osteocytes are derived from osteoblasts, which have been embedded in the bone matrix. They continue to secrete new matrix but are also important for mechanosensing (Urist, 1965). While osteoclasts are responsible to degrade redundant ECM (Long, 2001). All these cell types, apart from osteoclasts, are derived from a single multipotent progenitor cell type, known as mesenchymal stem cells (MSCs) (Lange et al, 2007).

2.1.3.2 Endochondral Ossification

Bone development via endochondral ossification involves bone tissue replacing hyaline cartilage. More specifically, endochondral ossification follows the hypertrophy of chondrocytes and synthesis of osteocyte and mineralisation factors (Bruder et al, 1994)(Figure 2.2). The process begins when osteoblasts produce osteoid around the fetal hyaline cartilage model (Sugiki et al, 2007). This leads to the calcification and deterioration of the cartilage matrix. As cavities form and the periosteal bone collars develop, calcellous bone replaces the remaining hyaline cartilage. Primary ossification centres cause the diaphysis to elongate and mature a medullary cavity via osteoclast activity (Noback & Robertson, 1951). Secondary ossification centres develop in the epiphyses and shortly after birth, these epiphyses ossify. Over time, bone fully replaces hyaline cartilage, except in the articular cartilages and epiphyseal plates.

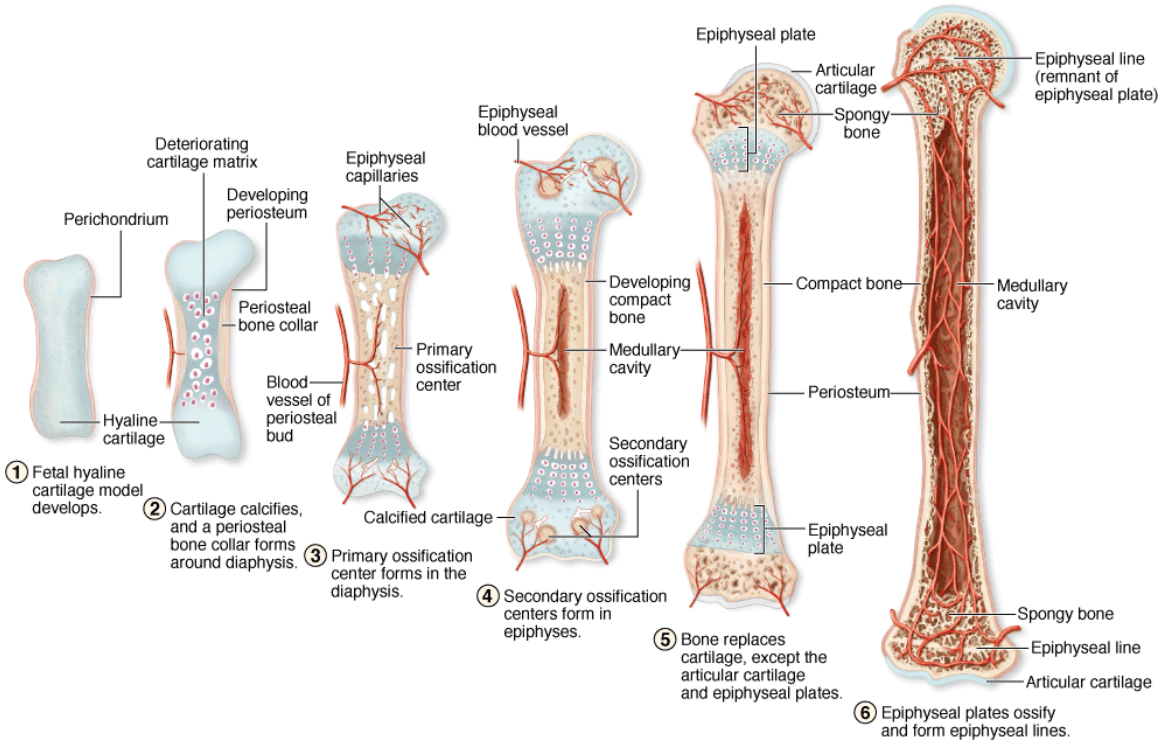

Figure 2.2 Development of long bones by endochondral ossification. Endochondral ossification forms the majority of bones in the skeleton and occurs in the fetus. The process involves the remodelling and calcification of hyaline cartilage into bone tissue. Primary ossification centres develop in the diaphysis. Secondary ossification centers develop later, in the epiphyses. The epiphyseal plate separates the primary and secondary ossification centers, which are responsible for bone elongation. Image adapted from: http://histonano.com/books/Junqueira's%20Basic%20Histology%20PDF%20WHOLE%20BOOK/8.%20Bone.htm

Postnatal growth in bone length occurs at secondary ossification centres in the epiphyses growth plates of long bones (Meirelles et al, 2006). Mineralisation of the growth plate can be divided into four regions; the resting zone, the proliferating zone, the hypertrophic zone and the calcified zone. The morphology and organisation of chondrocytes in the different zones is shown in Figure 2.3. The process involves rapid proliferation of chondrogenic progenitors (Zone 2), followed by cartilage calcification in the epiphyseal cores (Zone 4). Calcified cartilage is subsequently replaced by osteogenic tissue (Zone 5). In contrast, bone thickness is increased when osteoblasts synthesize *de novo* bone matrix beneath the periosteum (Morrison & Scadden, 2014).

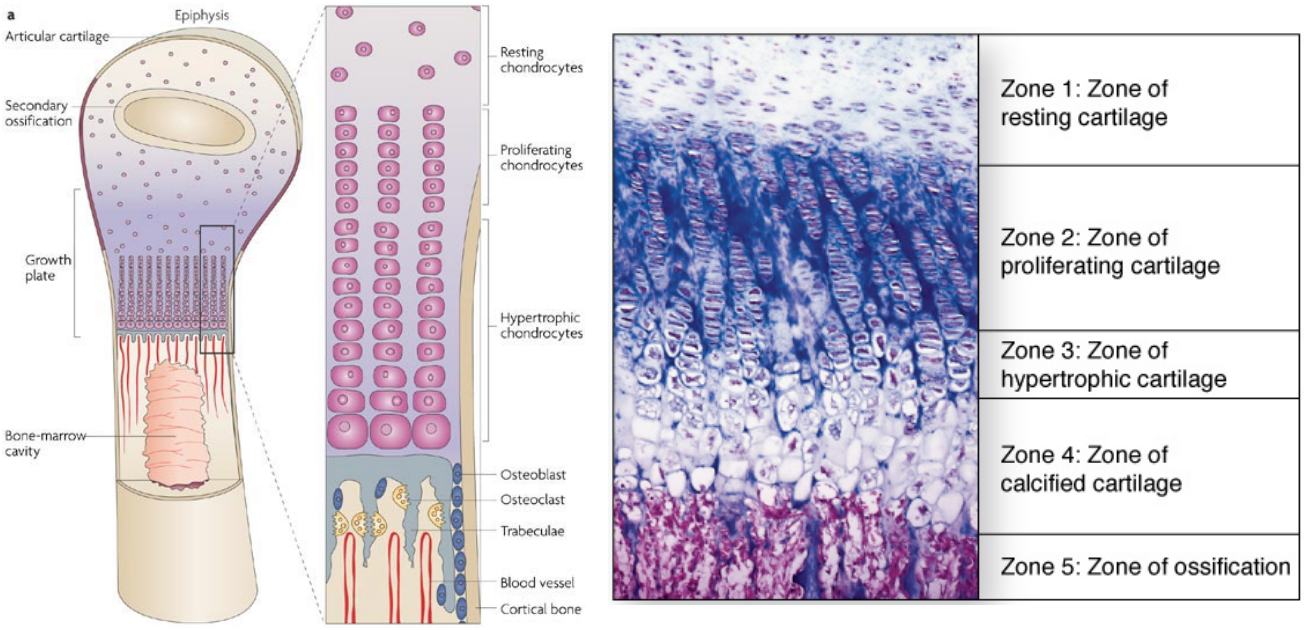

Figure 2.3 Epiphyseal growth plate. A plate of cartilage known as the epiphyseal growth plate separates primary ossification and secondary ossification centers. Cells in epiphyseal growth plates are responsible for continued elongation of bones until the body's full size is reached. Developments in epiphyseal growth plates occur in overlapping zones with distinct histological appearances. Moving from the epiphysis to the diaphysis, these zones include cells specialised for the following: (Zone 1) Resting hyaline cartilage, (Zone 2) proliferating chondrocytes aligned in lacunae as axial aggregates, (Zone 3) hypertrophic cartilage condensed matrix, (Zone 4) calcified cartilage, and (Zone 5) blood vessels and osteoblasts have invaded the lacunae of the old cartilage, producing marrow cavities and osteoid for new bone. Image adapted from: http://histonano.com/books/Junqueira's%20Basic%20Histology%20PDF%20WHOLE%20BOOK/8.%20Bone.htm and (Page-McCaw et al, 2007)

2.1.3.2.1 Matrix Vesicles in Mineralisation

Small, round, extracellular membrane bound organelles called matrix vesicles are the initiation site for the calcification of the bone matrix (Anderson, 1969). These vesicles form by budding from the plasma membranes of osteoblasts and hypertrophic chondrocytes (Kirsch et al, 1997). Importantly, matrix vesicles contain non-collagenous proteins called annexins, which have a strong affinity for calcium ions when associated with phosphatide serine. Phosphatases including alkaline phosphatase, trigger matrix mineralisation in three different ways (Majeska & Wuthier, 1975).

The mechanisms include increasing phosphate concentrations to begin calcium phosphate formation (Ali et al, 1970), hydrolysing inhibitors of hydroxyapatite formation, and connecting matrix vesicles to the bone matrix (Shapiro et al, 2015).

Ossification of the bone matrix begins with an influx of calcium ions into the matrix vesicles via channel proteins on the membranes of osteoblasts and hypertrophic chondrocytes (Anderson et al, 2005). As calcium ions bind to phospholipids in the plasma membrane, the activities of annexin-II and -V calcium channels are up regulated (Worch et al, 1998). The concentration of calcium ions reaches saturation and this marks the onset of hydroxyapatite crystal formation. Concurrently, alkaline phosphatase activity leads to an increase of phosphate ions inside the matrix vesicles (Golub, 2009), and amorphous calcium phosphate starts to precipitate due to the presence of both calcium and phosphate ions. Over time, the calcium phosphate is transformed into insoluble hydroxyapatite crystals that grow until they burst out of the matrix vesicles.

The newly formed hydroxyapatite crystals continue to grow outside the matrix vesicles, before large clusters are embedded between collagen fibres in the developing bone matrix. Crucially, hydroxyapatite formation is regulated by proteoglycans, osteocalcin and pH in the organic matrix. This inhibits detrimental mineralisation in regions such as cartilage and vascular tissue (Boivin et al, 2008).

2.1.3.3 Intramembranous Ossification

Bone growth through intramembranous ossification is a direct method of mineralisation observed during flat bone development and fracture healing (Ilizarov, 1989)(Figure 2.4). Intramembranous ossification begins at ossification centres with MSC condensation (Otto et al, 1997). This is followed by the differentiation of the adult stem cells into osteoblasts, which are responsible for mineralisation via the synthesis of Type I Collagen-based matrix. Importantly, in contrast to endochondral ossification, intramembranous ossification does not involve chondrogenic precursors (De Spiegelaere et al, 2010). As a consequence of matrix mineralisation, osteoblasts are embedded in the matrix. This triggers them to transform onto osteocytes, which function in bone matrix remodelling. Finally, large multinucleated cells known as osteoclasts resorb the bone matrix via acid phosphatases and proteolytic enzymes (Trebec et al, 2007).

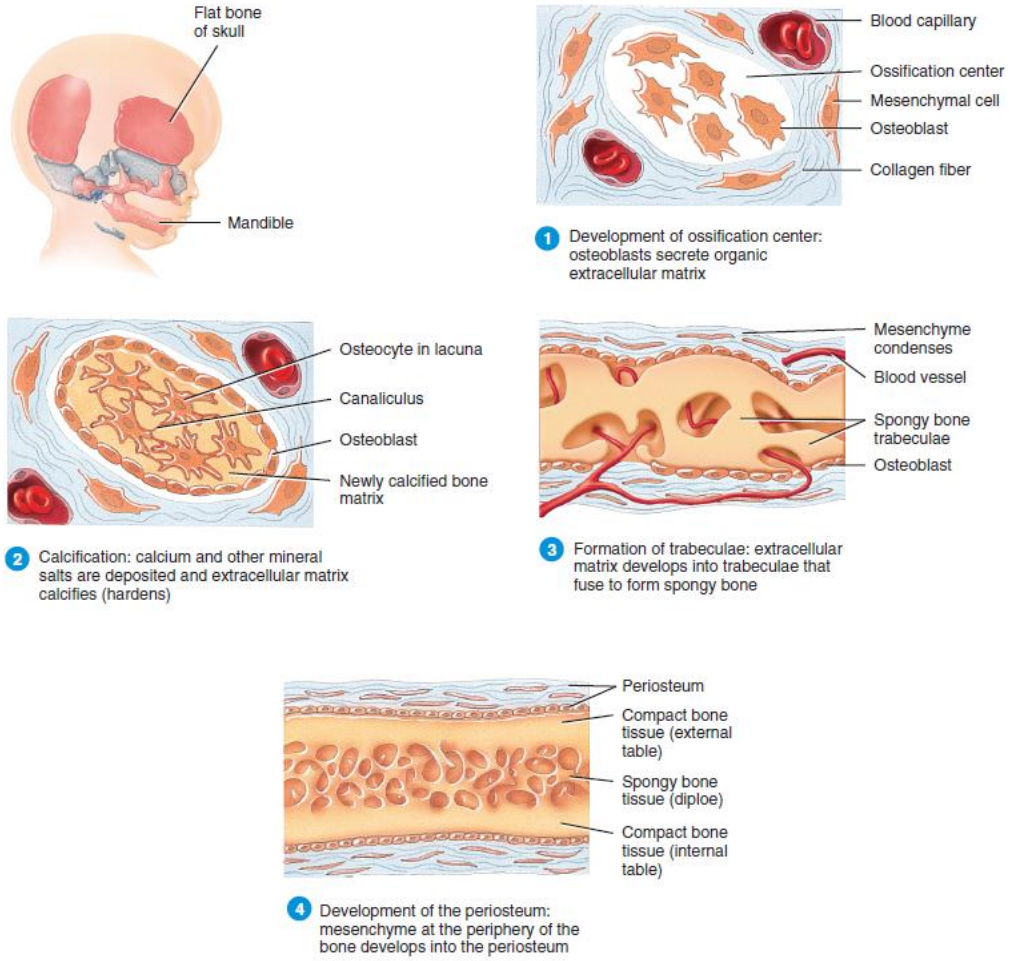

Figure 2.4 Intramembranous ossifications. This is a direct method of mineralisation observed during flat bone development and fracture healing. The process begins at ossification centres where MSCs condense and differentiate into osteoblasts. The osteoblasts start to secrete organic matrix in the form of Type I Collagen. The matrix calcifies as calcium salts are deposited and this leads to the fusion of trabeculae to form calcellous/ spongy bone. Over time, the spongy bone is remodeled into harder compact bone tissue. Image taken from: http://higheredbcs.wiley.com/legacy/college/tortora/0470565101/hearthis_ill/pap13e_ch06_illustr_audio_mp3_am/simulations/hear/ossification_intra.html

2.1.4 Osteogenic Homeostasis

Homeostasis in the adult skeleton is a balanced activity of bone remodelling through the formation of new tissue and resorption of existing bone (Kramer et al, 2010). Remodelling is primarily regulated by osteocytes and osteoclasts, which function in parallel to govern calcium homeostasis. Although repair of micro cracks is a regular occurrence, bone formation is accelerated at sites of repeated stress, and this can lead to bone thickening (Madsen et al, 2013). In contrast, bone resorption is ordered by osteoclasts and this can release minerals into the vascular system.

Parathyroid and calcitonin activities are balanced hormonal mechanisms for maintaining blood calcium homeostasis (Binnerts et al, 1992). Vitamin D is also important for systemic calcium concentrations (Sahota et al, 2004). In addition to this, bone homeostasis is influenced by mechanical stimuli and hormonal factors, including insulin growth factors (IGFs) and transforming growth factors (TGFs).

2.1.5 Osteochondral Repair and Regeneration

Cartilage has limited regenerative capacity after injury due to the lack of vasculature and limited numbers of chondrogenic progenitors in articular cartilage (Brittberg et al, 1994). Only injuries that infiltrate the subchondral bone can heal. However, the repaired articular cartilage does not match the biochemical or mechanical properties of the original tissue (Shapiro et al, 1993). Cartilage repair via autologous chondrocyte transplantation is unsuccessful because of limited cell numbers and the common calcification of transplanted tissues. Mesenchymal stem cells have been demonstrated to support chondrogenic repair. This happens through mechanisms observed in subchondral bone-facilitated repair where the stem cells can provide chondrogenic progenitors (Wakitani et al, 1994) and trophic factors (Caplan & Dennis, 2006).

In contrast to articular cartilage, bone fractures can been repaired with original structural and functional properties restored (Langer & Vacanti, 1993). Importantly, complete restoration only occurs in children. Bone repair through endochondral ossification involves four stages: hematoma formation, fibrocartilaginous callus formation, bone callus formation, and bone callus remodelling (Ferguson et al, 1999)(Figure 2.5). Bone healing can also occur via intramembranous ossification, where osteogenic progenitors differentiate directly into osteoblasts. This method does not include cartilage intermediates. Similar to endochondral ossification, woven bone is remodelled into stronger lamellar bone.

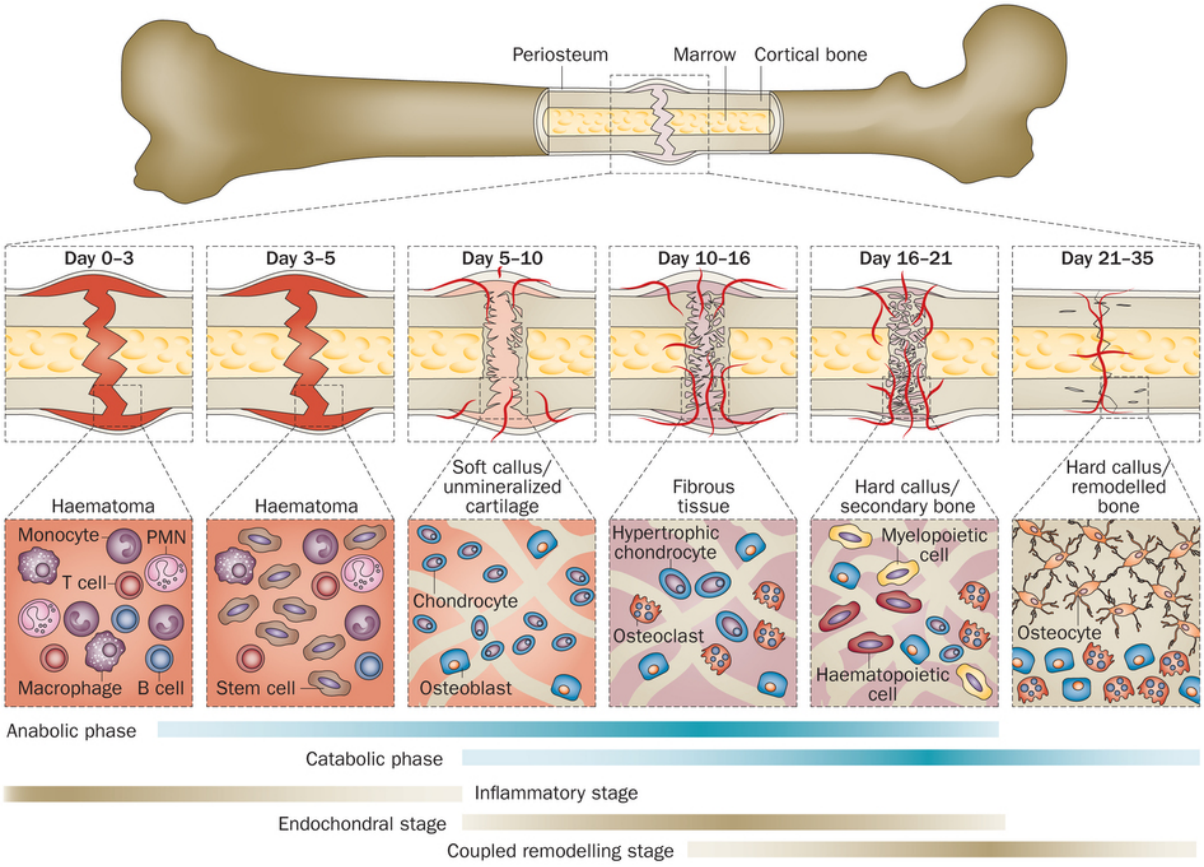

Figure 2.5 Long bone fracture repair. Bone repair through endochondral ossification involves four major stages: hematoma formation, un-mineralised cartilage callus formation, bone callus formation, and bone callus remodelling The metabolic phases (blue bars) of fracture healing overlap with biological stages (brown bars). Image taken from (Einhorn & Gerstenfeld, 2015).

Skeletal development and regeneration are complex processes, linked to various growth and transcriptional factors. Bone morphogenic proteins (BMPs) and transforming growth factors (TGFs) are the principal factors involved in joint healing. More specifically, TGF-βs are associated with chondrogenesis, while BMPs are responsible for cell proliferation and ossification, osteoblast recruitment and resorption of mineralised cartilage (van Beuningen et al, 1998). Although significant in joint repair, BMPs and TGFs function with a number of other signalling molecules, including insulin-like growth factors (IGFs), parathyroid hormone-related protein (PTHrP) and Wnt (Arvidson et al, 2011). These factors are not covered here.

2.1.6 Osteochondral Mechanics

Bone and cartilage are the principal tissue-types in joints and they both have different mechanical properties due to their different structure and function. Bone is load-bearing structural-tissue, while cartilage functions to reduce friction during joint movement and distribute loads (Hogan, 1985).

Bone mechanics vary depending on bone-type, age, diet and health (Morrison, 1970). For these reasons and variable testing conditions, there is discrepancy in the literature regarding the biomechanics of bone. Bone matrix is mostly composed of inorganic mineral (apatite) (Young's modulus of 130 GPa)(Khor et al, 2003) and Type 1 Collagen fibrils (Young's modulus of 5-11.5 GPa)(Wenger et al, 2007). Porous, cancellous bone has an average Young's modulus of 10-14 GPa, while cortical bone has an average modulus of 14-30 GPa (Rho et al, 1993; Rho et al, 1997).

The mechanical properties of cartilage are primarily linked to synovial fluid flow through the tissue during exposure to pressure (Gu & Li, 2011). The presence of solid and fluid phases in cartilage means that fluid flow is systematic through the tissue. The solid phase is an incompressible elastic material and the fluid phase is incompressible with low viscosity. Under high loading rates, there is insufficient time for the synovial fluid to move. In contrast, under low loading rates cartilage demonstrates viscoelastic properties (Mow et al, 1984). Additionally, compressive stiffness in cartilage is enhanced by electrostatic repulsion between negatively charged proteoglycans (Franz et al, 2001).

2.1.6.1 Mechanical Properties of Biomaterials for Joint Repair and Regeneration

Appropriate mechanical properties of materials are critical for the success and application of tissue engineering research. The material mechanics should be similar to the properties of the surrounding tissue. Nevertheless, this is not so important in biodegradable implants because over time, they are replaced by native tissue. Failure to meet mechanical requirements can lead to implant failure and the necessity for additional surgery. Table 2.1 lists popular biomaterials for orthopedic repair and compares their mechanical properties to native bone and articular cartilage. Osteochondral implants are often made of metals, but polymers and composites are becoming more popular as the technology is advanced.

Material	Tensile Strength (MPa)	Young's Modulus (GPa)
Metals		
Titanium	785	105
Stainless steel	465-950	200
Cobalt-Chronium alloys	655-1896	210-253
Polymers		
PMMA (Polymethylmethacrylate)	21	4.5
PEEK (Polyetheretherketone)	139	8.3
PLA (Polylactic acid)	28-50	1.2-3
PLGA (Polylactic-co-glycolic acid)	17	2
PCL (polycaprolactone)	10.5-16	0.3
Ceramics		
Zirconia	820	220
Alumina	300	380
Bioglass		75
Hydroxyapatite	117	40-50
Biological Tissues		
Tibia	140	18.1
Femur	121	17.2
Radius	149	18.6
Humerus	130	17.2
Cervical	3.1	0.23
Lumbar	3.7	0.16
Articular Cartilage	27.5	0.01

Table 2.1 Mechanical properties of skeletal tissues and commonly used biomaterials for orthopaedic repair. Adapted from (Katti, 2004).

2.2 Cartilage

Cartilage is connective tissue in the skeletal system, which can be separated into three distinct subgroups; elastic, hyaline and fibrocartilage (Brittberg et al, 1994). Elastic cartilage contains elastin and is located in flexible tissue including the outer ear, larynx and epiglottis (Eyre & Muir, 1975). Hyaline cartilage is primarily found at joint surfaces, and in the larynx, trachea and bronchi of the respiratory system (Muir, 1958). Importantly, articular cartilage refers to the hyaline cartilage at the surface of joints, and is derived from the interactions between ECM and chondrocytes at the end of long bones (Hunziker, 2002). Fibrocartilage is produced as a consequence of hyaline cartilage repair in tendons and ligaments. This type of cartilage can be defined by a dense and fibrous structure (Benjamin & Ralphs, 1998). Although fundamental and heavily utilised in the skeletal system, cartilage tissue is very restricted in its regeneration capacity. This is due to low metabolic activity and the lack of vasculature, lymphatic vessels and nerves (Buckwalter & Mankin, 1997).

2.2.1 Cartilage Structure

Articular cartilage comprises in an ordered structure of chondrocytes, collagens, proteoglycans and non-collagenous proteins (Mow et al, 1992). More specifically, the distance from the articular surface and their properties, classifies 4 inter-connected histological zones in cartilage (Modl et al, 1991)(Figure 2.4).

The superficial zone is defined by a Type II collagen fibre orientation, which is parallel to the joint surface (Schumacher et al, 1994). Proteoglycans are sparse and chondrocyte morphology is flattened. Furthermore, this is the only zone that contains articular cartilage progenitor cells (Dowthwaite et al, 2004). This zone accounts for 10-20% of the structures in articular cartilage.

The transitional zone is the thickest layer in articular cartilage and the orientation of collagen fibres is random (Thompson & Stockwell, 1983). Chondrocytes are round and proteoglycan content is high. Inter-connected to the transitional zone, is the radial zone.

The radial zone can be distinguished via Type 2 collagen fibres/ tubules perpendicular to the articular surface, and very high concentrations of proteoglycans (Ap Gwynn et al, 2000). The collagen fibres infringe into the tidemark. Additionally, round chondrocytes are organised in columns.

The tidemark in the joint surface separates the articular cartilage, from the calcified zone (Lane & Bullough, 1980). Crucially, the calcified zone is a remnant of endochondral ossification in the development of subchondral bone.

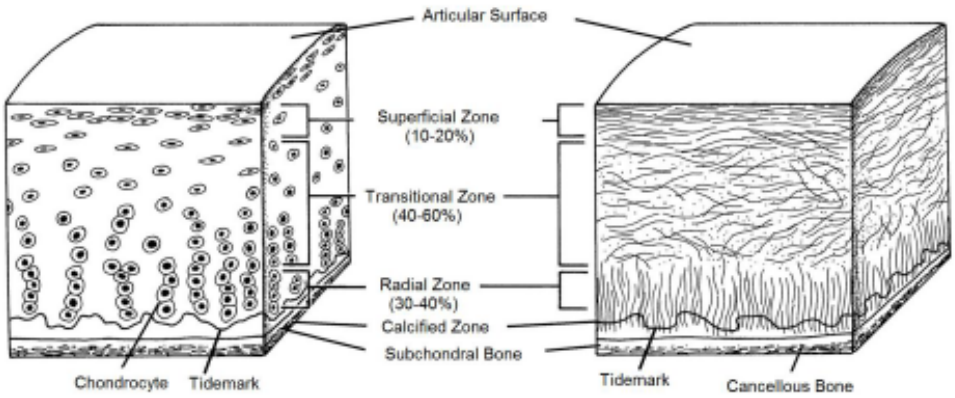

Figure 2.6 Structure of articular cartilage. The cellular organisation (left) and collagen fibre orientation (right) in the primary zones of articular cartilage. Image taken from (Newman, 1998).

2.2.2 Cartilage Composition

Articular cartilage has evolved the capacity to withstand high compressive forces through its structure and composition. The solid/ ECM phase of articular cartilage comprises up to a third of the whole tissue volume (Landis & Glimcher, 1982). This phase is primarily made up ECM proteins, including Type II collagen, glycoproteins and proteoglycans. Chondrocytes, another contributor to the solid phase, are sparsely present and account for around 5% of the cartilage tissue (Kusuzaki et al, 2001).

The fluid phase is accountable for the majority of the articular cartilage (65-85% of the tissue volume) (Mukherjee & Wayne, 1998), and contains water and ions (Berberat et al, 2009). Importantly, the water content of articular cartilage decreases over time (Armstrong & Mow, 1982) and this is a primary source of age-related joint degeneration (Torzilli et al, 1999).

2.2.2.1 Collagens

Collagens are the most abundant protein in mammals and account for more than 25% of the protein content in the body. Furthermore, collagens are the principal proteins in articular cartilage, and are fundamental for the structure and tensile strength of the joint tissue (Vanderrest & Garrone, 1991). To date, 28 types of collagen have been identified, but Type II and IX collagens are the main types specific to cartilage (Vondermark et al, 1977). In articular cartilage, Type II collagen makes up over 90% of the collagen and is responsible for fibril formation and structural strength in the matrix (Barry et al, 2001). Type IX collagen supports proteoglycan interactions and is essential for Type II collagen cross-linking into fibrils (Mendler et al, 1989).

2.2.2.2 Proteoglycans

A major component of ECM, proteoglycans are proteins covalently bound to glycosaminoglycans (GAGs) (Iozzo, 1998). Their main function involves the formation of structural complexes with other proteoglycans and fibrous matrix proteins. Chondroitin sulphate, keratin sulphate and hyaluronic acid are the principal GAGs in articular cartilage, and provide structural support and strength in the tissue (Bashir et al, 1999). Proteoglycans are also responsible for binding positively charged ions, such as sodium, potassium and calcium. This role regulates the water content of cartilage via osmosis (Loret & Simoes, 2010). Fibronectin, another important proteoglycan in articular cartilage, interacts via integrins with chondrocyte plasma membranes and Type II collagens, to stabilise the ECM and control cartilage development (DeLise et al, 2000).

2.2.3 Cartilage Development

The main functions of articular cartilage involve delivering a low friction surface for articulating joints, structural support and a template for endochondral ossification in long bone development (Hollister, 2005). Cartilage development begins when mesenchymal stem cells (MSCs) commit to a chondrogenic lineage via the condensation of the cells (Oldershaw & Hardingham, 2010).

The chondrogenic progenitors mature into chondroblasts and then chondrocytes, which express chondrogenic-specific markers and produce matrix proteins, including Type II Collagen, aggrecans and proteoglycans. Following chondrogenesis, the cells enter a resting phase to form articular cartilage or undergo proliferation (Goldring, 2012). This leads to terminal differentiation and chondrocyte hypertrophy; the beginning of endochondral ossification, where hypertrophic cartilage is replaced by bone. Chondrocytes have limited regenerative potential, and cartilage growth is based on maturation of immature chondrocyte progenitors (Pittenger et al, 1999). The chondrocytes do not have the ability to produce new ECM with the same initial properties.

2.2.3.1 Chondrocytes

Chondrocytes are the only cell type in cartilage, and are responsible for the synthesis and maintenance of the fundamental ECM structure (Johnstone et al, 1998). The shape, size and metabolic activity of chondrocytes varies depending on their location and level of maturity. Importantly, due to the high volume of ECM in articular cartilage, cellular interaction is limited. Cell response is regulated by other environmental factors, such as mechanical loading (Sun, 2010). Moderate mechanical loading is important for the maintenance of articular tissue. However, heavy use in joint tissue or lack of mechanical loading leads to matrix degradation. Nutrients are supplied to chondrocytes through diffusion in the synovial fluid and joint tissue. This process of nutrient supply is very inefficient and chondrocyte metabolism has to anaerobic (Egli et al, 2008). Furthermore, the level of metabolic activity is high for individual chondrocytes but low in the overall tissue due to sparse cell numbers.

2.2.3.2 Primary Chondrogenic Growth Factors and Transcription Factors

Differentiation of mesenchymal stem cells (MSCs) into chondrocytes is a complex process, which is tightly controlled by a range of chondrogenic growth and transcription factors (Figure 2.5). Here, the most important factors for chondrocyte differentiation and maintenance will be briefly described.

At the beginning of the chondrogenesis, transforming growth factor-βs (TGF-βs) stimulate the condensation of MSCs and the onset of early chondrogenesis (Jakob et al, 2001). Later, TGF-βs delay cartilage degradation by inhibiting hypertrophic proliferation in chondrocytes.

Bone morphogenic proteins including BMP-2 also promote mesenchymal stem cell condensation and the onset of joint formation (Grunder et al, 2004). The presence of BMP-2 factors is important through all stages of chondrogenic development.

After the initial development of chondro-progenitors from MSCs, fibroblast growth factors (FGFs) encourage proliferation in progenitor and pre-hypertrophic chondrocytes (Martin et al, 1999).

SOX9 transcription factor is expressed throughout articular cartilage development (Aigner et al, 2003). The factor is first detected after mesenchymal stem cell aggregation. Crucially, SOX9 is responsible for Type II Collagen gene expression and inhibition in the formation of hypertrophic chondrocytes to maintain cartilage.

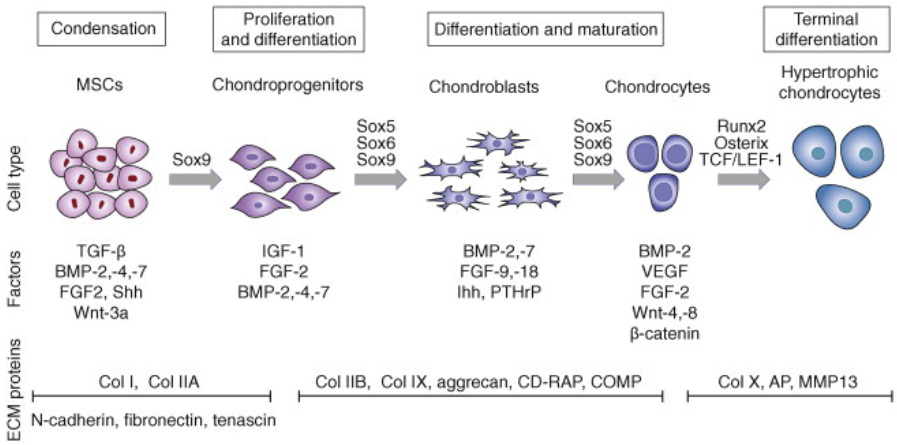

Figure 2.7 Differentiation of mesenchymal stem cells into chondrocytes. The expression profiles of the growth factors (below cells) and the main transcription factors (above arrows) involved in each step of chondrogenic differentiation. Proteins representative of the extracellular matrix (ECM) at various stages are highlighted. Image taken from (Vinatier et al, 2009).

2.3 Mesenchymal Stem Cells

Multipotency of cells was first recognised in the late 19th century. However, the concept was later defined by (Friedenstein et al, 1968), and (Tavassoli & Crosby, 1968). These researchers conducted original experiments in 1960s and 1970s to demonstrate multipotent potential of cells by transplanting bone marrow derived cells into heterotopic sites. Over time, the transplanted cells developed into osteogenic lineages. The mesenchymal stem cell term was later proposed by Arnold Caplan (Caplan, 1991).

Mesenchymal stem cells (MSCs) have the potential to differentiate into multiple lineages including osteoblasts, chondrocytes and adipocytes (Pittenger et al, 1999; Sottile et al, 2002). Furthermore, they have been proven to form muscle and connective tissue, as well as stromal cells for hematopoietic support (Caplan, 2007).

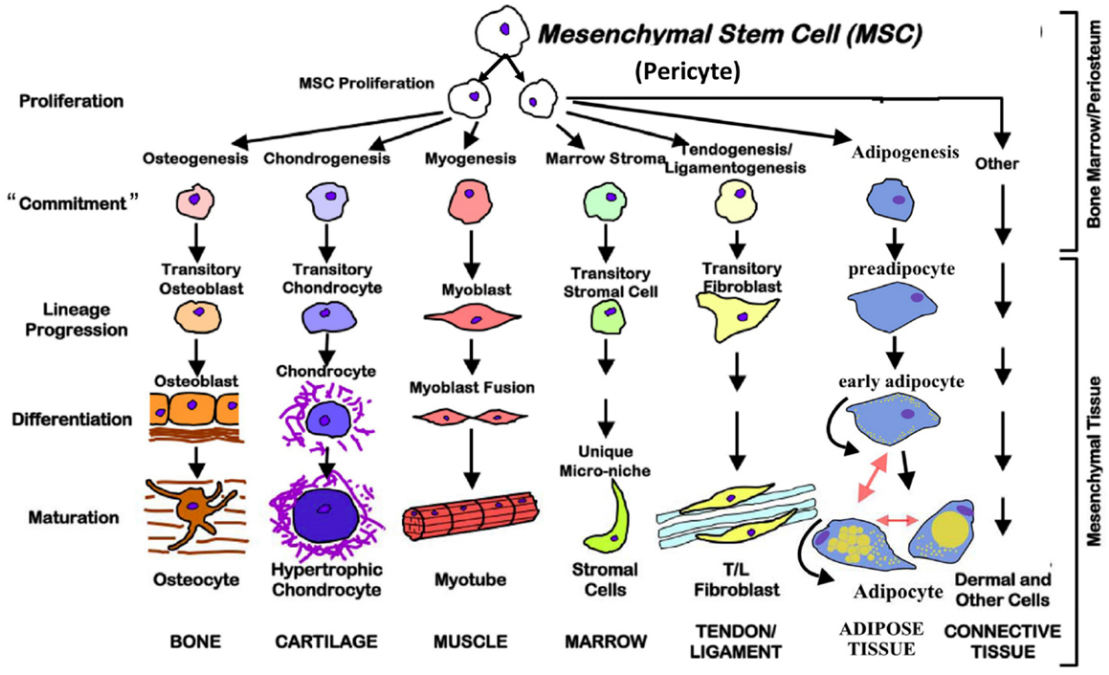

Figure 2.8 Mesengenic process: mesenchymal stem cell proliferation and differentiation. Multipotent differentiation of mesenchymal stem cells to differentiate into; bone, cartilage, muscle, bone marrow, tendons/ ligaments, adipose tissue and connective tissue. Image adapted from (DiMarino et al, 2013).

2.3.1 Initiating Differentiation of Mesenchymal Stem Cells

In the body, MSC differentiation is a tightly controlled process, which can be stimulated via lineage-specific chemical, topographical or mechanical cues.

2.3.1.1 Chemical Stimuli

Chemical influences in culture media, such as nutrient and growth factor supplementation, can initiate stem cell differentiation. Osteogenic differentiation is commonly achieved in 2D cultures via the addition of dexamethasone, ascorbic acid and β-glycerophosphate (Pittenger et al, 1999). More complex osteogenic media contain growth factors, such as bone morphogenetic proteins (BMPs). BMPs are important regulators in vertebrate development and promote osteogenesis (Hogan, 1996). In mesenchymal stem cells, up regulation of alkaline phosphatase activity is the trigger for extracellular matrix mineralisation and the onset of advanced-stage bone development (Weinreb et al, 1990).

Chondrogenic differentiation of mesenchymal stem cells requires culture media supplemented with transforming growth factor-β (TGF-β) (Mackay et al, 1998), dexamethasone, ascorbic acid, insulin-transferrin-selenium (ITS) and sodium pyruvate (Johnstone et al, 1998; Yoo et al, 1998). Chondrogenesis was originally conducted in 3D pellet cultures (Cao et al, 2015; Kafienah et al, 2007) but new protocols have been developed to allow differentiation in 2D monolayers (Caron et al, 2012; Henderson et al, 2011). Furthermore, cartilage formation has been enriched in low glucose media (Heywood et al, 2014) and low oxygen tension environments (Kurz et al, 2004; Saini & Wick, 2004). Increased synthesis of Type II Collagen proteins and proteoglycans are direct indicators of chondrogenic differentiation. This protein synthesis is a result in the up regulation of chondrogenic genes, such as SOX9 and collagen alpha 1 (II) (Bi et al, 1999).

2.3.1.2 Topographical Stimuli

Topographical microenvironments can effect mesenchymal stem cell differentiation, and moderate the necessity for growth factors. The use of surface roughness/ nanoscale disorder has been demonstrated to stimulate human mesenchymal stem cells (MSCs) to produce bone mineral *in vitro*, in the absence of

osteogenic supplements (Dalby et al, 2007). This approach had similar efficiency to that of cells cultured with osteogenic media. Importantly, the topographically treated MSCs displayed distinct differentiation profiles compared with those treated with osteogenic media. The biological testing considered cell morphology, cytoskeleton and adhesion formation, followed by cell growth and differentiation analysis (Dalby et al, 2006).

Porosity and pore size of biomaterial scaffolds are important for *in vitro and in vivo* bone formation (Karageorgiou & Kaplan, 2005a). *In vitro,* lower porosity has been demonstrated to stimulate osteogenic differentiation via suppressed cell proliferation and forced aggregation of cells. This is the opposite of what is observed *in vivo,* where higher porosity and pore size lead to enhanced bone development. Pore size in scaffolds can vary between applications and research groups. However, 100 μm is identified as the minimum requirement in pore size to accommodate for cell size, migration requirements and transport within the scaffold (O'Brien et al, 2005). Pore sizes greater than 300 μm are promoted for osteogenesis due to enhanced differentiation and the formation of vascularisation/ capillaries. Well-vascularised large pores lead straight to osteogenesis. In contrast, hypoxic environments in small pores favor osteochondral formation before bone development.

(Duan et al, 2014) investigated the *in vivo* effects of pore size in bi-layered scaffolds using a rabbit model of osteochondral defects. They fabricated five types of bi-layered poly(lactide-co-glycolide) (PLGA) scaffolds with different pore sizes to support osteogenic and chondrogenic layers (50-100 μm, 100-200 μm, 200-300 μm, and 300-450 μm). A small proportion of bi-layered scaffolds with allogeneic bone marrow MSCs were implanted in rabbit osteochondral defects. The results showed that all constructs supported the regeneration of articular cartilage and subchondral bone. The best differentiations were found in PLGA scaffolds with 100-200 μm pores in the chondral layer and 300-450 μm pores in the osteogenic layer.

(Yan et al, 2010) prepared collagen/ chitosan composite scaffolds for articular cartilage regeneration. The biodegradable scaffolds were cross-linked with genipin. The researchers evaluated the effects of chitosan content and genipin concentration on the physiochemical and biological properties of the porous scaffolds. The results showed that increase chitosan concentrations led to structural transition from fiber to sheet morphology of the material.

At low concentration of chitosan (under 25%), genipin cross-linking had significant control on scaffold porosity and pore size. The swelling ratio of the biomaterial was regulated via chitosan content or cross-linking. Importantly, cross-linking improved the stability of the chitosan material in aqueous environments, such as cell culture media. The biocompatibility of the scaffolds was evaluated through *in vitro* culture of rabbit chondrocytes. The chondrocytes exhibited good cell viability and attachment to the biomaterial surface. Collagen/ chitosan composites cross-linked with genipin are a feasible solution for osteochondral regeneration.

2.3.1.3 Mechanical Stimuli

Mesenchymal stem cells are adapted to respond to mechanical stimulation *in vivo* and *in vitro* (Butler et al, 2008; Luu et al, 2009; Wang et al, 1993). Importantly, cell gene expression and differentiation is primarily regulated by growth factors but can be enhanced via compressive and tensile loading (Kelly & Jacobs, 2010). Tensile forces and shear stress have been demonstrated to control osteogenic gene expression (Carter et al, 1998; Morinobu et al, 2003), while cyclic compression loading is important for chondrogenic development (Angele et al, 2003; Huang et al, 2004).

2.3.2 Assessing Differentiation of Mesenchymal Stem Cells

Differentiation of mesenchymal stem cells into osteogenic and chondrogenic lineages have been well documented and quantification methods are becoming more advanced (Caplan, 2007). Originally, stem cell differentiations were assessed using qualitative imaging techniques, which allowed limited quantification and required endpoint analysis (Zhu et al, 2006). Non-disruptive quantitative methods are preferred to allow assessments of cell proliferation, differentiation and viability during experiments.

Osteogenic differentiation is commonly evaluated by analysing cell morphology, bone-specific alkaline phosphatase activity, mineral deposition and osteocalcin expression (Caplan, 1991). Notably, alkaline phosphatase can be quantified at multiple time points during differentiation experiments.

Alizarin red staining can also be quantified after imaging, by extracting the stain from the bone matrix (Tataria et al, 2006). Alizarin red stains for mineralisation by binding to calcium in the bone matrix. This is important because it allows more detailed understanding of the osteogenic differentiation process.

Cartilage differentiation of mesenchymal stem cells is traditionally conducted in 3D pellet culture and confirmed by observing the cell pellet size and morphology. Histological stains, such as Safranin-O and 1,9-dimethylmethylene blue (DMMB), are used to imagine GAG production. In addition to this, immunohistochemistry and RT-PCRs assess Type II and X Collagen expression (Chung & Burdick, 2008). These approaches rely on sectioning of pellets and staining, which is not quantitative but very time consuming. More recently, studies have explored chondrogenic differentiation in 2D monolayer culture to allow for more high throughput and quantitative assessments (Henderson et al, 2011).

2.4 Tissue Engineering and Osteochondral Repair

Tissue engineering is a interdisciplinary scientific approach that combines the principals of biology and engineering to develop functional tissues (Langer & Vacanti, 1993). The purpose of this field of research is to improve healthcare by developing (cell-seeded) biomaterials that can be implanted into patients to regenerate damaged tissues, such as bone, cartilage, skin, vascular vessels etc. (Hutmacher et al, 2001). Tissue engineered implants can either be permanent or biodegradable, where they are replaced by native tissues over time.

The overall process of tissue development begins with the selection of suitable cells and/ or biomaterials for the intended application (Lutolf & Hubbell, 2005). These components are combined and cultured in supportive conditions, which contain biochemical and biophysical factors. At this stage, bioreactors are often utilised to enhance the culture environment by providing stimuli experienced by native tissue *in vivo* (El Haj & Cartmell, 2010). As tissues develop *in vitro,* cells proliferate and differentiate. Once sufficient development has been achieved, the constructs are implanted into patients where they continue to develop and remodel into functional tissues.

Improved understanding of the regulatory roles of biological, chemical and physical factors in tissue development and repair, are necessary to improve the quality of engineered tissues (Drury & Mooney, 2003). This is particularly true for constructs in osteochondral repair.

In recent years, with a progressively ageing population, pain and diseases of the joint such as osteoarthritis have become more common (Vater et al, 2011). There has also been a sharp increase in the number of joint-related injuries, due to more active lifestyles in the population. At present, such injuries are treated using a number of therapies, including surgical repair, transplantation of artificial devices and drug therapy (Martins et al, 2009). Joint injuries can be divided into two types; chondral when only the articular cartilage is damaged, and osteochondral when subchondral bone is also affected (Buckwalter, 2002). Spontaneous repair via mesenchymal stem cell mechanisms is observed in osteochondral injuries but this leads to the formation of fibrocartilage, and tissues may remain compromised.

In contrast, injuries only to cartilage do not have regenerative capacity because chondrocytes have limited self-renewal potential. Joint diseases are an obvious challenge for the near future and there is a clear demand for alternative regenerative therapies for osteochondral trauma (Pound et al, 2007).

2.4.1 Current Approaches to Osteochondral Repair

Treatment of joint trauma is currently inconsistent and the approach taken depends on the size, shape and location of the osteochondral defect (Newman, 1998; Taniyama et al, 2015). Joints defects can be reconstructed in total knee replacement (TKR) procedures using bone grafts or biomaterial implants (Bentley et al, 2003). For less severe injuries there are a number of regenerative methods.

The Ilizarov technique is used in large breaks to promote bone regeneration by maintaining a fracture for extended periods of time (Ilizarov, 1988; 1989; Paley, 1990). Unfortunately, this complex procedure requires very long recovery periods. In smaller defects, cartilage regeneration can be stimulated using microfracturing or laser therapy (Bedi et al, 2010; Steadman et al, 2003). Autologous mosaicplasty involves the transplantation of an osteochondral cylinder into a damaged joint (Hangody & Fules, 2003; Hangody et al, 2004). Limited donors and injury to donor sites are the main limitations of this technique.

2.4.1.1 Cell-based Techniques

Autologous chondrocyte implantation (ACI) has been applied to cartilage regeneration for over two decades (Brittberg et al, 1994). The procedure begins with a biopsy of cartilage from a healthy donor site and this is followed by enzymatic digestion of the cartilage tissue to remove extracellular matrix components. Autologous chondrocytes are expanded *in vitro,* before cells are delivered back into the patient (under the periosteal flap of the knee) (Peterson et al, 2000). The procedure promotes the formation of a ‘cartilage-like’ site with good chondral functionality. However, limitations such as the calcification of implants and fibrosis mean that research into osteochondral repair is concentrated on developing 3D scaffolds (Abarrategi et al, 2010; Chen et al, 2011; Duan et al, 2014; Haasper et al, 2008; Malafaya & Reis, 2009; Oliveira et al, 2006; Rodrigues et al, 2012).

2.4.1.2 Tissue Engineering Techniques

The necessities to improve the limitations of first generation techniques for osteochondral repair has focused research onto the potential of cell seeded constructs. These constructs are the basis of second-generation tissue engineering techniques.

One approach uses fresh osteochondral allografts (Ghazavi et al, 1997). However, these grafts are very limited in number and require compatible donors, to avoid immune rejection. For these reasons, biomaterial scaffolds that are seeded with autologous cells seem to be the most promising solution. Scaffolds specific to osteochondral repair can be made up of one individual scaffold, or separate scaffolds for bone and cartilage. A range of commercial products for osteochondral repair are summarised in Table 2.2. More recently, third generation techniques have combined biomaterial scaffolds with growth factors to enhance tissue formation.

Product	Chondro-Gide ®	ChondroMimetic®	MaioRegen®	Novocart ®
Material	Bovine Collagen I/ III	Collage, GAGs and calcium phosphate	Equine Collagen 1 plus Mg-HA	Biphasic Collagen I
Culture time (days)	N/A	N/A	N/A	8-9 (2D and 3D)
Transplant size (mm)	40x50	Unlimited	Unlimited	30x50
Cell numbers	N/A	N/A	N/A	$15x10^6$
Fixation type	Fibrin glue	Fibrin glue	Fibrin glue	Suture
Company	Geistlich-Pharma	Collagen Solutions	Finceramica	Tetec-AG

Table 2.2 Commercially available tissue-engineered products for osteochondral repair.

2.4.1.3 Cell Sources

In tissue engineering, cells for osteochondral constructs are typically derived from bone and cartilage grafts, or bone marrow progenitor cells (Chamberlain et al, 2007). Primary cells from bone and cartilage are perfect for osteochondral repair, although they have restricted expansion and are obtained in limited numbers (Zuk et al, 2001). Furthermore, cell harvesting introduces additional sites of injury.

Human mesenchymal stem cells (hMSCs) are the gold standard for osteochondral applications because they have the potential to differentiate into all the major cell types in joints (Caplan & Bruder, 2001). In addition to this, the cells are highly proliferative and have the capacity to adapt to their environment (Bruder et al, 1994). MSCs have been discovered to be involved in paracrine signalling and immunomodulation (Chase et al, 2010). More specifically, MSCs can prevent graft-versus-host disease after transplantation by regulating T-cell and B-lymphocyte proliferation and differentiation (Perez-Simon et al, 2011). This immunomodulation is achieved by the migration of MSCs to sites of injury (Aggarwal & Pittenger, 2005). Other paracrine signalling functions include the release of growth factors for hematopoietic stem cell proliferation (Zhou et al, 2012).

All of the described properties of MSCs demonstrate the benefits for these cells to be used in the development of modern therapeutic applications including bone and cartilage regeneration, prevention of graft-versus-host disease, improved engraftment of bone marrow transplants and even the treatment of metabolic diseases (Bacigalupo, 2007). Consequently, many research groups have focused on studying MSCs in the laboratory.

2.4.2 Properties of Effective Osteochondral Constructs/ Scaffolds

Scaffolds are fundamental for the success of tissue engineering strategies because they provide a template for cellular interactions and tissue development. Scaffolds are required to mimic the physiological extracellular matrix and maintain the cell's capacity to proliferate and differentiate (Hutmacher, 2000). Successful scaffolds should have the following properties:

- Inter-connected porous structure for cell growth and mass transport of nutrients and metabolic waste. Pore size and porosity to promote differentiation of cells, and possibly vascularisation.
- Biocompatible scaffold material with a degradation rate similar to the healing rate in native tissue.
- Biomaterial surface properties to promote cell attachment, proliferation and differentiation.
- Mechanics to match the native tissues.

2.4.2.1 Pore Size and Porosity

Scaffolds should consist of highly porous 3D structures with inter-connected porosity in order to facilitate *in vitro* cell attachment and proliferation, and *in vivo* differentiation and vascularisation (O'Brien et al, 2005). Furthermore, highly porous architectures will enhance mass transport of nutrients and metabolic waste, and prevent the formation of necrotic cores (Silva et al, 2006). Although highly porous structures are good for mass transport, increased porosity has a detrimental effect on the mechanical characteristics of scaffolds (Marklein & Burdick, 2010).

In osteochondral applications, scaffolds are required to be at least 70% porous to achieve good *in vitro* bone and cartilage tissue formation (Hutmacher, 2000; Oliveira et al, 2006). In addition to this, scaffold pore size has a great effect on the differentiation potential of cells and this is an important consideration when designing osteochondral constructs (Table 2.3). Osteogenic differentiation can be achieved in a broad range of pore sizes, while chondrogenesis is realised in smaller pores (Duan et al, 2014). For this reason, osteochondral constructs should accommodate a gradient of pore sizes. This can be accomplished by combining individual scaffolds or by producing a single scaffold with graduated pore sizes.

Tissue Type	Optimal Pore Size (μm)
Bone	100-400
Cartilage	50-200
Vascular/ Endothelial	<50
Fibroblast	100-500

Table 2.3 Examples of pore sizes suitable for culturing a range of cell types related to osteochondral repair. Taken from (Im et al, 2012; Karageorgiou & Kaplan, 2005a; McHugh et al, 2013; O'Brien et al, 2005).

2.4.2.2 Biological Requirements

Biocompatibility is an essential requirement of any biomaterial that is intended for tissue engineering applications (Hutmacher et al, 2001). Cell attachment and proliferation can be improved by regulating the surface properties of biomaterials in a biomimetic manner. Such surface modifications include altered material morphology, wettability, charge and roughness (Shin et al, 2003).

In addition to this, cell response can be enriched through the attachment of biological molecules onto the biomaterial surface. This can be accomplished through mechanisms including adsorption and encapsulation in polymer particles.

Coating scaffolds with extracellular proteins such as fibronectin, collagen and laminin can significantly improve initial cell attachment (Pierschbacher & Ruoslahti, 1984). Cell attachment can further be maximised by incorporating RGD (arginine-glycine-aspartic acid) integrin sequences into the scaffold material (Hersel et al, 2003). Integrating growth factors, including bone morphogenetic proteins (BMPs), transforming growth factor-beta (TGF-β) and vascular endothelial growth factor (VEGF), into biomaterials can also enhance cell differentiation (Lutolf & Hubbell, 2005).

2.4.2.3 Mechanical Requirements

Engineered constructs are required to maintain their stability and mechanical integrity at least until the damaged tissues can regenerate (Carter et al, 1998). Furthermore, it is important for implants to match the mechanics of native tissue and prevent stress shielding, which can lead to reduced bone density (Sumner, 2015). Over time, a transfer of load from the construct to the tissue is desirable to encourage tissue repair via mechanotransduction mechanisms. Unfortunately, most osteochondral defect solutions do not match the mechanical properties of joints. Metal implants have significantly higher moduli to native tissues (Rho et al, 1997), while polymers are considerably weaker (Katti, 2004).

2.4.3 Current Approaches in Osteochondral Scaffold Engineering

The approaches to osteochondral scaffold design can be categorised into six categories, each dependent on scaffold characteristics and cell source (Figure 2.9).

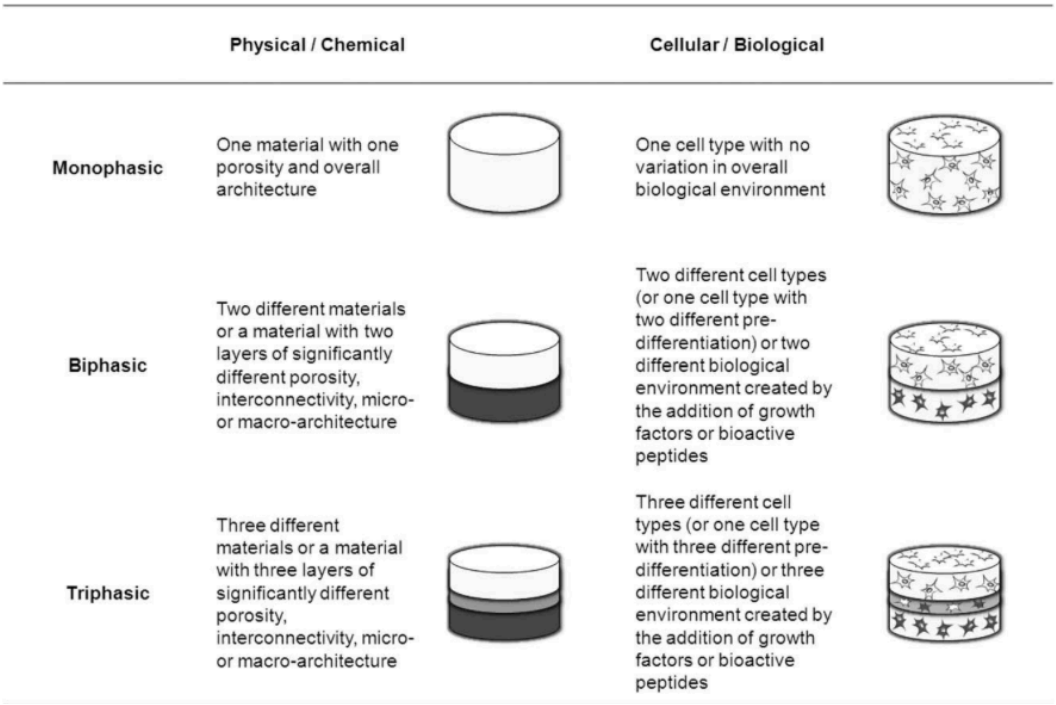

Figure 2.9 Osteochondral scaffold design approaches. Osteochondral tissue engineering strategies can be defined as monophasic, biphasic or triphasic. Scaffolds are further characterised based on the physical/ chemical and cellular/ biological properties of the scaffold. Adapted from (Jeon et al, 2014).

2.4.3.1 Individual scaffolds for bone and cartilage

Individual monophasic scaffolds can be cultured *in vitro* for osteogenic and chondrogenic components, before they are fused together by suturing or gluing. A limitation of this strategy is that layers can often separate under mechanical loading (Martin et al, 2007). Nevertheless, (Ibrahim et al, 2013) utilised this approach to produce a novel construct with a hydroxyapatite layer for osteogenesis and a N,O-carboxymethylated chitosan layer for cartilage. Human mesenchymal stem cells were successfully differentiated into both osteochondral lineages. When implanted into a rat model, the construct was not rejected by the host immune system and the scaffold layers did not delaminate.

In a similar manner, (Gao et al, 2002) seeded osteogenic progenitors onto a porous ceramic, and cartilage progenitor onto a hyaluronic acid sponge. The individual constructs were joined together with fibrin glue and over time, lamellar bone was detected on the ceramic biomaterial. Notably, the results failed to demonstrate any chondrogenesis on the hyaluronic acid scaffold.

(Schaefer et al, 2000) sutured PGA meshes seeded with autologous chondrocytes to collagen-HA sponges loaded with mesenchymal progenitor cells. This study showed that the Young's modulus of tissue engineered cartilage (0.68-0.8 MPa) was analogous to native articular cartilage (0.84 MPa).

2.4.3.2 Bi-Layered/ Biphasic Scaffolds

Biphasic scaffolds are composed of two different materials or one material with two layers of significantly different porosity (Jeon et al, 2014). The two layers must be interconnected and this can make fabrication of these scaffolds challenging.

One example of biphasic scaffolds was produced by (Rodrigues et al, 2012). These researchers developed a bi-layered scaffold starch/ polycaprolactone (SPCL) scaffold for osteogenesis and an agarose hydrogel for chondrogenesis. Amniotic fluid-derived stem cells were cultured on the scaffolds for up to 2 weeks in medium containing osteogenic and chondrogenic differentiation factors. Both osteochondral lineages were achieved, although chondrogenic supplements appeared to be essential in generating cartilage.

(Oliveira et al, 2006) designed novel hydroxyapatite/ chitosan (HA/CS) biphasic scaffolds by combining sintering and freeze-drying techniques. Results demonstrated that the biomaterials were biocompatible, and supported the *in vitro* proliferation and differentiation of goat marrow stromal cells into osteoblasts and chondrocytes, respectively. In addition to this, the seeded cells were able to adhere to the scaffolds and remain viable.

Further work by Oliveira in 2007, tested the suitability of corn starch-polycaprolactone (SPCL) scaffolds for cartilage tissue engineering. Bovine articular chondrocytes were seeded on SPCL scaffolds under dynamic conditions using spinner flasks and cultured under orbital agitation for 6 weeks. SPCL construct results demonstrated typical chondrocyte morphological features, with good cell distribution and extracellular matrix deposition throughout the scaffolds.

Glycosaminoglycans, and collagen types I and II were detected with higher levels of collagen type II compared to collagen type I.

Magalhaes *et al.*, (2008) developed implantable stimuli responsive constructs from 2-ethyl (2-pyrrolidone) methacrylate (EPM) and hyaluronic acid (HA) composites. Investigating a range of different EPM-HA ratios and cross-linkers produced hydrogels with different porous structures. Due to the physical and structural properties of the developed hydrogels, the materials were proposed for cartilage tissue engineering. Bovine chondrocytes were seeded and cultured under agitation for a period of 6 weeks. Following the culture period, the bovine chondrocytes demonstrated good cell morphology, viability and cell distribution within the EPM-HA hydrogels. The presence of cartilage factors was not assessed.

2.4.3.3 Homogenous Scaffolds

Homogenous scaffolds allow dual differentiation of a single cell source, by providing spatially resolved environments, each supportive of one of principal osteochondral cell lineages. Furthermore, the inter-connected structure of these scaffolds avoids issues with delamination.

(Malafaya & Reis, 2009) designed a homogenous biphasic scaffold using a particle aggregation method. One half was made from 100% chitosan, while the other was a 4:1 mixture of chitosan and hydroxyapatite. The scaffold pore diameters were in the 225-290 μm ranges, but the overall porosity of the scaffolds was only 30%. Importantly, scaffolds showed good mechanical properties compared to other chitosan-based porous materials (Young's modulus of 6.26 ± 1.04 MPa). Differentiation potential was not assessed on the scaffolds but they were considered non-cytotoxic.

Another homogenous scaffold with graduated pore characteristics was produced by (Duan et al, 2014). Scaffolds with five different pore sizes and 85% overall porosity were made from poly(lactide-co-glycolide) (PLGA). The pore sizes ranged between 50–100 μm, 100–200 μm, 200–300 μm, and 300–450 μm. To check biocompatibility and osteochondral differentiation potential, constructs were seeded with bone marrow derived mesenchymal stem cells and implanted into a rabbit knee defect model. The results showed that chondrogenic differentiation was observed in 100-200 μm pores, while bone differentiation was detected in the 300–450 μm pores.

2.5 Chitosan

2.5.1 Chitin and Chitosan

Chitosan is a cationic, biodegradable polymer derived from the deacetylation of chitin (Drury & Mooney, 2003). Chitosan is the second most abundant polysaccharide after cellulose, and even has a similar structure composed of N-glucosamine and N-acetyl-glycosamine units. The two biopolymer structures differ because of an amine group in chitosan instead of a hydroxyl group at position C(2) (Figure 2.9). The chitosan polymer contains reactive functional groups (amine group with two hydroxyl groups) that provide a high charge density when in solution. This allows for a number of chemical modifications, including the ability to form ionic complexes with therapeutically relevant anionic compounds, such as heparin (Shi et al., 2006).

Chitosan has potential uses in wound healing, drug delivery systems, bone filling and regeneration, and tissue engineering of cartilage and bone (Sendemir-Urkmez & Jamison, 2007). Chitosan promotes cell adhesion, proliferation and differentiation (Muzzarelli, 2011), while it shows biocompatibility, biodegradability by lysozyme (controlled by level of deacetylation) (Shi et al, 2006) and anti-inflammatory/ antibacterial properties (Wang & Stegemann, 2011). Although, chitosan can promote chondrogenesis due to a fundamental structure related to GAGs (Chondroitin sulfates) in cartilage, the material lacks the mechanical strength necessary in initial bone development (Malafaya et al, 2007).

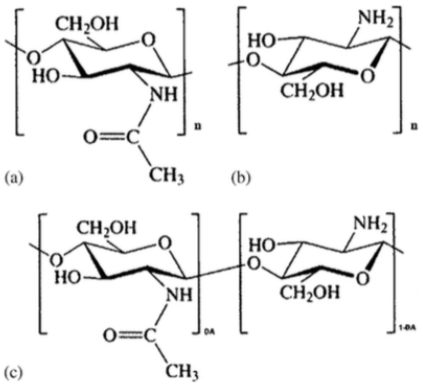

Figure 2.10 Chemical structures of chitin and chitosan. Structures of (A) chitin and (B) chitosan repeat units. (C) Partially acetylated chitosan, a copolymer characterised by its average degree of acetylation DA. Adapted from (Rinaudo, 2006).

2.5.2 Production of Chitosan

Chitosan can be derived from the exoskeletons of crustaceans, insects and marine invertebrates (Wang & Stegemann, 2011). The polymer has also been obtained from fungi (Yokoi et al, 1998). More specifically, chitosan is produced by the alkaline chemical or enzymatic N-deacetylation of chitin (Pillai et al, 2009). Alkali treatment results in the production of a more evenly deacetylated chitosan with a higher overall degree of deacetylation (Zhao et al, 2010)(Figure 2.10). In contrast, enzymatic deacetylation is less efficient due to the large enzyme molecules and their inability to access the highly crystalline chitin particles (Pangburn et al, 1982).

During the deacetylation process, proteins are removed using 1-2% aqueous NaOH, while minerals are purified out using HCl. Carotenoids, responsible for the pigmentation of crustacean shells, can be removed with EDTA in warm ethanol. It has been demonstrated that aqueous acetic acid treatment can demineralise and decolour simultaneously.

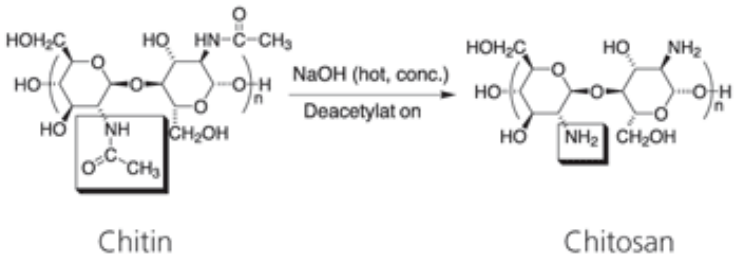

Figure 2.11 Producing chitosan from chitin through deacetylation. Image adapted from www.sigmaaldrich.com/materialsscience/biomaterials/tutorial.html

2.5.3 Deacetylation of Chitin

Deacetylation of chitin using alkaline chemicals is a harsh process due to the highly crystalline polymer structure, and the extensive inter- and intra-chain hydrogen bonding (Pugnaloni et al, 1988). For this reason, deacetylation requires high alkaline concentrations (40-50% NaOH), high temperatures (100-140 °C) and extended reaction times (Zhao et al, 2010). In these conditions the NaOH cleaves acetyl groups from the chitin to produce chitosan with 75% free amine groups. However, deacetylation is more efficient in amorphous regions compared to crystalline regions and this leads to heterogeneous products.

Homogeneous deacetylation has been explored where increased alkaline concentrations or temperatures greatly influenced the degree of deacetylation (Chang et al, 1997). Importantly, the degree of deacetylation was reduced when both variables were increased simultaneously.

2.5.3.1 Degree of N-Acetylation in Chitosan

Chitosans are a range of copolymers consisting of 2 repeating units of N-acetyl-D-glucosamine (A unit) and D-glucosamine (D unit). The ratio of the two units is an indicator of the degree of deacetylation, degree of N-acetylation and number of free amine or acetyl groups (Pillai et al, 2009). The degree of N-acetylation and the number of free amine groups are inversely proportional. Crucially, the degree of N-acetylation is an important characteristic in chitosan for consistent and reproducible results.

2.5.4 Cross-linking

Diepoxides, diacylchlorides and dialdehydes are usually utilised for the cross-linking of chitosan. Examples of such chemicals used for this application include glutaraldehyde, genipin and tripolyphosphate (Monteiro & Airoldi, 1999; Wang & Stegemann, 2011).

Glutaraldehyde is the most popular cross-linking reagent due to its availability and efficient cross-linking. The reaction involves the formation of a Schiff's base (condensation between an amine and an aldehyde or ketone) between two amino groups (Muzzarelli, 2009b). Furthermore, cross-linking can occur within or between polymeric chitosan chains. Although glutaraldehyde increases the mechanical strength of the chitosan, this cross-linking reaction leads to cytotoxic properties in the biomaterial due to the presence of free aldehyde groups (Sung et al, 1999). Genipin is another suitable cross-linker of chitosan.

Genipin is a naturally derived compound, with no reported cytotoxicity (Silva et al, 2008). Importantly, this cross-linker provides stable bonds via the same mechanisms as glutaraldehyde, while mildly enhancing the mechanical properties of chitosan more than glutaraldehyde (Jin et al, 2004).

2.5.5 Tissue Engineering with Chitosan

Chitosan is a biocompatible, biodegradable material that is able to reduce inflammation and can be moulded into a range of porous structures (Dash et al, 2011). Furthermore, the biological, physical and chemical properties of the material can tailored for tissue engineering application, including osteochondral defect repair (Abarrategi et al, 2010).

Chitosan has received FDA approval for a number of commercially available wound healing products, including SoftSeal-C Pad® (Chitogen Inc., Minneapolis, USA) and Sentrex BioSponge MPD® (Bionova Medical Inc., Tennessee, USA). However, the polymer has not been approved yet for osteochondral repair.

The cationic nature of chitosan allows for electrostatic interactions with negatively charged molecules, such as proteoglycans, glycosaminoglycans and DNA (Di Martino et al, 2005). The capacity to bind growth factors makes chitosan ideal for drug delivery applications (Shi et al, 2006).

2.5.5.1 Chitosan in Bone Regeneration

Chitosan has potential in bone regeneration because the polymer can promote osteoblast growth and mineralisation (Costa-Pinto et al, 2009). These properties are enhanced when chitosan composites are produced with ceramics, such as calcium phosphate, hydroxyapatite and β-tricalcium phosphate (Oliveira et al, 2006; Sendemir-Urkmez & Jamison, 2007).

Porous chitosan sponges reinforced with β-tricalcium phosphate ceramics demonstrated improved mechanical properties compared to chitosan alone (Zhang & Zhang, 2002). The Young's modulus and yield stress increased from 4 to 16 MPa and 1 to 4.5 MPa, respectively. This was significantly lower compared to native skeletal tissue. Human osteoblast-like MG63 cells showed good cell attachment and migration when seeded onto the composite scaffolds. Additionally, osteocalcin expression and alkaline phosphatase activity were improved (Zhang et al, 2003).

More recently, research has focused on optimising the biocompatibility, biodegradability and mechanical properties of composite scaffolds (Muzzarelli, 2011). To achieve this aim, hydroxyapatite has been in situ combined into chitosan scaffolds (Kong et al, 2006). Monitoring apatite formation and osteoblast progenitor activity assessed the bioactivity of the scaffolds.

The results showed that addition of nano-hydroxyapatite improved the bioactivity of the scaffolds. The composition of the substrate affected apatite formation, and pre-loaded hydroxyapatite enhanced the apatite coating. Furthermore, on the apatite-coated composite scaffolds cells demonstrated increased proliferation and alkaline phosphatase activity compared to chitosan-only scaffolds coated with apatite.

Other research has also focused of producing composite scaffolds in situ. Calcium phosphate cement was injected into chitosan to form biodegradable scaffolds with excellent osteoconductivity (Moreau & Xu, 2009). Furthermore, the chitosan reinforced the mechanical properties of the cement. Mesenchymal stem cells differentiated into osteogenic lineages and expressed high levels of alkaline phosphatase. The calcium phosphate cement-chitosan scaffold has potential for bone regeneration in moderate load-bearing orthopedic applications.

β-glycerophosphate, an osteogenic medium supplement was used to initiate cross-linking of chitosan-collagen composites at physiological pH and temperature (Wang & Stegemann, 2010). Subsequently, human bone marrow-derived stem cells were encapsulated in the chitosan-collagen hydrogels, and exhibited good biocompatibility and osteogenic differentiation. This study shows that chitosan-collagen composite materials may be advantageous for cell encapsulation and delivery, or as in situ gel-forming materials for tissue repair.

2.5.5.2 Chitosan in Cartilage Regeneration

Chitosan is a suitable for cartilage regeneration due to the polymer's ability to mimic the natural environment of the articular cartilage matrix (Di Martino et al, 2005). There are structural similarities between extracellular matrix components found in articular cartilage, such as Type II Collagen and glucosaminoglycans (GAGs), and chitosan (Muzzarelli et al, 2012). For this reason, chitosan is a popular scaffold material for cartilage regeneration.

In one example of cartilage repair with chitosan, a chitosan-gelatin composite was produced via a freezing and lyophilising technique (Xia et al, 2004). Autologous chondrocytes were isolated from pigs and seeded onto the chitosan-gelatin scaffolds. 16 weeks after implantation, the engineered cartilages acquired the histological, biochemical and mechanical properties of native cartilage tissue.

More specifically, the engineered elastic cartilage showed chondrocytes enclosed in the lacuna as well as, the presence of elastic fibrils and Type II Collagen. Glucosaminoglycan concentrations were up to 90% of what is observed in native tissues. At the same time, mechanical stiffness in the engineered constructs was 15% lower than in articular cartilage.

Alves da Silva *et al.* (2007 and 2010) assessed extracellular matrix (ECM) formation in two types of chitosan-based scaffolds, using bovine articular chondrocytes (BACs). More specifically, the effects of scaffolds porosity, pore size and morphology, on the formation of chondrogenic tissues were evaluated. Compression moulding and salt leaching were utilised to produce chitosan-poly(butylene succinate) scaffolds with different porosities and pore sizes. Next, BACs were seeded onto the scaffolds and cultured in static or dynamic conditions for 4 weeks. Both materials permitted good cell attachment and the articular chondrocytes were able to secrete ECM. Proteoglycans and collagen type II production were enhanced in large pores with random geometry but pore structure had the opposite effect on GAG production. Notably, dynamic culture conditions improved GAG production in both types of scaffold.

While porous scaffolds have been established to allow mesenchymal stem cell differentiation into chondrogenic lineages, hydrogels are being increasingly studied because they permit minimally invasive implantation (Garg et al, 2012; Hong et al, 2007). (Richardson et al, 2008) investigated temperature-sensitive chitosan-glycerophosphate hydrogels for invertebral disk repair. Gels were seeded with mesenchymal stem cells before gene expression analysis for chondrocytic-cell marker genes, demonstrated differentiation of MSCs to an articular chondrocyte phenotype. Further, differentiated cells lacked the expression of osteogenic or hypertrophic markers and cells secreted both proteoglycans and collagens.

The ability of chitosan to bind negatively charged molecules has been exploited to produce advanced scaffolds for tissue regeneration. One group designed novel porous chitosan scaffolds intended to enhance chondrogenesis, with the ability to release transforming growth factor-β1 (TGF-β1)(Kim et al, 2003). First, an emulsion method was used to load chitosan microspheres with the growth factor. Then the spheres were used to fabricate porous chitosan scaffolds. Finally, chondrocytes were seeded and the results showed that the chitosan scaffolds permitted good cell proliferation and production of extracellular matrix.

2.5.5.3 Chitosan in Osteochondral Regeneration

Even though chitosan has been demonstrated to support chondrogenic lineages, osteochondral constructs made purely from chitosan are rare. This could be explained by the fact that the osteogenic response in chitosan is significantly improved when the polymer is combined with ceramics, such as calcium phosphates.

The most popular method for fabricating osteochondral constructs involves bi-layered structures with the ability to support osteogenesis and chondrogenesis, simultaneously.

This is achieved by providing microenvironments tailored to each lineage. Furthermore, scaffolds for osteochondral regeneration are generally biphasic by incorporating composite materials.

(Abarrategi et al, 2010) investigated the effects of chitosan molecular weight, degree of deacetylation, and calcium content on osteochondral repair. The researchers prepared porous chitosan scaffolds, and implanted them into rabbit knee osteochondral defects. The results were varied depending on the properties of chitosan used. Notably, chitosan with the lowest molecular weight (11.49 KDa), and lowest deacetylation degree (83%), and intact mineral content, allowed both subchondral bone and cartilaginous tissue regeneration. The results prove that scaffolds made purely from chitosan are suitable for osteochondral repair.

In 2006, another group developed novel hydroxyapatite-chitosan bi-layered scaffolds for osteochondral applications by combining sintering and a freeze-drying techniques (Oliveira et al, 2006). The scaffolds produced contained open inter-connected pores in the range of 50-350 μm. There was no evidence of material-induced cytotoxicity, while goat bone marrow cells were able to adhere and proliferate. Osteogenesis was identified in the hydroxyapatite layer after 14 days and chondrogenesis was detected after 21 days. Notably, the researchers did not attempt to attain both lineages within the same construct and there are no mechanical tests.

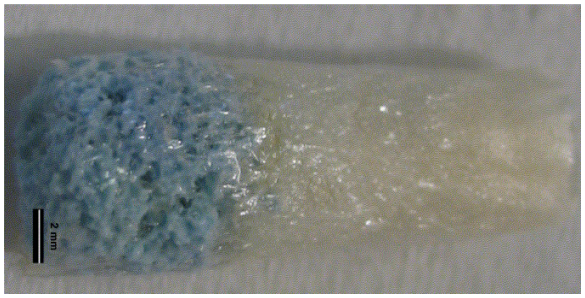

Figure 2.12 Hydroxyapatite-chitosan composite scaffold produced by Oliveira et al. Image taken from (Oliveira et al, 2006).

(Malafaya & Reis, 2009) produced bi-layered chitosan scaffolds using a particle aggregation method. More specifically, scaffolds were made with one side wholly chitosan and the other side containing a composite of 80% chitosan and 20% hydroxyapatite. The results showed that the developed scaffolds were highly inter-connected and contained suitable pore sizes for osteochondral applications.
Wet scaffolds were mechanically stable under dynamic compression and the composites had a Young's modulus of 6.26 MPa. Crucially, scaffolds had distinct regions of chondrogenic and osteogenic cell lineages after differentiation in a perfusion bioreactor system. Risks of delamination were alleviated due to the nature of the particle aggregation method used.

2.6 Bioreactors

The success of tissue engineering will depend on the ability to translate and scale-up research in a safe, reproducible and cost effective manner (Langer & Vacanti, 1993). Engineering of tissues necessitates the use of bioreactors, even for small-scale applications, as such systems allow for important parameters to be optimised. Bioreactors permit biological or biochemical processes to happen under tightly controlled conditions, with high degrees of reproducibility, control and automation (Hutmacher, 2000). Furthermore, bioreactors can improve *in vitro* 3D cultures by providing efficient cell nutrition and environmental stimuli, for controlled cell behavior.

2.6.1 Bioreactor Design

Bioreactors should create *in vitro* environments that are able to support fast and systematic tissue development (Martin et al, 2007). The ultimate characteristics of bioreactor systems include (Martin & Vermette, 2005):

- The ability to support mass transfer between cells and their environment via efficient nutrient supply and waste removal.
- Robust control of environmental variables, including temperature, pH, osmolality and oxygen content.
- Physiologically relevant signaling, including shear stress, compression and stretch.

From all the factors listed above, mass transfer has proved to be the most difficult to achieve and this has limited the potential to develop highly cellularised and vascularised tissues *in vitro*. Oxygen content is principal in extracellular matrix production. However, in terms of osteochondral applications there are discrepancies in the literature.

This is because cartilage has been produced in both high and low oxygen environments (Lennon et al, 2001). Mechanical stimulation can also promote tissue regeneration, and shear stress has been identified as the most important signal for mechanotransduction (Wang et al, 1993).

2.6.2 Types of Bioreactors

Bioreactors are designed depending on their intended application and each focuses on improving cell seeding, mass transfer or to provide external stimuli. The advantages and disadvantages of each of the major systems will be discussed.

2.6.2.1 Spinner Flasks

Issues with low seeding efficiencies and uneven cell distribution during static seeding of cells onto scaffolds, have been alleviated through the use of spinner flasks (Vunjak-Novakovic et al, 1998). Spinner flasks provide well-mixed environments, which allow for improved cell seeding and extracellular matrix production (Sikavitsas et al, 2002). Furthermore, this system is simple to use and results are reproducible. The size of tissue-engineered constructs can be a limitation for spinner flasks because mass transfer is not very efficient at low stirring rates. Turbulent flow as a consequence of faster spin speeds can lead to detrimental shear stress (Kurosawa, 2007).

2.6.2.2 Perfusion

Static culture of 3D scaffolds can cause the formation of necrotic cores and the subsequent failure of tissue engineered constructs (Martin et al, 2004). Perfusion bioreactors overcome this limitation by providing medium flow through the cores of scaffolds. More efficient nutrient transfer and hydrodynamic stimulation can improve cell proliferation and differentiation (Bilgen & Barabino, 2007). Furthermore, pulsatile perfusion has been shown to enhance osteogenic differentiation and mineralisation (El Haj & Cartmell, 2010). Interestingly, perfusion flow also creates cell alignment that can be important for tissue function, especially in cartilage (Temenoff & Mikos, 2000).

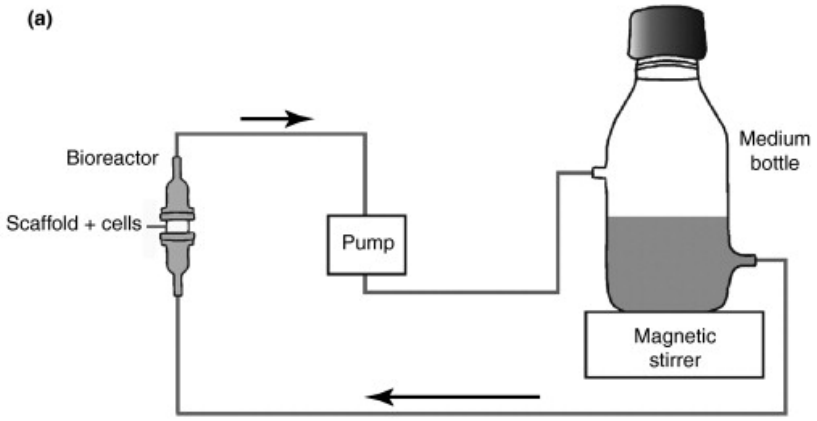

Figure 2.13 Perfusion bioreactor system suitable for cartilage tissue engineering using porous cell-seeded scaffolds. Image adapted from (Mahmoudifar & Doran, 2012).

2.6.2.3 Pulsatile Flow

Tissue engineering of vascular tissues is dependent on the ability of bioreactors to provide pulsatile forces, which mimic the *in vivo* environment. Vascular grafts have been produced using pulsatile perfusion bioreactors from marine collagen-PLGA fibres (Jeong et al, 2007; Jeong et al, 2005). The pulsatile perfusion system improved smooth muscle cell and endothelial cell proliferation, and alignment. Immunohistochemical analyses indicated the expressions of smooth muscle α-actin and myosin. Furthermore, endothelial cell nitric oxide was up regulated in constructs exposed to the hydrodynamic stimuli.

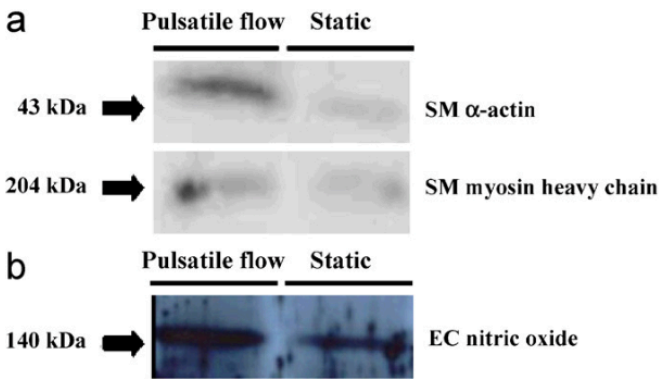

Figure 2.14 Development of vascular tissues in a pulsatile perfusion bioreactor system. Western blot analysis for (A) smooth muscle α-actin and myosin heavy chain and (b) endothelial cell nitric oxide in tissues engineered under static and pulsatile flow conditions Image adapted from (Jeong et al, 2007).

2.6.2.4 Rotating-Wall Vessels

Although shear stress is desirable for many tissue types it can also be damaging to others. For this reason, rotating-wall vessel bioreactors were first developed by NASA to provide minimal shear (Granet et al, 1998)(Figure 2.14). This bioreactor system is designed to balance gravitational, centrifugal and drag forces, while offering high mass transfer and limited shear stress (Schwarz et al, 1992; Unsworth & Lelkes, 1998). One disadvantage of rotating-wall vessels includes the fact that tissue growth is often non-uniform. In addition to this, prolonged exposure to centrifugal force can be detrimental to tissues, cell attachment and matrix deposition (Begley & Kleis, 2002).

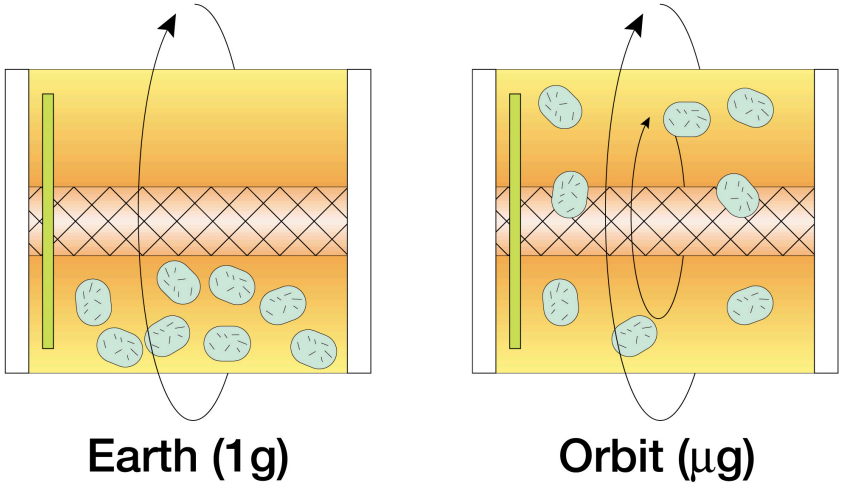

Figure 2.15 Rotating-wall bioreactors developed by NASA. This bioreactor system is designed to balance gravitational, centrifugal and drag forces, while offering high mass transfer and limited shear stress. Tissue constructs are cultured in microgravity environments. Image adapted from https://mix.msfc.nasa.gov/IMAGES/HIGH/0101761.jpg

2.6.2.5 Bioreactors for Osteochondral Constructs

Tissue engineering is principally focused on generating single tissue types, however this is inadequate for more complex repairs where stratified tissues are required (Bhumiratana & Vunjak-Novakovic, 2015; Mikos et al, 2006; Mosher et al, 2015). This is particularly important for developing osteochondral constructs, which contained both articular cartilage and subchondral bone. This aim can be achieved with the design of novel bioreactor systems capable of distinguishing between the different environments necessary to culture two tissues simultaneously.

The most popular bioreactors for osteochondral constructs are based on a double-chamber perfusion design, with individual chambers for bone and cartilage. (Malafaya & Reis, 2009) produced a double chamber system with the capacity for culturing six osteochondral constructs at the same time (Figure 2.15). The bioreactor setup proved to be successful with individual culture media for each tissue type. Furthermore, each compartment was separated by a silicon septum.

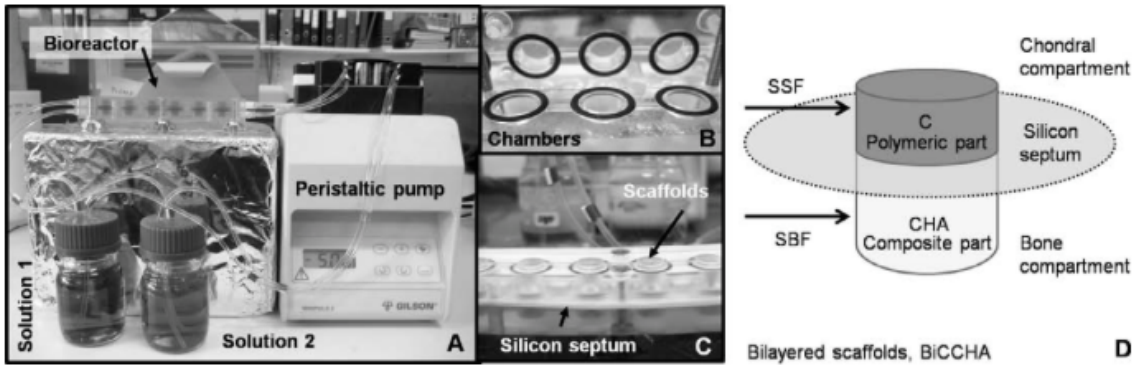

Figure 2.16 Double-chamber perfusion system for osteochondral constructs. Malafaya et al. designed this bioreactor system, to provide individual compartments and culture environments for bone and cartilage within a single scaffold. Image taken from (Malafaya & Reis, 2009).

A similar double-chamber system was utilised by (Gottardi et al, 2014). However, this setup allowed for high throughput culture via a bioreactor platform for the simultaneous culture of 96 osteochondral constructs (Figure 2.16). In addition to this study, there are a number of other research groups that have achieved independent culture of osteoblasts and chondrocytes within single-unit scaffolds, simultaneously (Chang et al, 2004; Kuiper et al, 2014; Liu & Jiang, 2013; Pei et al, 2014).

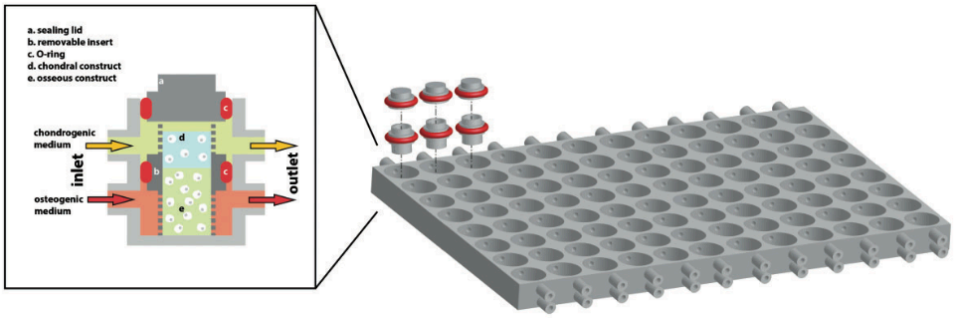

Figure 2.17 96-well Double-chamber perfusion system for osteochondral constructs. Image taken from (Alexander et al, 2014).

A more advanced bioreactor for osteochondral constructs was designed by (Haasper et al, 2009). Here, perfusion and mechanical stress could be applied at different frequencies to different parts of the scaffold. More specifically, the bioreactor was able to apply cyclic mechanical stretching to bone regions and cyclic compressive loading to cartilage regions (Haasper et al, 2008). The setup improved the commitment of mesenchymal stem cells to osteochondral lineages.

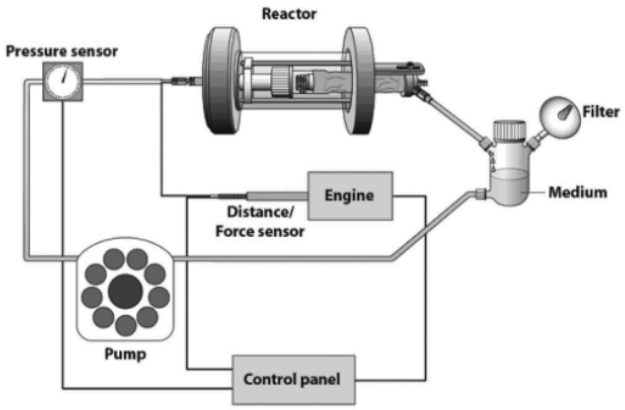

Figure 2.18 Cyclic-perfusion system for osteochondral repair, developed by Haasper et al. The bioreactor contains a chamber to enclose the construct. A peristaltic pump provides perfusion flow, while an electric engine drives cyclic mechanical loading. Image taken from (Haasper et al, 2008).

2.7 Project Aims

The overall aim of this project was to explore a model, and possible alternative therapy for osteochondral injuries. This literature review has discussed the background behind designing tissue-engineered scaffolds for this application. In producing osteochondral constructs, particular attention has to be applied to the biomaterial properties and architecture, as well as the cell source used.

At present, the most common approach for producing osteochondral constructs involves the culture of individual scaffolds for bone and cartilage. Scaffolds are then joined through the use of sutures or fibrin glue. Unfortunately, these constructs often fail due to delamination. A solution to this problem involves the production of a single scaffold with the capacity to maintain two different cell lineages simultaneously. Furthermore, a scaffold with these properties would allow the use of a single cell source, such as mesenchymal stem cells.

Tissue constructs made from chitosan, represent such a therapeutic strategy because they have been demonstrated to support the differentiation of human mesenchymal stem cells into both osteoblast and chondrocyte lineages. The current project intends to overcome limitations associated with specific differentiation media requirements for each lineage by providing scaffolds with spatially resolved environments, each supportive of one of these osteochondral lineages. More specifically, the understanding that scaffold pore size can regulate stem cell differentiation will be exploited.

Additionally, osteochondral differentiation will be enhanced through the use of a perfusion bioreactor system. This type of bioreactor has been widely used for the development of osteochondral constructs although published setups often rely on culturing separate scaffolds for bone and cartilage. This project will use a perfusion system that is capable of housing a single material scaffold, and still achieve osteogenic and chondrogenic lineages.

3. Materials and Methods

This section is dedicated to the materials and methods utilised throughout this whole research project. Section 3.2 describes the osteogenic differentiations of mesenchymal stem cells, and the subsequent analyses and quantifications. Section 3.3 describes the same aspects in chondrogenic differentiation. Sections 3.4 and 3.5 center on serum content analysis and polymerase chain reactions, respectively. Section 3.6 describes the use of ELISA to quantify osteocalcin expression. Sections 3.7-3.9 outline the protocols for the fabrication of bi-layered chitosan scaffolds. 3D culture in a perfusion bioreactor is summarised in Section 3.10. Section 3.11 describes the statistical analysis applied.

3.1 Cell Culture and Analysis

Immortalised bone marrow-derived human mesenchymal stem cells (hMSCs) (Sottile et al., 2003) and primary MSCs (Lonza) were maintained in a monolayer culture, stored in a humidified atmosphere at 37 ºC and 5% CO_2. Cells were typically grown in standard medium consisting of low glucose Dulbecco's Modified Eagle Medium (DMEM), 1% (v/ v) L-Glutamine, 1% (v/v) non-essential amino acids (NEAA) and 1% (v/v) antibiotics/ antimycotics (Invitrogen, UK), supplemented with either 10% (v/v) foetal calf serum (SC+FCS) (Invitrogen, UK) or with human serum (SC+HS) (Lonza). Cells were passaged using trypsin/ EDTA (Invitrogen, UK), see (Sottile et al., 2003), and routinely split 1:4. Human embryonic kidney (HEK) 293 and NTERA carcinoma cells lines were cultured under the same conditions.

3.1.1 Cryopreservation and Thawing

After trypsinisation and centrifugation, cell pellets were resuspended in 1:1 combination of culture media to freeze mix (80 % (v/v) culture media with serum, and 20 % (v/v) DMSO). Cell suspensions were transferred to sterile cryotubes and stored at -80 ºC overnight. Tubes were then moved to liquid nitrogen for long-term storage.

Frozen cells were thawed in a 37 ºC water bath for less than 1 minute. DMSO was neutralised with culture media and the thawed cell suspension was centrifuged at 200 g for 5 minutes. Cell pellets were resuspended in fresh culture media and stored in a humidified atmosphere at 37 ºC and 5% CO_2.

It was important to ensure 80% confluency prior to the first passage. Cells were passaged at least twice after freezing before differentiation experiments were started.

3.1.2 Plate Coatings for Cell Attachment

Tissue culture plastic plates were coated to ensure constant cell attachment during 14 and 21-day differentiation experiments. Rat tail Collagen I (Life Technologies) was diluted in 0.02 M acetic acid to a working concentration of 50 µg/ ml. Plates were incubated at room temperature with collagen for 1 hour. Coated-plates were then washed 3 times with PBS before immediate use or stored in the fridge for future use.

Plates can also be coated with fibronectin from bovine plasma (Sigma). Stock fibronectin was diluted in PBS to 50 µg/ ml. Tissue culture plastic was then incubated with fibronectin for 45 minutes before immediate use.

Matrigel^{TM}-coating (BD Bioscience) was achieved by diluting the stock extracellular matrix gel (500X) in cold Dulbecco's Modified Eagle Medium (DMEM). Plates were incubated with Matrigel^{TM} at room temperature for 15 minutes before use.

For gelatin coating (Life Technologies), stock gel from the fridge was liquefied at 37 ºC. Afterwards gelatin was diluted in PBS to a working concentration of 0.1%. Plates were incubated at room temperature for 1 hour, and then washed 3 times with PBS before use.

Mouse laminin I (Trevigen) was diluted in cold DMEM to a working concentration of 1-2 µg/ ml. Plates were incubated at 37 ºC with laminin for 4 hours. Coated-plates were then washed 3 times with PBS and used straight away.

3.2 Osteogenic Differentiation

Human MSCs were seeded into 24-well plates at a concentration of $2x10^4$ cells/ ml and allowed to attach for 24 hours in standard culture (SC) medium with FCS before differentiation was initiated. Furthermore, cells were seeded on Matrigel^{TM}-coated (BD Bioscience) tissue culture vessels to improve adhesion during osteogenic differentiation.

Osteogenic differentiation of hMSCs was assessed at various time-points following the replacement of the SC+FCS medium with one of the following treatments:

(1) OS+FCS (osteogenic medium containing FCS): (DMEM) supplemented with 10% (v/v) FCS, 1% (v/v) L-Glutamine, 1% (v/v) non-essential amino acids (NEAA), 1% (v/v) antibiotics/antimycotics, dexamethasone (0.1 μM), ascorbic acid phosphate (50 μM), and β-glycerophosphate (10 mM) (Sigma-Aldrich).
(2) OS+HS (osteogenic medium containing human serum): same as (1) but with HS instead of FCS.
(3) OS 5-Day serum (osteogenic supplements with no FCS or HS). Cells were treated with OS+FCS or OS+HS for the first 5 days before switching to OS without serum.
(4) SC+FCS (SC medium with FCS used as an undifferentiated control).
(5) SC+HS (SC medium with HS used as an undifferentiated control).
(6) SC 5-Day serum (SC medium with no FCS or HS used as a serum-free control). Cells were treated with SC+FCS or SC+HS for the first 5 days before switching to SC without serum.

Six independent wells were cultured for each condition per assay, and the medium was changed every 3 days for 14 or 21 days, depending on the experiment.

3.2.1 Flow Cytometry

Human MSCs were characterised by assessing the expression of MSC-specific surface markers using CD29 (Abcam), CD90 (eBioscience), CD105 (AbD Serotec) and SSEA4 (eBioscience) antibodies. Cells were harvested as described in section 3.1, and 1 ml of cell suspension was added to each Fluorescence Activated Cell Sorting (FACS) tube. The tubes were centrifuged at 200 g for 5 minutes, the supernatant was discarded and 5 μl of antibody was added to suspend the cells. Solutions were incubated at room temperature in the dark for 30 minutes, followed by the addition of 2 ml of medium to wash away unbound antibody. Tubes were centrifuged again for 5 minutes before pellets were re-suspended in 1 ml of fresh medium, and samples were stored on ice in the dark until analysis using a Beckman Coulter FC500 flow cytometer.

3.2.2 Phalloidin Stain for Actin Filaments

Phalloidin is a bicyclic peptide belonging to a family of toxins isolated from the deadly *Amanita phalloides* “death cap" mushroom. The peptide is commonly used in imaging applications to selectively label filamentous actin. The phalloidin vial (Life Technologies) was dissolved in 1.5 ml methanol to yield a final stock concentration of 6.6 µM. After the culture period, cells were washed twice in PBS and fixed in ice cold 4% paraformaldehyde for 15 minutes. Samples were washed twice with PBS before a 0.1% Triton X-100 solution was used for 5 minutes to permeate the cells further. Samples were washed twice with PBS before 205 µl of phalloidin stain was applied to each slide (5 µl phallotoxin stock diluted with 200µl PBS). Slides were incubated with the stain in the dark for 20 minutes. Finally, samples were washed twice with PBS and mounted onto microscope slides, using Vectashield mounting medium containing DAPI (Vector Laboratories). Staining was observed using fluorescent light microscopy.

3.2.3 Apoptosis Assay

The percentage of live, apoptotic and necrotic cells after 14 days of osteogenic differentiation with FCS or HS was determined using a commercially available Annexin-V-FLUOS staining kit (Roche). Manufacturer’s instructions were followed. In short, cells were washed in PBS, centrifuged at 200 g for 5 minutes and pellets were re-suspended in 100 µl Annexin-V-FLUOS labeling solution. After 15 minutes of incubation, cells were analysed using a Beckman Coulter FC500 flow cytometer.

3.2.4 PrestoBlue™ Cell Metabolic Assay

Cell metabolic activity/ viability was determined using a PrestoBlue™ assay (Invitrogen, UK) after 7 days of culture. The assay incorporates a fluorometric/ colourimetric oxidation-reduction (REDOX) indicator, known as resazurin (O'Brien et al, 2000). In brief, culture medium was aspirated and monolayers were washed with 37 °C PBS. 500 µl of warm PrestoBlue™ working solution (10% v/v PrestoBlue™ stock solution, 90% v/v Hanks Balanced Salt Solution (HBSS)) was transferred to each well. Three empty wells were filled as blanks, and the plate was incubated at 37 °C, 5% CO_2 for 35 minutes.

The plate was then wrapped in aluminum foil and agitated on a plate shaker for 10 minutes. 100 µl triplicates of the PrestoBlue™ solution per culture well were transferred to a 96-well plate and the fluorescence was measured at 560 nm excitation and 590 nm emission, using a Tecan Infinite 200 micro-plate reader. Subtracting the average fluorescence values for blank wells from culture well values eliminated background signals.

3.2.5 Hoechst 33258 DNA Assay

Cell proliferation was determined by assaying for total DNA contents after the 21-day culture period, as previously described (Rashidi et al, 2012). The fluorochrome Hoechst 33258 (Sigma-Aldrich, UK) binds cellular DNA resulting in enhanced fluorescence, which is directly proportional to the DNA content. To lyse the cells, the culture medium was replaced with 1 ml sterile dH_2O, and the well plate was stored at -20 ºC. Once frozen, the well plate was placed into the incubator at 37 °C to thaw, and the cycle repeated 3 times. Aliquots of 100 µl from each well were transferred to a 96-well plate, along with 100 µl Hoechst stain (10mg/ ml in dH2O) used at a working dilution of 1:50 in TNE buffer (10 mM Tris (hydroxymethyl) methylamine, 1 mM EDTA and 2 mM NaCl in distilled water, pH 7.4). The plate was gently agitated in the dark and fluorescence was measured at 360 nm excitation and 460 nm emission, using a Tecan Infinite 200 micro-plate fluorescence reader. A standard curve of DNA was produced using known concentrations of DNA from calf thymus (Sigma-Aldrich, UK) reconstituted in 0.01 M NaCl to a concentration of 20 µg/ ml.

3.2.6 PicoGreen DNA Assay

The fluorochrome PicoGreen (Life Technologies) is a more sensitive alternative to Hoechst dye. PicoGreen binds cellular DNA resulting in enhanced fluorescence, which is directly proportional to the DNA content. To lyse the cells, the culture medium was replaced with 1 ml sterile dH_2O, and the well plate was stored at -20 ºC. Once frozen, the well plate was placed into the incubator at 37 °C to thaw, and the cycle was repeated 3 times. The stock PicoGreen reagent was diluted 200-fold in 1X dilution buffer. Aliquots of 100 µl from each well were transferred to a 96-well plate, along with 100 µl 1X PicoGreen reagent.

The plate was gently agitated in the dark for 5 minutes. Fluorescence was measured at 480 nm excitation and 520 nm emission, using a Tecan Infinite 200 micro-plate fluorescence reader. A standard curve of DNA was produced using known concentrations of lambda DNA (Invitrogen).

3.2.7 Alizarin Red Staining and Quantification

After 14 days and 21 days of culture, cells were fixed using 4% paraformaldehyde (PFA) for at least 20 minutes. Wells were washed three times with PBS and 1 ml of 1% aqueous Alizarin red solution (Sigma-Aldrich) was added per well. Alizarin red was used to stain for calcium phosphate deposits in mineralised bone nodules. Briefly, the plate was incubated at room temperature for 10 minutes with occasional agitation. Following the incubation period, wells were washed with distilled water until all excess stain had been removed (Gregory et al., 2004).

Bone nodules were viewed using a phase contrast microscope. Quantification of Alizarin red staining was attained using a de-stain solution (20% methanol, 10% acetic acid in dH_2O) (Tataria et al., 2006). Plates were treated in the de-stain solution for 15 minutes with gentle agitation on a plate shaker and the Alizarin red concentrations per well were determined by measuring the absorbance at 405 nm using a Tecan Infinite 200 micro-plate reader.

3.2.8 Von Kossa Staining

Von Kossa staining was used to quantify mineralisation in osteogenic cell cultures and tissue sections from the bioreactor differentiations. The main principle behind the stain is a precipitation reaction in which silver ions react with phosphate (not calcium) in the presence of acidic material. Photochemical degradation of silver phosphate to silver then occurs under light illumination. In brief, samples were fixed in 4% PFA and washed three times with dH_2O. Osteogenic sections were then covered with a 1% silver nitrate solution (Sigma) and placed under a UV light source. It was important to ensure that all wells were exposed before samples were covered with aluminium foil. During UV exposure, samples were inspected every 10 minutes for brown/ black nodule staining. This can take up to 1 hour for weakly mineralised samples. Afterwards, the silver nitrate solution was removed and disposed of in the appropriate toxic waste container.

Samples were washed three times in dH_2O, before a 2.5% sodium thiosulphate solution (Sigma) was added. Samples were incubated for 5 minutes in the dark and thoroughly washed with dH_2O. Bone nodules were viewed using a brightfield microscope. Alizarin red staining has to be performed after Von Kossa staining to avoid photo bleaching of the red dye during incubations.

3.2.9 Immunocytochemistry

Cells were fixed in ice-cold 4% PFA for 15 minutes and washed in PBS + 0.1% Tween20 (PBT) for 10 minutes. Non-specific antibody binding was blocked via incubation for 1 hour with 1X Animal-Free Blocker™ (SP-5030) (Vector Laboratories) in PBT. Cells were then exposed to the primary antibody (bone-specific alkaline phosphatase antibody (B4-78) from DSHB; osteocalcin antibody (ab13418) from Abcam) at a dilution of 1:200 in PBT and stored at 4 ºC overnight. Next, samples were washed three times in PBT at 15 minute intervals, and the cells were incubated with a 1:200 dilution of Texas red-conjugated secondary antibody (Vector Laboratories) for 1 hour in the dark. Unbound secondary antibody was removed by washing four times in PBS for 15 min each. The samples were finally mounted onto microscope slides, using Vectashield mounting medium containing DAPI (Vector Laboratories) and analysed using fluorescent light microscopy.

3.2.10 Alkaline Phosphatase

Alkaline phosphatase (ALP) enzyme activity was used as a marker for early osteogenic differentiation (Mastrogiacomo et al., 2005), using a commercially available enzyme immuno assays kit (SIGMAFAST™ p-Nitrophenyl phosphate tablets from Sigma-Aldrich). Manufacturer's instructions were followed. Briefly, wells were washed twice with warm PBS and 200 µl of p-Nitrophenyl phosphate substrate solution was added to each well. The plate was incubated in the dark for 30 minutes at room temperature before 100 µl duplicates of the p-Nitrophenyl phosphate substrate solution per culture well were transferred to a 96-well plate. The absorbance for the reactions was read at 405 nm using a Tecan Infinite 200 micro-plate reader and 1:5 dilutions were required for readings outside the range of the plate reader. Untreated p-Nitrophenyl phosphate solution was added to three wells and these absorbance readings were used as blanks.

3.3 Chondrogenic Differentiation

Human mesenchymal stem cells were grown in T175 flasks until the required number of cells were achieved. Cells were trypsinised for 30 seconds and washed in standard culture media (20 ml per T175 flask). After 5 minutes of centrifugation at 200 g, pellets were re-suspended in chondrogenic medium without TGF-β ($5x10^6$ MSCs per ml). 200 µl of cell the suspension was added per well of a V-bottom 96-well plate. Plates were centrifuged for 5 minutes at 1000 g, before pellets were re-suspended in 200 µl chondrogenic medium with TGF-β. A final 5-minute centrifugation at 1000 g was used to condense the cells and begin chondrogenic pellet formation. Plates were then cultured at 37 ºC, 5% CO_2.

Chondrogenic differentiation of hMSCs was assessed at various time-points following the replacement of the SC+FCS medium with one of the following treatments:

(1) CHO (serum-free chondrogenic medium): high glucose (4.5 g/ L) DMEM supplemented with 1% (v/v) L-Glutamine, 1% (v/v) non-essential amino acids (NEAA), 1% (v/v) antibiotics/antimycotics, dexamethasone (0.1 µM), ascorbic acid phosphate (50 µM), sodium pyruvate (1 mM), proline (40 µg/ ml), 1X insulin-transferrin-selenium (ITS) and TGF-β (10 mM) (Life Technologies PHG9204).

(2) CHO 5-Day serum (chondrogenic supplements with 10% FCS or HS). Cells were treated with CHO+FCS or CHO+HS for the first 5 days before switching to CHO without serum (1).

(3) SC 5-Day serum (SC medium with no FCS or HS used as a serum-free undifferentiated control). Cells were treated with SC+FCS or SC+HS for the first 5 days before switching to SC without serum.

Six independent pellets were cultured for each condition per assay, and the medium was changed every 2 days for 14 or 21 days, depending on the experiment.

3.3.1 Papain Digest and DMMB GAG Assay

After the differentiation period, chondrogenic pellets were washed with PBS to remove any culture media. 100 µl dH_2O was added to each well and plates were freeze-thawed three times.

The proteolytic enzyme papain was used to solubilise cell pellets further and allowed the dissociation of sulphated glycosaminoglycans (GAGs) from other glycoproteins. Samples were incubated with 100 µl papain solution for 24 hours at 60 °C (0.1% papain (Sigma-Aldrich): papain buffer (sodium phosphate 0.1 M, cysteine hydrochloride 0.005 M, EDTA 0.005 M and dH_2O)). The pH of the papain solution was adjusted to pH 6.5 using 1 M HCl or NaOH as appropriate. Plates were sealed with parafilm to prevent evaporation. Papain solution without cells was also incubated as a control solution of heat-treated papain.

DMMB (1,9-dimethylmethylene blue) is a cationic dye that binds to sulphate and carboxylate groups within GAGs, to produce a concentration dependent colour change. 50 µl aliquots of papain-digested pellets were transferred to clean 96-well plates and 50 µl of DMMB solution (Sigma-Aldrich) was added to each sample. Wells were mixed well and the absorbance for the reactions was measured at 525 nm using a Tecan Infinite 200 micro-plate reader. It was important to quantify the absorbance immediately because the GAG-DMMB complex is not stable in solution.

3.3.2 Haematoxylin and Safranin-O Staining

Chondrogenic pellets were processed and embedded in paraffin wax (see Sections 3.10.4-3.10.5). To prepare pellet sections for histological staining analysis, paraffin wax was removed by immersing slides in Histoclear™ for 10 minutes. This was repeated twice. The sections were then rehydrated in a decreasing methanol gradient (MeOH: 100% [v/v] x 2, 75% [v/v], 50% [v/v] and 25% [v/v]). Pellet sections were rinsed with dH2O. Sections were then incubated in Mayer's haematoxylin for 5 minutes and rinsed under running tap water, until blue cell nuclei were visible. Slides were then immersed in a 0.1% Safranin-O solution for 10 minutes to stain for proteoglycans in cartilage. Samples were then dehydrated through an increasing methanol gradient (MeOH: 25% [v/v], 50% [v/v], 75% [v/v] and 100% [v/v] x 2). Finally, sections were cleared in xylene and mounted using DPX. Staining was observed under a brightfield microscope.

3.4 Biochemical Serum Analysis

In order to test for batch variability, as well as fundamental differences in fetal calf serum and human serum, 10 ml samples were sent to the Clinical Pathology lab at the Queen's Medical Centre, Nottingham. Samples were analysed for the content of 1,25-dihydroxyvitamin D, albumin, alkaline phosphatase, calcium, cortisol, glucose, insulin and phosphate.

3.5 RT-PCR

3.5.1 RT-PCR Primers

Primers used for PCRs were purchased from Eurofins MWG, Germany and are detailed in Appendix 2. Specific primers were used for bone-specific alkaline phosphatase and osteocalcin. Collagen II primers were designed for validation of chondrogenic samples. Clathrin was used as a positive control.

3.5.2 RNA Extraction

Cell suspensions were homogenised in TRI-reagent (Sigma) at a concentration of 1-5x10^6 cells per 0.5 ml. This allowed for DNA, RNA and proteins to be released from cells. The homogenised cultures were left at room temperature for 5 minutes before 0.1 ml aliquots of chloroform were added per 0.5 ml TRI-reagent. Samples were mixed vigorously through shaking before they were left to stand at room temperature for 15 minutes. Next, centrifugation at 12,000 g for 15 min at 4 °C allowed the mixture to be separated into 3 phases: a red organic phase containing protein, an interphase containing DNA, and a colourless upper (aqueous) phase containing RNA. The upper aqueous phase was carefully transferred to a clean 2 ml tube and at this stage; the volume of the aqueous phase was measured.

A column-based RNA Clean & Concentrator^{TM}-25 kit (Zymo Research) was used to purify the RNA from phenol residues left behind from the TRI-reagent.
2 volumes of RNA Binding Buffer were added to each volume of RNA sample. The minimal recommended sample volume was 50 µl and samples with a volume less than this were adjusted with RNase-free water. 1 volume of ethanol (95-100%) was added to the RNA-RNA Binding Buffer mixture (e.g. 150 µl ethanol to 150 µl mixture). The mixture was then transferred to a Zymo-Spin^{TM} II Column in a Collection Tube and centrifuged at ≥12,000 g for 1.5 minutes.

The flow-through was discarded and 400 µl RNA Preparation Buffer was added to the column before it was centrifuged at ≥12,000 g for 1.5 minutes. Again, the flow-through was discarded and 800 µl RNA Wash Buffer was added to the column. The column was centrifuged at ≥12,000 g for an additional 1 minute and the flow-through was replaced with 400 µl RNA Wash Buffer. Then, the Zymo-Spin™ II Column was centrifuged in an emptied Collection Tube at ≥12,000 g for 2 minutes. The column was carefully removed from the Collection Tube and transferred to a RNase-free tube. 25 µl RNase-free water was added directly to the column and left to stand for 4 minutes at room temperature. Finally, the tube was centrifuged at 10,000 g for 1 minute before the eluted RNA was used immediately or stored at -80 °C.

RNA content was quantified in each sample using spectrophotometry. In brief, 1 µl of each sample was analysed using a Nanodrop™ instrument, at wavelengths of 260 nm and 280 nm. The 260 nm wavelength measured RNA and the 280 nm wavelength measured protein content. It was important that the ratio of the RNA: protein was around 2 because this was a good indicator of a pure RNA sample. Lastly, samples were then diluted for cDNA synthesis and reverse transcription with RNase-free water to a concentration of 10 µg/ µl.

3.5.3 cDNA Synthesis Using SuperScript III

RNA samples were diluted to a concentration of 15 µg RNA per 14 µl total volume. RNA aliquots were incubated with 2 µl 10X DNase Reaction Buffer and 2 µl DNase for 15 minutes at 25 °C. Afterwards, 2 µl of 25 mM EDTA (pH 8) was added to each sample and incubated for 10 minutes at 65 °C. This step was important to inactivate the DNase reaction. Each sample was then split into 2 aliquots (each 10 µl), one for the +RT sample and one for the –RT sample. Samples were stored on ice.

At this stage a primer master mix was prepared by mixing random primer (pdN15) with dNTPs (see manufacturers instructions for details). 7.9 µl of primer master mix was added to each sample and incubated at 65 °C for 5 minutes. Samples were then placed on ice while buffer master mix was prepared. The buffer master mix consisted of 5X First-Strand Buffer, 0.1 M DTT and dH_2O (see manufacturers instructions for details).

The buffer master mix was split into 2 for the +RT and –RT. 12.1 µl –RT buffer master mix was added to each of the –RT samples on ice. Distilled H_2O was added to the –RT buffer master mix instead of reverse transcriptase. Similarly, 12.1 µl +RT buffer master mix was added to each of the +RT samples on ice, however samples were supplemented with reverse transcriptase enzyme instead of dH_2O. Next, samples were thermocycler incubated for 10 minutes at 25 °C, 1 hour at 50 °C, then for a further 15 minutes at 70 °C. Finally, samples were cooled at 4 °C for 2 minutes. The cDNA was used directly as input for PCRs or stored at -20 °C.

3.5.4 Polymerase Chain Reaction

Polymerase chain reaction was used to amplify cDNA fragments. Firstly, a master mix was made and stored on ice (0.9 µl dNTP, 2 µl 10x PCR buffer, 0.6 µl $MgCl_2$, 0.15 µl Taq polymerase and 14.35 µl dH_2O per reaction). 1.5 µl of primer mix was added per sample. Importantly, separate mixes were made for individual primers. The cDNA, master mix and primers were centrifuged at 10,000 g for 1 minute to ensure that all the solution was at the bottom of the tube. The tubes were then placed in a Labnet Multigene PCR machine. The programme consisted of the following cycles: 95 °C for 5 minutes, then 30-40 cycles (dependent on primer) of 95 °C for 1 minute, 60 °C for 30 seconds and 72 °C for 1 minute. The final cycle was at 72 °C for 10 minutes. Samples were used immediately, or stored at -20 °C.

3.5.5 Gel Electrophoresis

A stock solution of 50X TAE buffer (242 g Tris base, 57.1 ml glacial acetic acid and 18.6 g EDTA diluted in 1 litre dH_2O) was diluted to 1X TAE with dH_2O. A 1% agarose gel was prepared by dissolving agarose powder in 1X TAE buffer. The mixture was heated in a microwave to fully dissolve the agarose, before it was allowed to cool down. Next, 1 µl of ethidium bromide (10 mg/ ml)(Sigma) per 25 ml of gel was added. The gel was cast in a gel tray with the appropriate comb, and allowed to set at room temperature. Once set, the gel was submerged in a gel tank containing 1X TAE buffer and the comb was carefully removed. To each individual well, 15 µl of PCR product was added with 3 µl of loading buffer. 3 µl of molecular weight marker was loaded as a reference sample. Finally, the tank was closed and run at 100V for 60 minutes. The gel was assessed under UV at 290 nm wavelength.

3.6 ELISA for Osteocalcin

An osteocalcin ELISA kit (Invitrogen, UK) was used to quantify osteocalcin concentrations after osteogenic differentiation of (primary) hMSCs. Manufacturer's instructions were followed. The assay uses monoclonal antibodies targetted against epitopes of human osteocalcin. Levels of labelled enzyme to antibody complexes are measured through a chromogenic reaction using tetramethylbenzidine. The assay is based on colorimetric absorbance of the sample, which is proportional to the human osteocalcin concentration. To lyse the cells, the culture medium was replaced with 1 ml sterile dH_2O, and the well plate stored at -20 ºC. Once frozen, the well plate was placed into the incubator at 37 °C to thaw, and the cycle repeated 3 times. 200 µl aliquots of samples, standards and controls were added to each well (well plate provided in kit). Next, each well was supplemented with 100 µl of Anti-OST-HRP conjugate and incubated in the dark at room temperature for 2 hours. After the incubation period, the solution was discarded and wells were washed 3 times with wash solution. Within 15 minutes of the washing, 100 µl of Stabilised Chromagen solution was added to each well. The plate incubated in the dark for a further 30 minutes at room temperature. After the incubation period, 100 µl of Stop Solution was added to each well. At this stage, the plate was agitated to encourage a colour change from blue to yellow. The absorbance was measured at 450 nm within 1 hour of adding the Stop Solution. Untreated Stabalised Chromogen solution was added to three wells and these absorbance readings were used as blanks. A standard curve was generated from the osteocalcin standards in the kit. This allowed the concentration of unknown samples to be calculated.

3.7 Scaffold Components

3.7.1 Clean-up of Heavy Metal Ions from Chitosan Powder

Chitosan was initially cleaned of heavy metal ions to reduce any possible cytotoxicity. A chitosan slurry was produced by dissolving 250 g of chitosan powder and ~1.5 litres of distilled H_2O. Glass wool was added to a filter column (to act as a sieve), before the chitosan slurry was poured into the column. Then, the column was topped-up with 1 M sulphuric acid and liquid was allowed to flow through the column, at 1 drop/ second. Next, the chitosan was treated with aqueous ammonia. After all liquid had passed through the column, the chitosan was collected and washed thoroughly with distilled H_2O, to remove any traces of sulphuric acid or ammonia. Finally, the chitosan was dried and ground to a powder.

3.7.2 Production of 4% Chitosan Solution

A 4% chitosan solution was prepared by adding 8 g of chitosan (degree of deacetylation 84%, MW: 471,000 Da)(Weifeng Kehai Ltd, China) to 200 ml of distilled H_2O. The solution was mixed using a magnetic stirrer until uniformly dispersed, before 5 ml of glacial acetic acid was added. The acetic acid aided the full dissolution of chitosan in the solution and allowed gelation. The chitosan was stirred manually for 10 minutes before it was covered in cling film and left in a fume hood overnight.

3.7.3 PCL Porogen

Polycaprolactone (PCL) (MW: 65 kDa)(Sigma-Aldrich) was used as the porogen for the chitosan scaffolds. The porosity of the scaffolds was controlled via the volume fraction and the sieved particle size of the PCL.

3.7.3.1 Granules

PCL flakes were ground to a powder in a stainless steel coffee grinder. Liquid nitrogen was added to crystallise the PCL and prevent the hot metal blades from melting the porogen (low melting temperature of ~60 °C). The ground powder was sieved through 180-300 μm and 300-425 μm aperture sieves to achieve particles suitable for the required pore sizes of the scaffold.

3.7.3.2 Microspheres

An alternative, emulsion method was also used to produce PCL microspheres as the porogen particles. First, a 0.3% polyvinyl alcohol (PVA) solution was prepared to act as an emulsion stabiliser, by dissolving 3 g of PVA (MW: 13-23 kDa, 87-89% hydrolysed) in 1 litre of distilled H_2O. The solution was stirred at 400 rpm overnight, before any un-dissolved granules were filtered. Afterwards, PCL (24% w/v) was dissolved in 20 ml of dichloromethane. The dissolved PCL was added drop-wise to 400 ml PVA solution and stirred at 400 rpm for 3 hours, and at room temperature. This allowed the dichloromethane to fully evaporate and leave PCL microspheres. The microspheres were thoroughly washed in deionised water, before they were freeze-dried for 24 hours. Finally, the PCL spheres were sieved, and 180-300 µm and 300-425 µm particles were collected. PCL outside these ranges was re-emulsified in dichloromethane and recycled in the method.

3.8 Scaffold Construction

3.8.1 Glutaraldehyde Cross-linking

After the 4% chitosan solution had gelled and become viscous, a cross-linking solution of 0.5% glutaraldehyde (Sigma-Aldrich) was prepared by diluting the 25% stock solution in distilled H_2O. For scaffold production, 20 g of chitosan was mixed with 10 g PCL porogen (300-425 µm granules or microspheres). 4 ml of 0.5% glutaraldehyde solution was added to the chitosan-PCL complex and stirred vigorously. The 300-425 µm mixture was then poured into a mould lined with cling film, and allowed to cross-link until the composite began to set. At this point, a second scaffold layer was prepared in the same way as the first, but 10 g of PCL (300-425 µm granules or microspheres) was replaced with 10 g of PCL (180-300 µm granules or microspheres). The second layer was gently poured onto the first layer and the whole construct was allowed to completely set, before it was covered and stored at -20 °C overnight (*Figure 3.1* illustrates the scaffold layering process).

The frozen composite structure was removed from the freezer and treated in a 1:1 solution of ethanol and aqueous ammonia. Importantly, the solution was pre-cooled to -20 °C before use. The chitosan in ethanol-aqueous ammonia was stored at -20 °C in an airtight container for 48 hours.

Afterwards, the chitosan construct was copiously washed in ethanol before it was left to dehydrate in an ethanol bath for two days at room temperature.

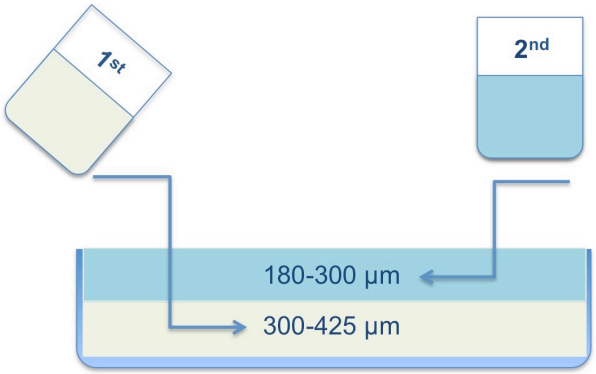

Figure 3.1 Layering of chitosan scaffolds. Mixing 4% chitosan solutions with PCL porogen particles at a 2:1 ratio produces scaffolds. Glutaraldehyde or genipin cross-linking agents are added before individual layers are pored into a mould. Note: The second layer is prepared once the first layer begins to set.

3.8.2 Genipin cross-linking

Chitosan scaffolds were also produced using an alternative, less cytotoxic cross-linking agent to glutaraldehyde. In brief, the method outlined in *3.8.1 Glutaraldehyde Cross-linking* was followed but 4 ml of 0.5% glutaraldehyde solution was replaced with 4 ml of 0.3% genipin (MW: 226.2, ≥98% purity)(Cambridge Bioscience, UK). The stock genipin crystalline powder was dissolved in ethanol. With genipin cross-linking, it was obvious when chitosan layers had started to set because the chitosan turned from yellow to blue in colour.

3.8.3 Porogen Extraction and L-glutamine Treatment

Individual scaffolds were cut out from the chitosan composite block using a 9 mm cork-borer. At this stage, 5 g of potassium hydroxide granules were dissolved in 200 ml ethanol. The mixture was magnetically stirred for 1 hour. The scaffolds were then immersed in the solution and incubated in an airtight container for 4 hours at 50 °C. Next, scaffolds were rinsed in ethanol and any cytotoxic, free aldehyde groups from the glutaraldehyde were tied up by soaking in cell culture-grade L-glutamine for 24 hours. Finally, the porous chitosan constructs were allowed to dry in a fume hood.

3.9 Characterisation of Chitosan Scaffolds

3.9.1 Porogen Particle Size Analysis

The size distribution of PCL porogen particles was assessed using a Malvern Mastersizer 3000 laser diffraction particle size analyser.

3.9.2 SEM Imaging

Scaffold pore size was determined by firstly mounting scaffold slices onto aluminum stubs. Then, the samples were platinum-coated for 90 seconds in argon using an Emscope SC500 sputtering coater. Samples were examined using a Philips XL30 electron microscope, at accelerating voltages between 10-20 KeV and spot sizes between 3-5.

3.9.3 Microcomputed Tomography

Microcomputed Tomography was used to determine the porosity of the chitosan scaffolds. Samples were placed in a 16 mm holder and scanned in a Scanco μCT 40, operated at 55 kV with a voxel resolution of 16 μm. For high resolution scans, a XRADIA Versa XRM-500 was used with a voxel resolution of 1 μm. The reconstruction threshold was set to 30.

3.9.4 Scaffold Compression Testing

The mechanical properties of porous scaffolds cross-linked with glutaraldehyde and genipin, were determined using a compression-testing machine (Instron Universal Testing Instruments, 5960 series). Compression properties data was analysed using Bluehill® 2 software. The test assessed the stress and strain of scaffolds at loads between 0-5 N. Scaffolds were tested dry, as well as after they were wetted in PBS for 2 hours. The compression test was performed at a rate of 1 mm per minute. Each type of scaffold was tested in triplicate. Finally, stress and strain data was used to calculate the Young's modulus of the chitosan scaffolds.

3.9.5 Scaffold Degradation Study

A degradation study of the chitosan scaffolds was conducted according to the standard BS EN ISO 10993-13 (2010). Scaffolds were placed individually into tubes.

The tubes were filled with 50 ml standard medium consisting of low glucose Dulbecco's Modified Eagle Medium (DMEM), 1% (v/v) L-Glutamine, 1% (v/v) non-essential amino acids (NEAA) and 1% (v/v) antibiotics/ antimycotics (Invitrogen, UK), supplemented with 10% (v/v) foetal calf serum (SC+FCS) (Invitrogen, UK). Scaffolds were maintained in a humidified atmosphere at 37 ºC and 5% CO_2. At various time points, the samples were removed and freeze-dried for 24 hours before weighing. The scaffolds were placed back into the tubes containing the same culture media. At each time point, 5 scaffolds were measured and the average reported. The pH of the culture media was also recorded with the scaffold weight. The percentage mass loss (M_L) was calculated using the following equation:

$$M_L = \left(\frac{M_d - M_i}{M_i}\right) \times 100\ (\%)$$

Where M_i is the initial mass of the scaffold and M_d is the mass of the degraded sample after freeze-drying for 24 hours.

3.9.6 FTIR Analysis of Chitosan Films

Structural changes in chitosan material cross-linked with glutaraldehyde were assessed after treatment with either L-glutamine or sodium borohydride for up to 24 hours. Chitosan samples were treated in this way to neutralise cytotoxic free-aldehyde groups from the cross-linking process. 10 µm thick films were cast from a 4% chitosan solution and assessed using a Cary 630 FTIR Spectrometer with an ATR attachment (Agilent Technologies). All spectra were recorded at room temperature at the resolution of 8 cm^{-1} and 32 scans. The FTIR analysis was focused on identification of absorption bands with the vibrations of functional aldehyde groups. The band wave numbers (cm^{-1}) were observed at:

- 1740-1690 aldehyde C=O stretch (strong intensity).
- 2820-2850 and 2720-2750 aldehyde =C-H stretch (medium intensity, 2 peaks).

3.9.7 Rheology to Assess Rate of Cross-linking

The rheological properties of 4% chitosan gels cross-linked with either 0.5% glutaraldehyde or 0.3% genipin were studied using an Anton Paar MCR 301 series rheometer. Rheology was applied to assess the rate of cross-linking of the gels. A parallel plate (PP50) measuring system was employed with 4 g of chitosan solution mixed with 800 µl cross-linking reagent as the volume per sample. Importantly, all gels were covered with mineral oil in order to prevent water evaporation and drying-out of samples during the cross-linking reactions. The elastic/ storage modulus (G') and the viscous/ loss modulus (G"), as a function of time, were determined from the oscillatory measurements at a frequency (ω) of 10 rad/ s. The strain (γ) was kept constant at 0.5%. Complete cross-linking and curing of the gels was determined as the time at which G' reached a plateau.

3.10 hMSC Culture on Chitosan Scaffolds

3.10.1 Dynamic Cell-seeding of Scaffolds

To prevent floatation and allow fluid flow to the scaffold-cores, the chitosan constructs were pre-wet and sterilised in ethanol, using a syringe-vacuum method developed by Felstead (University of Nottingham). See *Figure 3.2* for details.

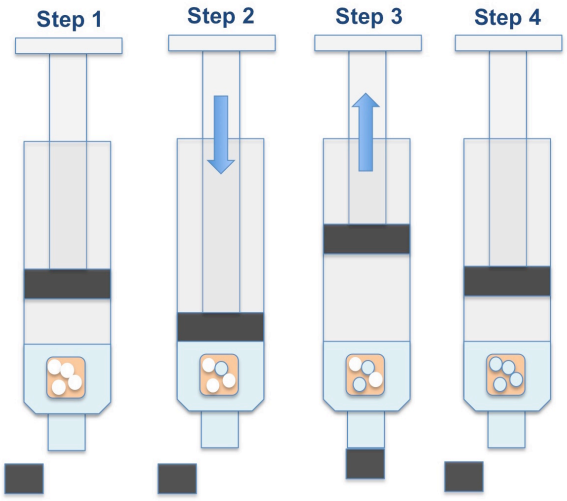

Figure 3.2 Pre-wetting and sterilisation of chitosan scaffolds. (Step 1) 50 ml syringe containing 10 ml ethanol and up to 3 scaffolds. (Step 2) Excess air is expelled from the syringe. (Step 3) A vacuum is formed and scaffolds are shook repeatedly under these conditions. (Step 4) Scaffolds are exposed to atmospheric pressure before the process is repeated twice more.

Cell seeding efficiency was improved when scaffolds were treated for 1.5 hours with 50 µg/ ml fibronectin (Sigma-Aldrich) diluted in PBS. Then, scaffolds were washed in PBS and submerged in culture medium for at least 1 hour. Seeding involved gentle pipetting of $1x10^6$ cells/ ml to the top of each scaffold, before plates were incubated overnight on a plate shaker (200 rpm) at 37 °C and 5% CO_2.

3.10.2 Bioreactor Sterilisation

To ensure sterility of the bioreactor system prior to the introduction of cell-seeded scaffolds, components were autoclaved for 10 minutes at 15 psi and 120 °C. After sterilisation, each bioreactor was assembled inside a sterile class II culture hood. The assembled components were then transferred to a sterile incubator, where the complete loop for the bioreactor system was completed. Silicone tubing was selected with a 3 mm bore and high permeability to CO_2. To guarantee thorough sterility of the system, each loop was perfused with ethanol for 1 hour. The system was then washed for 1 hour with PBS, before DMEM was circulated for a further hour. Finally, the cell-seeded scaffolds were introduced to the dynamic culture environment.

3.10.3 Culture in Perfusion Bioreactor

Bioreactors were manufactured in-house from polyetheretherketone (PEEK) (RS Components). The bioreactors are an adapted design from GKSS Research Centre, Germany and provide an inlet at the bottom, and an outlet at the top. Two glass-viewing windows enabled fluid flow to be monitored during experimental runs. To ensure leak-free bioreactors, silicone gaskets were inserted under each bioreactor cover. *Figure 3.3* shows the whole perfusion bioreactor system.

Scaffolds were introduced to the sterile, perfusion bioreactor system with specific orientation. Large pores were positioned at the bottom of the bioreactor (closest to the inflow), while small pores were at the top. This was designed to provide mechanical shear-stress to the bone-half of scaffolds only. The Watson Marlow 520S series peristaltic pump was switched on and basal culture medium was circulated at 1 ml per minute. After 48 hours, bioreactors were treated with differentiation-specific culture media, such as media containing factors for osteogenic and chondrogenic lineages.

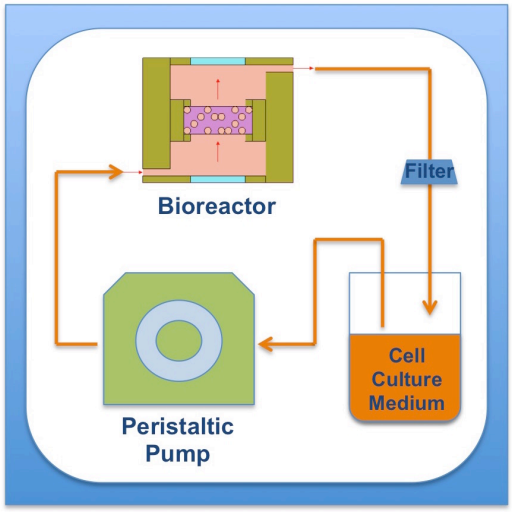

Figure 3.3 Diagram of the perfusion bioreactor system. Arrows indicate direction of cell culture medium flow.

3.10.4 Wax-embedding and Sectioning

After the culture period, scaffolds were removed from the bioreactors and washed 3 times in PBS before they were fixed in ice-cold 4% PFA for 2 hours. The scaffolds were washed in PBS and dehydrated via an increasing ethanol gradient (EtOH: 70% [v/v], 95% [v/v], 100% [v/v]). Next, samples were xylene cleared and embedded in paraffin wax. The paraffin blocks were attached onto a Leica RM2165 microtome and 10-20 µm sections were cut before they were stretched out in a 55 °C water bath. Finally, sections were mounted onto Superfrost™ microscope slides and dried at 50 °C overnight. The same protocol was also used to section cell pellets after chondrogenic differentiation.

3.10.5 De-waxing of Sections

To prepare chitosan sections for immunocytochemistry analysis, the paraffin wax was removed by immersing slides in Histoclear™ for 10 minutes. This was repeated twice. The sections were then rehydrated in a decreasing methanol gradient (MeOH: 100% [v/v] x 2, 75% [v/v], 50% [v/v] and 25% [v/v]). Slides were rinsed with PBT for 5 minutes and mounted using a DAPI-containing mounting medium, such as Vectashield™. The same protocol was used to section cell pellets after chondrogenic differentiation.

3.11 Statistical Analysis

Statistical significance at the 95% interval was determined using ANOVA analysis with Tukey post hoc comparison in GraphPad Prism™ 6 software. Mean values, standard deviations and standard error of the mean were calculated in Excel.

4. Transient FCS and HS Regimes to Support MSC Differentiation

4.1 Introduction

In the body, the structure of joints principally consists of bone, covered by a layer of articular cartilage for reduced friction. Bone is composed of hydroxyapatite crystals surrounded by a type I collagen matrix (Karageorgiou & Kaplan, 2005b). Furthermore, bone is living matter, which is continuously remodelled by native cells. The main cell types in bone are osteoblasts, which maintain a mineralised extracellular matrix (ECM), osteocytes, which produce new matrix and are important for mechanosensing, and osteoclasts, which degrade redundant ECM (Long, 2001). Cells from the osteoblast and osteocyte lineages are derived from a single multipotent progenitor cell type, known as mesenchymal stem cells (MSCs) (Lange et al, 2007). Articular cartilage comprises of a type II collagen and Chondroitin sulfate matrix (Hutmacher, 2000). Chondrocytes are present in cartilage to produce the ECM.

The main source of MSCs in the body is the stromal layer of bone marrow, although MSCs can also be found in umbilical cord blood, adipose tissue and muscle (Mastrogiacomo et al, 2005). In 1976, Friedenstein was the first to study and characterise bone marrow stromal cells. It was found that the main trait of MSCs is their ability to differentiate into osteocytes, chondrocytes and adipocytes (Lange et al, 2007).

These non-hematopoietic bone marrow cells (Vater et al, 2011) also have the ability to adhere to plastic surfaces without the need for pre-coating (Lange et al, 2007). Importantly, there is no single specific surface marker for the isolation of MSCs. However, MSCs do express CD29, CD90, CD105 and CD106, while they lack the hematopoietic markers CD34 and CD45 (Aicher et al, 2011).

Recently, MSCs have been discovered to be involved in paracrine signaling and immunomodulation (Chase et al, 2010). More specifically, MSCs can prevent graft-versus-host disease after transplantation by regulating T-cell and B-lymphocyte proliferation and differentiation (Perez-Simon et al, 2011). This immunomodulation is achieved by the migration of MSCs to sites of injury (Aggarwal & Pittenger, 2005). Other paracrine signalling functions include the release of growth factors for hematopoietic stem cell proliferation (Zhou et al, 2012).

All of the described properties of MSCs demonstrate the potential for these cells to be used in the development of modern therapeutic applications including bone and cartilage regeneration, prevention of graft-versus-host disease, improved engraftment of bone marrow transplants and even the treatment of metabolic diseases (Bacigalupo, 2007). Consequently, many research groups have focused on studying MSCs in the laboratory.

Isolated MSCs usually demonstrate a fibroblastic morphology, although there is some variation in the size and shape of cells (Mastrogiacomo et al, 2005), due to heterogeneity in the populations cultured *in vitro* (Vater et al, 2011). Osteogenic differentiation is achieved by supplementing standard culture medium with β-glycerophosphate, ascorbic acid, and dexamethasone. Once they have differentiated into osteoblasts, the MSCs morph from their fibroblastic morphology into a cuboidal shape. Alizarin red can be used to stain for calcium deposits and bone nodule formation after ECM has been produced by osteoblasts (Vater et al, 2011), while alkaline phosphatase activity is an early marker for osteogenesis (Jaiswal et al, 1997). Controversially, serum in culture medium has been suggested to contain factors that reduce osteogenesis of MSCs (Kuznetsov et al, 2000).

Serum is typically used for MSC culture as a source of nutrients, ECM proteins and growth factors (Bieback et al, 2009) (Liu et al, 2007). There is also evidence that serum may act as an antioxidant for cells (Meuleman et al, 2006). Nevertheless, there are problems associated with using serum such as batch-to-batch variation. Critically, foetal calf serum (FCS) contains animal-derived proteins/ molecules that may lead to the transmission of animal proteins, viruses and disease if cells cultured using FCS are used for human therapies (Lange et al, 2007). There is evidence that FCS may also induce hypersensitive reactions in patients. Methods of removing the majority of animal antigens in FCS exist, but all risks are not alleviated (Perez-Ilzarbe et al, 2009). Studies have demonstrated that bovine proteins remain in sera after many washes and most importantly, this can potentially lead to antibody formation and the non-engraftment of transplants (Stute et al, 2004). Hence, there has been increasing demands towards the development of serum-free media, and the possible use of human-derived serum (Aldahmash et al, 2011).

The aims of this investigation were to develop new serum conditions for the osteogenic differentiation of human MSCs and reduce the exposure of cells to FCS.

The current standard of using continuous FCS-containing medium was compared to osteogenic medium containing an alternative human serum (HS). Further, the study investigated whether a 5-day only treatment with human serum may be sufficient to sustain MSC differentiation in culture for up to 21 days. Attempts to standardise osteogenic differentiation of MSCs can provide more reliable differentiation results (Schallmoser et al, 2010) and serum-free conditions would additionally allow better understanding of the differentiation process by removing batch disparity of serum as a variable factor (Solmesky et al, 2010).

4.2 Results

4.2.1 Cell Characterisation

In order to successfully develop an osteochondral construct for joint repair using human mesenchymal stem cells (hMSCs), it is important for the cell culture conditions to be optimised. To come closer to achieving this aim, a comparison between the characteristics of MSCs cultured in foetal calf serum (FCS) or human serum (HS) was conducted.

Human mesenchymal stem cells were cultured in either FCS or HS for 2 passages before their morphology was observed using bright field microscopy. Figure 4.1A shows that cells cultured in both serum types exhibited the typical fibroblastic morphology associated with MSCs. Cells spread well across the surfaces of the culture flasks, suggesting that standard culture medium supplemented with either FCS or HS was suitable for maintaining MSCs. One difference between the two conditions was that cells cultured in HS appeared to proliferate at a greater rate than the equivalent cells cultured in FCS. Figure 4.3A demonstrates that cells in HS were over 1% more confluent than cells in FCS over a 24-hour period (not statistically significant). This observation is further supported in Figure 4.3B, where DNA content at Days 14 and 21, is significantly higher in HS culture than FCS culture ($p<0.05$ for both time points).

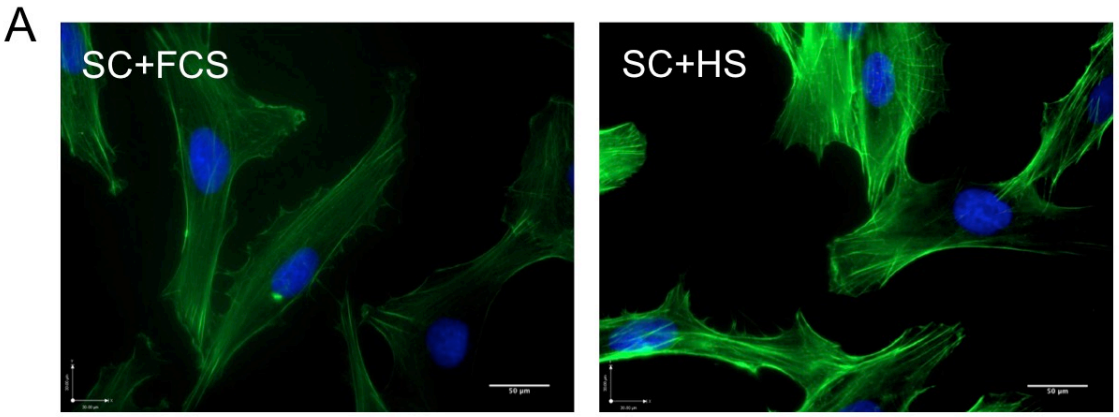

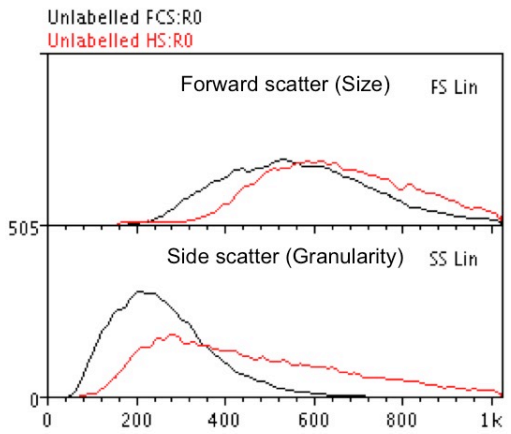

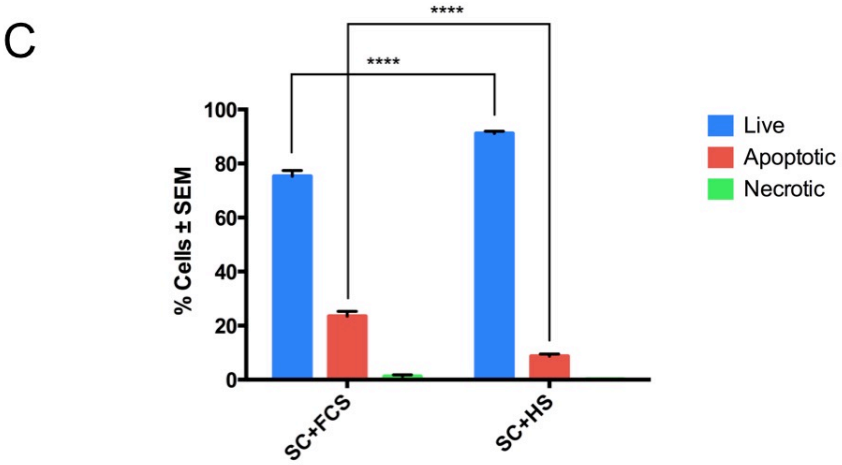

D

	SC+FCS (%) ± SEM	SC+HS (%) ± SEM
CD29	99.03 ± 0.563	98.76 ± 0.724
CD90	98.74 ± 0.591	98.53 ± 0.513
CD105	95.36 ± 0.978	92.91 ± 1.275

Figure 4.1 Characterisation of human mesenchymal stem cells cultured in fetal calf serum (FCS) and human serum (HS). (A) Fluorescence images showing the morphology and Actin filaments of hMSCs cultured in SC+FCS or SC+HS for 2 days. (B) Flow cytometry histograms comparing the size and granularity of cells cultured for 2 passages in SC+FCS and SC+HS. (C) The percentage (± S.E.M) of live, apoptotic and necrotic hMSCs after 14 days of culture on Matrigel coated plates in Standard Culture (SC) medium containing FCS or HS. n=3 (D) Flow cytometry data for the expression of MSC related surface markers CD29, CD90 and CD105 of cells cultured for 2 passages in SC+FCS or SC +HS. Scale bar represents 50 µm. ****<0.00005 significance threshold after ANOVA analysis with Tukey post hoc tests, comparing different sera types at the same time point.

A further morphological difference between MSCs cultured in the two serum types was that HS-cultured cells seemed to be more cuboidal in shape than cells in FCS (Figure 4.1A). However, forward-scatter data from the flow cytometry analysis (Figure 4.1B) proved that there was no difference in cell size between MSCs cultured in FCS or HS. Interestingly, the side-scatter data from the same analysis indicated cells cultured in HS to be more granular than cells in FCS. This information was supported by bright field microscopy observations of the cells, where MSCs in HS appeared darker than cells in FCS when observed under the same light intensity (data not shown).

The percentage of apoptotic and necrotic cells after 14 days of standard culture medium supplemented with FCS or HS (SC+FCS or SC+HS) was determined using a commercially available Annexin-V staining kit. Flow cytometry analysis indicated that there were higher numbers of apoptotic cells in FCS-culture than cells cultured with HS after 14 days (Figure 4.1C). Importantly, there were greater percentages of live MSCs in medium supplemented with HS than medium with FCS. Levels of necrosis were negligible for the two conditions.

Further flow cytometry analysis of the MSCs included a comparative assessment of the expression of CD29, CD90 and CD105 surface markers. These surface antigens are important markers for identifying a purified MSC population. Figure 4.1D indicated marginally different levels of CD29, CD90 and CD105 expression in cells cultured in HS and cells grown in the presence of FCS. 92.91% of MSCs cultured with HS expressed CD105, while 95.36% of FCS cells were positive for the same marker. CD90 expression was similar for the two conditions, whereas CD29 levels were 0.27% higher in FCS culture. Figure 4.2 shows detailed flow cytometry analysis of surface marker expression in mesenchymal stem cells cultured with FCS or HS.

4.2.2 Cell Attachment

Preliminary studies have shown that over prolonged culture periods, hMSCs begin to detach from their culture vessels as the cells proliferate and cell density increases. For this reason, initial studies compared the capacity of the hMSCs to remain attached to different types of commercially available tissue culture vessels, for up to 21 days in standard (SC) and osteogenic (OS) culture conditions.

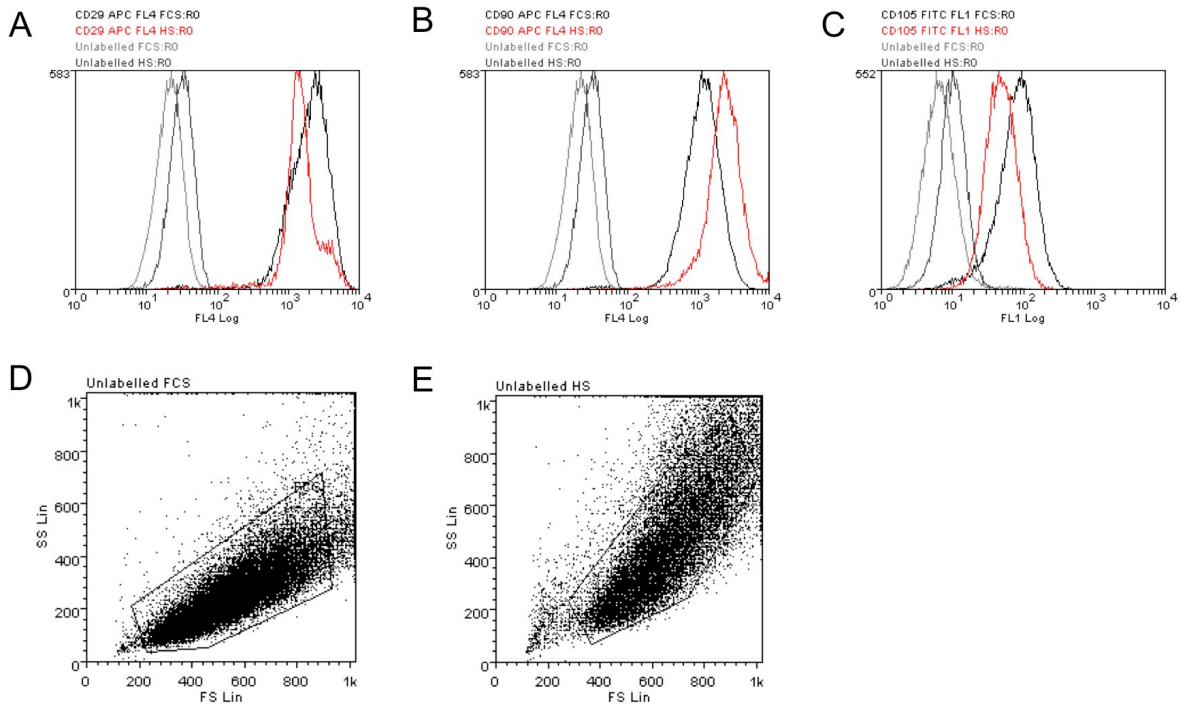

Figure 4.2 Detailed flow cytometry analysis of human mesenchymal stem cells cultured in fetal calf serum (FCS) and human serum (HS) for 2 passages. (A, B and C) Histograms for the expression of the MSC-related surface markers CD29 [A], CD90 [B] and CD105 [C] in human cells. (D and E) Population plots comparing the size (FS Lin) and granularity (SS Lin) of cells cultured for 2 passages in SC+FCS [D] and SC+HS [E]. Each sample was analysed for 50000 events. N=3.

First, the standard polystyrene plates available in our lab (BD Falcon™) were compared to an equivalent product from a different manufacturer, which has been frequently used for embryonic stem cell culture, and had demonstrated good cell attachment. The product used was the NUNC Nunclon™Δ polystyrene dishes. These experiments supported previous observations in terms of the fibroblastic morphology associated with MSCs and good cell spreading across the surfaces of the culture vessels. However, after 14 days of culture the layers of cells began to lift off at the well's edges and curl-up into balls. This detachment was most substantial in OS conditions with HS.

Next, it was decided that commercially available pre-coated culture dishes should also be tested, so samples of BD Purecoat Amine and BD Purecoat Carboxyl dishes were ordered. These plates are designed to improve cell attachment in serum-free conditions, increase cell proliferation and enhance post-thaw recovery. Furthermore, standardised pre-coating can reduce assay variability. After 7 days of culture, the hMSCs failed to attach in any conditions on the Amine-coated plates.

While cells on the Purecoat Carboxyl dishes successfully attached, they grew very sparsely and failed to demonstrate signs of osteogenic differentiation (data not shown).

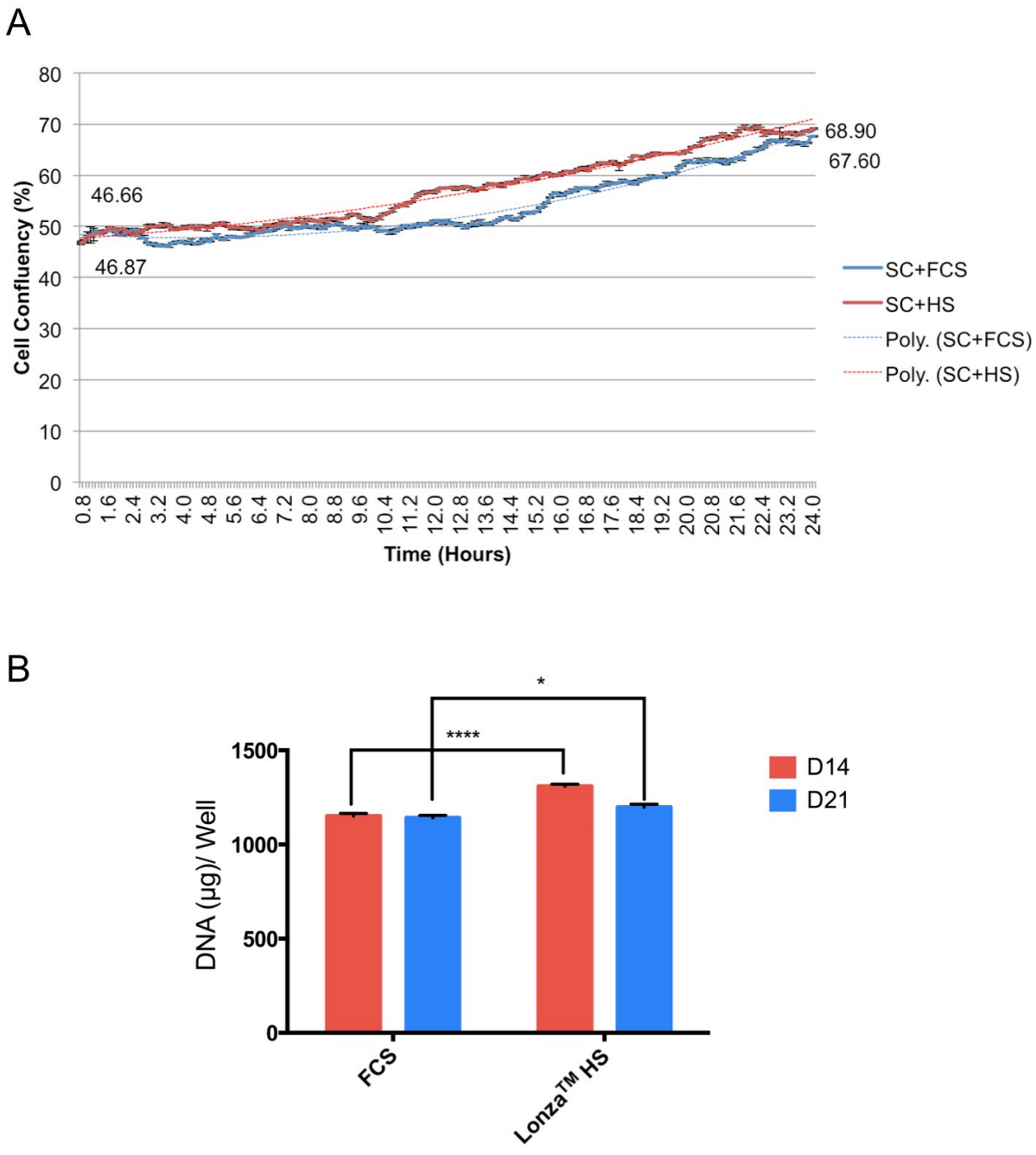

Figure 4.3 Human mesenchymal stem cell proliferation rates after culture in fetal calf serum (FCS) or Lonza™ human serum (HS). (A) Average cell confluency (%) after culture in SC+FCS and SC+HS for 24 hours. N=3. (B) DNA content (µg) per well after culture in SC+FCS and SC+HS for 14 and 21 days. n=6. *<0.05 and ****<0.00005 significance threshold after ANOVA analysis with Tukey post hoc tests, comparing different sera types at the same time point.

Since none of the commercial products designed to promote adherence worked with the hMSCs, the resulting step was to coat untreated polystyrene culture vessels with gelatin, collagen, fibronectin, Matrigel™ or laminin. MSCs attached well on all the coatings, apart from laminin after 7 days culture in proliferative media (Figure 4.4A). For this reason, the use of laminin was discontinued.

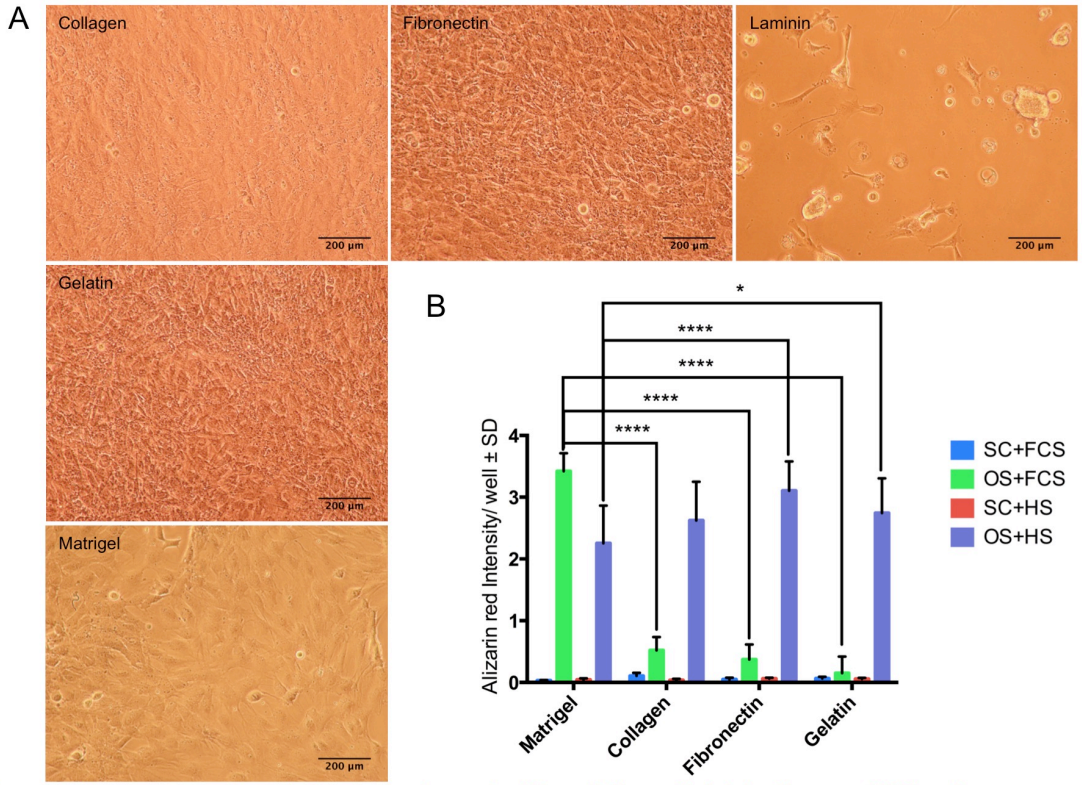

Figure 4.4 Human mesenchymal stem cell osteogenic differentiation with fetal calf serum (FCS) or human serum (HS), on different substrates for cell attachment. (A) Day 7 hMSC morphology on plates coated with Collagen, Fibronectin, Laminin, Gelatin or Matrigel™. (B) Day 21 Alizarin red staining intensity per well for hMSCs cultured on Matrigel™, Collagen, Fibronectin and Gelatin plates in SC and OS culture media with FCS and HS. Means ± S.D. shown. n=6. *<0.05 and ****<0.00005 significance thresholds after ANOVA analysis with Tukey post hoc tests, comparing the effects of substrate-type on mineralisation.

Figure 4.4B illustrates that after 21 days, significant mineral deposition was only found in hMSCs treated with osteogenic media. The amount of mineral deposited in wells supplemented with FCS was lower on plates coated with gelatin, collagen or fibronectin, than in cells grown on Matrigel™.

Mineral deposition on collagen, fibronectin and gelatin plates in OS+FCS conditions were significantly lower than the level observed on the same coatings with OS+HS media. Alizarin red levels were higher in the fibronectin-coated plates with HS, then any of the other coatings.

In terms of cell attachment, MSCs began to detach from the culture vessels after 14 days when collagen or fibronectin were used. Matrigel™ and gelatin coatings both revealed no signs of MSC detachment after 21 days of culture, although the mineralisation was consistently high on Matrigel™, regardless of the serum-type used. For this reason, it was decided that Matrigel-coated plates were most suitable for the comparison in osteogenic differentiation of hMSCs in media supplemented with either FCS or HS.

4.2.3 Serum Analysis

Human sera from three different manufacturers were test for their effect on hMSC metabolic activity and ALP activity (Figure 4.5). Sera were selected from Lonza™, Cellect™ and Seralab™, and it was shown that metabolic activity in hMSCs was lower with HS than FCS (Figure 4.5A). Human serum from Lonza™ allowed for the highest cell metabolism when compared to HS from Cellect™ and Seralab™. Interestingly, 0.2 µm filtration of all sera tested prior to medium preparation seemed to reduce the metabolic activity in hMSCs (not statistically significant). Further, analysis of DNA content per well indicates that cell proliferation is higher with HS than FCS. HS from Lonza™ and Seralab™ allowed for the highest rate of proliferation.

ALP response in hMSCs was significantly higher with all batches of HS than with FCS (Figure 4.5B)($p<0.00005$). Lonza™ and Seralab™ HS supported similar ALP activity, while Cellect™ was closer to FCS. As seen for metabolic activity data, filtration of sera reduced the ALP activity.

An important observation is that all the sera tested have natural ALP activity in the absence of cells. In terms of ALP activity in medium only, filtration had the least detrimental effect on the Cellect™ HS (23.4% reduction) (Figure 4.5C). This is compared to 38% reduction in Lonza™ HS and 24% reduction in Seralab™ HS.

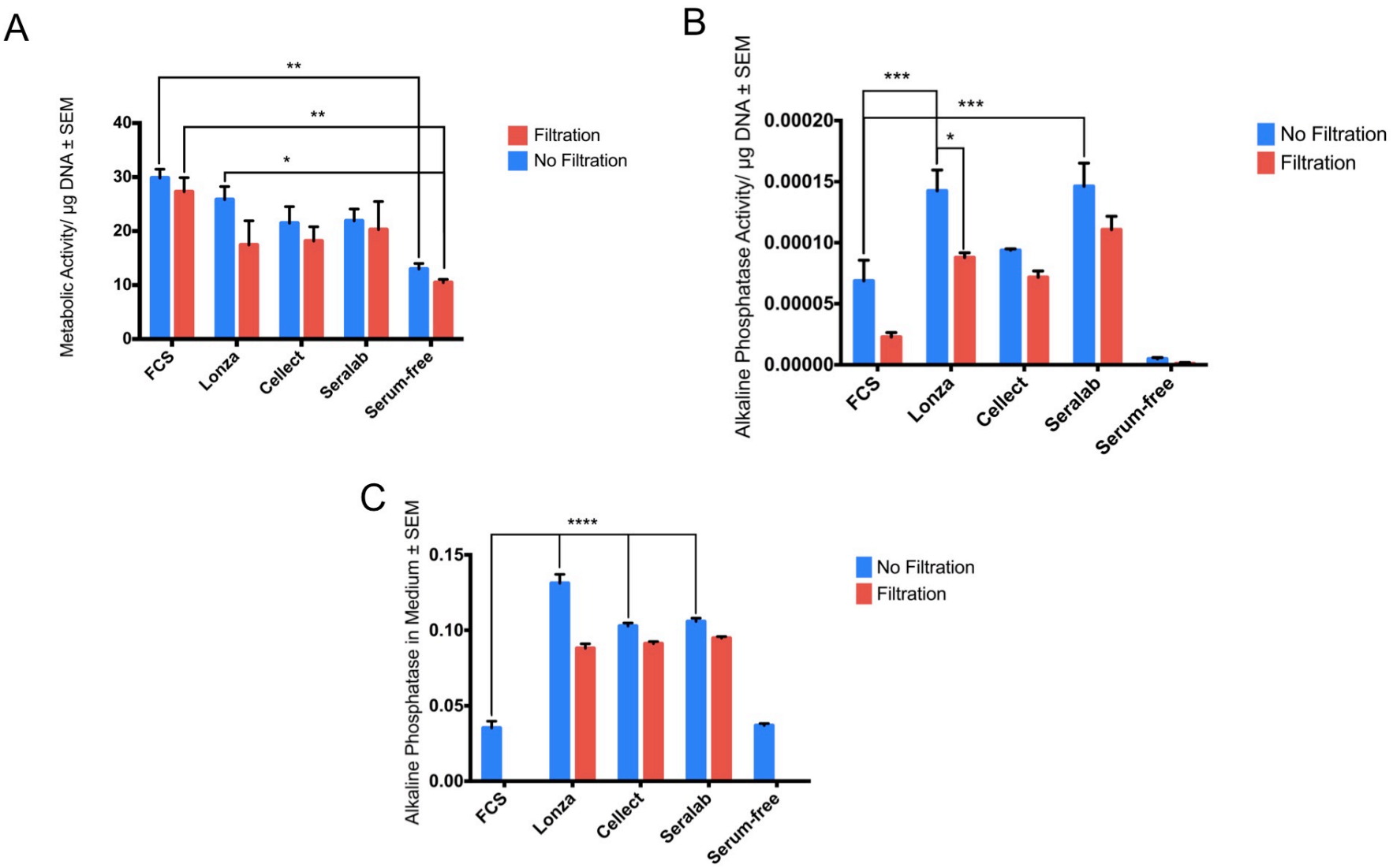

Figure 4.5 Variable hMSC response during serum test. (A) Metabolic assay for hMSCs cultured for 5 days in SC culture media, with FCS, Lonza™ HS, Cellect™ HS and Seralab™ HS. Filtered versus unfiltered sera are compared. (B) Alkaline Phosphatase activity for hMSCs cultured for 5 days in SC culture media, supplemented with a range of sera. (C) Alkaline Phosphatase activity measured in culture media only, with FCS, Lonza™ HS, Cellect™ HS and Seralab™ HS. Filtered versus unfiltered sera are compared. n=6. *<0.05, **<0.005, ***<0.0005 and ****<0.00005 significance thresholds after ANOVA analysis with Tukey post hoc tests, comparing different sera type at the same time point, and the effects of filtration.

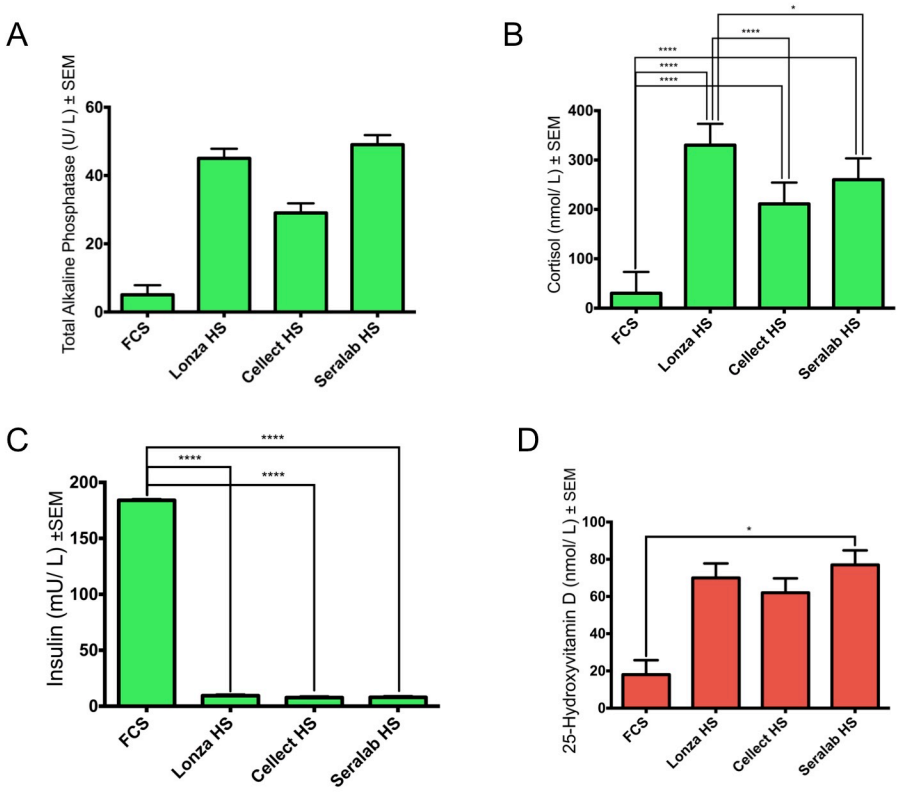

Figure 4.6a Human serum test. Biochemical analysis of FCS, Lonza™ HS, Cellect™ HS and Seralab™ HS for the content of (A) Total Alkaline Phosphatase, (B) Cortisol, (C) Insulin and (D) 25-Hydroxyvitamin D. N=1. *<0.05 and ****<0.00005 significance thresholds after ANOVA analysis with Tukey post hoc test, comparing different sera types.

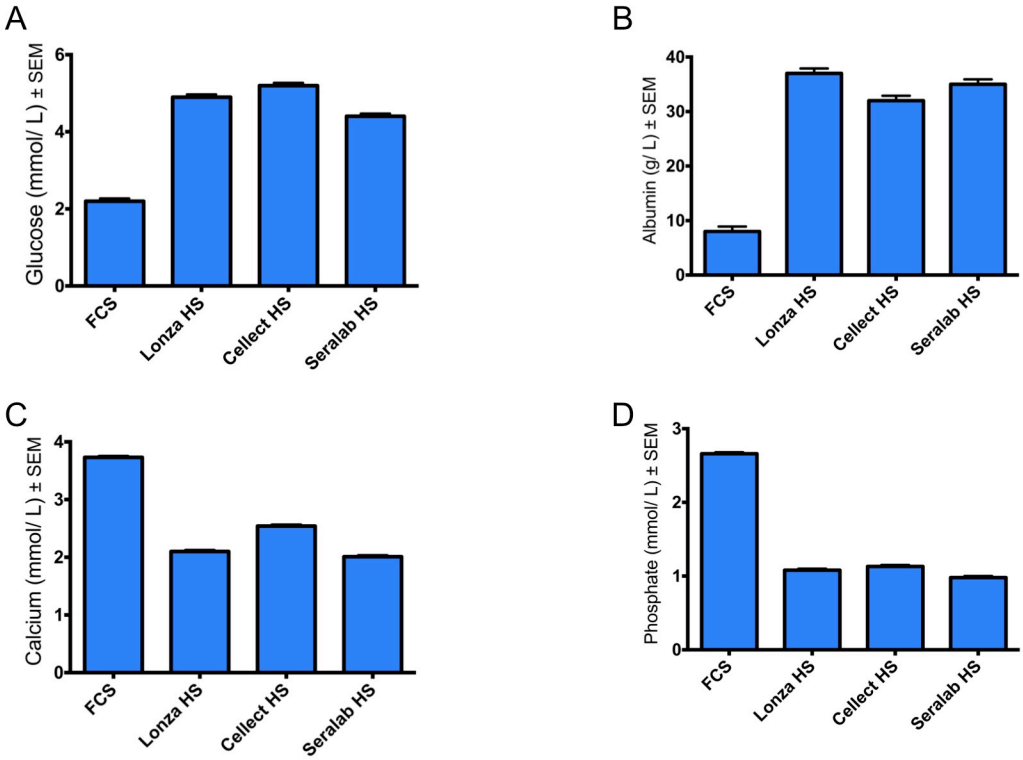

Figure 4.6b Human serum test. Biochemical analysis of FCS, Lonza™ HS, Cellect™ HS and Seralab™ HS for the content of (A) Glucose, (B) Albumin, (C) Calcium and (D) Phosphate. N=1. *<0.05 significance thresholds after ANOVA analysis with Tukey post hoc test, comparing different sera types.

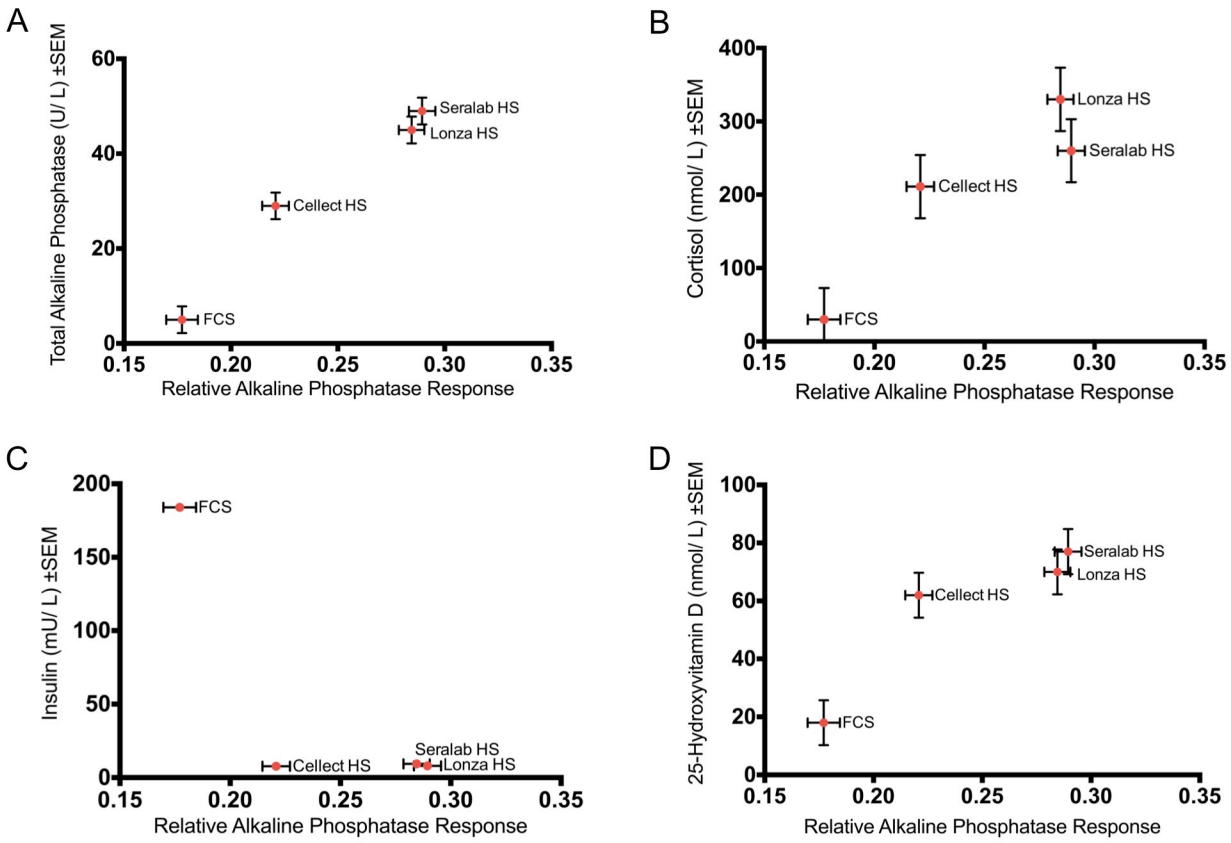

Figure 4.7a Human serum test. Multivariate analysis of FCS, Lonza™ HS, Cellect™ HS and Seralab™ HS correlating biochemical content of (A) Total Alkaline Phosphatase, (B) Cortisol, (C) Insulin and (D) 25-Hydroxyvitamin D, with the relative osteogenic effect of each sera-type (Alkaline Phosphatase activation) on mesenchymal stem cells. N=1.

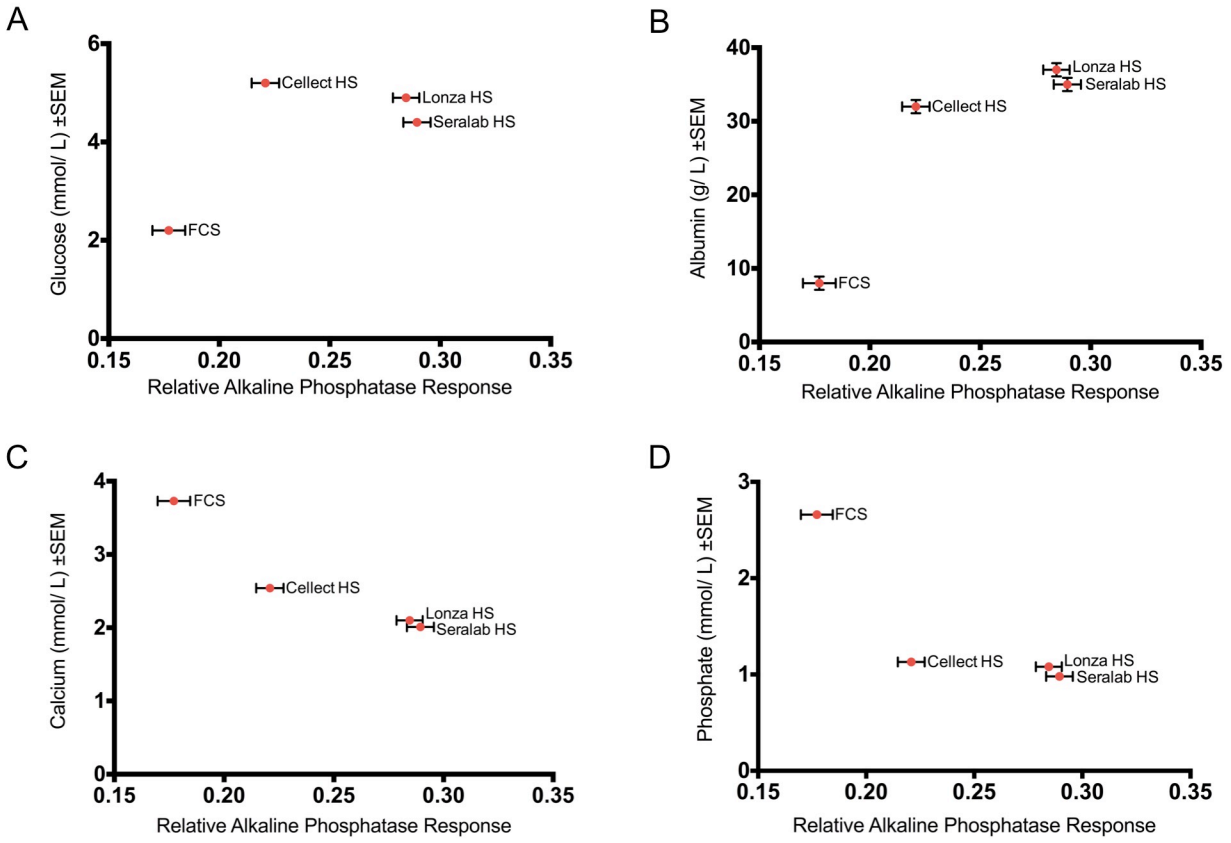

Figure 4.7b Human serum batch test. Multivariate analysis of FCS, Lonza™ HS, Cellect™ HS and Seralab™ HS correlating biochemical content of (A) Glucose, (B) Albumin, (C) Calcium and (D) Phosphate, with the relative osteogenic effect of each sera-type (Alkaline Phosphatase activation) on human mesenchymal stem cells. N=1.

Biochemical analysis of human serum from Lonza™, Cellect™ and Seralab™ was conducted to quantify any content differences compared to fetal calf serum. Human serum samples were tested for the following constituents;

- Glucose,
- Albumin,
- Calcium,
- Phosphate,
- Cortisol,
- Alkaline phosphatase,
- Insulin,
- 25-Hydroxyvitamin D.

The analysis showed that levels of glucose, albumin, cortisol, alkaline phosphatase and 25-Hydroxyvitamin D were higher in human serum than in fetal calf serum (Figures 4.6a and 4.6b). There were also differences between human serum samples. More specifically, samples that supported enhanced osteogenic differentiation (Lonza™ and Seralab™), displayed higher levels of cortisol, alkaline phosphatase and 25-Hydroxyvitamin D (Figures 4.7a and 4.7b). The multivariate analysis of the human serum batches indicated that Seralab™ HS stimulated the highest ALP response from hMSCs (Figures 4.7a and 4.7b). Lonza™ HS was second best and Cellect™ was significantly less effective. This data was supported by visual observations during differentiation experiments. Glucose levels were also higher in human serum than fetal calf serum. Interestingly, levels of calcium, phosphate and insulin were higher in the animal-derived serum.

4.2.4 Osteogenic Differentiation

Osteogenic differentiation of MSCs is crucial for the development of an osteochondral cellular construct. This type of differentiation is most commonly achieved using FCS in the laboratory, so it was important to determine if osteogenesis was different in osteogenic (OS) medium supplemented with Lonza™ HS and even in osteogenic medium with transient serum conditions (OS 5-Day FCS or HS).

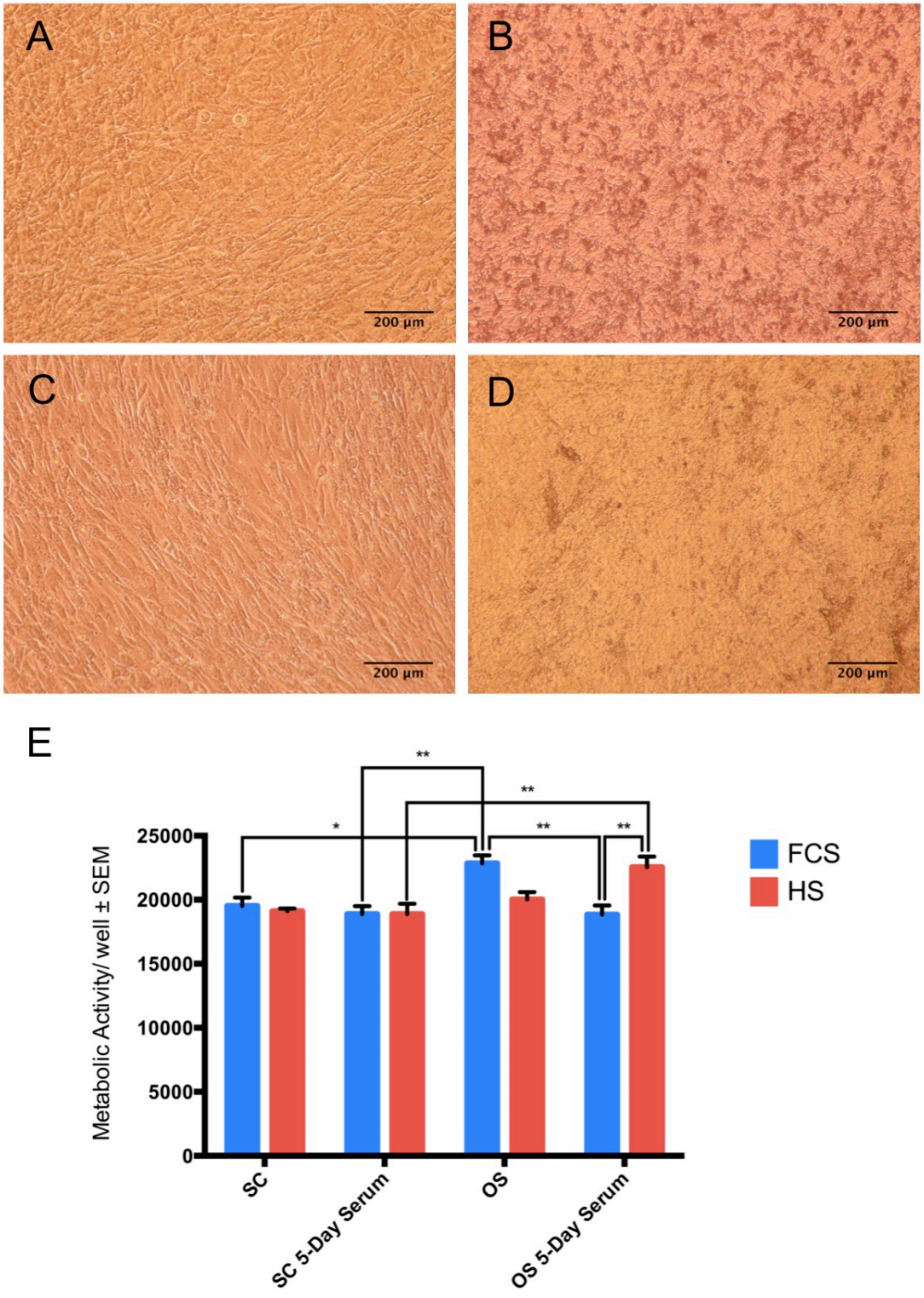

Figure 4.8 Morphological and metabolic changes during human mesenchymal stem cell osteogenic differentiation with FCS or HS. hMSCs cultured for 14 days in (A) SC +FCS, (B) OS+FCS, (C) SC 5-Day FCS and (D) OS 5-Day FCS medium. (E) Metabolic assay for hMSCs cultured for 14 days on Matrigel plates in SC and OS culture media, with FCS or Lonza™ HS. n=6. *<0.05 and **<0.005 significance thresholds of ANOVA analysis with Tukey post hoc tests comparing FCS versus HS at the same time point and media-type.

Human MSCs underwent considerable morphological changes during their osteogenic differentiation (Figure 4.8A-4.8D). MSCs transition from a fibroblastic-like phenotype to more flattened, polygonal morphology. Figure 4.8A shows that MSCs cultured in SC+FCS medium became very confluent after 14 days and therefore, the typical fibroblast morphology was not so obvious. Cells cultured in serum-free standard culture medium demonstrated less confluency (Figure 4.8C). In this culture condition, fibroblastic morphology was observed but cells were smaller in size than cells grown in serum-containing medium. Figure 4.8B shows significant mineral deposition in cells that had received osteogenic medium containing FCS. MSCs in complete osteogenic medium for the first 5 days of culture only (OS 5-Day FCS) had less mineral deposition than OS with FCS present throughout (Figure 4.8D). Importantly, these MSCs in differentiation medium had a stellate structure, which is characteristic of osteoblasts. Essentially, the same morphological trends in hMSCs were seen across all the serum conditions tested i.e. trends observed in osteogenic conditions are similar in media with FCS or HS, as well as trends with transient-sera treatments regardless of the serum type.

A PrestoBlue™ assay was conducted to measure the metabolic activity of human MSCs undergoing osteogenic differentiation at Day 14 (Figure 4.8E). Overall, metabolic levels were higher in wells treated under osteogenic conditions than control medium (SC). After 14 days, the metabolism for MSCs cultured in OS 5-Day FCS medium, was marginally lowest. Levels of metabolism for standard culture were similar with both serum types. Cells cultured in medium containing serum throughout the duration of the experiment, did not show higher levels of metabolic activity or viability in comparison to transient serum conditions.

In preliminary experiments, the observation that monolayers of cells detached in wells with human serum indicated that the initial results might be artifact. For this reason, osteogenic differentiation of MSCs was repeated on plates coated with Matrigel™ to promote adherence. Surprisingly, there were also signs of adipogenesis and lipid-droplet formation instead of osteogenesis in some HS differentiation experiment (data not shown).

Alkaline phosphatase (ALP) activity was used as an early indicator of osteogenic differentiation. Figures 4.9A shows that ALP levels were higher in osteogenic medium than SC medium regardless of whether the medium was supplemented with serum. Figure 4.9A also illustrates that levels of enzymatic activity are higher in

osteogenic medium with serum, than serum-free medium, although the levels are comparable. Importantly, Figure 4.9A demonstrates that ALP levels were higher after 21 days of culture than 14 days ($p<0.0005$). This was also observed in osteogenic medium with serum for the first 5 days only. Generally, culture conditions with FCS supported higher ALP activity than conditions with HS (Figure 4.9A). This data opposes the findings in 2.3 Serum Analysis. It was interesting to see at Day 14, that SC+HS medium showed similar levels of ALP to full osteogenic and OS-ve conditions with the same serum (Figure 4.4A). However, this trend had changed by Day 21 because the ALP activity was higher in osteogenic conditions than standard culture conditions.

Alizarin red staining was used as an indicator of osteogenesis and more specifically, calcium deposition. Figure 4.9B specifies that mineralisation was only present in medium containing dexamethasone, ascorbic acid phosphate and β-glycerophosphate. Direct comparison of cultures with FCS or HS at Day 14 indicated that the level of mineralisation was higher when osteogenic media was supplemented with HS than the equivalent media with FCS (Figure 4.10). This observation was also supported by quantitative analysis of the Alizarin red intensity (Figure 4.9B). Additional comparisons of Day 14 data show that hMSCs cultured in HS exhibited a cuboidal morphology before becoming more aligned than cells in media with FCS. Finally, mineralisation was greater after 21 days of differentiation than 14 days irrespective of which serum was used or whether serum exposure was transient. Furthermore, Figure 4.9B indicates that there was more intense Alizarin red staining in full osteogenic medium with FCS than the equivalent OS 5-Day Serum condition. Human serum results show the opposite trend where osteogenic conditions with transient serum showed greater mineral deposition than full osteogenic medium (Figure 4.9B).

Osteocalcin ELISA and immunocytochemistry for ALP were completed. The reason for this was because in the past it has proved difficult to demonstrate the presence of osteocalcin protein using immunocytochemistry. The Day 21 ELISA data was also inconclusive because osteocalcin protein was only found in osteogenic cultures with FCS (Figure 4.11A). For all other treatments, osteocalcin was not detected. The data does suggest that immortalised hMSCs have higher expression of the protein than primary hMSCs ($p<0.0005$). Primary MSC osteogenic differentiation is covered later in Section 4.2.4.

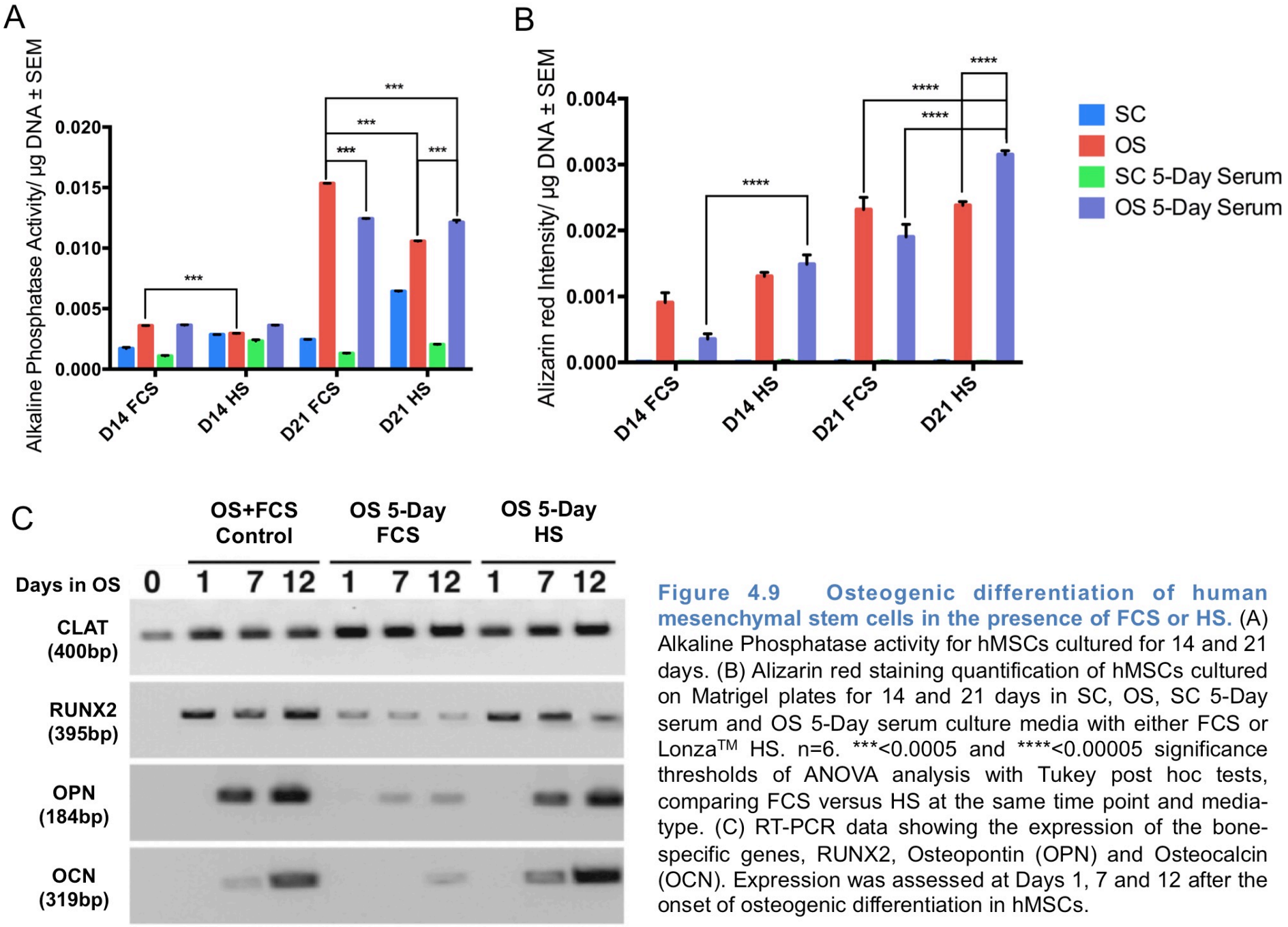

Figure 4.9 Osteogenic differentiation of human mesenchymal stem cells in the presence of FCS or HS. (A) Alkaline Phosphatase activity for hMSCs cultured for 14 and 21 days. (B) Alizarin red staining quantification of hMSCs cultured on Matrigel plates for 14 and 21 days in SC, OS, SC 5-Day serum and OS 5-Day serum culture media with either FCS or Lonza™ HS. n=6. ***<0.0005 and ****<0.00005 significance thresholds of ANOVA analysis with Tukey post hoc tests, comparing FCS versus HS at the same time point and media-type. (C) RT-PCR data showing the expression of the bone-specific genes, RUNX2, Osteopontin (OPN) and Osteocalcin (OCN). Expression was assessed at Days 1, 7 and 12 after the onset of osteogenic differentiation in hMSCs.

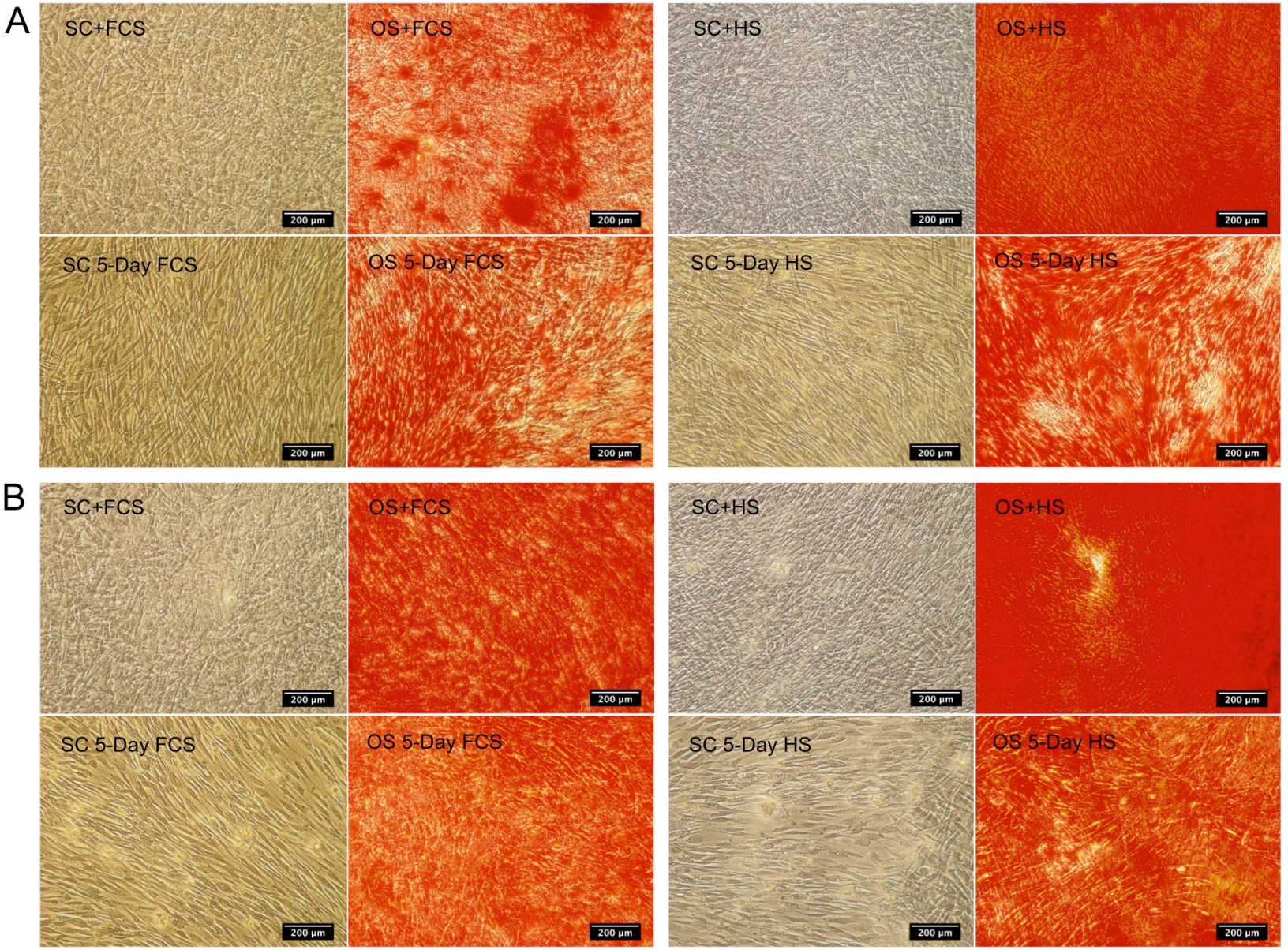

Figure 4.10 Osteogenic response of human mesenchymal stem cells exposed to FCS or Lonza™ HS, including transient-serum treatments. Alizarin red staining for calcium deposits in hMSCs cultured for (A) 14 and (B) 21 days in SC, OS, SC 5-Day serum and OS 5-Day serum culture media with FCS or HS. Scale bar represents 200 µm.

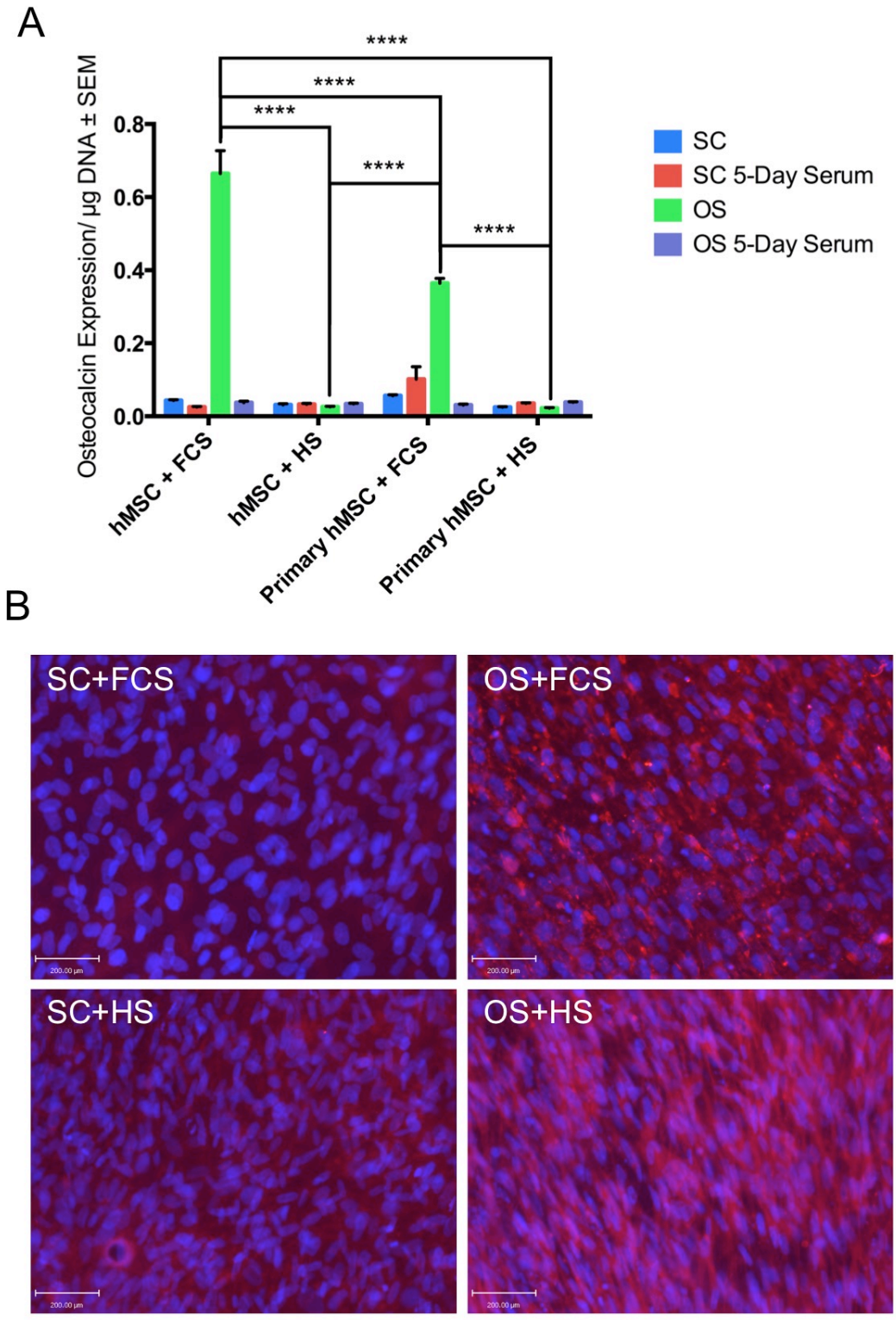

Figure 4.11 Osteogenic response of human mesenchymal stem cells in the presence of FCS or Cellect™ HS. (A) ELISA for Osteocalcin expression in hMSCs on Matrigel plates cultured for 21 days. n=6. ****<0.00005 significance threshold of ANOVA analysis with Tukey post hoc tests, comparing FCS versus HS at the same time point and media-type. (B) Bone-specific Alkaline Phosphatase immunostaining for hMSCs treated for 14 days. Scale bar represents 200 µm.

Further, with transient exposure to fetal calf serum the osteocalcin expression was diminished. Differentiation samples with human serum failed to show any osteocalcin signal, even though previous analysis for Alizarin red staining and alkaline phosphatase suggested good osteogenic differentiation of these samples. Figure 4.11B illustrates that ALP protein is found in Day 14 osteogenic cultures supplemented with FCS and HS. The location of ALP in FCS cultures is more defined than with HS. Further, the immunostaining also confirms that ALP is expressed at low levels in proliferative cultures with HS.

Pico Green DNA assays were conducted, as an indicator of MSC proliferation via correlating DNA content with relative cell numbers. This was important to allow metabolic activity, ALP and mineral deposition data to be normalised to well contents. Generally, DNA content in cultures was higher after 21 days than 14 days of culture. Also, cell numbers were generally higher in standard culture compared to osteogenic culture. Conditions with transient-serum exposure had less DNA content than serum-containing environments.

In addition to this, osteogenic differentiation of hMSCs was further analysed using RT-PCRs for the bone-specific genes, Runt-related transcription factor 2 (RUNX2), osteopontin (OPN) and osteocalcin (OCN)(Figure 4.9C). After primers were carefully chosen for each gene, the parameters for each primer pair were optimised. Temperature and cycle numbers were adjusted to allow the expression of single, clear bands on the PCR gels. The data for OS Control samples showed that RUNX2 was always detected, and up regulated during osteogenic differentiation. Osteopontin and osteocalcin were detected after Day 7 of osteogenic differentiation. The level of osteocalcin expression was highest at Day 12 of differentiation. Trends in the control samples were also observed in osteogenic differentiations with 5-Day exposures to FCS or HS. However, the expression level of the 3 genes in samples with transient FCS, were significantly lower.

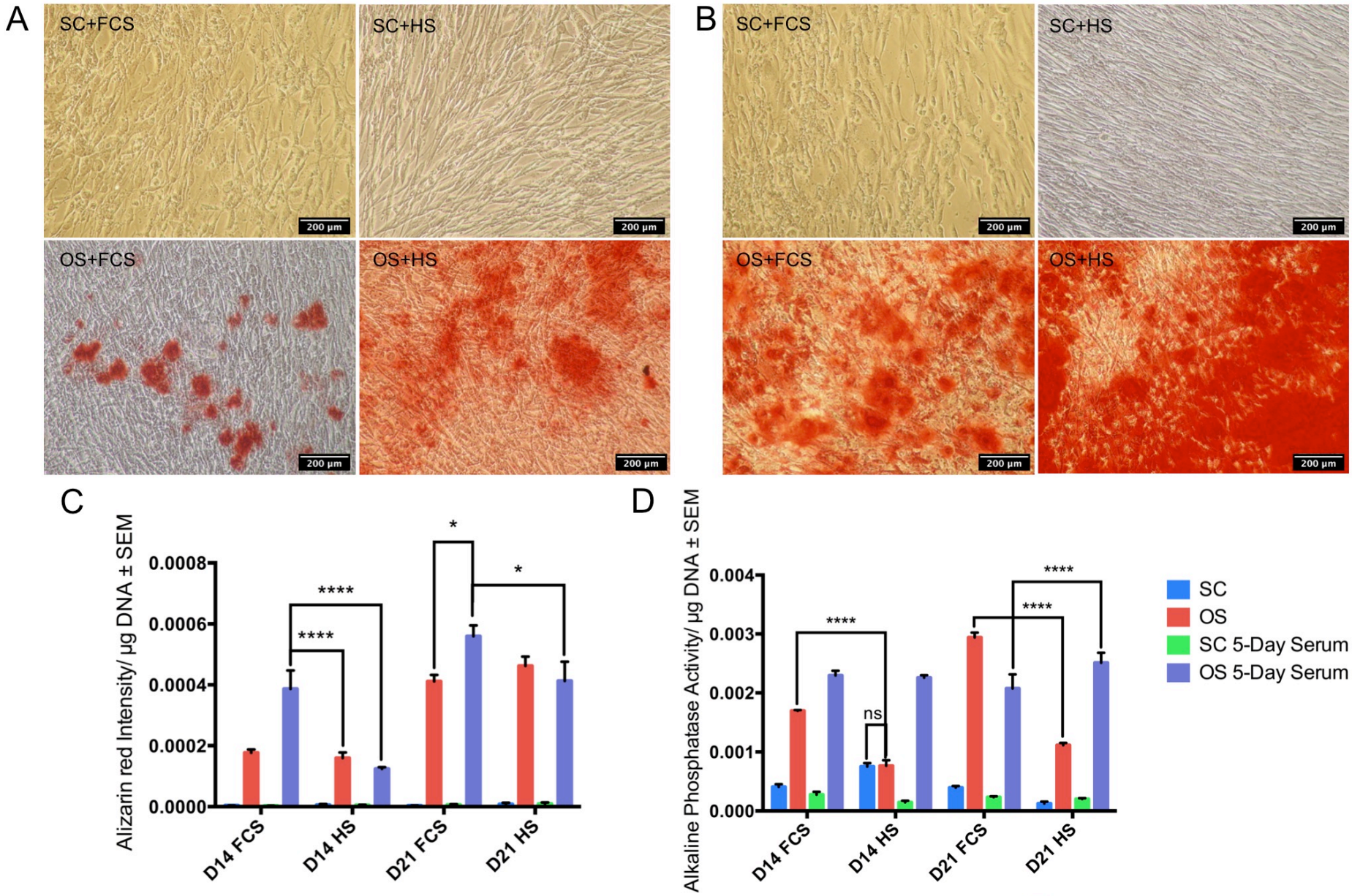

Figure 4.12 Osteogenic differentiation of primary hMSCs in the presence of FCS or Seralab™ HS. (A) Alizarin red stain of hMSCs cultured for 14 and 21 days in SC, OS, SC 5-Day serum and OS 5-Day serum culture media with FCS or Seralab™ HS. (B) Alizarin red staining quantification and (C) Alkaline Phosphatase activity for hMSCs cultured for 14 and 21 days. n=6. *<0.05 **<0.005 and ****<0.00005 significance thresholds of ANOVA with Tukey post hoc tests, comparing FCS versus HS.

The osteogenic differentiation potential of primary mesenchymal stem cells was assessed, to evaluate whether the culture conditions were suitable for cells from multiple sources (previously tested immortalised cell line)(Figure 4.12). Differentiation was evaluated through Alizarin red staining and alkaline phosphatase quantification. The results showed that primary mesenchymal stem cells have the ability to successfully respond to differentiation media supplemented with either fetal calf serum or human serum, and that transient serum regimes were also able to trigger this response. At Days 14 and 21, cells cultured in osteogenic conditions supplemented with HS appeared to mineralise more than primary hMSCs in FCS (Figure 4.12A and 4.12B). However, once mineral deposition was quantified and normalised to DNA content, cells cultured in FCS showed higher levels than HS cells (Figure 4.12C). An interesting observation was that cells treated with 5-Day FCS deposited more mineral than cells in FCS throughout the differentiation. MSCs cultured in OS+FCS also had higher ALP activity than cells in HS (Figure 4.12D). Overall the Alizarin red and ALP analysis showed that primary MSCs demonstrated lower levels of osteogenic differentiation than immortalised MSCs.

4.2.5 Chondrogenic Differentiation

Since the overreaching aim of the project is to develop an osteochondral cellular construct, chondrogenic differentiation of MSCs is just as important as osteogenic differentiation. Differentiation of MSCs to cartilage is generally achieved in serum-free conditions, so it was important to determine if chondrogenesis is possible in chondrogenic (CHO) medium supplemented with transient serum conditions (CHO 5-Day FCS or Seralab^{TM} HS).

Chondrogenic pellets were formed successfully in serum-free and transient-serum differentiation samples (Figure 4.13B). Pellets in control medium could not hold their shape. Serum-free chondrogenic pellets and pellets with 5-Day HS exposure were large and similar in size, while 5-Day FCS pellets were smaller.

Dimethylmethylene blue (DMMB) assays were used on chondrogenic samples to test for the presence of the glycosaminoglycan (GAG) chondroitin sulfate (Figure 4.13A). Serum-free chondrogenic and chondrogenic samples with 5-Day exposure to FCS samples demonstrated the highest levels of GAGs, compared to control samples and chondrogenic samples with 5-Day exposure to Seralab^{TM} HS ($p<0.005$).

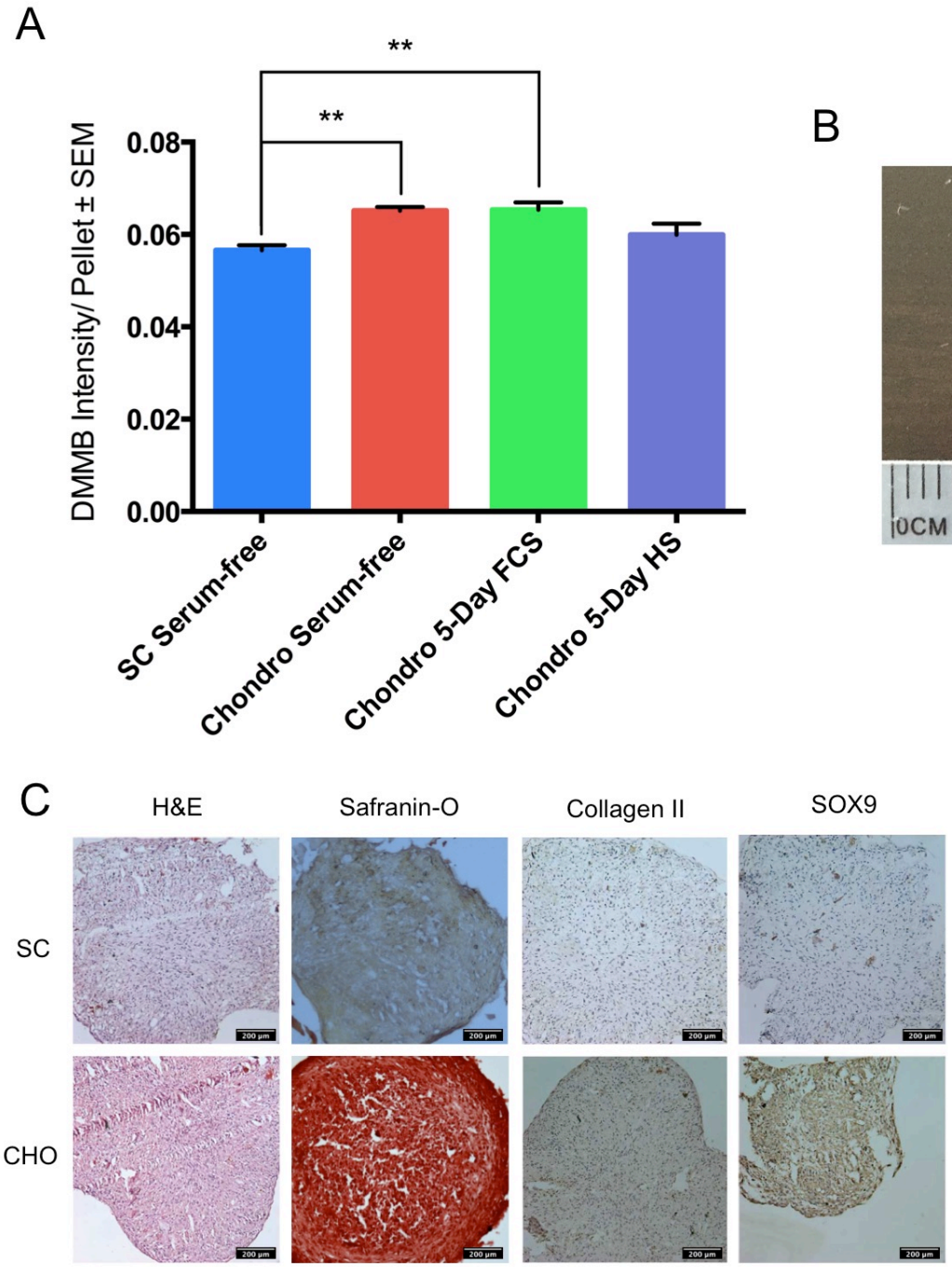

Figure 4.13 Chondrogenic differentiation of human mesenchymal stem cells in the presence of transient exposure to FCS or Cellect™ HS. (A) Day 21 Dimethyl methylene blue (DMMB) assay for hMSC pellet cultures in chondrogenic media, with FCS or HS for the first 5 days only. DMMB levels are normalised to cell metabolic activity. n=6. **<0.005 significance threshold of ANOVA analysis with Tukey post hoc comparison tests of serum-free versus transient-serum chondrogenic conditions. (B) Chondrogenic pellet morphology after 21 days in culture. (C) Haematoxylin and eosin (H&E), Safranin-O staining for proteoglycans in cartilage pellets and, immunostaining for Collagen II and SOX9 expression. Scale bar represents 200 µm.

However, when data was normalised to cell metabolic activity, chondrogenic samples with transient exposure to HS had the highest GAG levels. The remaining chondrogenic samples had similar levels to untreated controls.

Safranin-O staining for proteoglycans in cartilage pellets and, immunostaining for Collagen II and SOX9 expression were successfully achieved in serum-free chondrogenic samples (Figure 4.13C). Control samples in proliferative media (SC) stained negatively for these chondrogenic markers. Immunostaining in chondrogenic samples with transient exposure to FCS or Seralab™ HS was not as effective as serum-free differentiations (data not shown).

4.2.6 Live Alkaline Phosphatase

A new Life Technologies Alkaline Phosphatase Live Stain™ was tested as an alternative method to end-point ALP detection. The main advantage of this kit is that cells remain viable and differentiations can be maintained after the assay. Human MSCs, HEK293 and NTera2 cells were chosen (Figure 4.14A). HEK293 were used as a negative control, while the natural ALP activity in NTera2 cells allowed for a positive control. Human MSCs were tested in proliferative and osteogenically differentiated states. Figure 4.14B confirm that differentiated MSCs and NTera2 cells express ALP activity using the standard enzymatic end-point method. However, ALP cannot be detected using the Alkaline Phosphatase Live Stain™ (Figure 4.14C).

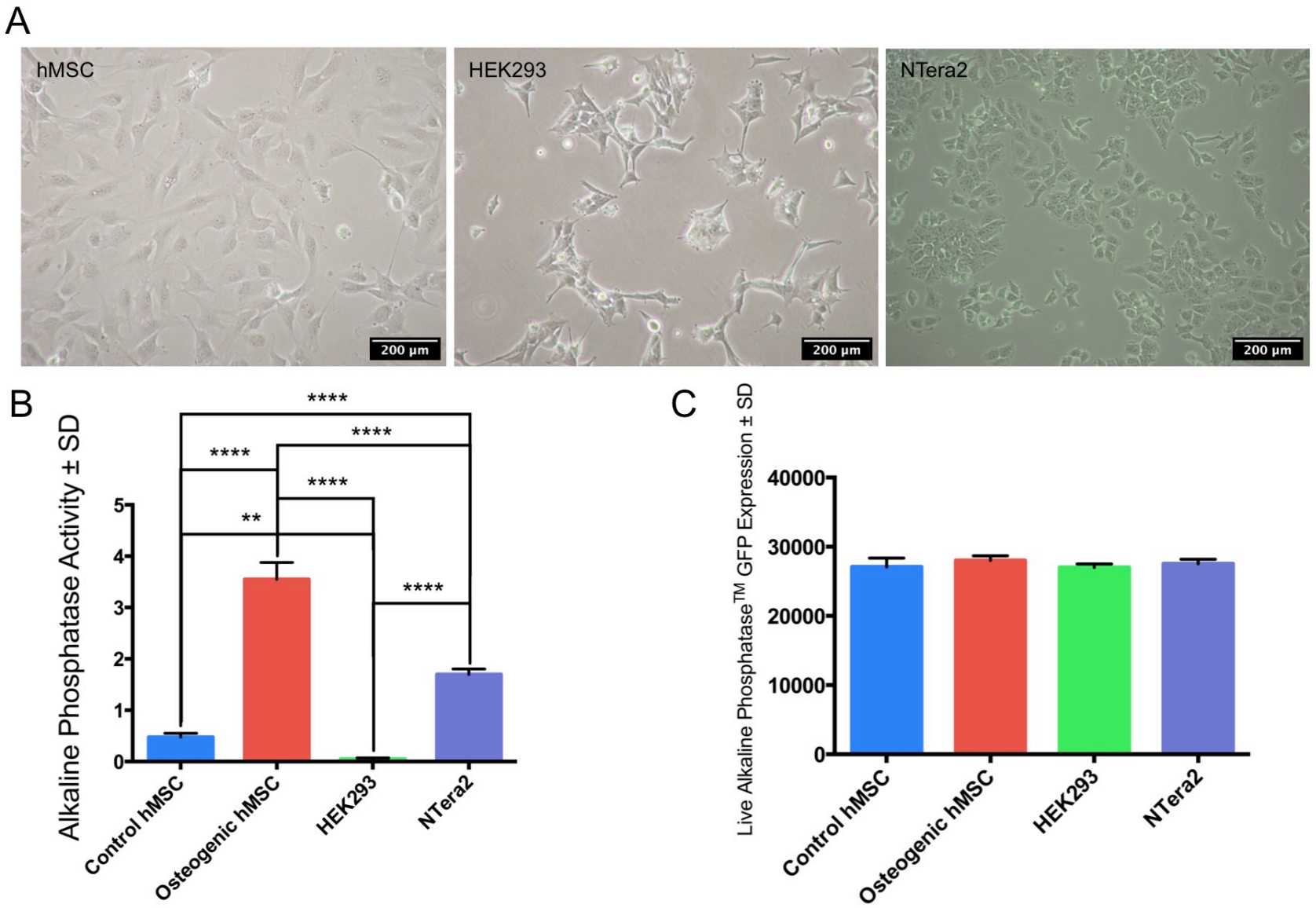

Figure 4.14 Life Technologies Alkaline Phosphatase Live Stain™ test. (A) Morphology of human MSC, HEK293 and NTera2 cells used to assess the potential of using Alkaline Phosphatase Live Stain™ to quantify enzyme activity and maintain cell viability. (B) Day 7 Alkaline Phosphatase activity of cells using standard/ end-point Alkaline Phosphatase kit from Sigma™. (C) Day 7 Alkaline Phosphatase activity of cells using new Alkaline Phosphatase kit from Life Technologies™. Means ± S.D. shown. n=6. **<0.005 and ****<0.00005 significance thresholds after ANOVA analysis with Tukey post hoc tests.

4.3 Discussion

4.3.1 MSC Culture and Osteogenic Differentiation

Serum is an important supplement in culture media for stem cells because it provides cells with nutrients, ECM proteins and growth factors required for proliferation and differentiation (Bieback et al, 2009). The primary objective of this investigation was to compare osteogenic differentiation of hMSCs in medium containing either FCS or HS. Although most commonly used, FCS may not be suitable for regenerative therapies because of possible transmission of animal viruses to patients (Lange et al, 2007). Testing of HS rather than FCS may allow for autologous serum use (Honmou et al, 2011). Therefore, commercially available HS was tested, as well as the possibility of transient serum-treatment of cells (Choi et al, 2013; Cobb & Walker, 1961).

First, comparisons were made between hMSCs cultured in SC+FCS or SC+HS media. The results suggest that cells in SC+HS medium were more cuboidal than the stereotypical fibroblastic morphology of hMSCs cultured with FCS. Flow cytometry analysis indicated that there was no significant difference in cell size between the two serum conditions, although cells in HS were more granular. MSCs in HS did not express hMSC-specific surface antigens at a significantly higher level than cells in SC+FCS, indicating that HS does not induce a more purified population of hMSCs than FCS.

Furthermore, proliferation and DNA content/ cell number data indicates that hMSCs in HS proliferated at a higher rate than cells cultured in FCS. This observation is reinforced by other research in the literature by (Mizuno et al, 2006) and (Tateishi et al, 2008). Apoptotic analysis showed that after 14 days in SC+HS there was less cell death and more live cells, than MSCs in SC+FCS. However, Meuleman et al. (2006) propose that during prolonged cell culture periods, small, proliferating cells are replaced by large, slow growing cells. Continued use of heterologous HS in culture leads the hMSCs to exhibit growth arrest and death within 6 weeks (Lange et al, 2007). Here, cells were only cultured for up to 3 weeks and therefore further experiments with prolonged culture periods would be required to confirm what the literature indicates. Importantly, there are similar studies into the use of heterologous HS, which demonstrate that the cells do not degenerate over time (Abdallah et al, 2006; Mannello & Tonti, 2007).

All known studies comparing FCS with autologous HS suggest higher cell numbers in HS culture (Lange et al, 2007) (Mizuno et al, 2006). The higher cell death in FCS could be explained by the fact that, due to high levels of ECM formation, Day 14 cells were difficult to detach from culture vessels and required extended trypsinisation during harvesting.

According to some reports, transient serum exposure reduces the viability of hMSCs. MSCs adopt a distinct growth pattern and smaller, fibroblastic morphology than cells in serum treatments (Chase et al, 2010). The literature also proposes that completely serum-free media cannot support proliferation of MSCs without initial transient serum exposure (Tonti & Mannello, 2008). These suggestions are sustained by the findings of this study, as cells in transient-serum environments adopt obvious growth patterns, and growth rates are reduced compared to MSCs in continued serum exposure. Notably, MSCs cultured in serum-free conditions apparently exhibit longer telomeres and an increased proliferative capacity (Pochampally et al, 2004). The study into transient-serum regimes with HS is an extension to an initial paper from our group, which investigated transient FCS treatment and the differentiation potential of MSCs (France et al, 2012).

Next, the ability of hMSCs to differentiate into osteogenic lineages was studied. The results here put forward that metabolic activity is lower in the proliferative conditions than in osteogenic media (Munoz et al, 2014). More specifically, metabolic activity is higher in osteogenic media supplemented with FCS than HS. While in transient-serum condition, HS leads to increased MSC metabolism. (Pattappa et al, 2011) found that there were no metabolic differences in MSCs during proliferation and subsequent differentiation into osteogenic lineages.

ALP activity, an early marker of osteogenic differentiation that is involved in preparing ECM for mineralisation (Sendemir-Urkmez & Jamison, 2007), was quantified using colorimetric assays. The results here validate that ALP activity is significantly higher in osteogenic conditions, than in standard culture. Furthermore, the ALP levels in MSCs treated with osteogenic medium containing FCS for the first 5 days only were lower than when serum was present throughout the whole culture period. The opposite was observed in osteogenic cultures with HS. This observation would signify that the onset of osteogenic differentiation is slower in cells cultured in transient FCS conditions (Shahdadfar et al, 2005) but not in transient HS.

Interestingly, initial ALP levels of cells cultured in SC+HS media were very similar to those revealed in osteogenic conditions with human serum, and in general cells in HS have greater ALP levels than cells in FCS, regardless of the conditions. This is especially true at Day 14. High levels of ALP enzymatic activity have also been confirmed in other undifferentiated cultures, such as embryonic stem cells (Adewumi et al, 2007).

There is research, which indicates that MSCs expressing high ALP levels in standard conditions, do not mineralise in OS medium (Vater et al, 2011). This cannot be supported in this investigation, as mineralisation was greater in osteogenic cultures with HS than FCS. As expected, there was no osteogenic differentiation in conditions without dexamethasone, β-glycerophosphate and ascorbic acid supplementation (Kyllonen et al, 2013; Sekiya et al, 2002). Transient-serum exposure allows for the osteogenic differentiation of MSCs, but the intensity of mineralisation is lower (Pisciotta et al, 2012). This supports the ALP findings that differentiation is slower in the absence of serum.

Differentiation samples with human serum failed to show any osteocalcin signal, even though previous analysis for Alizarin red staining and alkaline phosphatase suggested good osteogenic differentiation of these samples. Osteocalcin is a protein secreted by osteoblasts and is involved in mineral deposition and calcium homeostasis (Ducy et al, 1997; Komori et al, 1997). One possible explanation for the absence of osteocalcin could be the higher levels of calcium mineral deposits and ECM production in human serum samples. Therefore, it was more difficult to break-up these samples and release the osteocalcin protein for the ELISA kit to detect.

Runt-related transcription factor 2 (RUNX2), Osteopontin (OPN) and Osteocalcin (OCN) genes are all fundamentally involved in the osteogenic differentiation of MSCs. The data showed that RUNX2 was always detected, and up regulated during osteogenic differentiation. RUNX2 controls MSC commitment to osteogenic lineages and there is a direct correlation between gene expression and the level of osteoblast differentiation (Zhang et al, 2009). Osteopontin and Osteocalcin were detected after Day 7 of osteogenic differentiation. Both proteins are important in the later stages of bone development and remodelling, therefore it is expected that gene activation is delayed (Kyllonen et al, 2013; Merry et al, 1993).

The osteogenic differentiation potential of primary mesenchymal stem cells was assessed, to prove that the culture conditions are suitable for cells from multiple sources (Kartsogiannis & Ng, 2004). The majority of experiments described in this study are based on an immortalised MSC line. Differentiation was evaluated through Alizarin red staining and alkaline phosphatase quantification. The results showed that primary mesenchymal stem cells have the ability to successfully differentiate into bone lineages in media supplemented with either fetal calf serum or human serum. Transient serum regimes were also suitable. Levels of differentiation were lower in primary cells than in the immortalised cell line. However, there is conflicting data in the literature, as some groups suggest that primary MSCs have the highest differentiation potential (Zhao et al, 2009).

4.3.2 Serum Analysis

Chemical composition of sera is highly variable between types, manufacturers or batches and this can provide significant impact on cell function. Samples that supported enhanced osteogenic differentiation (Lonza™ and Seralab™), displayed higher levels of cortisol, alkaline phosphatase and 25-Hydroxyvitamin D. All of these have been documented in the literature as being important factors for the osteogenic differentiation of mesenchymal stem cells.

In the literature, cortisol has been revealed to decrease expression of bone formation markers and reduce bone density via resorption (Misra et al, 2004). For this reason hypercortisolism can be a direct cause of osteoporosis (Mundy et al, 1976). Here it was shown that human serum with high cortisol levels lead to increased osteogenesis. Therefore, cortisol levels in serum may not be very important in MSC bone development.

Alkaline phosphatase is essential in the onset of MSC osteogenic differentiation and preparation for mineral deposition (Roach, 1999). Data in this study supports this fact because sera with naturally high alkaline phosphatase levels performed better during bone differentiations.

25-Hydroxivitamin D is another factor that was present at high levels in serum samples with greater osteogenic potential. Deficiency in vitamin D like hypercortisolism is linked to increased bone resorption and disease (Girgis et al, 2015; Morrison et al, 1994).

Vitamin D and its associated receptors regulate mineral and skeletal homeostasis by increasing calcium transport in the intestines (Goltzman et al, 2015).
Furthermore, vitamin D has been demonstrated to increase osteocalcin expression (Staal et al, 1998). However, there is contrasting data in the literature as some studies suggest that increased sensitivity to vitamin D in joints may be linked to osteoarthritis development (Mabey & Honsawek, 2015).

Glucose levels were also higher in human serum than fetal calf serum and this could explain the higher rates in proliferation observed with human serum (Li et al, 2007). Some researchers disagree with this observation and suggest that glucose levels do not effect growth factor production and proliferation in mesenchymal stem cells (Weil et al, 2009).

Interestingly, levels of calcium, phosphate and insulin were higher in the animal-derived serum. These are also well-documented factors involved in osteogenic differentiation. However, they do not appear to be as important as cortisol, alkaline phosphatase and 25-Hydroxyvitamin D. Calcium and phosphate are major minerals in bone, and there is a co-dependence of both factors during bone development (Shapiro & Heaney, 2003). For this reason, calcium phosphates are popular ceramic biomaterials for bone regeneration (Hench, 1991). Nevertheless, calcium levels may only be crucial in diseased tissue, which is prone to bone resorption. (O'Brien et al, 1998). High levels of insulin are also linked to low bone mineral density (Sayers et al, 2012). Here, FCS contained the highest level of insulin and didn’t allow for the highest level of mineral deposition. Human serum with low insulin levels did. Thus, insulin levels in serum may be an important factor for osteogenic differentiation in MSCs.

Fetal bovine serum is more commonly utilised in cell culture supplementation than human serum. For this reason, Vetsch and colleagues (2015) studied the impact of four different FBS types on the mineralisation of acellular and cell-seeded silk fibroin (SF) scaffolds. The results presented that spontaneous mineralisation on SF scaffolds with certain FBS types, was observed even in acellular conditions. Furthermore, cell-mediated mineralisation was only detected under osteogenic conditions but the ion composition was the same for both types of mineralisation. The research provides clear evidence for the influence of FBS type on mineralisation but highlights that FBS medium supplementation can reduce reproducibility of results due to batch variability.

4.3.3 Chondrogenic Differentiation

Chondrogenic differentiation of MSCs is usually achieved in serum-free conditions because serum has been shown to inhibit cartilage formation (Lee et al, 2009). Here cartilage development was assessed in a number of ways. Dimethylmethylene blue (DMMB) assays were used to test for the presence of the glycosaminoglycan (GAG) chondroitin sulfate (Templeton, 1988). Serum-free chondrogenic and chondrogenic samples with 5-Day exposure to FCS samples exhibited the highest levels of GAGs. Proliferative control samples with FCS, and chondrogenic samples with 5-Day exposure to Seralab^{TM} HS had lower levels of expression. The data suggests that it is feasible to achieve proteoglycan synthesis in transient-FCS conditions but not with transient-HS.

Additional Safranin-O staining for proteoglycans in cartilage pellets and, immunostaining for Collagen II and SOX9 expression were successfully achieved in serum-free chondrogenic samples. However, staining could not be demonstrated with transient exposure to serum. Collagen II is a major protein in cartilage and levels can be associated with intensities of chondrogenic differentiation (Johnstone et al, 1998). SOX9 is present after MSC condensation and has a primary function in collagen production (Akiyama et al, 2002; DeLise et al, 2000). Therefore, it is unexpected that the proteins were absent in transient-serum regimes, when successful cartilage differentiation was demonstrated via proteoglycan synthesis. FCS is good for chondrocyte culture but not for the differentiation of MSCs into chondrocytes (Tallheden et al, 2005). Enhanced chondrogenesis has been achieved with HS (Chua et al, 2007) and this indicates that the presence of serum is not an issue for cartilage culture, as long as stem cells are already committed to chondrogenic lineages.

4.4 Summary

HS supports a highly proliferative MSC population that avoids the risks associated with FCS culture. Rates of osteogenic differentiation are higher using HS compared to FCS culture. Significantly, all known studies comparing FCS with autologous HS have similar conclusions as described in this investigation (Mizuno et al, 2006). However, HS is expensive and can have batch variation leading to unreliable results, as indicated in this study. Furthermore, obtaining sufficient quantities of HS from an autologous donor is difficult (Lange et al, 2007). In addition to this, it was demonstrated that chondrogenesis in MSCs could be achieved with transient exposure to FCS but not HS. Further analysis is required. Although serum is important for good viability and differentiation of MSCs, cells can survive in transient-serum conditions, but express reduced proliferation and differentiation rates. Alternative solutions to FCS and HS include the use of human platelet lysate (Perez-Ilzarbe et al, 2009) or serum-free defined medium (Lange et al, 2007). Serum content analysis here, has shown that high levels of alkaline phosphatase and 25-Hydroxyvitamin D could enhance osteogenic differentiation of MSCs. It is important to keep levels of cortisol and insulin low because they are linked to bone resorption. This study provides evidence that the use of HS is a feasible alternative to FCS.

5. Production of Bi-layered Chitosan Scaffolds

5.1 Introduction

In recent years, with a progressively ageing population, diseases of the joint such as osteoarthritis and rheumatoid arthritis have become more common (Vater et al, 2011). There has also been a sharp increase in the number of joint-related injuries, due to more active lifestyles in the population. At present, such injuries are treated using a number of therapies, including surgical repair, transplantation of artificial devices and drug therapy (Martins et al, 2009). For more details see Section 2.4 *Tissue Engineering and Osteochondral Repair*. Osteochondral pathologies are an obvious challenge for the near future and there is a clear demand for alternative regenerative therapies for joint trauma (Pound et al, 2007).

The majority of research relating to regenerative medicine is conducted in a 2D environment to allow easy culture and good cell viability. However, culture in 2D may misrepresent *in vivo* conditions required for the generation of tissues (Mazzoleni et al, 2009). In particular, 2D culture *in vitro* lacks the architecture that ECM provides *in vivo,* and the vasculature required for regulated transport of nutrients to cells.

Constructs for cell seeding, known as scaffolds, can present more physiological culture conditions for cells by providing an artificial 3D environment for tissue development (Thein-Han et al, 2008). Scaffolds for developing osteochondral constructs, such as sponges, fibers and gels, are made from a variety of polymers, including chitosan (Muzzarelli, 2009a). For more details, see Section 2.4.2 *Properties of Effective Osteochondral Constructs/ Scaffolds.*

Chitosan is a polysaccharide obtained from the exoskeletons of crustaceans (Wang & Stegemann, 2011). It is the second most abundant polysaccharide after cellulose and has potential uses in ‘wound healing, drug delivery systems, bone filling and regeneration, and tissue engineering of cartilage and bone’ (Sendemir-Urkmez & Jamison, 2007). Chitosan promotes cell adhesion, proliferation and differentiation (Muzzarelli, 2011), while it shows biocompatibility, biodegradability by lysozyme (controlled by level of deacetylation) (Shi et al, 2006) and anti-inflammatory/ antibacterial properties (Wang & Stegemann, 2011).

Although, chitosan can promote chondrogenesis due to a fundamental structure related to GAGs (Chondroitin sulfates) in cartilage, the material lacks the mechanical strength necessary in initial bone development (Malafaya et al, 2007).

The aim of this investigation was to explore a model, and possible alternative therapy for osteochondral injuries. Tissue constructs made from chitosan, represent such a therapeutic strategy where the ability to support the differentiation of human mesenchymal stem cells (hMSCs) into osteoblast and chondrocyte lineages, in a single scaffold would be desirable. To date, osteochondral repair strategies have relied on separate scaffolds for bone and cartilage, before they are combined as single a graft (Martin et al, 2007). These implants often fail due to delamination. In addition to this, the current project intends to overcome problems associated with specific differentiation medium requirements for each lineage by providing scaffolds with spatially resolved environments, each supportive of one of these cell lineages. More specifically, this research aims to produce a scaffold with graduated porosity and the capacity to regulate stem cell differentiation (Duan et al, 2014; Karageorgiou & Kaplan, 2005a). An important distinction is that whereas cultures aimed at osteogenic lineages include the use of sera, such as foetal calf serum (FCS)(Vater et al, 2011), culture protocols for *in vitro* chondrogenesis are fundamentally serum-free. The work reported here describes the influence of porogen type on the production of bi-layered, chitosan scaffolds containing two distinct pore sizes to control mesenchymal stem cell differentiation into osteogenic and chondrogenic lineages. Furthermore, a comparison of scaffolds that are cross-linked with glutaraldehyde and genipin is investigated to maximise biocompatibility.

5.2 Results

5.2.1 Chitosan Scaffold Development

In the development of an osteochondral construct for joint repair, a 3D cell culture environment is required and this can be achieved by seeding MSCs onto a biomaterial scaffold. This section describes how a suitable scaffold was produced from chitosan.

A number of different scaffolds were manufactured from chitosan (Figure 5.1). A preliminary study was performed to find the optimum concentration of glutaraldehyde solution for the cross-linking of chitosan. A range of glutaraldehyde concentrations between 0.1-1% were tested, and it was concluded that 4 ml of 0.5% glutaraldehyde solution was most suitable because it allowed the chitosan to set in a relatively quick time (20 minutes). This was also sufficient time for air bubbles caused by the production process, to escape before the chitosan had completely set. Further preliminary studies compared setting times of 4% and 5% chitosan solutions. 4% chitosan was chosen because 5% solutions proved to be too viscous and air bubbles were formed, which led to uncontrolled scaffold porosity (data not shown).

The chitosan material is derived from the shells of crustaceans living in the sea. For this reason, the material is naturally polluted with heavy metal ions and this can have cytotoxic effects. For this reason, before scaffold development began, the chitosan powder was filtered in a sulphuric acid column to remove heavy metal residues (Ozer, 2007). Untreated chitosan stained black with Remazol Blue dye (Santos et al, 2008). However, the same material did not stain after the heavy metals were removed. It was also important to wash away all sulphuric acid deposits after the treatment cycle because any acid bound to the chitosan prevented the full dissolution of the material. This problem was identified when the chitosan began to sediment during the making of chitosan solutions from powder (data not shown).

The first chitosan scaffolds were made from 4% chitosan, 4 ml of 0.5% glutaraldehyde solution and, 300-425 µm and 180-300 µm polycaprolactone granules. These scaffolds were frozen directly after the second layer was poured and left to set in a -20 °C freezer for 72 hours.

This length of time proved to be too extensive because when individual scaffolds were cut out (Figure 5.2), the pores were enlarged and deformed due to obvious ice crystal formation. It was also established that the chitosan had to be fully cross-linked at room temperature before it could be frozen.

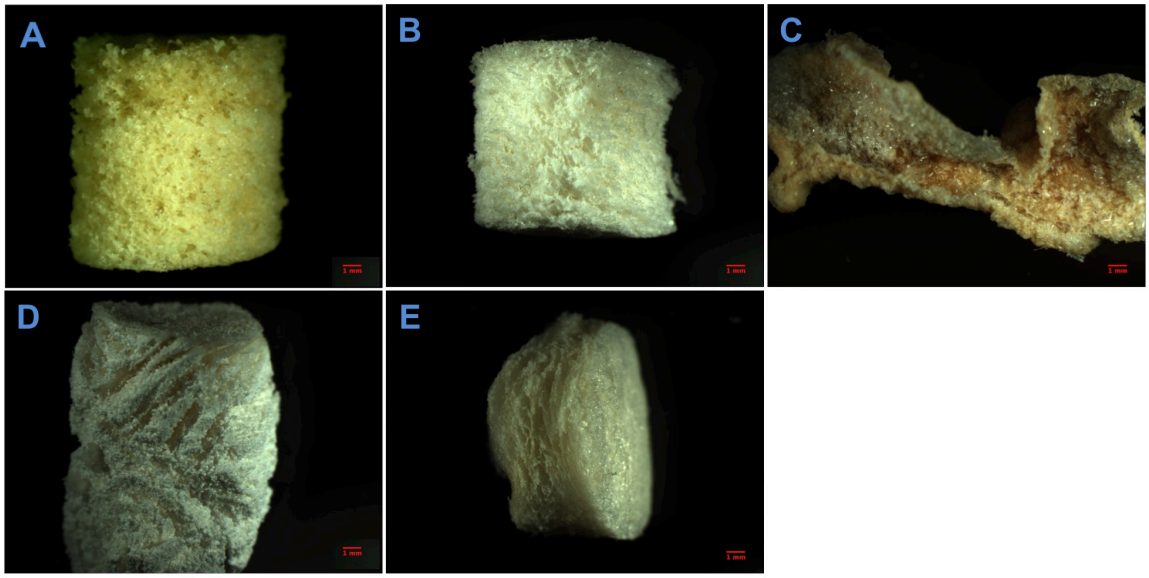

Figure 5.1 Bi-layered chitosan scaffold preparation and post-crosslinking processing. (A) 4% chitosan scaffold produced with 0.5% glutaraldehyde solution and, 180-300 µm and 300-425 µm polycaprolactone (PCL) granules as porogen. (B) Chitosan scaffold produced with 2.5X more glutaraldehyde solution than scaffold (A) and, 180-300 µm and 300-425 µm PCL particles. (C) Scaffold [A] after treatment with 8% (w/v) glutamic acid in 0.5 m HCl for 24 hours. This was intended to reduce cytotoxicity by removing any free aldehyde groups in the scaffolds. (D) Chitosan scaffold produced with glutaraldehyde solution and, 180-300 µm and 300-425 µm poly-hydroxy-byruvate (PHBV) porogen particles, instead of PCL. (E) Chitosan scaffold produced with 2X less glutaraldehyde solution than scaffold (A) and, 180-300 µm and 300-425 µm PCL particles. Scale bar represents 1 mm.

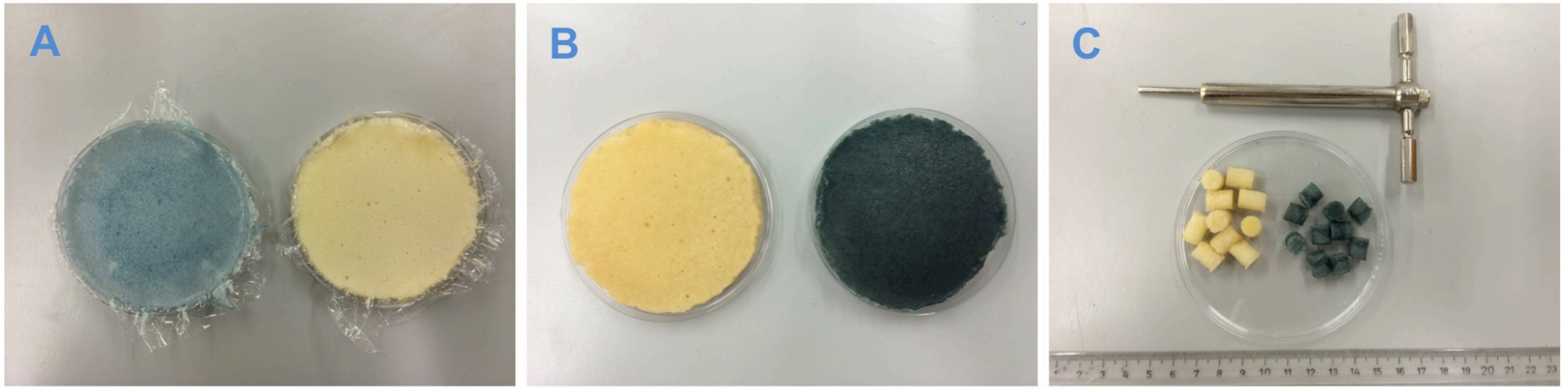

Figure 5.2 Production of bi-layered chitosan scaffolds for osteochondral modelling and repair. (A) 4% chitosan solutions are mixed with either 0.5% glutaraldehyde (yellow) or 1% genipin (green/ blue) crosslinking solutions. 180-300 µm and 300-425 µm PCL porogen particles are added and mixed solutions are poured into petri dishes for crosslinking at room temperature. (B) Mixtures in [A], 24 hours after crosslinking began. (C) Individual scaffolds are cut-out using a sharp core borer tool.

Subsequently, the second chitosan scaffold batch was made in the same way as the first, except these scaffolds were allowed to fully set at room temperature. Then, they were frozen in a -20 °C freezer overnight, to prevent significant ice crystal formation. These scaffolds appeared suitable for the culturing of cells until the scaffolds were treated with glutamic acid to tie up free, cytotoxic aldehyde groups from the glutaraldehyde cross-linking solution (Figure 5.1C).

At one stage of the scaffold development, due to low stocks of polycaprolactone, it was suggested that an alternative material should be used as a porogen. 300-425 μm and 180-300 μm particles of poly-hydroxy-byruvate (PHBV) were tested (Figure 5.1D). The different molecular weight of PHBV to polycaprolactone meant that 60 g of chitosan had to be mixed with the PHBV porogen (instead of the suggested 20 g in the Materials and Methods) to achieve a similar consistency in solution. In the end, the construct that was produced was found to be of a powdery consistency, not suitable for a scaffold. Furthermore, the PHBV porogen could not be extracted using potassium hydroxide.

The initial protocol proposed that scaffolds are soaked in 8% (w/v) glutamic acid diluted in 0.5 M hydrochloric acid for 24 hours (Mann & Weiner, 1999). However, the scaffolds initially swelled-up and later started to dissolve in the acidic solution. Figure 5.1C shows the dimensional instability of these chitosan scaffolds after they were treated and dried in a fume hood. To alleviate this issue, the same manufacturing process was repeated. However, this batch of scaffolds was treated with less concentrated cell culture L-glutamine to tie up free aldehyde groups. These scaffolds were successfully treated. However, it was decided that a stronger reducing agent would be more efficient at reducing cytotoxicity.

For this reason, another batch of scaffolds was treated for 1 hour in 1% $NaBH_4$. FTIR analysis of chitosan treated with either L-glutamine or $NaBH_4$ confirmed that the latter was more efficient at reducing aldehyde groups, thereby reducing cytotoxicity (Figure 5.3). The scaffolds reduced in 1% $NaBH_4$ were chosen for seeding and culturing of human MSCs.

In addition to this, chitosan scaffolds were produced with PCL microspheres. This aimed to establish if pore characteristics could be better controlled with uniform spheres instead of granules as porogen material. It should be noted that all the chitosan scaffolds produced in this investigation had high elasticity (spongy texture) and were easily compressed.

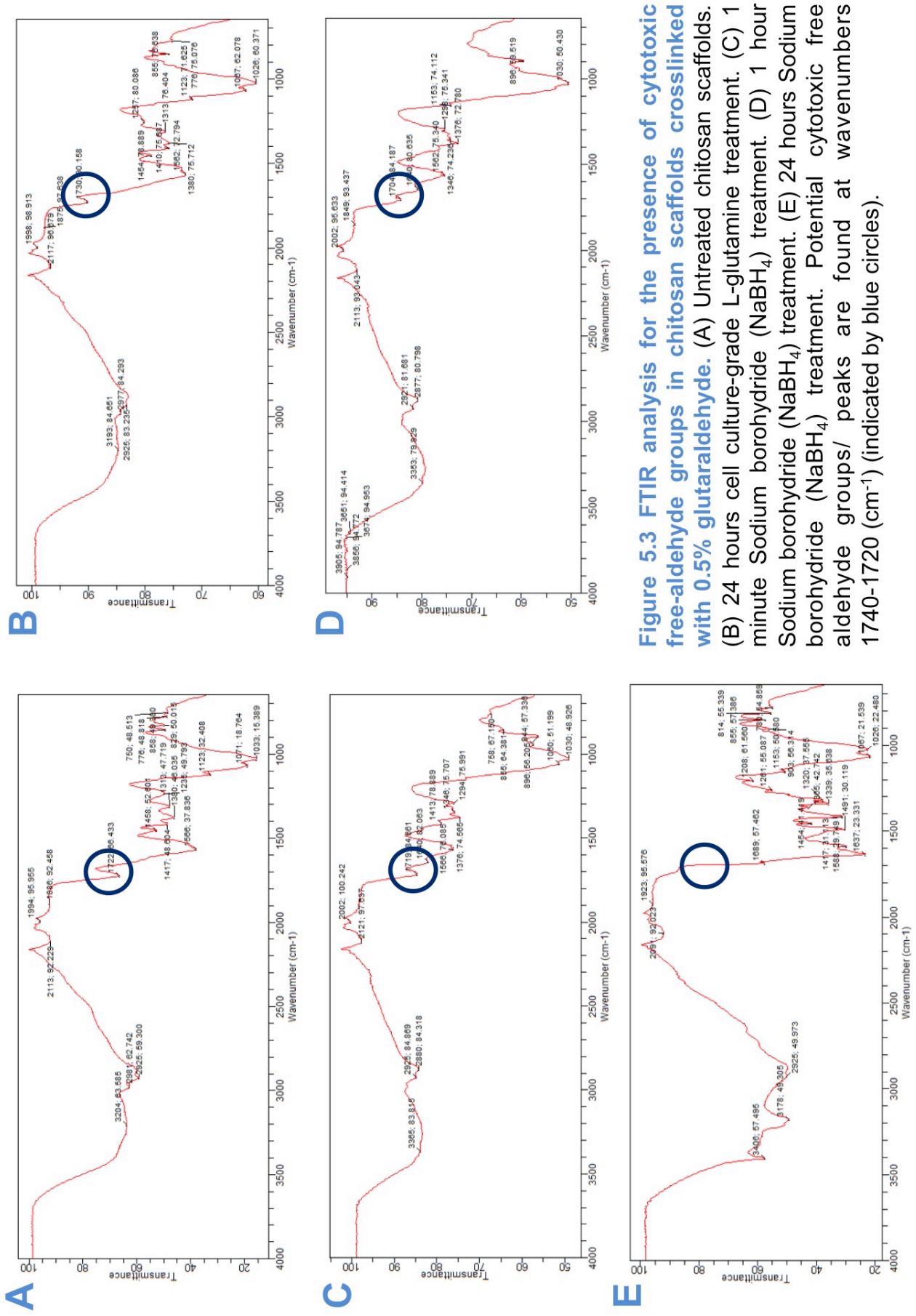

Figure 5.3 FTIR analysis for the presence of cytotoxic free-aldehyde groups in chitosan scaffolds crosslinked with 0.5% glutaraldehyde. (A) Untreated chitosan scaffolds. (B) 24 hours cell culture-grade L-glutamine treatment. (C) 1 minute Sodium borohydride ($NaBH_4$) treatment. (D) 1 hour Sodium borohydride ($NaBH_4$) treatment. (E) 24 hours Sodium borohydride ($NaBH_4$) treatment. Potential cytotoxic free aldehyde groups/ peaks are found at wavenumbers 1740-1720 (cm^{-1}) (indicated by blue circles).

5.2.2 Characterisation of Scaffold Porosity

The final chitosan scaffold batches produced with PCL granules (Figure 5.5A) and PCL microspheres (Figure 5.5B) were characterised in terms of pore morphology, size, interconnectivity and overall porosity. To investigate this, 5 scaffolds made with each of the two porogen-types were cut in half, mounted and sputter coated with platinum for SEM imaging. It was determined that chitosan scaffolds require weeks to fully dry, due to their strong affinity to water. Problems were encountered during the coating process as the argon molecules in the sputter coater caused the molecules in the damp chitosan scaffolds to be excited. This prevented the sputter coater from generating the required vacuum, and platinum from being deposited on the surface of the chitosan. A solution to this setback was to freeze-dry the chitosan in a vacuum for 2 hours before coating.

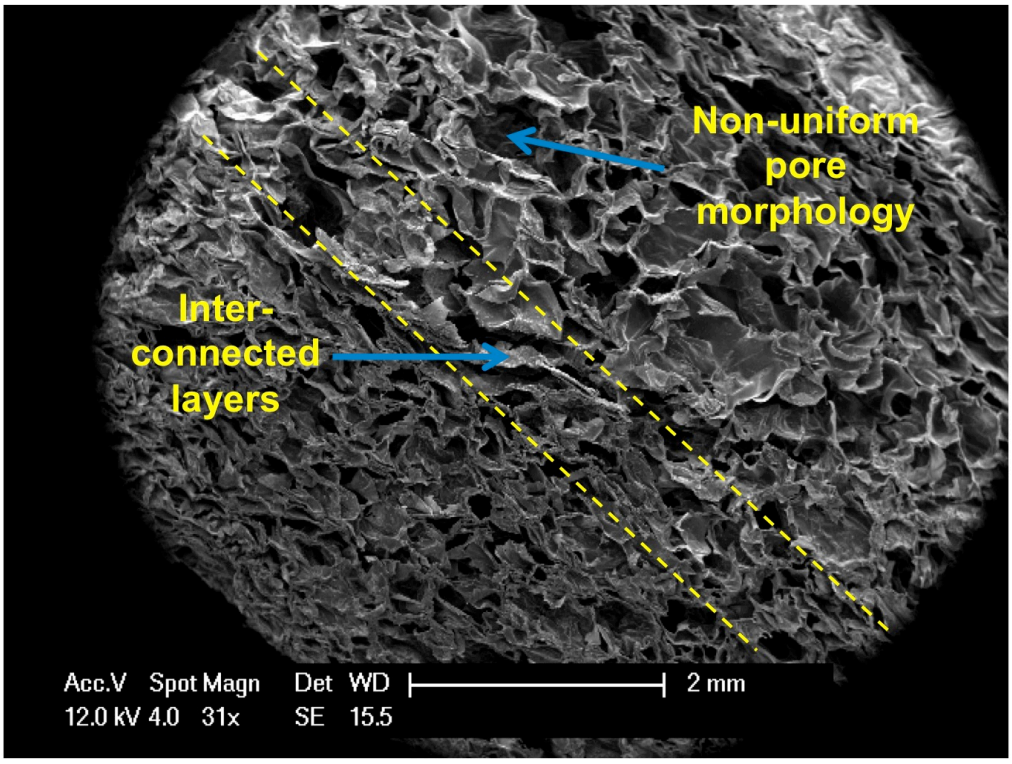

Figure 5.4. SEM image of bi-layered chitosan scaffold prepared with PCL granules as porogen. Cross-section shows dual porosity with 180-300 µm pores for the chondrogenic section of the scaffold, and 300-425 µm pores for the osteogenic region. The image highlights inter-connectivity between layers and non-uniform pore morphology when PCL granules are used for scaffold production

Once coated, scanning electron microscopy (SEM) was used to determine the pore sizes and morphologies within the scaffold. Figure 5.4 shows that there were pores present throughout the whole cross-section of the chitosan scaffolds, and that pores were relatively evenly distributed. The scaffolds were intended to have large 300-425 µm pores at one half and small 180-300 µm pores at the other half of the chitosan. Importantly, there are midsections within the scaffold where large and small pores were inter-connected (Figure 5.4). This same fundamental structure was also observed in scaffolds manufactured with PCL microspheres. However, pore size was more uniform with microspheres than with PCL granules.

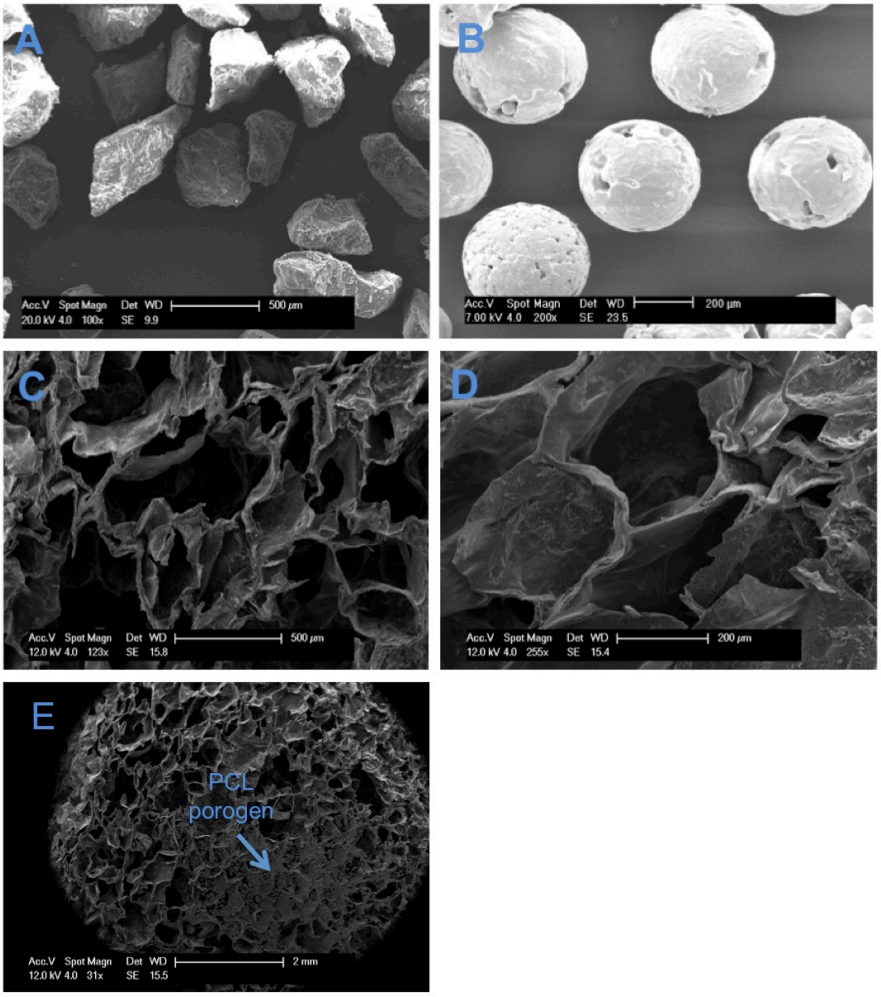

Figure 5.5 SEM analyses of chitosan scaffold pore size and morphology. (A-B) Polycaprolactone (PCL) porogen particles used in the production of bi-layered chitosan scaffolds for osteochondral modelling and repair. (A) PCL granules lead to non-uniform pore morphology in scaffolds (C). (B) PCL microspheres with uniform shape allow for more spherical/ controlled pore structure (D). (E) Scaffold core showing un-extracted PCL porogen after a 4-hour treatment with Potassium hydroxide solution [highlighted by arrow].

SEM imaging highlighted that pores within the scaffold produced with PCL granules were deformed. It was proposed that the compressive forces experienced by the spongy scaffolds, during scaffold cutting and trimming (Figure 5.2), caused this deformation. An attempt to resolve this included the soaking of scaffolds in phosphate buffer saline (PBS), freezing to expand the pores and drying in a vacuum. The method did not work since the pores shrunk again, once the scaffolds were exposed to atmospheric pressure. It was determined that the non-uniform nature of the granule porogen (Figure 5.5A) was the primary cause for deformed pores.

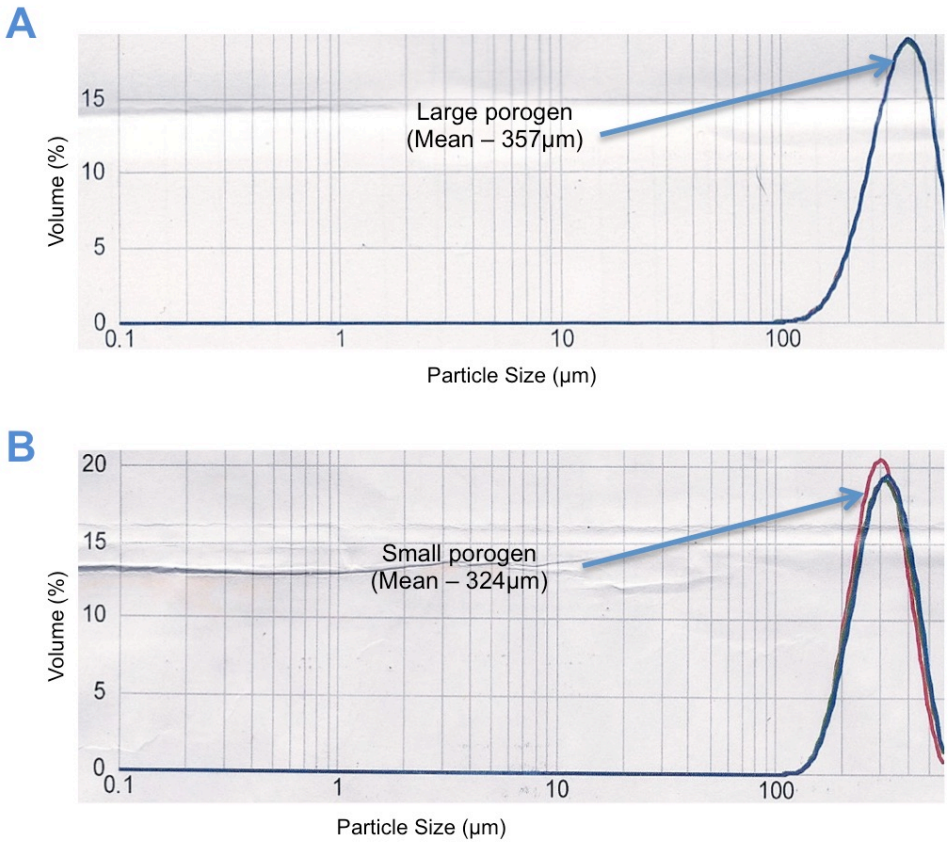

Figure 5.6 Particle size distribution of PCL granular porogen assessed using a Malvern Mastersizer 3000 laser diffraction particle size analyser. (A) PCL granules considered in the 300-425 µm size range after sieving. (B) PCL granules considered in the 180-300 µm size range after sieving.

Laser diffraction particle size analysis of the PCL granules suggested that these particles had a broad size-distribution (Figure 5.6) due to their non-uniform morphology. This problem was not observed when PCL microspheres were used as the porogen because these particles had a very uniform morphology, as illustrated in Figure 5.5B. Significantly, the compressive forces experienced by the spongy scaffolds, during scaffold cutting and trimming, did cause further deformation.

X-ray micro computed tomography (microCT) was utilised to evaluate the porosity of scaffolds produced with PCL granules and microspheres. Notably, this analysis showed that all scaffolds were at least 70% porous (Table 5.1), and that the porosity in scaffolds produced with porogen granules was slightly higher than with microspheres (Table 5.1). This correlated with the SEM observation of slightly larger, non-uniform pores when PCL granules are employed. Furthermore, three-dimensional image reconstruction pointed out that some of the polycaprolactone porogen had not been fully extracted from the scaffold cores. This was also illustrated via SEM analysis (Figure 5.5E). The observation changed the protocol of the porogen extraction time to be extended from 2 hours to 4 hours.

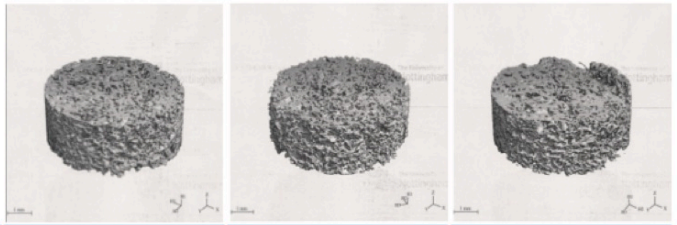

		Bottom	Middle	Top
Glutaraldehyde	% Porosity	74	73	73
	Pore size (µm) ± StDev	287 ± 10.5	232 ± 17.4	196 ± 5.9
Genipin	% Porosity	72	72	71
	Pore size (µm) ± StDev	302 ± 7.2	239 ± 19.8	189 ± 3.2

Table 5.1 Summary of X-ray micro-computed tomography (Micro-CT) analysis. Reconstruction images and quantification of the bottom, middle and top sections of chitosan scaffolds cross-linked with either 0.5% glutaraldehyde or 0.3% genipin. N=5. Segmentation parameters using Scanco Medical µCT 40 – Sigma: 0.7 Support: 1 Threshold: 30.

5.2.3 Genipin Cross-linking

After batches of chitosan scaffolds were successfully produced with glutaraldehyde cross-linking, alternative cross-linking procedures were investigated to identify less cytotoxic reagents, in an attempt to increase scaffold cytocompatibility. For this reason, a new batch of scaffolds was produced with the same PCL microsphere porogen and genipin as a cross-linking agent, instead of glutaraldehyde (Figure 5.7) (Muzzarelli, 2009b; Silva et al, 2008). SEM analysis showed that these scaffolds had the desired pore sizes (data not shown), while microCT scans of the genipin scaffolds indicated 72% average porosity and more uniform pore characteristics than in scaffolds produced with glutaraldehyde (Table 5.2). Genipin scaffolds were also shorter than glutaraldehyde ones. Furthermore, a colour change was noticeable when the chitosan had been completely cross-linked with genipin, as the material changed from yellow to blue/ green (Figure 5.8). Cross-linking time was estimated using time-lapse imaging and it took around 15 hours for cross-linking to occur when a 0.3% genipin solution was used (Figure 5.9). Although a range of genipin concentrations was tested (0.15% and 0.3%), time-lapse imaging was not a quantitative method for predicting the rate of chitosan cross-linking. Rheological analysis demonstrated that chitosan cross-links in 1.5 hours with 0.5% glutaraldehyde, and in around 18 hours with 0.3% genipin (Figure 5.10).

Further, by sourcing genipin from a cheaper supplier in China, it was possible to produce genipin scaffolds using a 1% cross-linking solution. Compared to the 0.3% concentration initially used, scaffolds were cured in 4 hours instead of 18 hours. This was a very important advance because it alleviated issues of porogen sedimentation due to slow cross-linking rates.

A

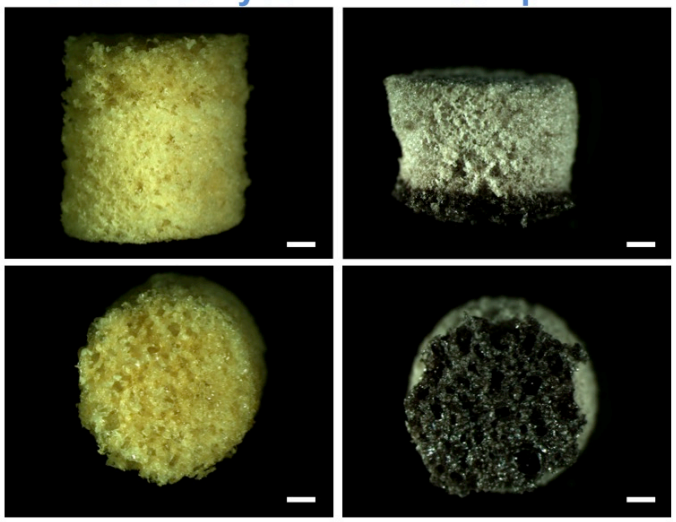

B

Glutaraldehyde	Genipin
Industrial organic compound	Biological compound
High toxicity	Low toxicity
Targets amine groups	Targets amine groups
Crosslinks chitosan in <1 hour (0.5%)	Crosslinks chitosan in ~24 hours (0.4%)
No colour change	Blue colour change
Autofluorescence	Autofluorescence
Poor stiffness	Improved stiffness
Cheap	Very expensive

C

Gardenia jasminoides

Figure 5.7 Alternative crosslinkers in the production of bi-layered chitosan scaffolds for osteochondral modelling and repair. (A) 4% chitosan scaffolds produced with 180-300 µm pores for chondrogenic differentiation of human mesenchymal stem cells (hMSCs), and 300-425 µm pores for osteogenesis. Scaffolds were either crosslinked with 0.5% glutaraldehyde solution (yellow scaffolds) or 0.3% genipin (blue scaffolds). Dark pigmentation indicates porogen sedimentation, due to slow crosslinking rate. (B) Table comparing the properties of glutaraldehyde and genipin crosslinkers. (C) Genipin is derived from South-East Asian plant, *Gardenia jasminoides*. Scale bar represents 1 mm.

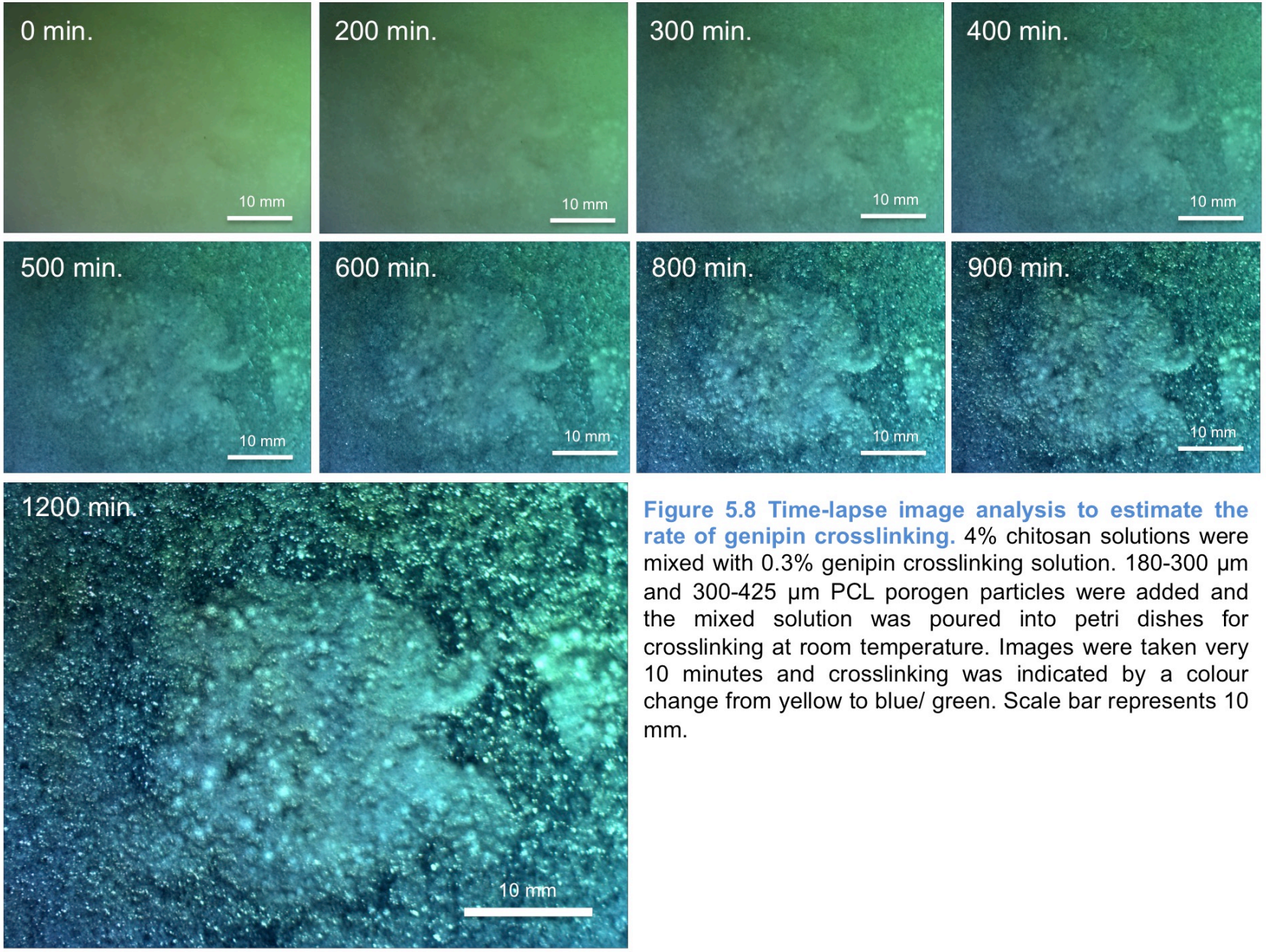

Figure 5.8 Time-lapse image analysis to estimate the rate of genipin crosslinking. 4% chitosan solutions were mixed with 0.3% genipin crosslinking solution. 180-300 µm and 300-425 µm PCL porogen particles were added and the mixed solution was poured into petri dishes for crosslinking at room temperature. Images were taken very 10 minutes and crosslinking was indicated by a colour change from yellow to blue/ green. Scale bar represents 10 mm.

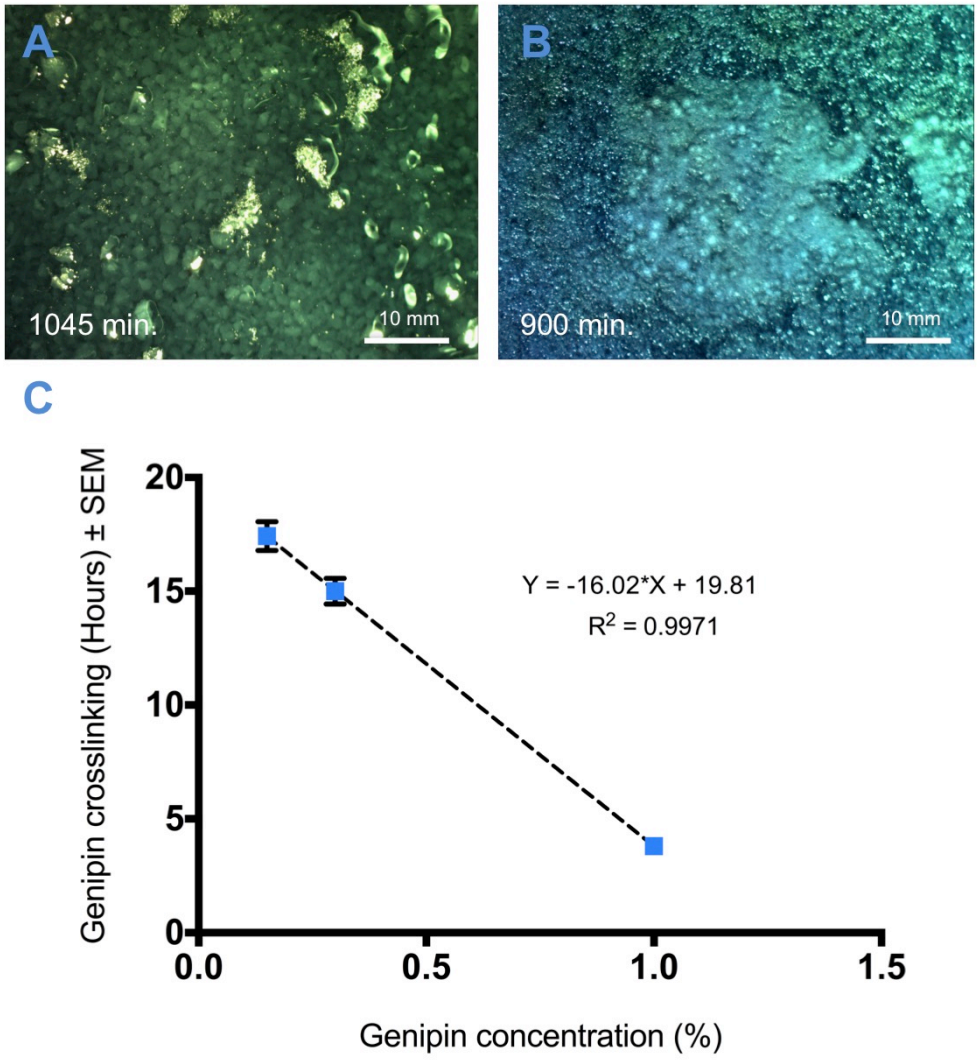

Figure 5.9 Rate of chitosan crosslinking with a range of genipin concentrations. (A) Endpoint image after crosslinking a 4% chitosan solution with 0.15% genipin.180-300 µm and 300-425 µm PCL porogen particles were added and the mixed solution was poured into petri dishes for crosslinking at room temperature. (B) Endpoint image after crosslinking a 4% chitosan solution with 0.3% genipin. Images were taken very 10 minutes and crosslinking was indicated by a colour change from yellow to blue/ green. Scale bar represents 10 mm. (C) Linear regression analysis showing the rate of chitosan crosslinking with 0.15%, 0.3% and 1% genipin solutions.

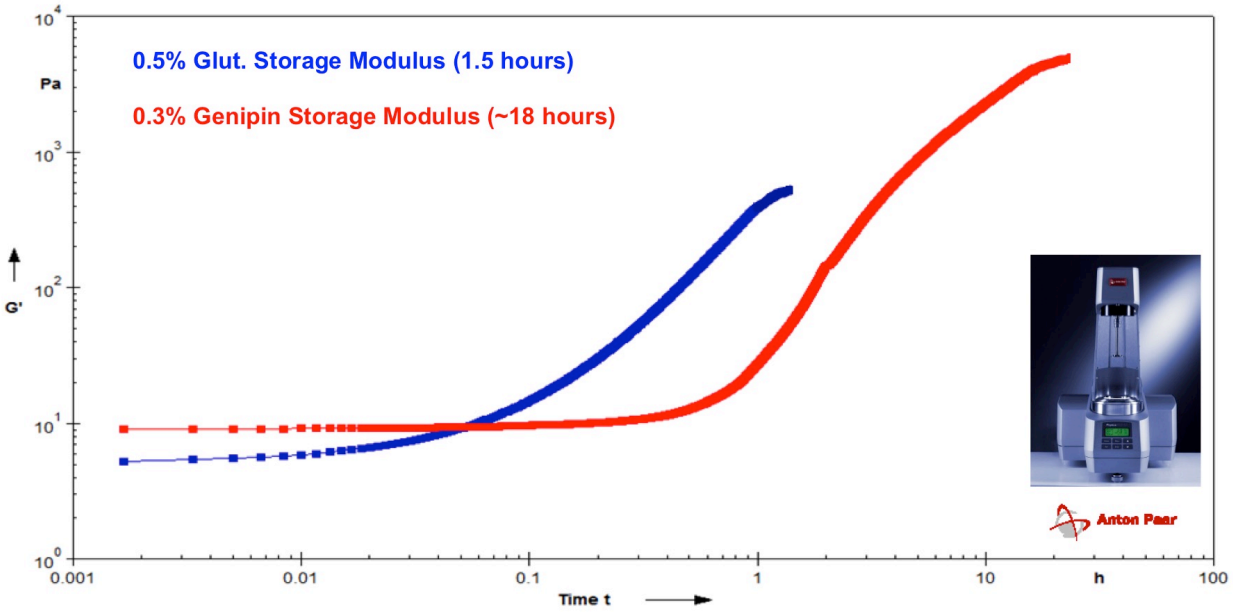

Figure 5.10. Quantification of the rate of chitosan cross-linking with 0.5% glutaraldehyde and 0.3% genipin solutions. The storage modulus (G')/ viscosity of 4% chitosan solutions was measured over 24 hours to assess the rate of cross-linking with glutaraldehyde and genipin. G' was measured using an Anton Paar MCR series rheometer and PP50-SN11649 attachment. All measurements were conducted at 20 °C. N=3.

5.2.4 Chitosan Degradation

A degradation study of chitosan scaffolds cross-linked with 0.5% glutaraldehyde was conducted over a 52-week period to assess the biodegradability potential of the constructs (Figure 5.11A). Scaffolds (n=5) were placed in cell culture media at 37 °C. Scaffold weight and medium pH were recorded at regular intervals. In the first 7 weeks of the experiment, scaffolds significantly increased in weight from 40 mg to 370 mg. Over the remainder of the degradation experiment, the chitosan scaffolds gradually decreased in weight to around 70 mg at week 52. Importantly, this was higher than the weight of the scaffolds at the beginning of the study. In terms of cell culture medium pH, a drop from 7.3 to 4.9 was observed over the 52-week study.

A

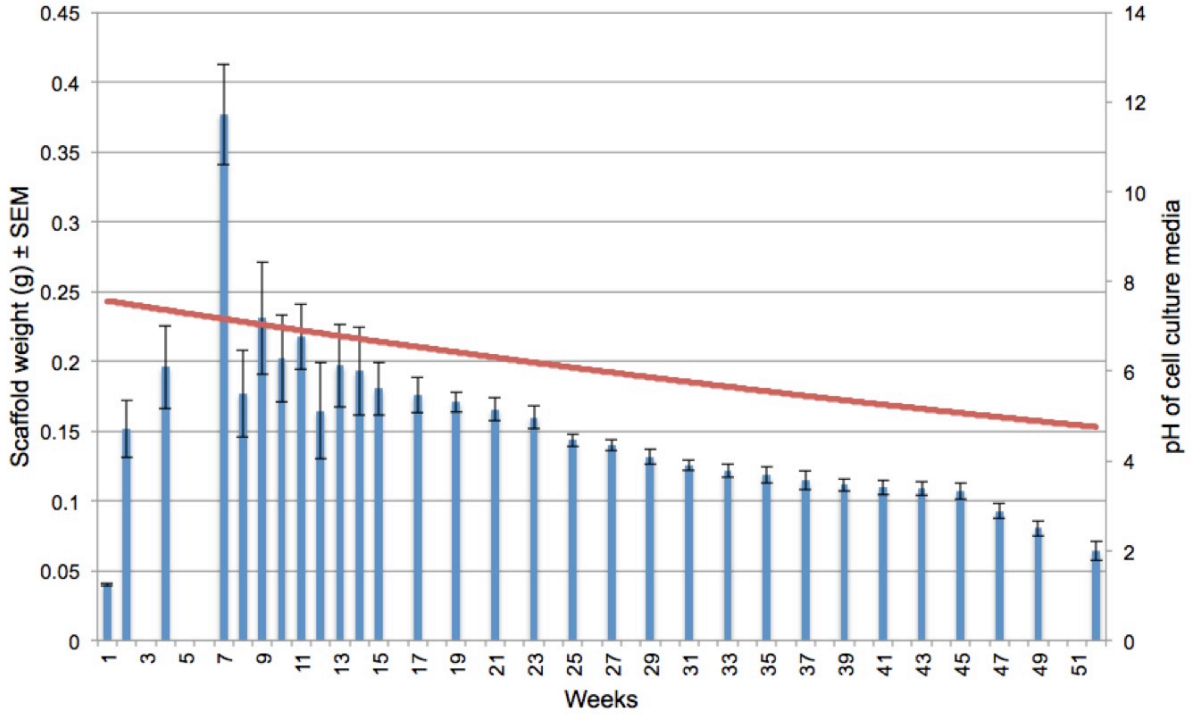

B

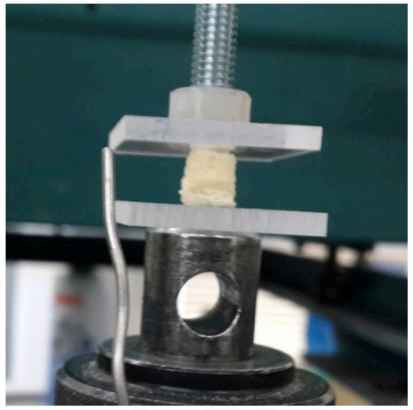

C

	Scaffold Young's Modulus (MPa)		
	0.5% Glutaraldehyde	0.3% Genipin	Native Cartilage
Dry	0.241 ± 0.12	0.493 ± 0.08	0.45 to 0.8 [1]
Wet	0.019 ± 0.01	0.032 ± 0.01	

Figure 5.11 Assessing the physical properties of bi-layered chitosan scaffolds for osteochondral modelling and repair. (A) 52-week degradation study of chitosan scaffolds crosslinked with 0.5% glutaraldehyde. Degradation was conducted in cell culture media at 37°C. Scaffold weight and media pH were recorded at each time point. N=5. (B) Mechanical test rig used to measure stress and strain in chitosan scaffolds. (C) Table showing the Young's Modulus (MPa) of chitosan scaffolds crosslinked with either 0.5% glutaraldehyde or 0.3% genipin. Scaffolds were tested both dry and wet. N=3. [1] (Mansour, 2013. *Biomechanics of cartilage.*)

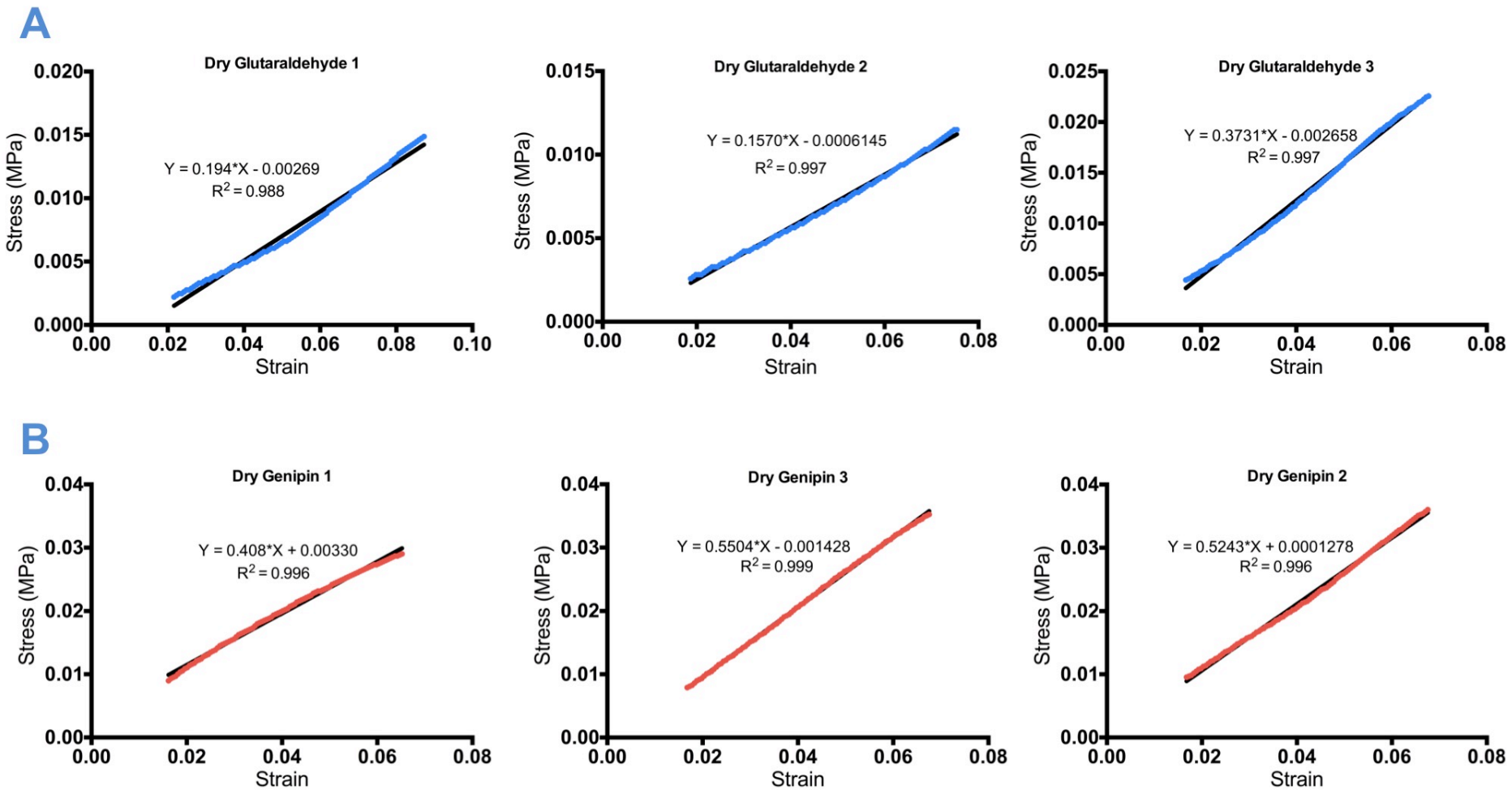

Figure 5.12 Compression testing of dry bi-layered chitosan scaffolds for osteochondral modelling and repair. Stress (MPa) against strain curves of chitosan scaffolds crosslinked with either (A) 0.5% glutaraldehyde or (B) 0.3% genipin. N=3.

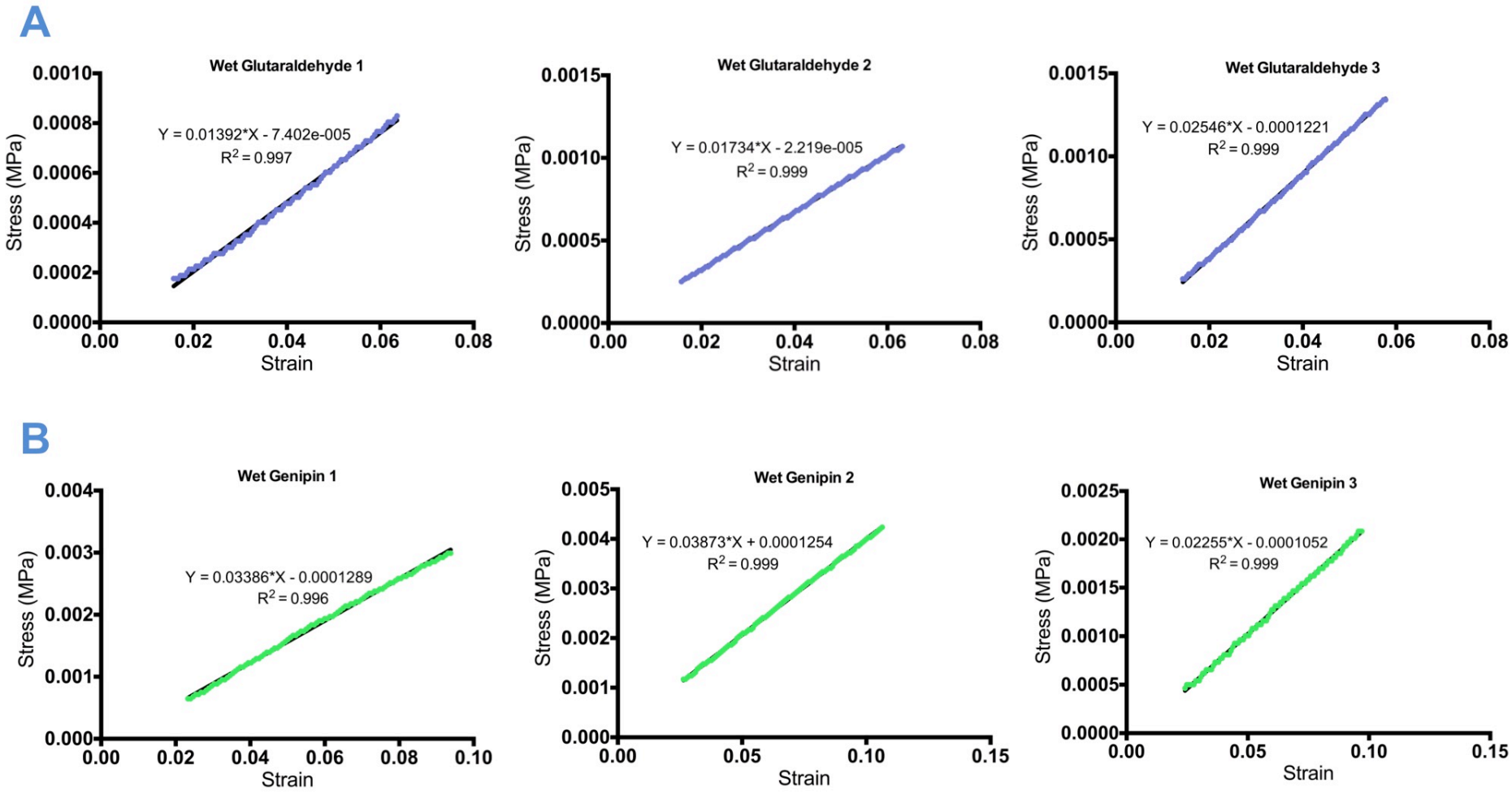

Figure 5.13 Compression testing of wet bi-layered chitosan scaffolds for osteochondral modelling and repair. Stress (MPa) against strain curves of chitosan scaffolds crosslinked with either (A) 0.5% glutaraldehyde or (B) 0.3% genipin. Scaffolds were wetted in PBS for 1 hour before testing. N=3.

5.2.5 Scaffold Compression Testing

Compression testing of scaffolds produced with 0.5% glutaraldehyde and 0.3% genipin was completed (Figure 5.11B). Note: all scaffolds were tested in their elastic region. The results of the mechanical tests indicated that dry genipin scaffolds have a Young's modulus of 0.493 ± 0.08 MPa; this was about twice that observed in glutaraldehyde scaffolds (0.241 ± 0.12 MPa) (Figure 5.11C). The compressive moduli for both types of scaffolds were lower than in native cartilage tissue (0.45-0.8 MPa)(Mansour, 2013). Once pre-wetted, the scaffold stiffness was significantly reduced. The modulus in genipin scaffolds dropped to 0.032 ± 0.01 MPa, while in the glutaraldehyde scaffolds the mechanical strength dropped to 0.019 ± 0.01 MPa. Detailed stresses against strain curves are also shown for both dry (Figure 5.12) and wet (Figure 5.13) scaffolds. Additionally, scaffolds produced with 1% genipin appeared to withstand compressive forces better than scaffolds cross-linked with 0.3% genipin (data not shown).

The compression results did not express the true moduli of the chitosan scaffolds because the conditions assumed that a solid, non-porous material was tested. All constructs were over 70% porous and only ~30% was chitosan. The true modulus of the chitosan was calculated with:

$$\frac{E^*}{E} = p^2$$

The formula is used to calculate the true Young's modulus in porous materials using the apparent modulus and porosity values (Straffelini et al, 1999). E^* is the apparent modulus, E is the true modulus and p is the fraction of chitosan material presented as a decimal. Table 3.2 shows the true moduli of the chitosan scaffolds cross-linked with glutaraldehyde or genipin.

Cross-linker	*p*	*E** (MPa)	*E* (MPa)
0.5% Glutaraldehyde *(Dry)*	0.27	0.214	2.936
0.5% Glutaraldehyde *(Wet)*	0.27	0.019	0.261
0.3% Genipin *(Dry)*	0.28	0.493	6.288
0.3% Genipin *(Wet)*	0.28	0.032	0.408

Table 5.2 True and apparent of compressive moduli of chitosan scaffolds. Compassion of chitosan scaffolds cross-linked with 0.5% glutaraldehyde or 0.3% genipin. All scaffolds were compression tested dry and wetted in PBS for 1 hour. E^* is the apparent modulus, E is the true modulus and p is the fraction of chitosan material presented as a decimal. N=3.

5.2.6 Scale-up of Microsphere Production

Following the success in improved morphology of the scaffold by using a spherical porogen it became important to develop a scale-up method to deliver sufficient amounts in a practical time scale. Therefore, the manufacturing process based on an emulsion method for the PCL microsphere porogen was modified, to improve efficiency and allow for the scale-up of scaffold production. The original methodology worked well but did not produce sufficient quantities of microspheres to allow fast production of scaffolds. From every 1 g of PCL only 0.63 g is utilised, and the maximum capacity was 5 g at any one time. The first step was to improve the capacity of the porogen manufacturing process. This was achieved by using 5 litre glass vessels instead of the 600 ml beakers that were initially employed. Automated syringe pumps were also added instead of manual pipettes for the droplet formation process.

Different setups were tested to allow the scale-up of the PCL microsphere/ porogen production. Spin speed, needle bore size and the concentration of PCL/ PVA were shown to be crucial for the efficient production of spheres in the 180-300 μm and 300-342 μm ranges (Figure 5.14). Higher concentrations in the continuous phase (PVA solution from 0.3% to 0.6%) or dispersion phase (PCL in dichloromethane from 24% to 48%) led to a greater proportion of microspheres in the smaller, <300 μm range.

However, the concentration of the continuous phase had a greater effect by producing nearly 50% more spheres in the 180-300 μm range than in the 300-425 μm sizes.

Needle bore size and spin speed also exhibited effects on microsphere size. Higher gauge needles with smaller diameter bores produced smaller porogen particles (Figure 5.14). In addition to this, smaller microspheres were principal at higher spin speeds. Figure 5.15 shows the experimental setup for the scale-up of PCL microsphere production.

In summary, using larger vessels increased the capacity of microsphere production. Automation also improved the efficiency of the process. The original manual method led to 63% useful porogen, while automation using identical parameters produced 80.2% of useful microspheres. The highest proportion of both 180-300 μm and 300-425 μm PCL spheres was attained in the 0.3% PVA, 24% PCL and 16 Gauge needle batch.

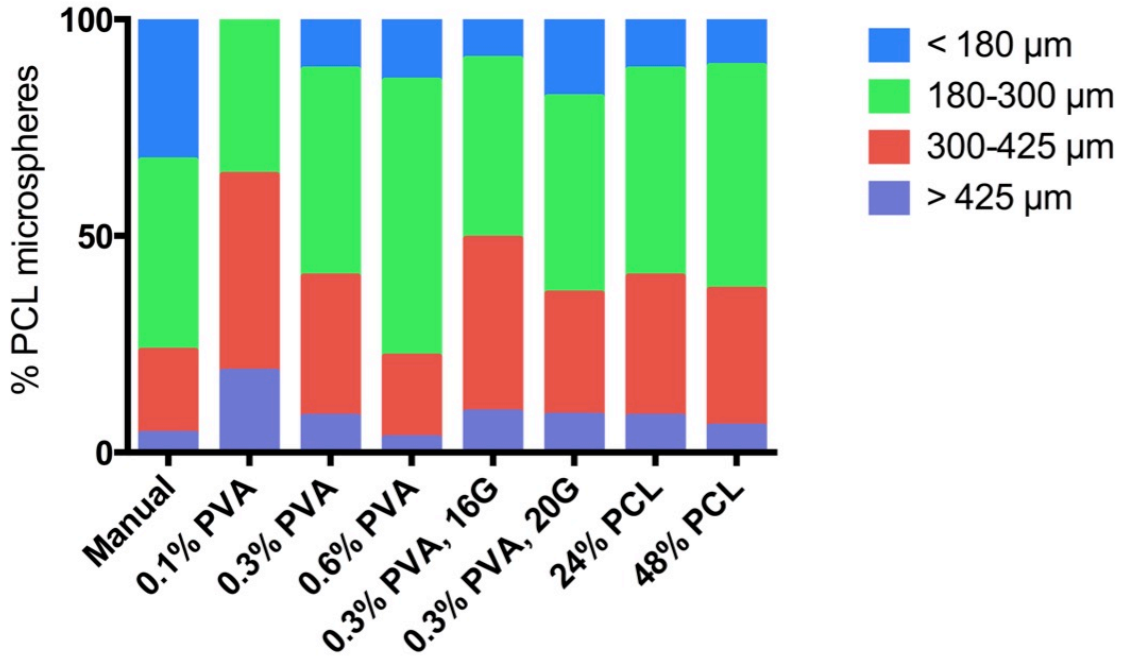

Figure 5.14. Batch yield and method comparison in the production of polycaprolactone (PCL) microspheres as porogen material for bi-layered chitosan scaffolds. The percentage of PCL microspheres in the <180 µm, 180 µm, 300 µm and 425 µm porogen size ranges was measured by sieving and weighing. Batches produced using a range of methodologies were compared. The Manual batch refers to the original production method where 600 ml glass beakers were used. For this, 24% PCL was added drop-wise using a manual pipette, to a 0.3% polyvinyl alcohol (PVA) solution and stirred for 3 hours at 400 rpm. All other batches were scale-up attempts in 5 litre glass vessels with a rotor-stirring blade. PCL droplet formation was automated using syringe pumps for more efficient and controlled droplet formation. The name of each batch refers to the variable that was altered from the original production method.

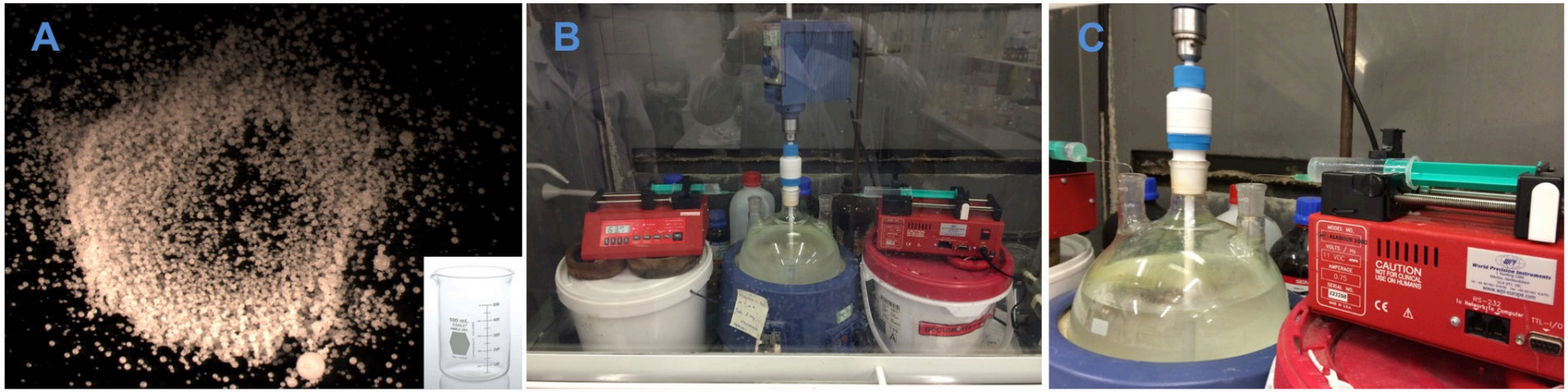

Figure 5.15 Scale-up in the production of polycaprolactone (PCL) microspheres as porogen material for bi-layered chitosan scaffolds aimed at osteochondral modelling and repair. PCL microspheres were produced by dissolving the porogen material in dichloromethane (24% v/w), before it was added drop-wise to a 0.3% polyvinyl alcohol (PVA) solution and stirred for 3 hours at 400rpm. (A) Initial methods for production of PCL porogen microspheres with 600ml glass beakers demonstrated limited production efficiency. (B) Glass beakers were replaced with 5 litre glass vessels with a rotor stirring blade to increase the manufacturing rate of porogen material. (C) Syringe pumps allowed for more efficient and controlled droplet formation.

5.3 Discussion

In regenerative therapies, chitosan scaffolds can provide the necessary biodegradability, together with anti-inflammatory and, toxin- and allergen-free characteristics (Abarrategi et al, 2010). For many years, chitosan has also been explored as a possible protein and drug delivery system (Illum, 1998). Together, these features can significantly accelerate the recovery time of patients.

In this project, an integrated bi-layered scaffold suitable for seeding mesenchymal stem cells was successfully developed from chitosan. This novel construct, which offers a progressive transition from a bone-like to a cartilage-like architecture, is degradable, amenable to scaled-up production, and can be combined with bioactive substances to further enhance its therapeutic potential as a surgical implant.

The methodology is readily adaptable without the necessity for complex equipment and can be scalable with no limit to thickness and cross sectional area. More importantly graded functionality can be easily achieved without the instability typically associated with the combination of distinct layers for each osteochondral lineage. This is important as the performance of current commercially available collagen-based scaffolds aimed at joint repair suffer delamination failure upon arthroscopic delivery (Fonseca et al, 2014; Tuan et al, 2013).

Chitosan also resolves concerns associated with commercially available collagen scaffolds for osteochondral repair, which rely on bovine or equine components (Moran et al, 2015). Xenogeneic collagen scaffolds run a potential risk of generating antigenic responses or facilitating disease transmission, despite the use of processing routes designed to alleviate such possibilities.

5.1.1 Glutaraldehyde and Genipin Cross-linking

Cross-linking is an important aspect of developing tissue engineered constructs from hydrogels because the process can significantly improve the stability and mechanical strength of the biomaterials (Lutolf et al, 2003; Peppas et al, 2006). Initially in this study, glutaraldehyde was used to cross-link the chitosan hydrogels. Chitosan is commonly cross-linked in this manner via interaction between primary amine or hydroxyl groups in the chitosan (Campos et al, 2013), and aldehyde groups in the glutaraldehyde cross-linker (Poon et al, 2014).

The bonds are stabilised by resonance with the adjacent ethylenic double bonds (Monteiro & Airoldi, 1999). However, this cross-linking reaction leads to cytotoxic properties in the biomaterial due to the presence of free aldehyde groups (Sung et al, 1999; Wang & Stegemann, 2011). Glutaraldehyde has also been demonstrated to increase scaffold autofluorescence and this is a major limitation for visualising cell seeding (Baschong et al, 2001).

To alleviate these potential cytotoxic effects, scaffolds were treated with L-glutamine to tie-up any free aldehyde groups (Karadeniz & Astley, 2013). The results here indicated that cell culture L-glutamine was not effective at neutralising these cytotoxic groups. Citric acid was identified as an alternative treatment to improve cell attachment after glutaraldehyde cross-linking but acidic conditions are detrimental to chitosan (Gulbins et al, 2003). This is because protonated amino groups on glucosamine increase the solubility of the chitosan polymer (Thein-Han et al, 2008). For this reason, aldehyde groups in scaffolds were successfully reduced with $NaBH_4$ (AbdelMagid et al, 1996). Interestingly, NaBH4 is most commonly used for hydrogen evolution and fuel cell applications (Amendola et al, 2000; Moon et al, 2008).

Even though cytotoxicity in the chitosan scaffolds was successfully reduced with $NaBH_4$, it is desirable to utilise cross-linking reagents with no initial cytotoxicity. Here we demonstrated that genipin is a suitable cross-linker of chitosan (Silva et al, 2008; Yan et al, 2010). The main advantages of genipin are that it is a naturally derived compound, with no cytotoxicity at low concentrations. The cross-linker provides stable bonds via the same mechanisms as glutaraldehyde (Muzzarelli, 2009b). Additionally, genipin can mildly enhance the mechanical properties of chitosan more than glutaraldehyde (Jin et al, 2004) and provides visual confirmation of cross-linking with a colour change. It was demonstrated that the compressive moduli of genipin cross-linked scaffolds is nearly double that observed when glutaraldehyde is used.

A significant drawback in using genipin is the cost involved; it is very expensive when used in higher concentrations that allow fast cross-linking times. In this study, low genipin concentrations (≤0.3%) led to problems in scaffold production because the PCL porogen was able to sediment over time. This is a significant drawback in producing scaffolds with spatially resolved microenvironments, however the issue was resolved when 1% genipin was tested.

Unfortunately the use of genipin, like that of glutaraldehyde, also caused scaffold autofluorescence (Chen et al, 2005), which may complicate the cellular characterisation procedures when using biological components for tissue engineering approaches. Other cross-linker alternatives such as β–glycerophosphate have also been used for scaffold production (Wang & Stegemann, 2010), and could be further tested alongside genipin to evaluate their respective performance.

5.1.2 Scaffold Compression Testing

All chitosan scaffolds produced were spongy and did not have the mechanical strength required for skeletal tissue engineering. In this study it was established that wet chitosan scaffolds cross-linked with genipin (0.408 MPa) had a higher compressive modulus than scaffolds cross-linked with glutaraldehyde (0.261 MPa). The Young's modulus in native articular cartilage is in the range of 0.45-0.8 MPa (Mansour, 2013). Additionally, higher concentrations of cross-linker tolerated compressive forces better than constructs produced with lower concentrations of cross-linker. Mechanical strength can further be increased by using chitosan with higher deacetylation, although biodegradability rates will decrease (Thein-Han et al, 2008).

The most popular methods of increasing mechanical strength in chitosan are based on composites materials (Karageorgiou & Kaplan, 2005b). Incorporating hydroxyapatite or calcium phosphate into chitosan can improve the mechanics as well as the osteoconductive properties of the material (Moreau & Xu, 2009). This can be achieved in the bi-layered scaffolds produced here, simply by mixing the fillers into the chitosan hydrogels before cross-linking (preliminary data not shown). Importantly, β-tricalcium phosphates are preferential to hydroxyapatites because they exhibit bioresorbable properties (Mathieu et al, 2006). Significantly, the level of improvement is highly dependent on the method used to incorporate the fillers (Reves et al, 2012).

5.1.3 Chitosan Degradation

An important characteristic of constructs for osteochondral repair is controlled biodegradability, where the whole implant can be replaced with native tissue as the site of injury regenerates. Notably in this investigation, the chitosan scaffolds cross-linked with glutaraldehyde failed to degrade after 1 year. Within the first few weeks, scaffolds increased in weight. This can be explained by the well documented swelling and adsorptive properties of chitosan. Fundamentally, it is suggested that the scaffolds adsorbed proteins from the cell culture media (Amidi et al, 2010). Later in the degradation experiment, scaffold weight did decrease but never below the initial weight. Scaffolds cross-linked with genipin were not assessed for degradation, but other groups have shown that genipin leads to slower degradation compared to glutaraldehyde (Mi et al, 2001).

Producing scaffolds from chitosan with an increased degree of deacetylation can increase the rate of degradation (Pillai et al, 2009). The chitosan used here had a deacetylation degree of 84%, which is reported to have a weight half-life in excess of 84 days (Ren et al, 2005). The literature further suggests that the degradation rate of the scaffolds produced here, may be accelerated *in vivo*, due the presence of lysozymes (Tomihata & Ikada, 1997).

5.1.4 Characterisation of Scaffold Porosity

Pore size and porosity are important factors in the differentiation of MSCs (Karageorgiou & Kaplan, 2005b). Most importantly, the distribution of pores requires greater control to support the differentiation of MSCs into osteoblasts and chondrocytes within different parts of the same scaffold. Similar work, where differentiation was controlled by pore size, has been described by (Oliveira et al, 2006) and (Chen et al, 2011).

Oliveira (2006) produced scaffolds with open inter-connected pores in the range of 50-350 μm. Osteogenesis was identified in the hydroxyapatite layer after 14 days and chondrogenesis was detected after 21 days. Notably, the researchers did not attempt to attain both lineages within the same construct and there is no mechanical testing.

It is believed that smaller scaffold pores provide low oxygen tension, which has been proven to regulate the chondrogenic differentiation of MSCs (Lennon et al, 2001). Furthermore, smaller pores allow cells to grow in confined spaces and this is similar to condensation of MSCs during *in vivo* chondrogenesis (Goldring et al, 2006). More details on the effects of scaffold porosity and pore size on differentiation of cells can be found in Sections 2.3.1.2 Topographical Stimuli and 2.4.2.1 Pore Size and Porosity.

The scaffolds produced here with PCL granules as porogen, had pores in the appropriate size ranges. There were large (300-425 μm) pore regions for osteogenesis and smaller (180-300 μm) pores for chondrogenesis. However, pores were deformed and not spherical. When PCL microspheres were applied, scaffolds showed more uniform pore characteristics. Likewise, an increase in mechanical strength of the chitosan scaffold would prevent further pore deformation during the forming process of individual scaffolds. Cutting scaffolds out before the PCL porogen is extracted with potassium hydroxide, is a partial resolution to this problem. Significantly, it has been recently presented that more uniform, rounder pores improve MSC proliferation and differentiation on biomaterial surfaces (Tunesi et al, 2013).

5.1.5 Scale-up of Microsphere Production

Due to the importance of controlled scaffold porosity, a method for producing PCL microspheres in a coordinated manner has been developed to improve the quality and efficiency of scaffold fabrication. In brief, dissolving PCL in dichloromethane solvent and adding this drop-wise to a PVA solution produced microspheres (Luciani et al, 2008). The size distribution of the microspheres was controlled by the stirring speed (Corrin et al, 2012). Faster speeds produced smaller particles.

Initially, it was very time consuming to produce sufficient quantities of particles in the 180-300 μm and 300-425 μm size ranges. For every 20 g of PCL in the method, less than 5 g were useful microspheres. Nonetheless, a major advantage of the emulsion protocol was that the microspheres that were not in the correct size range could be recycled.

Regardless, it was important to improve the efficiency of the fabrication method and this was successfully achieved via scale-up and automation. Larger vessels and stirring rotors were utilised instead of magnetic stirrers, to increase the yield to 63% useful porogen. Automation of droplet formation further improved efficiency to 80%.

The porogen technique used in this project is based on solvent casting/ particle leaching. This involves the dispersion of porogen with controlled particle size into a polymer solution (Yang et al, 2006).The method strengthens the polymer to produce a polymer-porogen network. Finally, the porogen particles are leached, or dissolved in a solvent to produce a porous network (Johnson et al, 2010). Although the leaching of PCL is employed, the literature shows that there are many other options (Smith et al, 2009).

Free-drying also known as lyophilisation, has been widely used for the fabrication of porous hydrogels (Deville, 2008). In this technique, rapid cooling of polymers causes thermodynamic instability and phase separation to create pores (Kang et al, 1999). (O'Brien et al, 2004) improved on conventional freeze-drying processes and created scaffolds with more defined pore characteristics. This was achieved by employing homogeneous freezing and the tight control over the rate of freezing during fabrication. Unfortunately, freeze-drying does not allow the control necessary to create bi-layered pore structures for osteochondral applications.

Dense gas foaming with CO_2 exploits the idea that the CO_2 gas is a fluid when above its critical temperature and pressure (Annabi et al, 2010). Furthermore, the physical properties of CO_2 in those conditions are intermediate to those of a true gas or liquid. However, this technique is not suitable for chitosan because dense gas CO_2 has a low solubility in hydrophilic polymers. It is more suitable for hydrophobic polymer scaffolds such as PLA, PLGA and PCL (Tai et al, 2007).

Finally, additive manufacturing and 3D printing techniques are becoming increasingly popular in all aspects of life, including the fabrication of macro-porous scaffolds for tissue engineering applications (Habibovic et al, 2008). In one recent example, (Petrochenko et al, 2015) manufactured porous scaffolds via the two-photon polymerisation (2PP) of biodegradable urethane and acrylate-based photoelastomer, with porosities greater than 60%. Most significantly, printing techniques permit the design and fabrication of scaffolds, which a considered to be structurally ‘perfect’.

5.2 Summary

A number of different dual porosity scaffolds were produced from chitosan, aimed at osteochondral modelling and repair. The work here demonstrates that PCL microspheres used as porogen allowed improved control of scaffold porosity and pore size, compared to PCL granules. This close control is important in order to achieve dual porosity within the scaffold, and provide differential environments for MSC differentiation towards osteogenic and chondrogenic lineages. In addition to this, two different cross-linking agents were tested. Although more difficult to use due to longer cross-linking times, genipin was able to generate scaffolds with improved mechanical strength compared to glutaraldehyde. The mechanical properties could be further improved by using higher concentrations of genipin, and this would also alleviate problems associated with slow cross-linking rates. Scaffolds cross-linked with glutaraldehyde failed to biodegrade in 1 year *in vitro*, while genipin scaffolds were not tested here. Significantly, it is suggested that genipin scaffolds degrade more slowly than glutaraldehyde (Jin et al, 2004; Muzzarelli, 2009b). For this reason, detailed degradation profiles of both scaffold-types need to be attained in future. Additionally, further analysis is required to assess the biocompatibility of the scaffolds and their suitability for osteochondral repair. This can be found in Section 6 *Assessing scaffold biocompatibility in a perfusion bioreactor system*.

6. Assessing Scaffold Biocompatibility in a Perfusion Bioreactor System

6.1 Introduction

As previously described, chitosan is suitable for osteochondral defect repair because it displays chondroinductive properties and can be produced in a range of geometries/ scaffolds (Elder et al, 2013). These desirable properties make the biomaterial appropriate for implantation in a variety of regenerative therapies, including bone and cartilage repair, and intervertebral disc surgery (Di Martino et al, 2005).

Tissue engineered scaffolds act as an interim synthetic extracellular matrix (ECM) that cells interact with prior to forming a new tissue (Smith et al, 2009). The success of constructs for tissue regeneration and 3D culture depend on a number of factors including:

- Good initial cell seeding (Sobral et al, 2011);
- Optimal nutrient supply to prevent necrotic core formation in scaffolds (Vunjak-Novakovic et al, 1998);
- Biocompatibility and no biomaterial-induced cytotoxicity (Smith et al, 1992);
- Chemical, topographical and mechanical cues to promote MSC differentiation (Caplan & Bruder, 2001), including biomimicry (Lu et al, 2010).

Scaffolds with spatially resolved environments (different pore sizes) were produced to support both osteogenic and chondrogenic differentiation of mesenchymal stem cells (see Section 5 *Production of bi-layered chitosan scaffolds*). This study investigated procedures to maximise cell-seeding efficiencies and determined the biocompatibility of the different chitosan scaffolds using human mesenchymal stem cells. A novel perfusion bioreactor system was used to optimise nutrient supply and investigate whether graded scaffold pore size can support osteochondral differentiation of mesenchymal stem cells. Furthermore, the bioreactor was designed to enhance osteogenic differentiation by applying mechanical shear stress to one half of scaffolds.

6.2 Results

6.2.1 Chitosan Biocompatibility

The biocompatibility of a range of chitosan scaffolds was assessed after seeding with human mesenchymal stem cells. Proliferation was monitored in scaffolds cross-linked with either glutaraldehyde or genipin, using an inverted light microscope and cell metabolic activity was quantified using the PrestoBlue™ assay at day 7 (Figure 6.1). As well as displaying improved pore morphology (Figures 6.1A and 6.1B, and also see Section 5 *Production of bi-layered chitosan scaffolds*), genipin scaffolds allowed for higher metabolic activity compared to scaffolds cross-linked with glutaraldehyde ($p<0.00005$) (Figure 6.1C). Importantly, cell metabolism in genipin scaffolds was similar to the levels observed in tissue culture plastic.

In an attempt to decrease the cytotoxic effects of glutaraldehyde, scaffolds were treated with either L-glutamine or $NaBH_4$ to reduce any free aldehyde groups in the biomaterial. Afterwards, cell viability was measured using the neutral red assay (Figure 6.2). In this assay, culture media was conditioned with the different scaffolds before MSCs were cultured in each medium for 24 hours. The level of neutral red uptake into the lysosomes/ endosomes and vacuoles of live cells correlated with their viability. For all the cultures treated with chitosan-conditioned media, cell viability was above the 70 % threshold for cytotoxicity. A small but non-statistically significant increase in viability was observed between untreated chitosan scaffolds and ones treated with L-glutamine (Figure 6.2). Significant differences were found between control scaffolds and $NaBH_4$-treated material ($p<0.001$). The positive control, phenol-conditioned cultures, had viability below 40% and this was significantly lower than any of the chitosan-conditioned cultures ($p <0.00005$).

6.2.2 Cell Imaging

It is desirable to be able to monitor cells after seeding onto scaffolds and during prolonged periods of culture. In this study, it was important to confirm that MSCs had successfully attached to the bi-layered chitosan scaffolds before osteochondral differentiation was initiated.

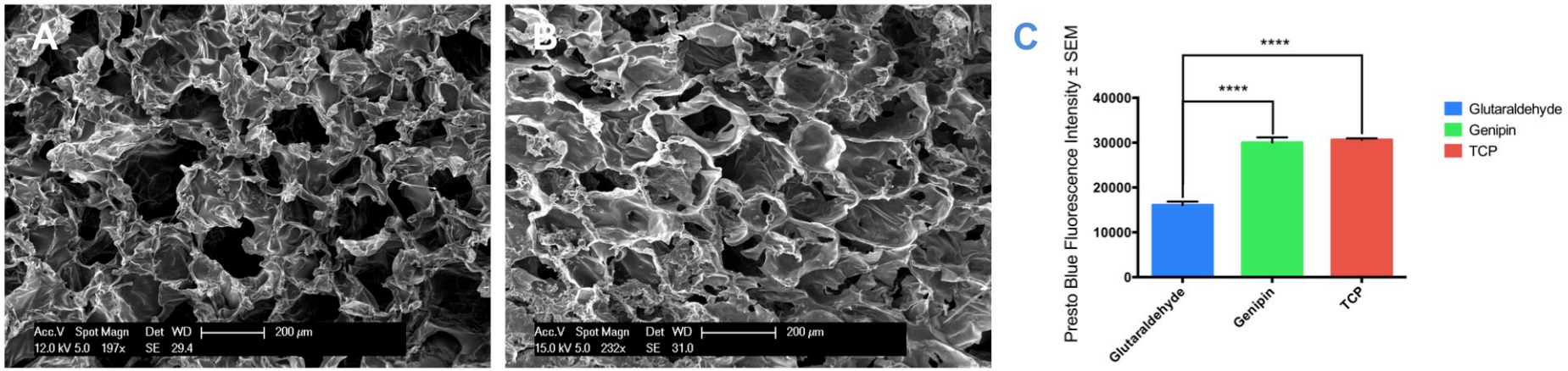

Figure 6.1 Comparison of chitosan scaffolds cross-linked with either glutaraldehyde or genipin. (A and B) SEM images of pore morphology in scaffolds cross-linked with 0.5% glutaraldehyde [A] and 0.3% genipin [B]. (C) Day 7 Presto Blue™ metabolic assay for hMSCs cultured on glutaraldehyde and genipin cross-linked chitosan scaffolds, and tissue culture plastic. n=9. ****<0.00005 significance threshold after ANOVA analysis with Tukey post hoc tests, comparing different scaffolds at the same time point.

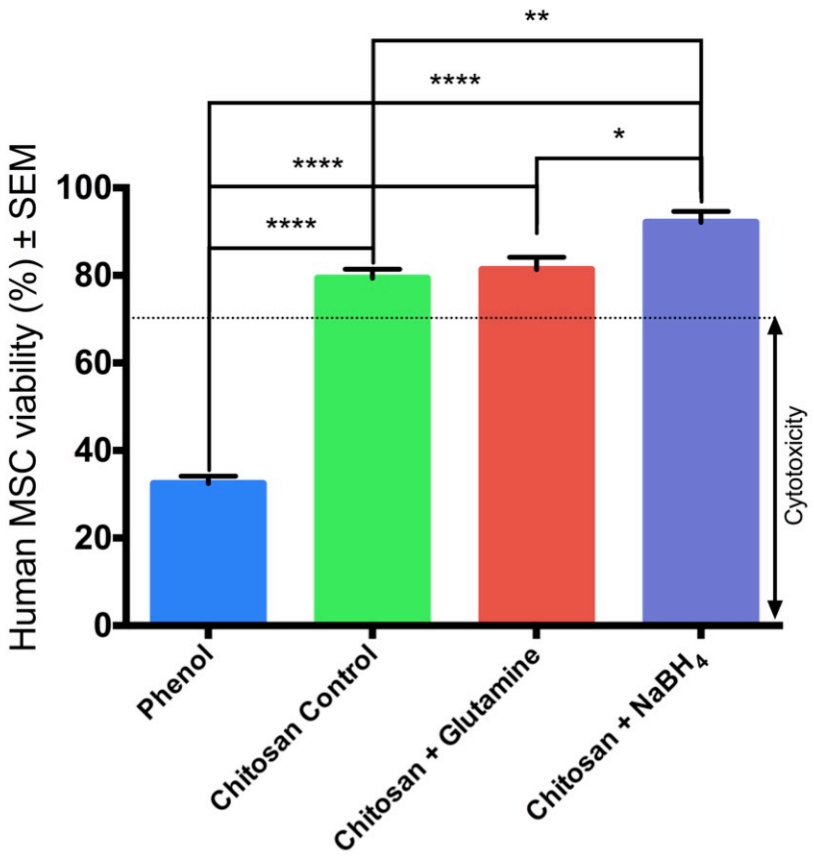

Figure 6.2 Biocompatibility of chitosan scaffolds cross-linked with glutaraldehyde. The viability of human mesenchymal stem cells after 24 hours culture in chitosan-conditioned media. Media was condition with untreated, glutamine-treated and $NaBH_4$-treated chitosan scaffolds. Phenol was used as a positive control. Cytoxicity is defined at viability levels below 70%. N=4. *<0.05, **<0.005 and ****<0.00005 significance threshold after ANOVA analysis with Tukey post hoc tests, comparing different scaffold treatments at the same time point.

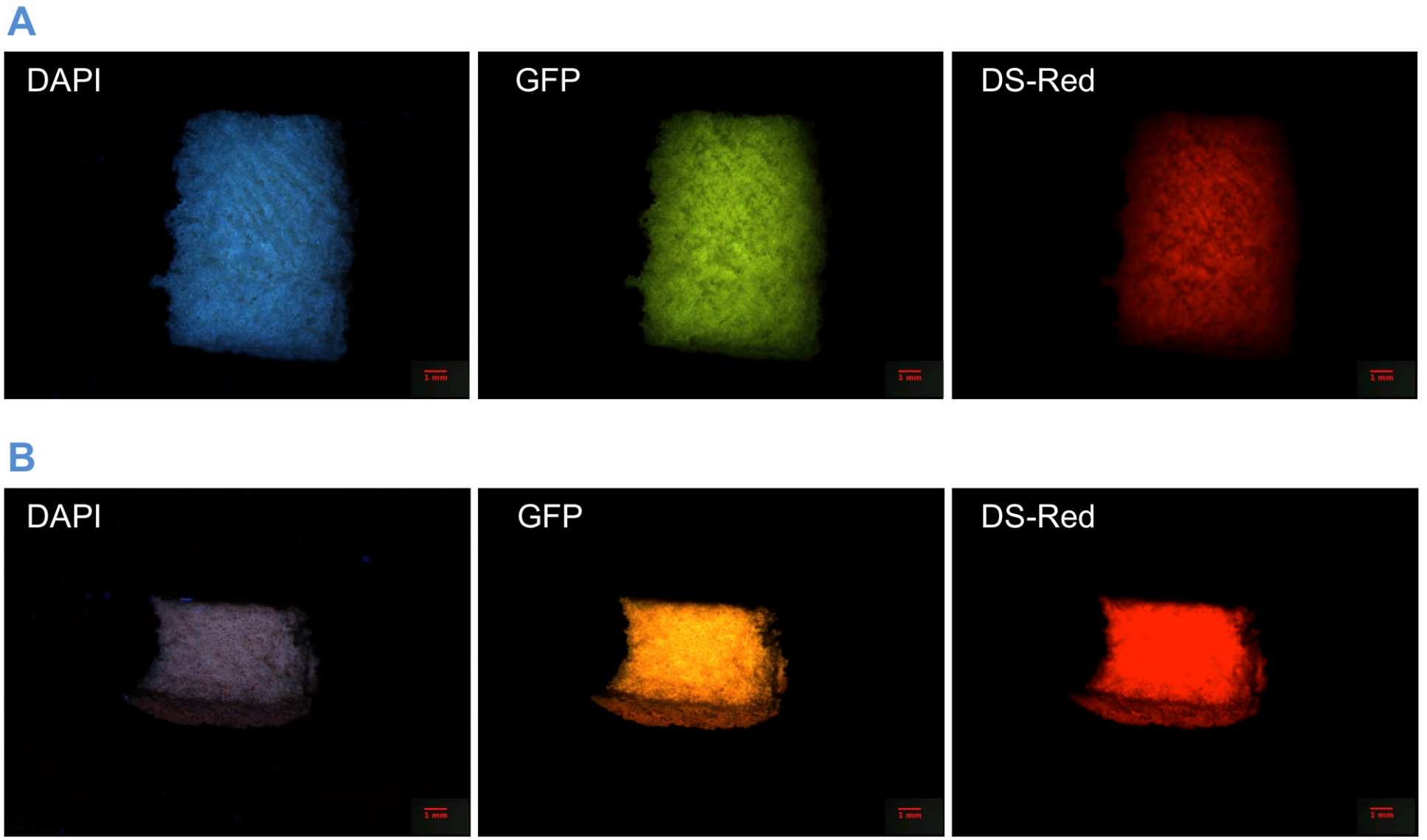

Figure 6.3 Scaffold auto-fluorescence during exposure to UV, GFP and DS-Red light wavelengths. Comparison of chitosan scaffolds cross-linked with either (A) glutaraldehyde or (B) genipin, and their potential to image fluorescently-tagged cells on them. Scale bar represents 1 mm.

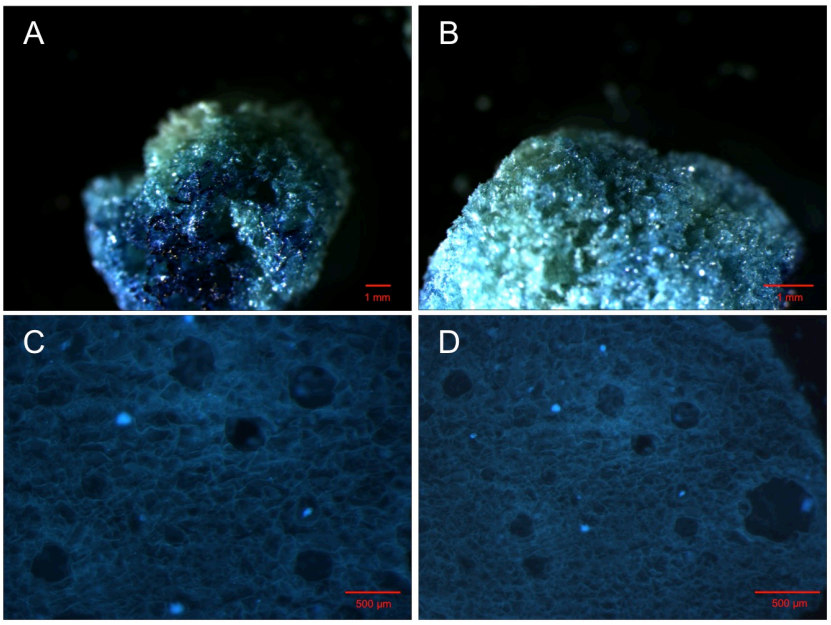

Figure 6.4 Imaging hMSCs after seeding on chitosan scaffolds cross-linked with glutaraldehyde. (A and B) Toluidine blue staining for DNA and membranes. Cell nuclei cannot be distinguished as chitosan material absorbs the stain. (C and D) UV fluorescence stereomicroscope images of cell nuclei (blue dots), 24 hours after seeding. DNA was stained with Hoechst 33258 dye.

Human MSCs tagged with green fluorescent protein were dynamically seeded onto fibronectin-coated chitosan scaffolds. Unfortunately, the chitosan constructs had strong auto-fluorescent properties when exposed to green fluorescent light; therefore, cells could not be distinguished from the porous biomaterial. It was determined that both chitosan scaffolds cross-linked with either glutaraldehyde or genipin, were autofluorescent when exposed to UV light and observed using a DAPI, GFP or DS-Red filters (Figure 6.3). Compared to glutaraldehyde, genipin scaffolds were less autofluorescent in the UV channel. This was proven when mesenchymal stem cells were treated with the nuclear dye Hoechst 33258 and visualised on scaffolds after UV exposure (Figures 6.4C and 6.4D). Additionally, MSCs were stained with Toluidine blue. Toluidine blue is a basic thiazine metachromatic dye, which has a high affinity for acidic tissue components. The dye successfully stained cellular DNA and membranes but was also absorbed by the chitosan scaffolds (Figure 6.4A and 6.4B). It was impossible to leach out excess staining from the chitosan and to image the cell seeding efficiency.

To resolve issues with cell imaging on the chitosan scaffolds, an innovative method was developed where MSCs were loaded with barium.

Barium was added to cell culture medium and over a 24-hour period, cells actively took-up the barium into their cytoplasm (Figure 6.5A). After this, loaded cells were seeded onto chitosan scaffolds and imaged using X-ray micro computed tomography. Groups of barium-loaded cells were visible as white dots on the chitosan scaffold (Figure 6.5B).

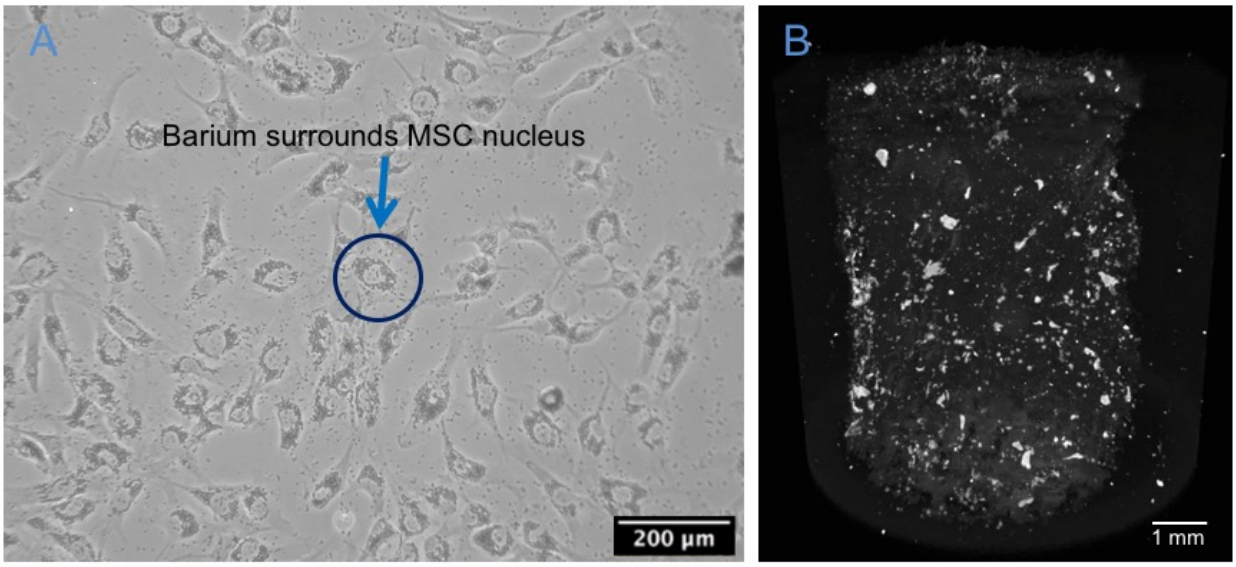

Figure 6.5 Imaging cell-seeding on chitosan scaffolds. (A) hMSCs loaded with barium nanoparticles after 24-hour incubation. (B) MicroCT reconstruction of chitosan scaffolds seeded with hMSCs loaded with barium nanoparticles. Clumps of cells are represented by the white barium dots and imaged 24 hours after seeding.

6.2.3 Scaffold Seeding

Cell seeding protocols were explored to establish the most efficient method for even distribution of cells throughout the scaffolds. It was also important that cells remained attached to scaffolds for the duration of differentiation. Four different seeding methods were tested (Figure 6.6):

- Standard seeding (control) where cell suspensions were slowly pipetted onto scaffolds. This was followed by static culture or dynamic culture on a plate shaker.
- Centrifuged scaffolds in cell suspension for 10 minutes at 350 g, to drive cells through the scaffold. Preliminary tests showed that longer centrifugation allowed for higher metabolic activity/ cell numbers (Figure 6.6A).

- A prototype scaffold-seeding chamber was produced using 3D rapid prototyping. The chambers were designed to enclose a scaffold, while 2 syringes on each side flushed cell suspensions through. 2 different chambers were manufactured using either small bead extrusion deposition or resin photopolymerisation (Figures 6.6B and 6.6C).

The seeding efficiency of each method was compared when barium-loaded MSCs were seeded onto scaffolds and imaged using MicroCT after 24 hours (Figure 6.7). All four methods allowed for even cell distribution throughout the scaffolds. However, standard seeding led to the formation of large cell clumps (Figure 6.7A), compared to centrifugation (Figure 6.7B) and chamber seeding (Figure 6.7C). In addition to this, the efficiencies were quantified using a PrestoBlue™ metabolic assay 24 hours after seeding (Figure 6.7D). Standard seeding followed by dynamic culture presented the highest metabolic activity of all the approaches tested, and was thus adopted for further experiments. The levels were significantly higher than standard seeding followed by static culture ($p < 0.00005$). Notably, the metabolic levels in the seeding device/ chamber sample were lowest and this could indicate poor seeding or cell damage.

6.2.4 MSC Differentiation for 21 Days in Perfusion Bioreactor

This section focused on assessing the biocompatibility of the chitosan scaffolds seeded with mesenchymal stem cells, and cultured in a perfusion bioreactor system. First, human MSCs were dynamically seeded onto scaffolds cross-linked with glutaraldehyde and genipin. After 24 hours, the MSCs had effectively attached to both types of chitosan scaffold. The seeded constructs were transferred to perfusion bioreactors for 14-day culture in standard culture medium. Figure 6.8 shows the bioreactor setup used. After culture for 7 and 14 days, the scaffolds were wax-embedded, sectioned and stained with DAPI to allow assessment of cells in centre of the scaffolds (Figure 6.9). This showed MSCs had attached to both types of chitosan scaffolds, and some cells were proliferating inside the pores. Notably, fewer cells were seen in smaller pores than larger pores. At Day 14, glutaraldehyde scaffolds were more sparsely populated, than the equivalent genipin scaffolds. No cells could be observed at Day 7 (Figure 6.9).

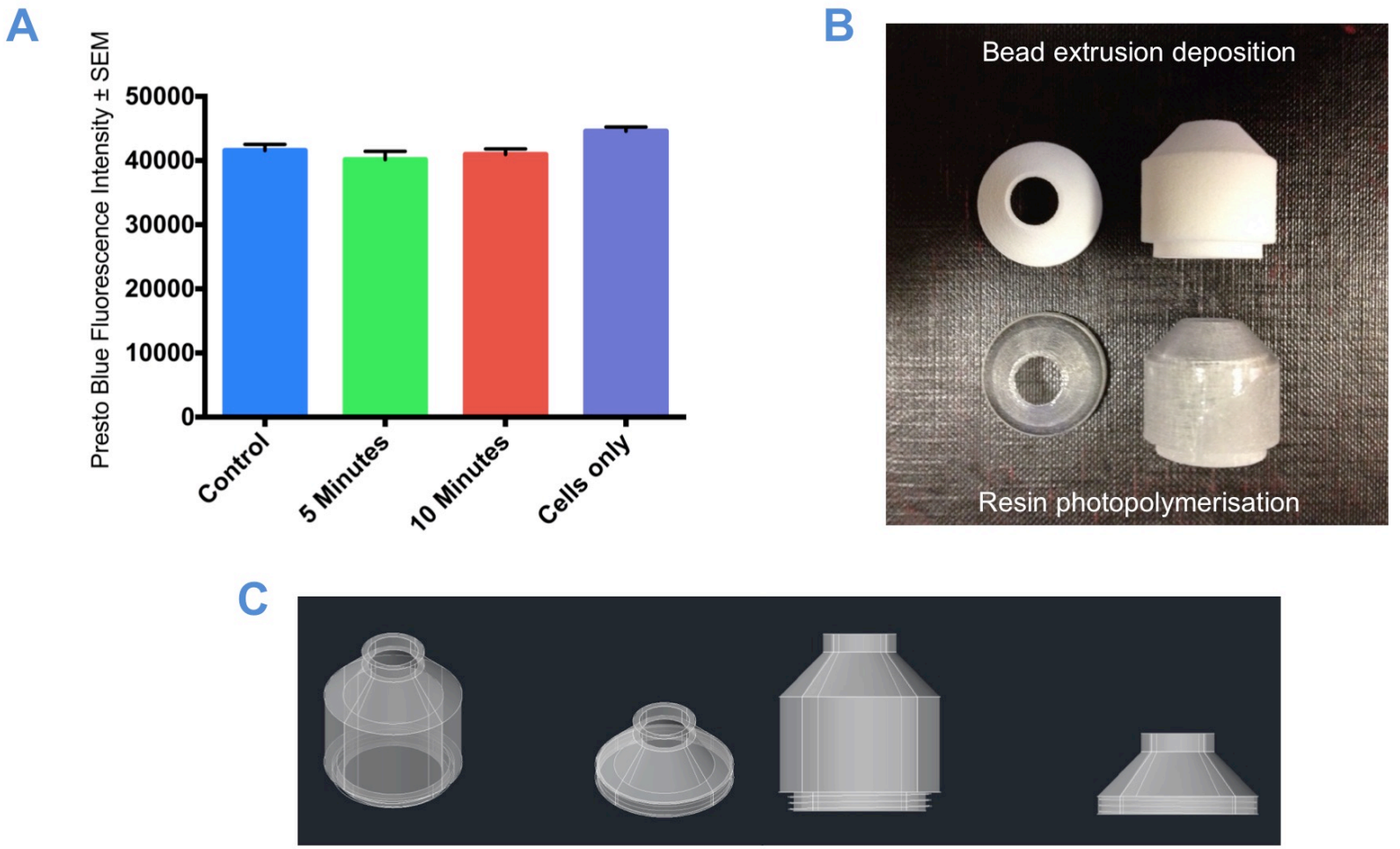

Figure 6.6 Scaffold seeding methods. (A) Day 5 Presto Blue™ metabolic assay for hMSCs cultured on glutaraldehyde-crosslinked chitosan scaffolds after centrifugation seeding at 350g for 5 and 10 minutes. Control method involves pipetting cells directly onto scaffold. Cells only control compares hMSCs on tissue culture plastic. (B) A prototype scaffold seeding chamber produced using 3D rapid prototyping. The chambers are designed to enclose scaffolds, while 2 syringes transfer cell suspensions through the scaffolds. Small bead extrusion deposition (top) provides minimal cytotoxicity but poor water tightness. UV photopolymerisation (bottom) of resin prevents leaks but is toxic to cells. (C) Autocad™ CAD drawings of seeding chamber.

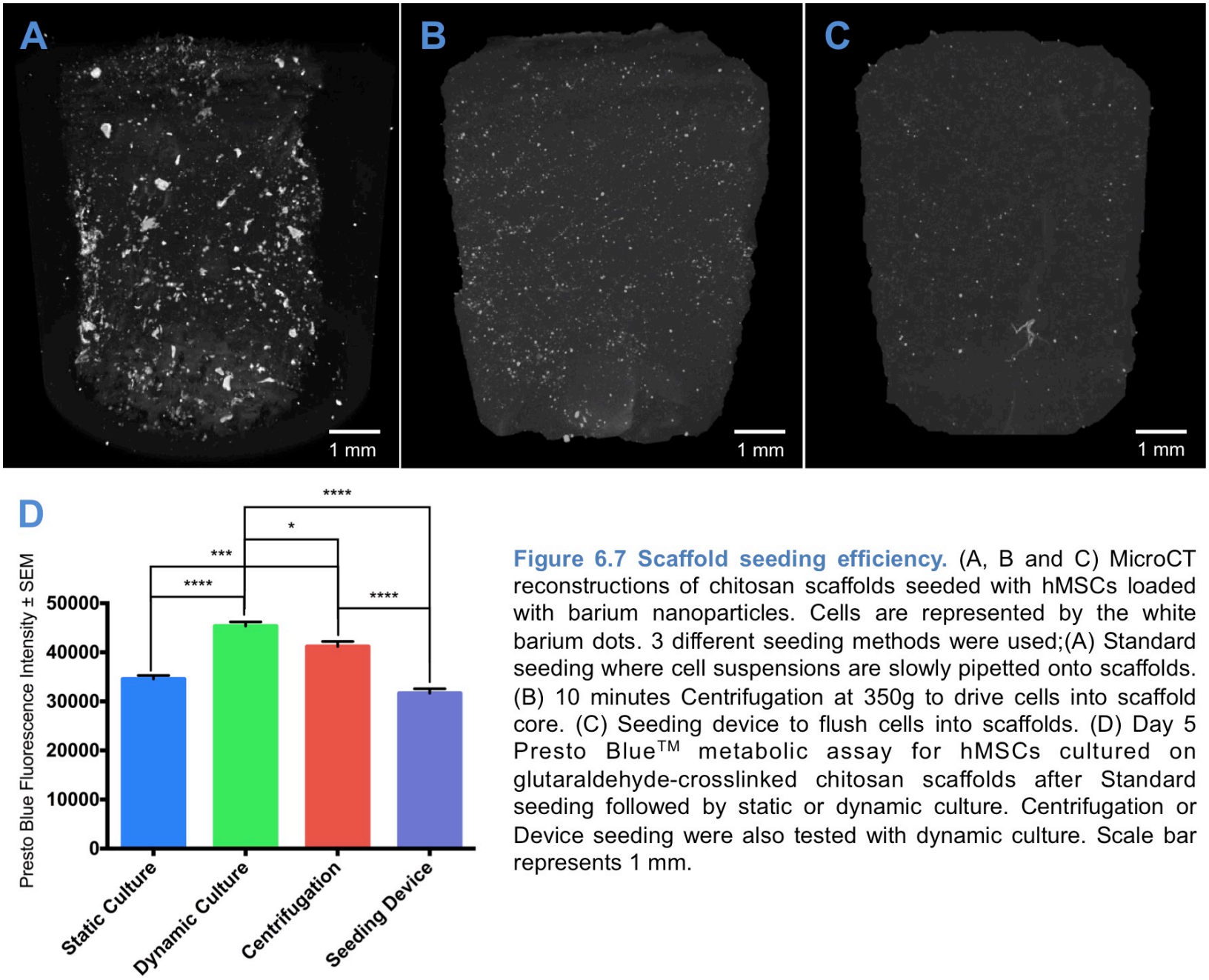

Figure 6.7 Scaffold seeding efficiency. (A, B and C) MicroCT reconstructions of chitosan scaffolds seeded with hMSCs loaded with barium nanoparticles. Cells are represented by the white barium dots. 3 different seeding methods were used;(A) Standard seeding where cell suspensions are slowly pipetted onto scaffolds. (B) 10 minutes Centrifugation at 350g to drive cells into scaffold core. (C) Seeding device to flush cells into scaffolds. (D) Day 5 Presto Blue™ metabolic assay for hMSCs cultured on glutaraldehyde-crosslinked chitosan scaffolds after Standard seeding followed by static or dynamic culture. Centrifugation or Device seeding were also tested with dynamic culture. Scale bar represents 1 mm.

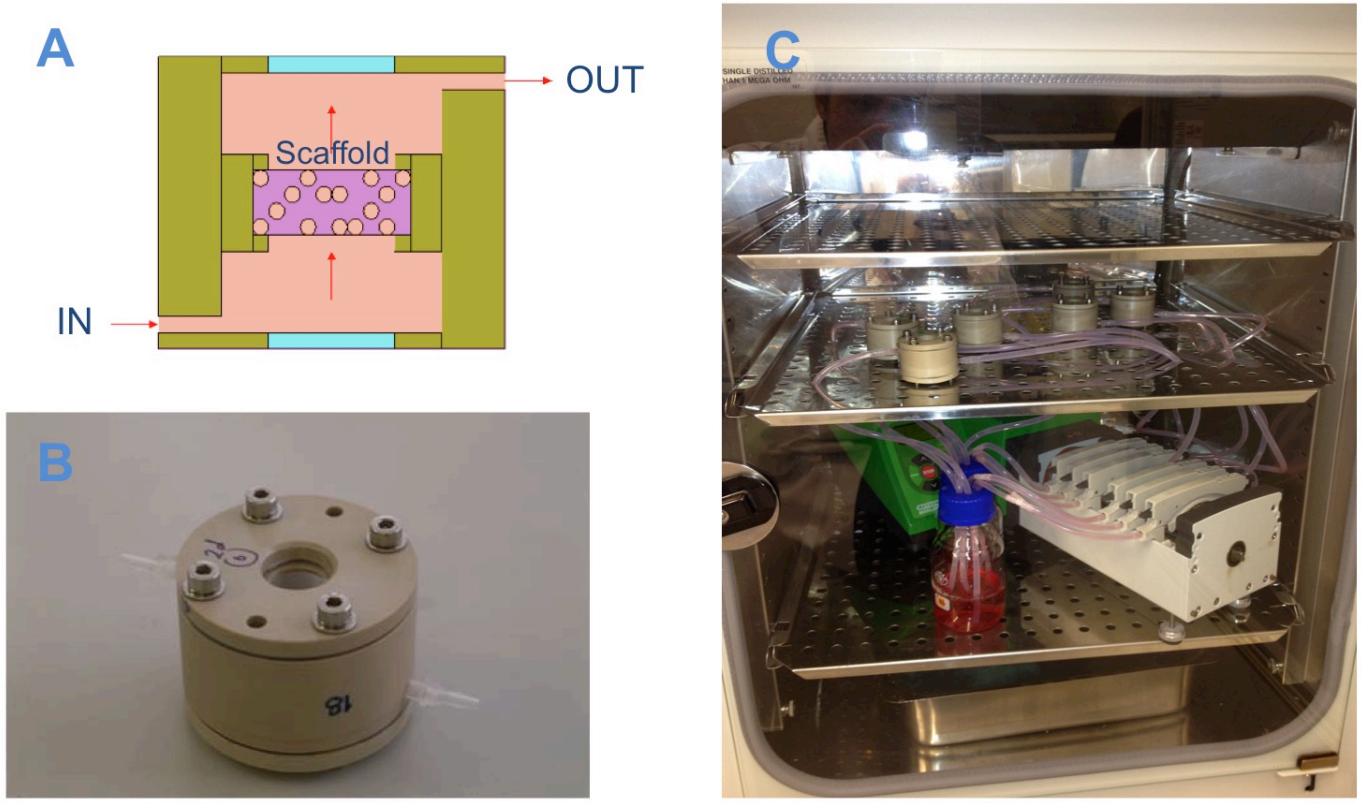

Figure 6.8 PEEK perfusion bioreactor for 3D biocompatibility and differentiation tests. (A) Diagram of custom-made perfusion bioreactor (green). This is a modified design from GKSS™ Germany and provides shear stress to bone-specific layer of chitosan scaffolds (purple) during culture media perfusion (pink). Shear stress is achieved by having the inflow and outflow at different elevations. Direction of flow is indicated by arrows. (B) Assembled perfusion bioreactor. (C) Perfusion bioreactors connected to a Watson Marlow 500 Series peristaltic pump.

Next, the differentiation of mesenchymal stem cells into osteogenic and chondrogenic lineages in the perfusion bioreactor system, was tested. Scaffolds cross-linked with glutaraldehyde were cultured for 21 days in the bioreactor system. Scaffolds were either cultured in standard medium or differentiation medium containing osteogenic and chondrogenic factors (Figure 6.10). In differentiation conditions, there was strong evidence of cell clustering in the scaffold region with smaller pores. There was no evidence of aggregate formation in the scaffold sections with larger pores. In the intermediate region between large and small pores, cells formed smaller clusters than those observed in small pores. Day 21 imaging of the scaffolds cultured in standard medium did not indicate any visible cell clustering.

Further, the metabolic activity of MSCs in standard and differentiation conditions was analysed after 21-day culture in the perfusion bioreactor system (Figure 6.11). Metabolic activity was lower in differentiation conditions than in the standard medium controls. However, this was not statistically different.

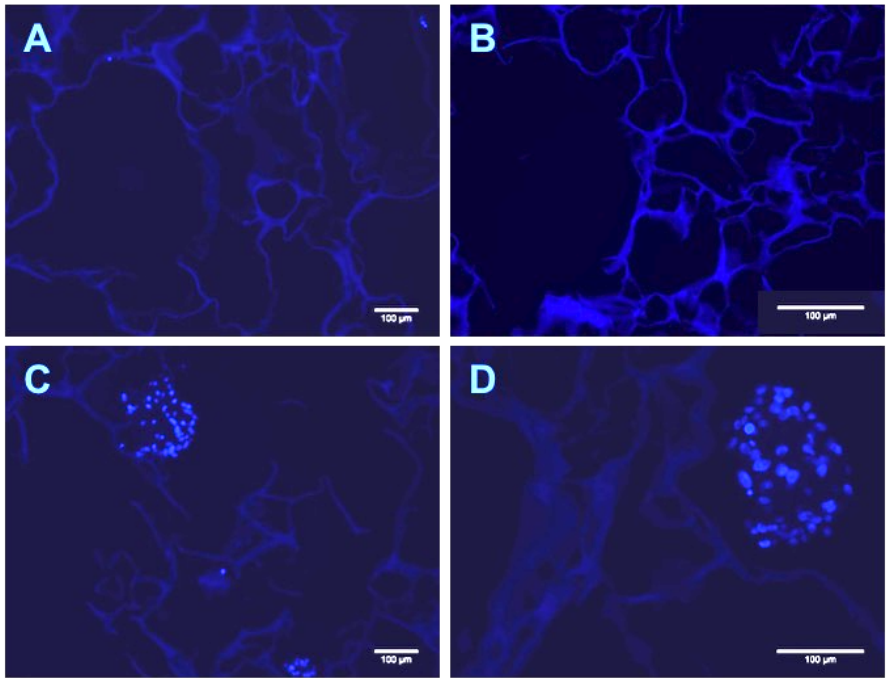

Figure 6.9. Porous chitosan scaffolds after 7 and 14 days of culture in PEEK perfusion bioreactors. DAPI staining of cross-sections in chitosan scaffolds cross-linked with glutaraldehyde and seeded with hMSCs. (A and B) Scaffolds cultured in standard medium for 7 days. (C and D) Scaffolds cultured in standard medium for 14 days. Cells formed clusters inside scaffold pores. Scale bar represents 100 µm.

6.2.5 Histochemical Analysis of MSC Differentiation

After 21 days of differentiation culture in the perfusion bioreactors, the scaffolds were fixed, wax-embedded, sectioned and stained to assess the levels of differentiation. Histochemical staining was examined using Alizarin red and Von Kossa to stain for mineral deposits/ calcium as indicator of osteogenic differentiation. The chitosan scaffolds were shown to absorb Alizarin red stain more intensely than cellular samples (Figure 6.13B), and it was decided that only Von Kossa staining should be used.

Hematoxylin and eosin staining confirmed the presence of cells, and showed that MSCs formed comprehensive multi-layered structures inside scaffold pores (Figure 6.12). Furthermore, there were distinct growth differences and cellular alignment between samples in standard or differentiation media, indicating suitable growth conditions.

Safranin-O staining, a marker for the presence of proteoglycans found in cartilage, was used to assess the chondrogenic differentiation. Importantly, sections confirmed that the chitosan scaffolds did not absorb much Safranin-O stain, allowing the observation of proteoglycan-based positive staining (Figure 6.13D).

The orientation of the scaffold within the bioreactor system had an impact on the differentiation of the MSCs (Figure 6.14). The large 300-425 μm pores supported osteogenic differentiation (Figure 6.14C and D). This was defined by Alizarin red and Von Kossa staining, which were more intense in the large pores cultured at the bottom. This was where the bioreactor provided mechanical shear. In addition to this, analysis of the scaffolds confirmed that the differentiation conditions used supported osteogenic differentiation in the large pores by detecting the expression of osteocalcin and alkaline phosphatase with peroxidase staining. Small pores (180-300 μm) promoted chondrogenic differentiation. This was confirmed by Safranin-O staining and bright-field imaging of cell clusters (Figure 6.14E and 6.14F).

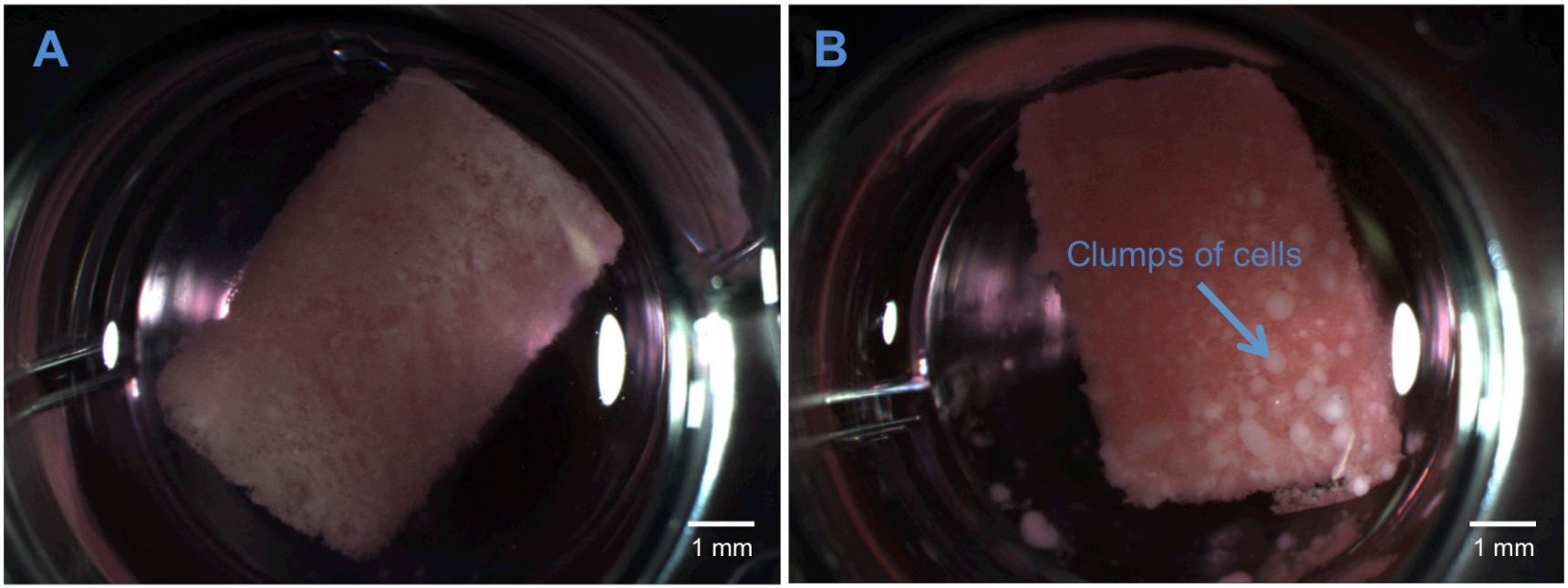

Figure 6.10 Chitosan scaffolds after 21 days culture in PEEK perfusion bioreactors. Chitosan scaffolds cross-linked with glutaraldehyde and seeded with hMSCs. Scaffolds were cultured in either (A) proliferative-only media or (B) differentiation media with osteogenic and chondrogenic growth factors. Clumps of cells in (B) indicate successful chondrogenic differentiation. Scale bar represents 1 mm.

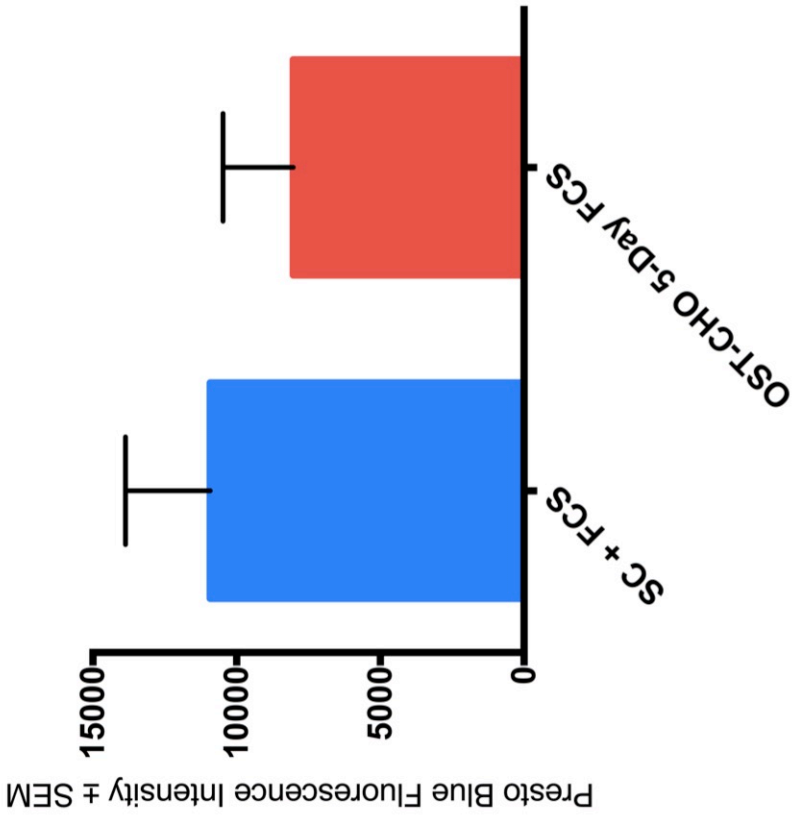

Figure 6.11 Comparison of cell metabolic activity in proliferative and differentiation culture conditions. Day 21 Presto Blue™ metabolic assay for hMSCs cultured on glutaraldehyde cross-linked chitosan scaffolds, in PEEK perfusion bioreactors. N=5. No statistical difference.

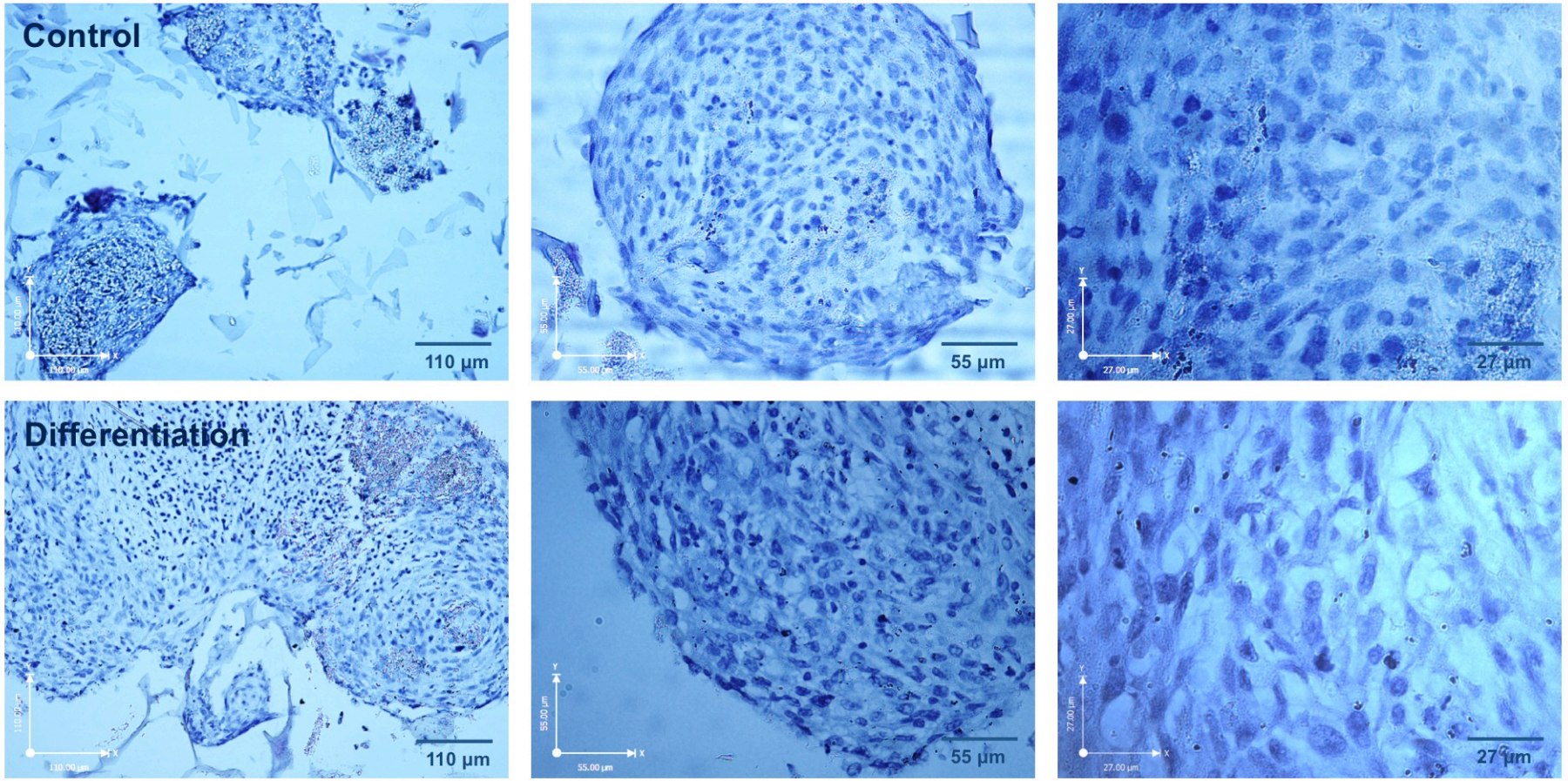

Figure 6.12 Porous chitosan scaffolds after 21 days culture in PEEK perfusion bioreactors. Haematoxylin and eosin staining in cross-sections of chitosan scaffolds cross-linked with glutaraldehyde and seeded with hMSCs. Scaffolds were cultured in either control proliferative-only media or differentiation media, with osteogenic and chondrogenic growth factors.

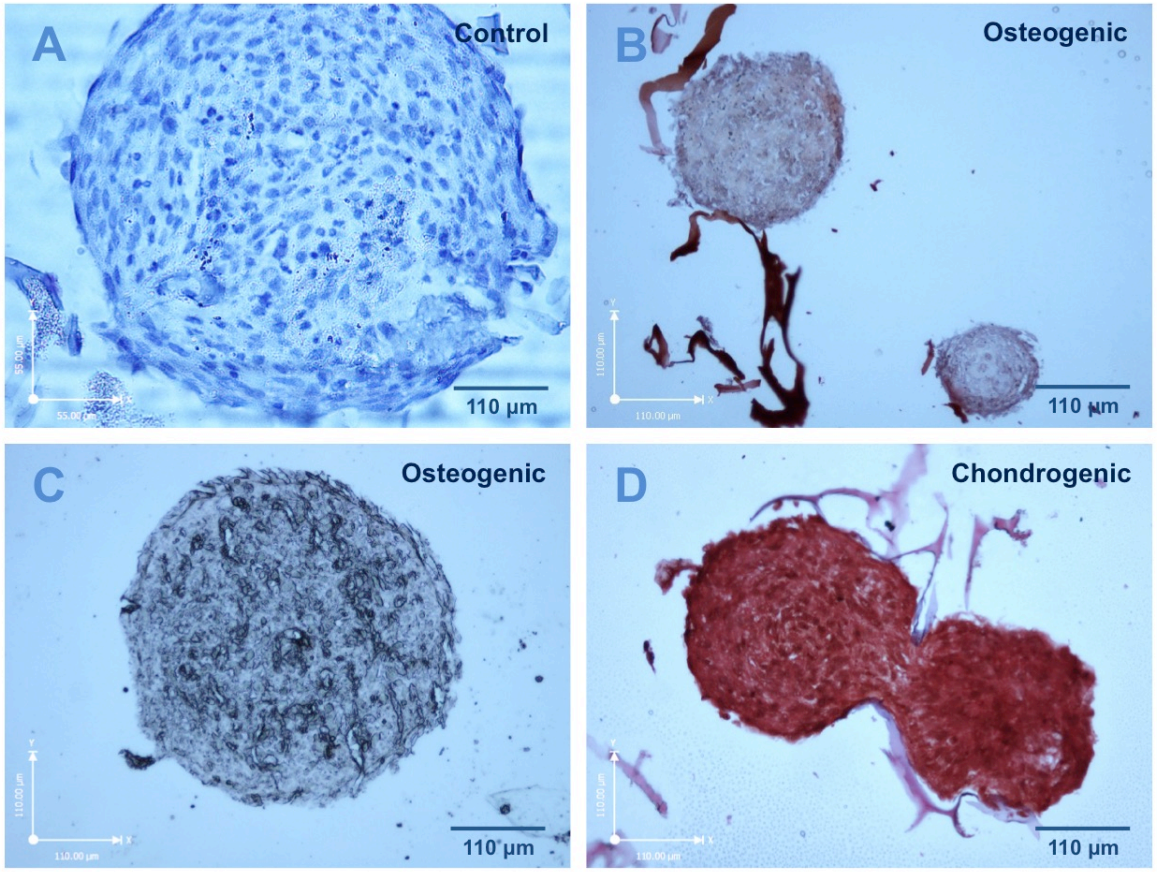

Figure 6.13 Types of differentiation stains for porous chitosan scaffolds after 21 days culture in PEEK perfusion bioreactors. Staining in cross-sections of chitosan scaffolds cross-linked with glutaraldehyde and seeded with hMSCs. Scaffolds were cultured in either control proliferative-only media or differentiation media, with both osteogenic and chondrogenic growth factors. (A) Haematoxylin and eosin stain of scaffolds in control/ proliferative conditions. (B and C) Osteogenic part (300-425 µm pores) of scaffolds with (B) Alizarin red and (C) Von Kossa staining for mineral deposition. (D) Chondrogenic part (180-300 µm pores) of chitosan scaffolds stained for proteoglycans with Safranin-O. Scale bar represents 110 µm.

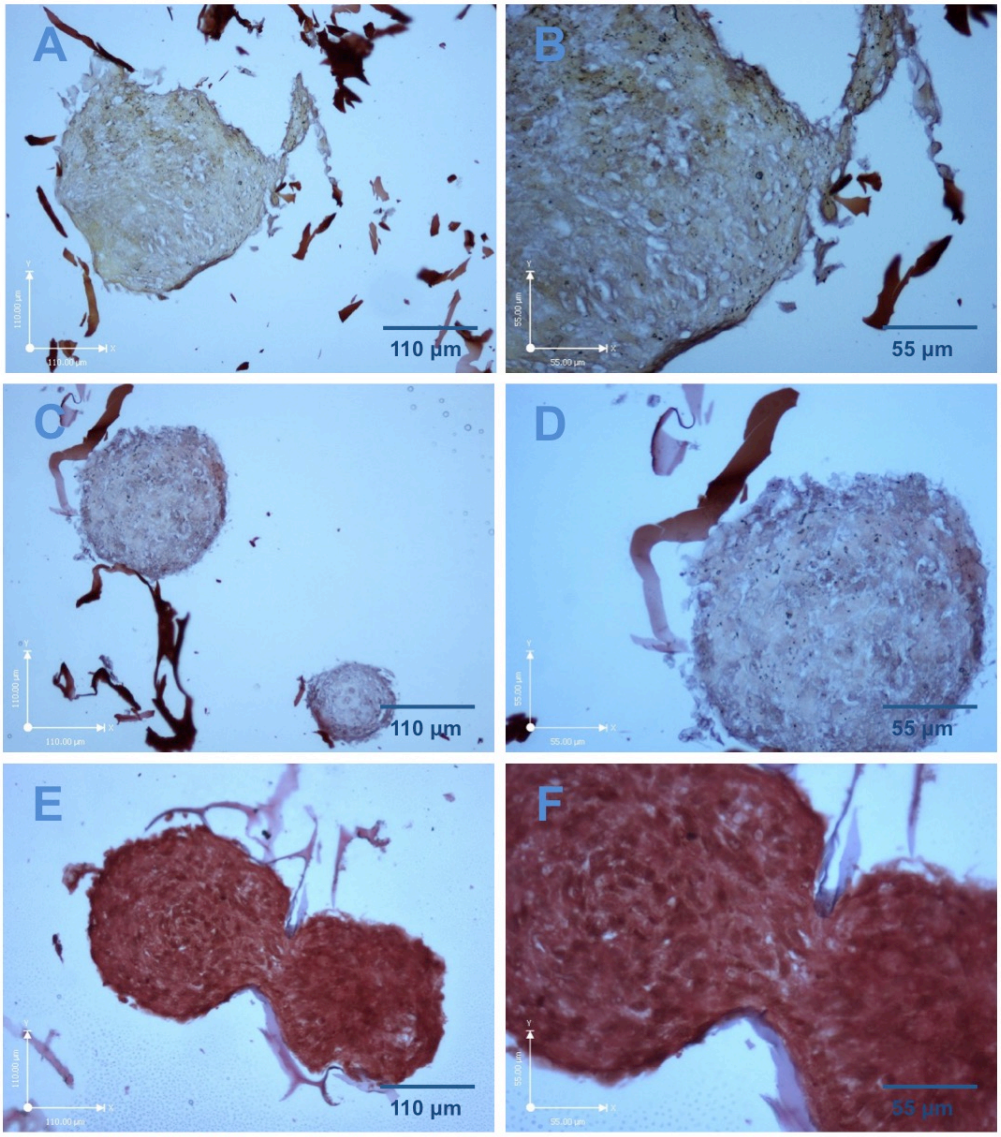

Figure 6.14 Differentiation staining of porous chitosan scaffolds after 21 days culture in PEEK perfusion bioreactors. Staining in cross-sections of chitosan scaffolds cross-linked with glutaraldehyde and seeded with hMSCs. Scaffolds were cultured in either standard media or differentiation media, with both osteogenic and chondrogenic growth factors. (A and B) Alizarin red scaffold stain in control/ proliferative conditions. (C and D) Osteogenic region (300-425 µm pores) of scaffolds with Alizarin red staining. (E and F) Chondrogenic region (180-300 µm pores) of chitosan scaffolds stained with Safranin-O.

6.3 Discussion

The purpose of this chapter was to combine the developments in Sections 4 and 5, and to advance the osteochondral differentiation of MSCs in a perfusion bioreactor system. More specifically, the perfusion system used here was intended to improve cell proliferation and differentiation by enhancing nutrient transportation and initiating mechanical stimulation via exposure of cells to fluid shear.

6.3.1 Chitosan Autofluorescence

In preliminary studies, human MSCs tagged with green fluorescent protein (GFP) were dynamically seeded onto fibronectin-coated chitosan scaffolds. Unfortunately, the chitosan auto-fluoresced when exposed to green fluorescent light, so cells could not be distinguished from the scaffold. Further investigation showed that chitosan scaffolds cross-linked with genipin and glutaraldehyde auto-fluoresce in the UV, GFP and DS-Red channels. Notably, chitosan scaffolds cross-linked with genipin were least auto-fluorescent in the UV channel. The auto-fluorescent nature of chitosan scaffolds is well documented and is principally caused by the cross-linking agents used in scaffold fabrication (Hwang et al, 2011; Wei et al, 2007). Acetic acid, which is essential in the production of the chitosan hydrogels, can also contribute to the auto-fluorescent properties of the scaffolds (Caric et al, 2004).

To mitigate this problem and allow good cell imaging on chitosan constructs, mesenchymal stem cells were successfully loaded with barium. The high molecular weight of barium allowed the visualisation of cells on the scaffolds using MicroCT 3D reconstructions. In the literature, liver cells and liposomes have also been loaded with barium to improve the quality of imaging tissues (Chakrabarti et al, 1992; Debbaut et al, 2009). Similar techniques have been applied to superparamagnetic iron oxide nanoparticles, where the active uptake of particles into cells improves the imaging contrast but also allows for the controlled migration of cells via magnetic fields (Gupta & Gupta, 2005; Laurent et al, 2008; Pankhurst et al, 2003). Importantly, the uptake of nanoparticles does not influence cell viability and differentiation potential (Harrison et al, 2014).

6.3.2 Scaffold Seeding

Before 3D differentiations into osteochondral lineages were attempted in the perfusion bioreactor system, it was important to improve the seeding efficiency of cells onto the scaffolds. Cell seeding is a fundamental part in developing tissue engineered constructs because it governs the success of tissue formation. More specifically, high seeding efficiencies can augment the use of limited cells and enhance tissue development (Jung et al, 2010; Sobral et al, 2011). Uniform seeding is also important for uniform extracellular matrix formation (Sendemir-Urkmez & Jamison, 2007).

Tissue engineered scaffolds can be seeded in static or dynamic conditions (Wendt et al, 2003). Static protocols involve surface seeding, while dynamic methods involve the movement of cell suspensions. Common methods for dynamic seeding include orbital shakers, centrifugation and spinner flasks (Godbey et al, 2004; Sikavitsas et al, 2002; Vunjak-Novakovic et al, 1998; Zhang et al, 2015).

In this project, barium-loaded cells were seeded onto scaffolds using a dynamic method (pipette the cells onto the material and leave on a plate shaker for 24 hours), as well as a centrifugation method (cells are forced into the scaffold cores through centrifugation). Additionally, 3D printing was used to produce a unique seeding chamber, which allowed 2 syringes to pipette cell suspensions through the scaffolds multiple times.

The literature suggests that centrifugal seeding is an efficient approach to achieve uniform cell distribution, especially at low cell concentrations (1.33×10^5 cells/ ml) (Godbey et al, 2004). Here, the results confirmed that centrifugal seeding leads to uniform distribution, but the nature of the method had a detrimental effect of cell metabolism.

The seeding chamber fabricated in this project utilised a similar strategy to scaffold seeding in a perfusion bioreactor system. This is a popular approach among the tissue engineering community (Kitagawa et al, 2006; Koch et al, 2010; Maidhof et al, 2010; Wendt et al, 2003). Unfortunately, this method led to the lowest seeding efficiencies and metabolic activities in the mesenchymal stem cells. The result could be explained by the fact that the chamber diameter was marginally larger than the scaffold diameters. This means that cell suspensions were flushed around the scaffold, instead of into their cores.

From the three seeding strategies, dynamic seeding was the simplest and the most efficient because it allowed for the highest metabolic activity.

Following the optimisation of cell seeding protocols, it was important to assess the biocompatibility of the chitosan scaffolds. Mesenchymal stem cell proliferation was investigated on chitosan scaffolds that have been treated with reducing agents to improve cell compatibility.

Chitosan scaffolds are commonly cross-linked with glutaraldehyde (Hsieh et al., 2007), but this leaves cytotoxic aldehyde groups on the surface of the material. For this reason, chitosan scaffolds cross-linked with glutaraldehyde were treated with glutamine or sodium borohydride (AbdelMagid et al, 1996; Baschong et al, 2001). The purpose of the reducing agents was to tie up any cytotoxic aldehyde groups from the glutaraldehyde. The results showed that both agents improved cell viability on the chitosan scaffolds, although sodium borohydride was more effective.

6.3.3 Perfusion Bioreactor Differentiations

Following the cell seeding tests, MSCs were dynamically seeded onto scaffolds cross-linked with either glutaraldehyde or genipin. Constructs were then cultured in the perfusion bioreactor for 7 days. These preliminary studies were important to determine scaffold biocompatibility. It was revealed that MSCs proliferate more on scaffolds cross-linked with genipin than they do when glutaraldehyde is used. Additionally, the metabolic activity of mesenchymal stem cells was significantly improved through the use of genipin instead of glutaraldehyde (Silva et al, 2008). This is possibly caused by the cytotoxic properties of glutaraldehyde (Sung et al, 1999). Genipin is a naturally derived compound with no cytotoxic effects, which cross-links via the same mechanisms as glutaraldehyde (Muzzarelli, 2009b).

Once biocompatibility of the scaffold was confirmed, osteochondral differentiations were conducted for 21 days in the perfusion bioreactor system. Chemical supplements were used in the cell culture medium to regulate the differentiation process. However, the purpose of this investigation was to demonstrate that scaffold architecture can guide mesenchymal stem cell differentiation into osteogenic and chondrogenic lineages.

Following the differentiation period, scaffolds were wax-embedded and sectioned. Sections were then stained with Von Kossa and Safranin-O.
Staining illustrated that there were both osteogenic and chondrogenic lineages present in single scaffolds.

Chondrogenesis was detected in small pore (180-300 μm) regions, and this was illustrated via cluster formation analogous to chondrogenic pellet culture (Mackay et al, 1998). The literature also suggests that cartilage differentiation of mesenchymal stem cells is preferential in smaller pores (Duan et al, 2014; Im et al, 2012). As well as forcing cell cluster formation, small pore regions can be considered to have hypoxic microenvironments. Hypoxia is considered beneficial for chondrogenic differentiation because it mimics the natural environment of cartilage tissues (Kanichai et al, 2008; Khan et al, 2007). Positive Safranin-O staining of small pore clusters was a good indication of proteoglycan synthesis (Barry et al, 2001).

Osteogenic differentiation of mesenchymal stem cells was observed in large pore (300-425 μm) regions of the bi-layered chitosan scaffolds. Von Kossa and Alizarin red staining in large pores recognised calcium deposition and the presence of bone-like mineral matrix. The quality and the methods of staining could be improved because the stains used here are specific to calcium. Chitosan can bind calcium from its environment (Bravo-Osuna et al, 2007) and this can lead to false positive staining.

Porosity and pore size of biomaterial scaffolds are important for *in vitro and in vivo* bone formation (Karageorgiou & Kaplan, 2005a). *In vitro,* lower porosity has been demonstrated to stimulate osteogenic differentiation via suppressed cell proliferation and forced aggregation of cells. Stem cells only begin differentiating after attaching to a substrate and lower scaffold porosity could influence this (Hutmacher, 2000). The opposite is observed *in vivo,* where higher porosity and pore size lead to enhanced bone development. Interestingly, (Gomes et al, 2006) showed that *in vitro,* larger porosities of 80% enhanced osteogenic differentiation compared 50% porous constructs.

Pore size in scaffolds can vary between applications and research groups. However, 100 μm is identified as the minimum requirement in pore size to accommodate for cell size, migration requirements and transport within the scaffold (O'Brien et al, 2005). Pore sizes greater than 300 μm are promoted for osteogenesis due to enhanced differentiation and the formation of vascularisation/ capillaries.

Importantly, the majority of chitosan scaffolds for osteogenic application are composites made with ceramic materials (Abarrategi et al, 2010; Malafaya & Reis, 2009; Oliveira et al, 2006). In this study, bone differentiation was achieved without osteogenic promoters, such as hydroxyapatite and calcium phosphates. However, in future ceramic fillers may be incorporated into the bi-layered chitosan scaffold to improve the mechanical characteristics and enhance the differentiation process (Zhang et al, 2003).

The perfusion bioreactor runs were a good preliminary test of the whole differentiation system and in future the differentiation period will have to be extended to allow whole scaffolds to be populated with differentiated cells. In this manner, scaffolds will mimic native osteochondral environment more closely and allow for improved tissue formation. Perfusion promoted fluid sheer to cells that were attached to the bi-layered chitosan scaffolds and mitigated mass transfer limitations (Bilgen & Barabino, 2007). More specifically, the novel bioreactor design allowed for this mechanotransduction to be applied to the osteogenic regions of the constructs, only. These forces are important in bone development (El Haj & Cartmell, 2010).

6.4 Summary

This chapter focused on optimising biocompatibility and maximising seeding efficiencies in the development of a construct for joint repair. It was demonstrated that chitosan scaffolds could be cross-linked with genipin to allow maximum viability of mesenchymal stem cells. Cell viability with glutaraldehyde scaffolds could also be improved through treatments with aldehyde-reducing agents, such as sodium borohydride. Due to the nature of the scaffold fabrication process, it was difficult to visualise fluorescently tagged cells on the scaffolds. A novel approach was utilised where cells were loaded with barium and imaged using MicroCT. Next, a range of scaffold seeding methods was explored. These included dynamic, centrifugation and perfusion-based seeding. Dynamic seeding proved to be most efficient and it was applied for all future experiments. Finally, the differentiation potential of the bi-layered chitosan scaffold was tested in a perfusion bioreactor. Preliminary results showed that mesenchymal stem cell differentiation could be regulated by scaffold pore size. Osteochondral lineages were detected after 21 days, however culture periods need to be extended significantly in future, to improve tissue development.

7. Conclusions and Future Work

This research project has explored the development of a novel chitosan scaffold for oteochondral modelling and potential repair. A range of relevant aspects were investigated, including transient FCS and HS regimes to support osteogenic and chondrogenic differentiation of human MSCs, the production of a novel chitosan scaffold with graduated pore sizes, and the assessment of scaffold biocompatibility in a perfusion bioreactor system.

7.1 Serum Conditions for MSC Differentiation

Human serum (HS) has been demonstrated to support a highly proliferative mesenchymal stem cell population, while avoiding the xeno-associated risks in FCS culture (Doucet et al, 2005). Rates of osteogenic differentiation are higher using HS compared to FCS culture. This was established via analyses including, Alizarin red staining, quantification of alkaline phosphatase activity and, PCRs for bone-specific genes. Alizarin red staining has important limitations because the assay stains for calcium ions the presence of which, may not be specific to early osteogenesis. Therefore, observations in this study need to be further validated with additional immunostaining and ELISA for proteins, such as osteocalcin, osterix, collagens type 1 and 2, and RUNX2. Significantly, all known studies comparing FCS with autologous HS have similar conclusions as described in this investigation (Mizuno et al, 2006). However, HS is expensive and can have batch variation leading to unreliable results, as indicated in this study. Furthermore, obtaining sufficient quantities of HS from an autologous donor is difficult (Lange et al, 2007).

Serum is an important component of culture medium for good viability, proliferation and osteogenic differentiation in MSCs. Nevertheless, in this project it has been shown that MSCs can survive transient-serum treatments with FCS and HS. Although the cells remain viable, they exhibit reduced proliferation and differentiation rates.

In addition to this, it was revealed that chondrogenesis in MSCs could be achieved with transient exposure to FCS but HS results are inconclusive. For this reason, more work is necessary on the chondrogenic differentiation of MSCs in transient-serum conditions. It is also desirable to test alternative culture environments, such as hypoxia and culture medium with high/ low glucose content.

Substitute solutions to FCS and HS include the use of human platelet lysate (Perez-Ilzarbe et al, 2009) and serum-free defined medium (Lange et al, 2007). Serum content analysis conducted here, is a novel and important approach in improving the understanding of stem cell differentiations. The results showed that high levels of alkaline phosphatase and 25-Hydroxyvitamin D could enhance osteogenic differentiation of MSCs. Furthermore, it is important to keep levels of cortisol and insulin low because they are linked to bone resorption (Goltzman et al, 2015).

This study provides evidence that the use of HS is a feasible alternative to FCS. However, alternatives such as platelet lysate and defined media should be explored. One strategy to realising defined media and improving the reliability of stem cell differentiations is through the use of growth factor mimics. Finally, FCS from different manufacturers should also be considered in future to strengthen the findings in the HS investigations.

7.2 Production of Bi-layered Chitosan Scaffolds

Production of scaffolds with the capacity to maintain osteogenic and chondrogenic cell lineages is a significant aspect in developing effective osteochondral constructs. In this project, a number of different dual-porosity scaffolds were produced from chitosan using novel freeze-gelation and porogen fabrication methods. Fundamentally, the scaffolds were designed with graduated pores sizes (180-300 μm and 300-425 μm) to regulate the differentiation of mesenchymal stem cells into subchondral bone and articular cartilage.

The work here, demonstrates that PCL microspheres used as porogen material allowed improved control of scaffold porosity and pore size, compared to PCL granules. This close control is important in order to achieve dual porosity within the scaffold, and provide differential environments for MSC differentiation towards osteogenic and chondrogenic lineages.

In addition to this, two different cross-linking agents were tested. Although more difficult to use due to longer cross-linking times, genipin was able to generate scaffolds with improved pore characteristics and mechanical strength compared to glutaraldehyde. The mechanical properties of scaffolds could be further improved by using higher concentrations of genipin.
This would also alleviate problems associated with slow cross-linking rates. As well as optimising genipin concentrations, it is desirable to further explore alternatives cross-linkers, such as β-glycerophosphate.

Scaffolds cross-linked with glutaraldehyde failed to biodegrade in 1 year *in vitro*, while genipin scaffolds were not tested here. Notably, the degree of deacetylation in chitosan has a large influence on cell adhesion and on the degradation properties of the scaffold, so it would be wise to investigate materials with a range of deacetylation degrees.

To maintain development and progress in future, more detailed characterisation of the mechanical and degradation properties of the glutaraldehyde and genipin constructs is compulsory. It is also important to scale-up production of the scaffold constructs and try to modify fabrication methods to alleviate the use of toxic chemicals, which can be detrimental to cell health. Additionally, the incorporation of dispersed degradable fillers such as calcium phosphates could improve the osteoconductive and mechanical properties of constructs. In brief, further developments and analyses are required to determine the biocompatibility of the scaffolds and their suitability for osteochondral repair.

7.3 Scaffold Biocompatibility in a Perfusion Bioreactor

The final aspect of this research focused on optimising biocompatibility and maximising seeding efficiencies in the 3D culture of osteochondral constructs. It was demonstrated that chitosan scaffolds could be cross-linked with genipin to allow maximum viability of mesenchymal stem cells. While, cell viability on glutaraldehyde scaffolds could also be improved through treatments with aldehyde-reducing agents, such as sodium borohydride.

Due to the nature of the scaffold fabrication process, it was difficult to visualise fluorescently tagged cells on the scaffolds. An innovative approach was utilised where cells were loaded with barium and imaged using MicroCT.
Scanning electron microscopy can be applied in future to compliment current MicroCT data.

A range of scaffold seeding methods was also explored. These included dynamic, centrifugation and perfusion-based seeding. Although the simplest to accomplish, dynamic seeding proved to be most efficient. For this reason, it was applied to all future experiments.

Finally, the differentiation potential of the bi-layered chitosan scaffold was tested in a perfusion bioreactor. Preliminary results showed that mesenchymal stem cell differentiation could be regulated by scaffold pore size. Osteochondral lineages were detected after 21 days, however culture periods must be extended significantly in future, to improve tissue development. The levels of osteogenic and chondrogenic differentiation must be quantified.

Once culture periods are prolonged, understanding of the scaffold biocompatibility and differentiation potential in the *in vitro* model will be enriched. Consequently, osteogenic and chondrogenic differentiations of mesenchymal stem cells can be enhanced by optimisation of scaffold pore sizes accordingly. There is also necessary scope to investigate the reasons for controlled differentiation i.e. cell cluster formation and hypoxic environments. Further, flow rates and fluid shear may have significant positive effects on osteogenic differentiation if parameters are optimised and/ or mathematical modelling is applied.

7.4 Overall Conclusions

The use of tissue-engineered scaffolds is an established strategy for the repair of joint trauma. Nevertheless, the application of single scaffolds to control simultaneous osteogenic and chondrogenic differentiation is a relatively novel concept. Importantly, the results of this project provide good foundations for the development of effective osteochondral constructs.

In the future, focus needs to be applied to demonstrating solid evidence on the capacity of the bi-layered chitosan scaffold to control stem cell differentiation. This must be achieved before further developments in the differentiation conditions and scaffolds characteristics are made. Examples of overarching improvements include the incorporation of osteoconductive fillers and encapsulated growth factors into the scaffold architecture. Finally, it would be realistic to include animal studies and explore the osteochondral potential of the chitosan scaffold *in vivo*.

8. References

Abarrategi, A., Lopiz-Morales, Y., Ramos, V., Civantos, A., Lopez-Duran, L., Marco, F. & Luis Lopez-Lacomba, J. (2010) Chitosan scaffolds for osteochondral tissue regeneration. *Journal of Biomedical Materials Research Part A*, 95A(4), 1132-1141.

Abdallah, B. M., Haack-Sorensen, M., Fink, T. & Kassem, M. (2006) Inhibition of osteoblast differentiation but not adipocyte differentiation of mesenchymal stem cells by sera obtained from aged females. *Bone*, 39(1), 181-188.

AbdelMagid, A. F., Carson, K. G., Harris, B. D., Maryanoff, C. A. & Shah, R. D. (1996) Reductive amination of aldehydes and ketones with sodium triacetoxyborohydride. Studies on direct and indirect reductive amination procedures. *Journal of Organic Chemistry*, 61(11), 3849-3862.

Adewumi, O., Aflatoonian, B., Ahrlund-Richter, L., Amit, M., Andrews, P. W., Beighton, G., Bello, P. A., Benvenisty, N., Berry, L. S., Bevan, S., Blum, B., Brooking, J., Chen, K. G., Choo, A. B. H., Churchill, G. A., Corbel, M., Damjanov, I., Draper, J. S., Dvorak, P., Emanuelsson, K., Fleck, R. A., Ford, A., Gertow, K., Gertsenstein, M., Gokhale, P. J., Hamilton, R. S., Hampl, A., Healy, L. E., Hovatta, O., Hyllner, J., Imreh, M. P., Itskovitz-Eldor, J., Jackson, J., Johnson, J. L., Jones, M., Kee, K., King, B. L., Knowles, B. B., Lako, M., Lebrin, F., Mallon, B. S., Manning, D., Mayshar, Y., McKay, R. D. G., Michalska, A. E., Mikkola, M., Mileikovsky, M., Minger, S. L., Moore, H. D., Mummery, C. L., Nagy, A., Nakatsuji, N., O'Brien, C. M., Oh, S. K. W., Olsson, C., Otonkoski, T., Park, K.-Y., Passier, R., Patel, H., Patel, M., Pedersen, R., Pera, M. F., Piekarczyk, M. S., Pera, R. A. R., Reubinoff, B. E., Robins, A. J., Rossant, J., Rugg-Gunn, P., Schulz, T. C., Semb, H., Sherrer, E. S., Siemen, H., Stacey, G. N., Stojkovic, M., Suemori, H., Szatkiewicz, J., Turetsky, T., Tuuri, T., van den Brink, S., Vintersten, K., Vuoristo, S., Ward, D., Weaver, T. A., Young, L. A., Zhang, W. & Int Stem Cell, I. (2007) Characterization of human embryonic stem cell lines by the International Stem Cell Initiative. *Nature Biotechnology*, 25(7).

Aggarwal, S. & Pittenger, M. F. (2005) Human mesenchymal stem cells modulate allogeneic immune cell responses. *Blood*, 105(4), 1815-1822.

Aicher, W. K., Buehring, H.-J., Hart, M., Rolauffs, B., Badke, A. & Klein, G. (2011) Regeneration of cartilage and bone by defined subsets of mesenchymal stromal cells-Potential and pitfalls. *Advanced Drug Delivery Reviews*, 63(4-5), 342-351.

Aigner, T., Gebhard, P. M., Schmid, E., Bau, B., Harley, V. & Poschl, E. (2003) SOX9 expression does not correlate with type II collagen expression in adult articular chondrocytes. *Matrix Biology*, 22(4), 363-372.

Akiyama, H., Chaboissier, M. C., Martin, J. F., Schedl, A. & de Crombrugghe, B. (2002) The transcrintion factor Sox9 has essential roles in successive steps of the chondrocyte differentiation pathway and is required for expression of Sox5 and Sox6. *Genes & Development*, 16(21), 2813-2828.

Aldahmash, A., Haack-Sorensen, M., Al-Nbaheen, M., Harkness, L., Abdallah, B. M. & Kassem, M. (2011) Human Serum is as Efficient as Fetal Bovine Serum in Supporting Proliferation and Differentiation of Human Multipotent Stromal (Mesenchymal) Stem Cells In Vitro and In Vivo. *Stem Cell Reviews and Reports*, 7(4), 860-868.

Alexander, P. G., Gottardi, R., Lin, H., Lozito, T. P. & Tuan, R. S. (2014) Three-dimensional osteogenic and chondrogenic systems to model osteochondral physiology and degenerative joint diseases. *Experimental Biology and Medicine*, 239(9), 1080-1095.

Ali, S. Y., Sajdera, S. W. & Anderson, H. C. (1970) Isolation and characterization of calcifying matrix vesicles from epiphyseal cartilage. *Proceedings of the National Academy of Sciences of the United States of America*, 67(3), 1513-&.

Alves da Silva, M., Crawford, A., Mundy, J., Correlo, V. M., Sol, P., Battacharya, M., Hatton, P. V., Reis, R. L. & Neves, N. M. (2007) Novel chitosan/poly (butylene succinate) scaffolds for cartilage tissue engineering. *Tissue Engineering*, 13(7), 1735-1736.

Alves da Silva, M. L. A., Crawford, A., Mundy, J. M., Correlo, V. M., Sol, P., Bhattacharya, M., Hatton, P. V., Reis, R. L. & Neves, N. M. (2010) Chitosan/polyester-based scaffolds for cartilage tissue engineering: Assessment of extracellular matrix formation. *Acta Biomaterialia*, 6(3), 1149-1157.

Amendola, S. C., Sharp-Goldman, S. L., Janjua, M. S., Kelly, M. T., Petillo, P. J. & Binder, M. (2000) An ultrasafe hydrogen generator: aqueous, alkaline borohydride solutions and Ru catalyst. *Journal of Power Sources*, 85(2), 186-189.

Amidi, M., Mastrobattista, E., Jiskoot, W. & Hennink, W. E. (2010) Chitosan-based delivery systems for protein therapeutics and antigens. *Advanced Drug Delivery Reviews*, 62(1), 59-82.

Anderson, H. C. (1969) Vesicles associated with calcification in matrix of epiphyseal cartilage. *Journal of Cell Biology*, 41(1), 59-&.

Anderson, H. C., Garimella, R. & Tague, S. E. (2005) The role of matrix vesicles in growth plate development and biomineralization. *Frontiers in Bioscience-Landmark*, 10, 822-837.

Angele, P., Yoo, J. U., Smith, C., Mansour, J., Jepsen, K. J., Nerlich, M. & Johnstone, B. (2003) Cyclic hydrostatic pressure enhances the chondrogenic phenotype of human mesenchymal progenitor cells differentiated in vitro. *Journal of Orthopaedic Research*, 21(3), 451-457.

Annabi, N., Nichol, J. W., Zhong, X., Ji, C. D., Koshy, S., Khademhosseini, A. & Dehghani, F. (2010) Controlling the Porosity and Microarchitecture of Hydrogels for Tissue Engineering. *Tissue Engineering Part B-Reviews*, 16(4), 371-383.

Ap Gwynn, I., Wade, S., Kaeaeb, M. J., Owen, G. R. & Richards, R. G. (2000) Freeze-substitution of rabbit tibial articular cartilage reveals that radial zone collagen fibres are tubules. *Journal of Microscopy (Oxford)*, 197(2), 159-172.

Armstrong, C. G. & Mow, V. C. (1982) Variations in the intrinsic mechanical proterties of human articular-cartilage with age, degeneration, and water-content. *Journal of Bone and Joint Surgery-American Volume*, 64(1), 88-94.

Arvidson, K., Abdallah, B. M., Applegate, L. A., Baldini, N., Cenni, E., Gomez-Barrena, E., Granchi, D., Kassem, M., Konttinen, Y. T., Mustafa, K., Pioletti, D. P., Sillat, T. & Finne-Wistrand, A. (2011) Bone regeneration and stem cells. *Journal of Cellular and Molecular Medicine*, 15(4), 718-746.

Bacigalupo, A. (2007) Management of acute graft-versus-host disease. *British Journal of Haematology*, 137(2), 87-98.

Barry, F., Boynton, R. E., Liu, B. S. & Murphy, J. M. (2001) Chondrogenic differentiation of mesenchymal stem cells from bone marrow: Differentiation-dependent gene expression of matrix components. *Experimental Cell Research*, 268(2), 189-200.

Baschong, W., Suetterlin, R. & Laeng, R. H. (2001) Control of autofluorescence of archival formaldehyde-fixed, paraffin-embedded tissue in confocal laser scanning microscopy (CLSM). *Journal of Histochemistry & Cytochemistry*, 49(12), 1565-1571.

Bashir, A., Gray, M. L., Hartke, J. & Burstein, D. (1999) Nondestructive imaging of human cartilage glycosaminoglycan concentration by MRI. *Magnetic Resonance in Medicine*, 41(5), 857-865.

Bedi, A., Feeley, B. T. & Williams, R. J., III (2010) Management of Articular Cartilage Defects of the Knee. *Journal of Bone and Joint Surgery-American Volume*, 92A(4), 994-1009.

Begley, C. M. & Kleis, S. J. (2002) RWPV bioreactor mass transport: Earth-based and in microgravity. *Biotechnology and Bioengineering*, 80(4), 465-476.

Benjamin, M. & Ralphs, J. R. (1998) Fibrocartilage in tendons and ligaments - an adaptation to compressive load. *Journal of Anatomy*, 193, 481-494.

Bentley, G., Biant, L. C., Carrington, R. W. J., Akmal, M., Goldberg, A., Williams, A. M., Skinner, J. A. & Pringle, J. (2003) A prospective, randomised comparison of autologous chondrocyte implantation versus mosaicplasty for osteochondral defects in the knee. *Journal of Bone and Joint Surgery-British Volume*, 85B(2), 223-230.

Berberat, J. E., Nissi, M. J., Jurvelin, J. S. & Nieminen, M. T. (2009) Assessment of interstitial water content of articular cartilage with T-1 relaxation. *Magnetic Resonance Imaging*, 27(5), 727-732.

Bhumiratana, S. & Vunjak-Novakovic, G. (2015) Engineering physiologically stiff and stratified human cartilage by fusing condensed mesenchymal stem cells. *Methods*, 84, 109-114.

Bi, W. M., Deng, J. M., Zhang, Z. P., Behringer, R. R. & de Crombrugghe, B. (1999) Sox9 is required for cartilage formation. *Nature Genetics*, 22(1), 85-89.

Bieback, K., Hecker, A., Kocaoemer, A., Lannert, H., Schallmoser, K., Strunk, D. & Klueter, H. (2009) Human Alternatives to Fetal Bovine Serum for the Expansion of Mesenchymal Stromal Cells from Bone Marrow. *Stem Cells*, 27(9), 2331-2341.

Bilgen, B. & Barabino, G. A. (2007) Location of scaffolds in bioreactors modulates the hydrodynamic environment experienced by engineered tissues. *Biotechnology and Bioengineering*, 98(1), 282-294.

Binnerts, A., Swart, G. R., Wilson, J. H. P., Hoogerbrugge, N., Pols, H. A. P., Birkenhager, J. C. & Lamberts, S. W. J. (1992) The effect of growth-hormone administration in growth-hormone deficient adults on bone, protein, carbohydrate and lipid homeostasis, as well as on body-composition. *Clinical Endocrinology*, 37(1), 79-87.

Boivin, G., Bala, Y., Doublier, A., Farlay, D., Ste-Marie, L. G., Meunier, P. J. & Delmas, P. D. (2008) The role of mineralization and organic matrix in the microhardness of bone tissue from controls and osteoporotic patients. *Bone*, 43(3), 532-538.

Bravo-Osuna, I., Millotti, G., Vauthier, C. & Ponchel, G. (2007) In vitro evaluation of calcium binding capacity of chitosan and thiolated chitosan poly(isobutyl cyanoacrylate) core-shell nanoparticles. *International Journal of Pharmaceutics*, 338(1-2), 284-290.

Brittberg, M., Lindahl, A., Nilsson, A., Ohlsson, C., Isaksson, O. & Peterson, L. (1994) Treatment of deep cartilage defects in the knee with autologous chondrocyte transplantation. *New England Journal of Medicine*, 331(14), 889-895.

Bruder, S. P., Fink, D. J. & Caplan, A. I. (1994) Mesenchymal stem-cells in in bone-development, bone repair, and skeletal regeneration therapy. *Journal of Cellular Biochemistry*, 56(3), 283-294.

Buckwalter, J. A. (2002) Articular cartilage injuries. *Clinical Orthopaedics and Related Research*(402), 21-37.

Buckwalter, J. A. & Mankin, H. J. (1997) Articular cartilage .2. Degeneration and osteoarthrosis, repair, regeneration, and transplantation. *Journal of Bone and Joint Surgery-American Volume*, 79A(4), 612-632.

Butler, D. L., Juncosa-Melvin, N., Boivin, G. P., Galloway, M. T., Shearn, J. T., Gooch, C. & Awad, H. (2008) Functional tissue engineering for tendon repair: A multidisciplinary strategy using mesenchymal stem cells, bioscaffolds, and mechanical stimulation. *Journal of Orthopaedic Research*, 26(1), 1-9.

Campos, E., Coimbra, P. & Gil, M. H. (2013) An improved method for preparing glutaraldehyde cross-linked chitosan-poly(vinyl alcohol) microparticles. *Polymer Bulletin*, 70(2), 549-561.

Cao, B., Li, Z., Peng, R. & Ding, J. (2015) Effects of cell-cell contact and oxygen tension on chondrogenic differentiation of stem cells. *Biomaterials*, 64, 21-32.

Caplan, A. I. (1991) Mesenchymal stem-cells. *Journal of Orthopaedic Research*, 9(5), 641-650.

Caplan, A. I. (2007) Adult mesenchymal stem cells for tissue engineering versus regenerative medicine. *Journal of Cellular Physiology*, 213(2), 341-347.

Caplan, A. I. & Bruder, S. P. (2001) Mesenchymal stem cells: building blocks for molecular medicine in the 21st century. *Trends in Molecular Medicine*, 7(6), 259-264.

Caplan, A. I. & Dennis, J. E. (2006) Mesenchymal stem cells as trophic mediators. *Journal of Cellular Biochemistry*, 98(5), 1076-1084.

Caric, D., Tomisic, V., Kveder, M., Galic, N., Pifat, G., Magnus, V. & Soskic, M. (2004) Absorption and fluorescence spectra of ring-substituted indole-3-acetic acids. *Biophysical Chemistry*, 111(3), 247-257.

Caron, M. M. J., Emans, P. J., Coolsen, M. M. E., Voss, L., Surtel, D. A. M., Cremers, A., van Rhijn, L. W. & Welting, T. J. M. (2012) Redifferentiation of dedifferentiated human articular chondrocytes: comparison of 2D and 3D cultures. *Osteoarthritis and Cartilage*, 20(10), 1170-1178.

Carter, D. R., Beaupre, G. S., Giori, N. J. & Helms, J. A. (1998) Mechanobiology of skeletal regeneration. *Clinical Orthopaedics and Related Research*(355), S41-S55.

Cengiz, I.F., Oliveira, J.M., and Reis, R.L., 2014. *3D Multiscale Physiological Human*, 4, 25-47.

Chakrabarti, A. C., Veiro, J. A., Wong, N. S., Wheeler, J. J. & Cullis, P. R. (1992) Generation and characterization of iron-loaded and barium-loaded liposomes. *Biochimica Et Biophysica Acta*, 1108(2), 233-239.

Chamberlain, G., Fox, J., Ashton, B. & Middleton, J. (2007) Concise review: Mesenchymal stem cells: Their phenotype, differentiation capacity, immunological features, and potential for homing. *Stem Cells*, 25(11), 2739-2749.

Chang, C. H., Lin, F. H., Lin, C. C., Chou, C. H. & Liu, H. C. (2004) Cartilage tissue engineering on the surface of a novel gelatin-calcium-phosphate biphasic scaffold in a double-chamber biorector. *Journal of Biomedical Materials Research Part B-Applied Biomaterials*, 71B(2), 313-321.

Chang, K. L. B., Tsai, G., Lee, J. & Fu, W. R. (1997) Heterogeneous N-deacetylation of chitin in alkaline solution. *Carbohydrate Research*, 303(3), 327-332.

Chase, L. G., Lakshmipathy, U., Solchaga, L. A., Rao, M. S. & Vemuri, M. C. (2010) A novel serum-free medium for the expansion of human mesenchymal stem cells. *Stem cell research & therapy*, 1(1), 8.

Chen, H. M., Wei, O. Y., Bisi, L. Y., Martoni, C. & Prakash, S. (2005) Reaction of chitosan with genipin and its fluorogenic attributes for potential microcapsule membrane characterization. *Journal of Biomedical Materials Research Part A*, 75A(4), 917-927.

Chen, J. N., Chen, H. A., Li, P., Diao, H. J., Zhu, S. Y., Dong, L., Wang, R., Guo, T., Zhao, J. N. & Zhang, J. F. (2011) Simultaneous regeneration of articular cartilage and subchondral bone in vivo using MSCs induced by a spatially controlled gene delivery system in bilayered integrated scaffolds. *Biomaterials*, 32(21), 4793-4805.

Choi, J., Chung, J.-H., Kwon, G.-Y., Kim, K.-W., Kim, S. & Chang, H. (2013) Effectiveness of autologous serum as an alternative to fetal bovine serum in adipose-derived stem cell engineering. *Cell and Tissue Banking*, 14(3), 413-422.

Chua, K. H., Aminuddin, B. S., Fuzina, N. H. & Ruszymah, B. H. I. (2007) Basic fibroblast growth factor with human serum supplementation: enhancement of human chondrocyte proliferation and promotion of cartilage regeneration. *SMJ Singapore Medical Journal*, 48(4), 324-332.

Chung, C. & Burdick, J. A. (2008) Engineering cartilage tissue. *Advanced Drug Delivery Reviews*, 60(2), 243-262.

Clarke, B. (2008) Normal Bone Anatomy and Physiology. *Clinical Journal of the American Society of Nephrology*, 3, S131-S139.

Cobb, J. P. & Walker, D. G. (1961) Effect of heterologous, homologous, and autologous serums on human normal and malignant cells in vitro. *Journal of the National Cancer Institute*, 27(1), 1-&.

Conaghan, P. G., Porcheret, M., Kingsbury, S. R., Gammon, A., Soni, A., Hurley, M., Rayman, M. P., Barlow, J., Hull, R. G., Cumming, J., Llewelyn, K., Moscogiuri, F., Lyons, J. & Birrell, F. (2015) Impact and therapy of osteoarthritis: the Arthritis Care OA Nation 2012 survey. *Clinical Rheumatology*, 34(9), 1581-1588.

Corrin, A. A., Ngai, M., Walthers, C. M., Dunn, J. C. Y., Wu, B. M. & Ieee (2012) Injectable Macroporous Microparticles for Soft Tissue Augmentation, *34th Annual International Conference of the IEEE Engineering-in-Medicine-and-Biology-Society (EMBS)*. San Diego, CA, Aug 28-Sep 01. NEW YORK: Ieee.

Costa-Pinto, A. R., Correlo, V. M., Sol, P. C., Bhattacharya, M., Charbord, P., Delorme, B., Reis, R. L. & Neves, N. M. (2009) Osteogenic Differentiation of Human Bone Marrow Mesenchymal Stem Cells Seeded on Melt Based Chitosan Scaffolds for Bone Tissue Engineering Applications. *Biomacromolecules*, 10(8), 2067-2073.

Dalby, M. J., Gadegaard, N., Tare, R., Andar, A., Riehle, M. O., Herzyk, P., Wilkinson, C. D. W. & Oreffo, R. O. C. (2007) The control of human mesenchymal cell differentiation using nanoscale symmetry and disorder. *Nature Materials*, 6(12), 997-1003.

Dalby, M. J., McCloy, D., Robertson, M., Agheli, H., Sutherland, D., Affrossman, S. & Oreffo, R. O. C. (2006) Osteoprogenitor response to semi-ordered and random nanotopographies. *Biomaterials*, 27(15), 2980-2987.

Dash, M., Chiellini, F., Ottenbrite, R. M. & Chiellini, E. (2011) Chitosan-A versatile semi-synthetic polymer in biomedical applications. *Progress in Polymer Science*, 36(8), 981-1014.

Day, T. F., Guo, X. Z., Garrett-Beal, L. & Yang, Y. Z. (2005) Wnt/beta-catenin signaling in mesenchymal progenitors controls osteoblast and chondrocyte differentiation during vertebrate skeletogenesis. *Developmental Cell*, 8(5), 739-750.

De Spiegelaere, W., Cornillie, P., Casteleyn, C., Burvenich, C. & Van den Broeck, W. (2010) Detection of Hypoxia Inducible Factors and Angiogenic Growth Factors during Foetal Endochondral and Intramembranous Ossification. *Anatomia Histologia Embryologia*, 39(4), 376-384.

Debbaut, C., Monbaliu, D., Casteleyn, C., Van Loo, D., Masschaele, B., Cornillie, P., Pirenne, J., Van Hoorebeke, L., Simoens, P. & Segers, P. (2009) Constructing a model of blood flow in human liver using contrast-loaded corrosion casting and micro-ct imaging. *International Journal of Artificial Organs*, 32(7), 451-451.

DeLise, A. M., Fischer, L. & Tuan, R. S. (2000) Cellular interactions and signaling in cartilage development. *Osteoarthritis and Cartilage*, 8(5), 309-334.

Deville, S. (2008) Freeze-casting of porous ceramics: A review of current achievements and issues. *Advanced Engineering Materials*, 10(3), 155-169.

Di Martino, A., Sittinger, M. & Risbud, M. V. (2005) Chitosan: A versatile biopolymer for orthopaedic tissue-engineering. *Biomaterials*, 26(30), 5983-5990.

DiMarino, A. M., Caplan, A. I. & Bonfield, T. L. (2013) Mesenchymal stem cells in tissue repair. *Frontiers in Immunology*, 4.

Doucet, C., Ernou, I., Zhang, Y. Z., Llense, J. R., Begot, L., Holy, X. & Lataillade, J. J. (2005) Platelet lysates promote mesenchymal stem cell expansion: A safety substitute for animal serum in cell-based therapy applications. *Journal of Cellular Physiology*, 205(2), 228-236.

Dowthwaite, G. P., Bishop, J. C., Redman, S. N., Khan, I. M., Rooney, P., Evans, D. J. R., Haughton, L., Bayram, Z., Boyer, S., Thomson, B., Wolfe, M. S. & Archer, C. W. (2004) The surface of articular cartilage contains a progenitor cell population. *Journal of Cell Science*, 117(6), 889-897.

Drury, J. L. & Mooney, D. J. (2003) Hydrogels for tissue engineering: scaffold design variables and applications. *Biomaterials*, 24(24), 4337-4351.

Duan, P., Pan, Z., Cao, L., He, Y., Wang, H., Qu, Z., Dong, J. & Ding, J. (2014) The effects of pore size in bilayered poly(lactide-co-glycolide) scaffolds on restoring osteochondral defects in rabbits. *Journal of Biomedical Materials Research Part A*, 102(1), 180-192.

Ducy, P., Desbois, C., Boyce, B., Pinero, G., Story, B., Dunstan, C., Smith, E., Bonadio, J., Goldstein, S., Gundberg, C., Bradley, A. & Karsenty, G. (1996) Increased bone formation in osteocalcin-deficient mice. *Nature*, 382(6590), 448-452.

Ducy, P., Zhang, R., Geoffroy, V., Ridall, A. L. & Karsenty, G. (1997) Osf2/Cbfa1: A transcriptional activator of osteoblast differentiation. *Cell*, 89(5), 747-754.

Egli, R. J., Bastian, J. D., Ganz, R., Hofstetter, W. & Leunig, M. (2008) Hypoxic expansion promotes the chondrogenic potential of articular chondrocytes. *Journal of Orthopaedic Research*, 26(7), 977-985.

Einhorn, T. A. & Gerstenfeld, L. C. (2015) Fracture healing: mechanisms and interventions. *Nature Reviews Rheumatology*, 11(1), 45-54.

El Haj, A. J. & Cartmell, S. H. (2010) Bioreactors for bone tissue engineering. *Proceedings of the Institution of Mechanical Engineers Part H-Journal of Engineering in Medicine*, 224(H12), 1523-1532.

Elder, S., Gottipati, A., Zelenka, H. & Bumgardner, J. (2013) Attachment, proliferation, and chondroinduction of mesenchymal stem cells on porous chitosan-calcium phosphate scaffolds. *The open orthopaedics journal*, 7, 275-81.

Engler, A. J., Sen, S., Sweeney, H. L. & Discher, D. E. (2006) Matrix elasticity directs stem cell lineage specification. *Cell*, 126(4), 677-689.

Eyre, D. R. & Muir, H. (1975) Distribution of different molecular species of collagen in fibrous, elastic and hyaline cartilages of pig. *Biochemical Journal*, 151(3), 595-602.

Ferguson, C., Alpern, E., Miclau, T. & Helms, J. A. (1999) Does adult fracture repair recapitulate embryonic skeletal formation? *Mechanisms of Development*, 87(1-2), 57-66.

Fonseca, C., Caminal, M., Peris, D., Barrachina, J., Fabregas, P. J., Garcia, F., Cairo, J. J., Godia, F., Pla, A. & Vives, J. (2014) An arthroscopic approach for the treatment of osteochondral focal defects with cell-free and cell-loaded PLGA scaffolds in sheep. *Cytotechnology*, 66(2), 345-354.

France, L., Scotchford, C., Grant, D., Rashidi, H., Popov, A. & Sottile, V. (2012) Dual differentiation of human mesenchymal stem cell driven by transient serum exposure regimes. *Human Gene Therapy*, 23(10), A87-A87.

Franz, T., Hasler, E. M., Hagg, R., Weiler, C., Jakob, R. P. & Mainil-Varlet, P. (2001) In situ compressive stiffness, biochemical composition, and structural integrity of articular cartilage of the human knee joint. *Osteoarthritis and Cartilage*, 9(6), 582-592.

Friedenstein, A., Petrakov, K., Kuroleso, A. & Frolova, G. P. (1968) Heterotopic transplants of bone marrow - analysis of precursor cells for osteogenic and hematopoietic tissues. *Transplantation*, 6(2), 230-247.

Gao, J., Dennis, J. E., Solchaga, L. A., Goldberg, V. M. & Caplan, A. I. (2002) Repair of osteochondral defect with tissue-engineered two-phase composite material of injectable calcium phosphate and hyaluronan sponge. *Tissue Engineering*, 8(5), 827-837.

Garg, T., Singh, O., Arora, S. & Murthy, R. S. R. (2012) Scaffold: A Novel Carrier for Cell and Drug Delivery. *Critical Reviews in Therapeutic Drug Carrier Systems*, 29(1), 1-63.

Ghazavi, M. T., Pritzker, K. P., Davis, A. M. & Gross, A. E. (1997) Fresh osteochondral allografts for post-traumatic osteochondral defects of the knee. *Journal of Bone and Joint Surgery-British Volume*, 79B(6), 1008-1013.

Girgis, C. M., Baldock, P. A. & Downes, M. (2015) Vitamin D, muscle and bone: Integrating effects in development, aging and injury. *Molecular and Cellular Endocrinology*, 410(C), 3-10.

Godbey, W. T., Hindy, B. S. S., Sherman, M. E. & Atala, A. (2004) A novel use of centrifugal force for cell seeding into porous scaffolds. *Biomaterials*, 25(14), 2799-2805.

Goldring, M. B. (2012) Chondrogenesis, chondrocyte differentiation, and articular cartilage metabolism in health and osteoarthritis. *Therapeutic advances in musculoskeletal disease*, 4(4), 269-85.

Goldring, M. B., Tsuchimochi, K. & Ijiri, K. (2006) The control of chondrogenesis. *Journal of Cellular Biochemistry*, 97(1), 33-44.

Goltzman, D., Hendy, G. N. & White, J. H. (2015) Vitamin D and its receptor during late development. *Biochimica Et Biophysica Acta-Gene Regulatory Mechanisms*, 1849(2), 171-180.

Golub, E. E. (2009) Role of matrix vesicles in biomineralization. *Biochimica Et Biophysica Acta-General Subjects*, 1790(12), 1592-1598.

Gomes, M. E., Holtorf, H. L., Reis, R. L. & Mikos, A. G. (2006) Influence of the porosity of starch-based fiber mesh scaffolds on the proliferation and osteogenic differentiation of bone marrow stromal cells cultured in a flow perfusion bioreactor. *Tissue Engineering*, 12(4), 801-809.

Gottardi, R., Lin, H., Lozito, T. P., Alexander, P. G., Clark, K. L., Sefton, E. C., Woodruff, T. K. & Tuan, R. S. (2014) An Osteochondral Microphysiological System to Study the Pathogenesis of Osteoarthritis and the Effect of Hormonal Exposure. *Tissue Engineering Part A*, 20, S34-S34.

Granet, C., Laroche, N., Vico, L., Alexandre, C. & Lafage-Proust, M. H. (1998) Rotating-wall vessels, promising bioreactors for osteoblastic cell culture: comparison with other 3D conditions. *Medical & Biological Engineering & Computing*, 36(4), 513-519.

Grunder, T., Gaissmaier, C., Fritz, J., Stoop, R., Hortschansky, P., Mollenhauer, J. & Aicher, W. K. (2004) Bone morphogenetic protein (BMP)-2 enhances the expression of type II collagen and aggrecan in chondrocytes embedded in alginate beads. *Osteoarthritis and Cartilage*, 12(7), 559-567.

Gu, K. B. & Li, L. P. (2011) A human knee joint model considering fluid pressure and fiber orientation in cartilages and menisci. *Medical Engineering & Physics*, 33(4), 497-503.

Gulbins, H., Goldemund, A., Anderson, I., Haas, U., Uhlig, A., Meiser, B. & Reichart, B. (2003) Preseeding with autologous fibroblasts improves endothelialization of glutaraldehyde-fixed porcine aortic valves. *Journal of Thoracic and Cardiovascular Surgery*, 125(3), 592-601.

Gupta, A. K. & Gupta, M. (2005) Synthesis and surface engineering of iron oxide nanoparticles for biomedical applications. *Biomaterials*, 26(18), 3995-4021.

Haasper, C., Colditz, M., Budde, S., Hesse, E., Tschernig, T., Frink, M., Krettek, C., Hurschler, C. & Jagodzinski, M. (2009) Perfusion and cyclic compression of mesenchymal cell-loaded and clinically applicable osteochondral grafts. *Knee Surgery Sports Traumatology Arthroscopy*, 17(11), 1384-1392.

Haasper, C., Zeichen, J., Meister, R., Krettek, C. & Jagodzinski, M. (2008) Tissue engineering of osteochondral constructs in vitro using bioreactors. *Injury-International Journal of the Care of the Injured*, 39, S66-S76.

Habibovic, P., Gbureck, U., Doillon, C. J., Bassett, D. C., van Blitterswijk, C. A. & Barralet, J. E. (2008) Osteoconduction and osteoinduction of low-temperature 3D printed bioceramic implants. *Biomaterials*, 29(7), 944-953.

Hangartner, T. N. & Gilsanz, V. (1996) Evaluation of cortical bone by computed tomography. *Journal of Bone and Mineral Research*, 11(10), 1518-1525.

Hangody, L. & Fules, P. (2003) Autologous osteochondral mosaicplasty for the treatment of full-thickness defects of weight-bearing joints - Ten years of experimental and clinical experience. *Journal of Bone and Joint Surgery-American Volume*, 85A, 25-32.

Hangody, L., Rathonyi, G. K., Duska, Z., Vasarhelyi, G., Fules, P. & Modis, L. (2004) Autologous osteochondral mosaicplasty. Surgical technique. *The Journal of bone and joint surgery. American volume*, 86-A Suppl 1, 65-72.

Harrison, R., El Haj, A. & Sottile, V. (2014) Magnetic Targeting for Enhanced Stem Cell Therapies. *Tissue Engineering Part A*, 20, S11-S11.

Hench, L. L. (1991) Bioceramics - from concept to clinic. *Journal of the American Ceramic Society*, 74(7), 1487-1510.

Henderson, S. E., Santangelo, K. S. & Bertone, A. L. (2011) Chondrogenic effects of exogenous retinoic acid or a retinoic acid receptor antagonist (LE135) on equine chondrocytes and bone marrow-derived mesenchymal stem cells in monolayer culture. *American Journal of Veterinary Research*, 72(7), 884-892.

Hersel, U., Dahmen, C. & Kessler, H. (2003) RGD modified polymers: biomaterials for stimulated cell adhesion and beyond. *Biomaterials*, 24(24), 4385-4415.

Heywood, H. K., Nalesso, G., Lee, D. A. & Dell'accio, F. (2014) Culture expansion in low-glucose conditions preserves chondrocyte differentiation and enhances their subsequent capacity to form cartilage tissue in three-dimensional culture. *BioResearch open access*, 3(1), 9-18.

Hogan, B. L. M. (1996) Bone morphogenetic proteins: Multifunctional regulators of vertebrate development. *Genes & Development*, 10(13), 1580-1594.

Hogan, N. (1985) The mechanics of multi-joint posture and movement control. *Biological Cybernetics*, 52(5), 315-331.

Hollister, S. J. (2005) Porous scaffold design for tissue engineering. *Nature Materials*, 4(7), 518-524.

Hong, Y., Song, H., Gong, Y., Mao, Z., Gao, C. & Shen, J. (2007) Covalently crosslinked chitosan hydrogel: Properties of in vitro degradation and chondrocyte encapsulation. *Acta Biomaterialia*, 3(1), 23-31.

Honmou, O., Houkin, K., Matsunaga, T., Niitsu, Y., Ishiai, S., Onodera, R., Waxman, S. G. & Kocsis, J. D. (2011) Intravenous administration of auto serum-expanded autologous mesenchymal stem cells in stroke. *Brain*, 134, 1790-1807.

Huang, C. Y. C., Hagar, K. L., Frost, L. E., Sun, Y. B. & Cheung, H. S. (2004) Effects of cyclic compressive loading on chondrogenesis of rabbit bone-marrow derived mesenchymal stem cells. *Stem Cells*, 22(3), 313-323.

Hunziker, E. B. (2002) Articular cartilage repair: basic science and clinical progress. A review of the current status and prospects. *Osteoarthritis and Cartilage*, 10(6), 432-463.

Hutmacher, D. W. (2000) Scaffolds in tissue engineering bone and cartilage. *Biomaterials*, 21(24), 2529-2543.

Hutmacher, D. W., Goh, J. C. H. & Teoh, S. H. (2001) An introduction to biodegradable materials for tissue engineering applications. *Annals Academy of Medicine Singapore*, 30(2), 183-191.

Hwang, Y.-J., Larsen, J., Krasieva, T. B. & Lyubovitsky, J. G. (2011) Effect of Genipin Crosslinking on the Optical Spectral Properties and Structures of Collagen Hydrogels. *Acs Applied Materials & Interfaces*, 3(7), 2579-2584.

Ibrahim, N. S., Krishnamurithy, G., Raghavendran, H. R. B., Puvaneswary, S., Ng Wuey, M. & Kamarul, T. (2013) Novel HA-PVA/NOCC bilayered scaffold for osteochondral tissue-engineering applications - Fabrication, characterization, in vitro and in vivo biocompatibility study. *Materials Letters*, 113, 25-29.

Ilizarov, G. A. (1988) The principles of the ilizarov method. *Bulletin of the Hospital for Joint Diseases Orthopaedic Institute*, 48(1), 1-11.

Ilizarov, G. A. (1989) The tension stress effect on the genesis and growth of tissues .2. The influence of the rate and frequency of distraction. *Clinical Orthopaedics and Related Research*(239), 263-285.

Illum, L. (1998) Chitosan and its use as a pharmaceutical excipient. *Pharmaceutical Research*, 15(9), 1326-1331.

Im, G. I., Ko, J. Y. & Lee, J. H. (2012) Chondrogenesis of Adipose Stem Cells in a Porous Polymer Scaffold: Influence of the Pore Size. *Cell Transplantation*, 21(11), 2397-2405.

Iorio, R., Robb, W. J., Healy, W. L., Berry, D. J., Hozack, W. J., Kyle, R. F., Lewallen, D. G., Trousdale, R. T., Jiranek, W. A., Stamos, V. P. & Parsley, B. S. (2008) Orthopaedic surgeon workforce and volume assessment for total hip and knee replacement in the united states: Preparing for an epidemic. *Journal of Bone and Joint Surgery-American Volume*, 90A(7), 1598-1605.

Iozzo, R. V. (1998) Matrix proteoglycans: From molecular design to cellular function. *Annual Review of Biochemistry*, 67, 609-652.

Jaiswal, N., Haynesworth, S. E., Caplan, A. I. & Bruder, S. P. (1997) Osteogenic differentiation of purified, culture-expanded human mesenchymal stem cells in vitro. *Journal of Cellular Biochemistry*, 64(2), 295-312.

Jakob, M., Demarteau, O., Schafer, D., Hintermann, B., Dick, W., Heberer, M. & Martin, I. (2001) Specific growth factors during the expansion and redifferentiation of adult human articular chondrocytes enhance chondrogenesis and cartilaginous tissue formation in vitro. *Journal of Cellular Biochemistry*, 81(2), 368-377.

Jeon, J. E., Vaquette, C., Klein, T. J. & Hutmacher, D. W. (2014) Perspectives in Multiphasic Osteochondral Tissue Engineering. *Anatomical Record-Advances in Integrative Anatomy and Evolutionary Biology*, 297(1), 26-35.

Jeong, S. I., Kim, S. Y., Cho, S. K., Chong, M. S., Kim, K. S., Kim, H., Lee, S. B. & Lee, Y. M. (2007) Tissue-engineered vascular grafts composed of marine collagen and PLGA fibers using pulsatile perfusion bioreactors. *Biomaterials*, 28(6), 1115-1122.

Jeong, S. I., Kwon, J. H., Lim, J. I., Cho, S. W., Jung, Y. M., Sung, W. J., Kim, S. H., Kim, Y. H., Lee, Y. M., Kim, B. S., Choi, C. Y. & Kim, S. J. (2005) Mechano-active tissue engineering of vascular smooth muscle using pulsatile perfusion bioreactors and elastic PLCL scaffolds. *Biomaterials*, 26(12), 1405-1411.

Jin, J., Song, M. & Hourston, D. J. (2004) Novel chitosan-based films cross-linked by genipin with improved physical properties. *Biomacromolecules*, 5(1), 162-168.

Johnson, T., Bahrampourian, R., Patel, A. & Mequanint, K. (2010) Fabrication of highly porous tissue-engineering scaffolds using selective spherical porogens. *Bio-Medical Materials and Engineering*, 20(2), 107-118.

Johnstone, B., Hering, T. M., Caplan, A. I., Goldberg, V. M. & Yoo, J. U. (1998) In vitro chondrogenesis of bone marrow-derived mesenchymal progenitor cells. *Experimental Cell Research*, 238(1), 265-272.

Jung, D.-Y., Yamada, T., Tsuchiya, T., Ryu, S.-C. & Han, D.-W. (2010) Effects of Cell-seeding Methods of Human Osteoblast Culture on Biomechanical Properties of Porous Bioceramic Scaffold. *Biotechnology and Bioprocess Engineering*, 15(2), 341-348.

Kafienah, W., Mistry, S., Dickinson, S. C., Sims, T. J., Learmonth, I. & Hollander, A. P. (2007) Three-dimensional cartilage tissue engineering using adult stem cells from osteoarthritis patients. *Arthritis and Rheumatism*, 56(1), 177-187.

Kang, H. W., Tabata, Y. & Ikada, Y. (1999) Fabrication of porous gelatin scaffolds for tissue engineering. *Biomaterials*, 20(14), 1339-1344.

Kanichai, M., Ferguson, D., Prendergast, P. J. & Campbell, V. A. (2008) Hypoxia promotes chondrogenesis in rat mesenchymal stem cells: A role for AKT and hypoxia-inducible factor (HIF)-1 alpha. *Journal of Cellular Physiology*, 216(3), 708-715.

Karadeniz, L. & Astley, S. T. (2013) Catalyst functional group cooperativity in the amino acid-catalysed nitroaldol condensation reaction. *Research on Chemical Intermediates*, 39(7), 3407-3415.

Karageorgiou, V. & Kaplan, D. (2005a) Porosity of 3D biomaterial scaffolds and osteogenesis. *Biomaterials*, 26(27), 5474-5491.

Karageorgiou, V. & Kaplan, D. (2005b) Porosity of 3D biornaterial scaffolds and osteogenesis. *Biomaterials*, 26(27), 5474-5491.

Kartsogiannis, V. & Ng, K. W. (2004) Cell lines and primary cell cultures in the study of bone cell biology. *Molecular and Cellular Endocrinology*, 228(1-2), 79-102.

Katti, K. S. (2004) Biomaterials in total joint replacement. *Colloids and Surfaces B-Biointerfaces*, 39(3), 133-142.

Kelly, D. J. & Jacobs, C. R. (2010) The Role of Mechanical Signals in Regulating Chondrogenesis and Osteogenesis of Mesenchymal Stem Cells. *Birth Defects Research Part C-Embryo Today-Reviews*, 90(1), 75-85.

Khan, W. S., Adesida, A. B. & Hardingham, T. E. (2007) Hypoxic conditions increase hypoxia-inducible transcription factor 2 alpha and enhance chondrogenesis in stem cells from the infrapatellar fat pad of osteoarthritis patients. *Arthritis Research & Therapy*, 9(3).

Khor, K. A., Li, H. & Cheang, P. (2003) Characterization of the bone-like apatite precipitated on high velocity oxy-fuel (HVOF) sprayed calcium phosphate deposits. *Biomaterials*, 24(5), 769-775.

Kim, S. E., Park, J. H., Cho, Y. W., Chung, H., Jeong, S. Y., Lee, E. B. & Kwon, I. C. (2003) Porous chitosan scaffold containing microspheres loaded with transforming growth factor-beta 1: Implications for cartilage tissue engineering. *Journal of Controlled Release*, 91(3), 365-374.

Kirsch, T., Nah, H. D., Shapiro, I. M. & Pacifici, M. (1997) Regulated production of mineralization-competent matrix vesicles in hypertrophic chondrocytes. *Journal of Cell Biology*, 137(5), 1149-1160.

Kitagawa, T., Yamaoka, T., Iwase, R. & Murakami, A. (2006) Three-dimensional cell seeding and growth in radial-flow perfusion bioreactor for in vitro tissue reconstruction. *Biotechnology and Bioengineering*, 93(5), 947-954.

Koch, M. A., Vrij, E. J., Engel, E., Planell, J. A. & Lacroix, D. (2010) Perfusion cell seeding on large porous PLA/calcium phosphate composite scaffolds in a perfusion bioreactor system under varying perfusion parameters. *Journal of Biomedical Materials Research Part A*, 95A(4), 1011-1018.

Kojimoto, H., Yasui, N., Goto, T., Matsuda, S. & Shimomura, Y. (1988) bone lengthening in rabbits by callus distraction - the role of periosteum and endosteum. *Journal of Bone and Joint Surgery-British Volume*, 70(4), 543-549.

Komori, T., Yagi, H., Nomura, S., Yamaguchi, A., Sasaki, K., Deguchi, K., Shimizu, Y., Bronson, R. T., Gao, Y. H., Inada, M., Sato, M., Okamoto, R., Kitamura, Y., Yoshiki, S. & Kishimoto, T. (1997) Targeted disruption of Cbfa1 results in a complete lack of bone formation owing to maturational arrest of osteoblasts. *Cell*, 89(5), 755-764.

Kong, L. J., Gao, Y., Lu, G. Y., Gong, Y. D., Zhao, N. M. & Zhang, X. F. (2006) A study on the bioactivity of chitosan/nano-hydroxyapatite composite scaffolds for bone tissue engineering. *European Polymer Journal*, 42(12), 3171-3179.

Kozielski, M., Buchwald, T., Szybowicz, M., Blaszczak, Z., Piotrowski, A. & Ciesielczyk, B. (2011) Determination of composition and structure of spongy bone tissue in human head of femur by Raman spectral mapping. *Journal of Materials Science-Materials in Medicine*, 22(7), 1653-1661.

Kramer, I., Halleux, C., Keller, H., Pegurri, M., Gooi, J. H., Weber, P. B., Feng, J. Q., Bonewald, L. F. & Kneissel, M. (2010) Osteocyte Wnt/beta-Catenin Signaling Is Required for Normal Bone Homeostasis. *Molecular and Cellular Biology*, 30(12), 3071-3085.

Kuiper, N. J., Wang, Q. G. & Cartmell, S. H. (2014) A Perfusion Co-Culture Bioreactor for Osteochondral Tissue Engineered Plugs. *Journal of Biomaterials and Tissue Engineering*, 4(2), 162-171.

Kurosawa, H. (2007) Methods for inducing embryoid body formation: In vitro differentiation system of embryonic stem cells. *Journal of Bioscience and Bioengineering*, 103(5), 389-398.

Kurz, B., Domm, C., Jin, M. S., Sellckau, R. & Schunke, M. (2004) Tissue engineering of articular cartilage under the influence of collagen I/III membranes and low oxygen tension. *Tissue Engineering*, 10(7-8), 1277-1286.

Kusuzaki, K., Sugimoto, S., Takeshita, H., Murata, H., Hashiguchi, S., Nozaki, T., Emoto, K., Ashihara, T. & Hirasawa, Y. (2001) DNA cytofluorometric analysis of chondrocytes in human articular cartilages under normal aging or arthritic conditions. *Osteoarthritis and Cartilage*, 9(7), 664-670.

Kuznetsov, S. A., Mankani, M. H. & Robey, P. G. (2000) Effect of serum on human bone marrow stromal cells: Ex vivo expansion and in vivo bone formation. *Transplantation*, 70(12), 1780-1787.

Kyllonen, L., Haimi, S., Mannerstrom, B., Huhtala, H., Rajala, K. M., Skottman, H., Sandor, G. K. & Miettinen, S. (2013) Effects of different serum conditions on osteogenic differentiation of human adipose stem cells in vitro. *Stem Cell Research & Therapy*, 4, 15.

Landis, W. J. & Glimcher, M. J. (1982) Electron-optical and analytical observations of rat growth plate cartilage prepared by ultra-cryomicrotomy - the failure to detect a mineral phase in matrix vesicles and the identification of heterodispersed particles as the initial solid-phase of calcium-phosphate deposited in the extracellular-matrix. *Journal of Ultrastructure Research*, 78(3), 227-268.

Lane, L. B. & Bullough, P. G. (1980) Age-related-changes in the thickness of the calcified zone and the number of tidemarks in adult human articular-cartilage. *Journal of Bone and Joint Surgery-British Volume*, 62(3), 372-375.

Lange, C., Cakiroglu, F., Spiess, A. N., Cappallo-Obermann, H., Dierlamm, J. & Zander, A. R. (2007) Accelerated and safe expansion of human mesenchymal stromal cells in animal serum-free medium for transniantation and regenerative medicine. *Journal of Cellular Physiology*, 213(1), 18-26.

Langer, R. & Vacanti, J. P. (1993) Tissue engineering. *Science*, 260(5110), 920-926.

Laurent, S., Forge, D., Port, M., Roch, A., Robic, C., Elst, L. V. & Muller, R. N. (2008) Magnetic iron oxide nanoparticles: Synthesis, stabilization, vectorization, physicochemical characterizations, and biological applications. *Chemical Reviews*, 108(6), 2064-2110.

Lee, S., Kim, J. H., Jo, C. H., Seong, S. C., Lee, J. C. & Lee, M. C. (2009) Effect of Serum and Growth Factors on Chondrogenic Differentiation of Synovium-Derived Stromal Cells. *Tissue Engineering Part A*, 15(11), 3401-3415.

Lennon, D. P., Edmison, J. M. & Caplan, A. I. (2001) Cultivation of rat marrow-derived mesenchymal stem cells in reduced oxygen tension: Effects on in vitro and in vivo osteochondrogenesis. *Journal of Cellular Physiology*, 187(3), 345-355.

Li, Y. M., Schilling, T., Benisch, P., Zeck, S., Meissner-Weigl, J., Schneider, D., Limbert, C., Seufert, J., Kassem, M., Schutze, N., Jakob, F. & Ebert, R. (2007) Effects of high glucose on mesenchymal stem cell proliferation and differentiation. *Biochemical and Biophysical Research Communications*, 363(1), 209-215.

Liu, C.-H., Wu, M.-L. & Hwang, S.-M. (2007) Optimization of serum free medium for cord blood mesenchymal stem cells. *Biochemical Engineering Journal*, 33(1), 1-9.

Liu, X.-g. & Jiang, H.-k. (2013) Preparation of an osteochondral composite with mesenchymal stem cells as the single-cell source in a double-chamber bioreactor. *Biotechnology Letters*, 35(10), 1645-1653.

Long, M. W. (2001) Osteogenesis and bone-marrow-derived cells. *Blood Cells Molecules and Diseases*, 27(3), 677-690.

Loret, B. & Simoes, F. M. F. (2010) Effects of pH on transport properties of articular cartilages. *Biomechanics and Modeling in Mechanobiology*, 9(1), 45-63.

Lu, H. H., Subramony, S. D., Boushell, M. K. & Zhang, X. (2010) Tissue Engineering Strategies for the Regeneration of Orthopedic Interfaces. *Annals of Biomedical Engineering*, 38(6), 2142-2154.

Luciani, A., Coccoli, V., Orsi, S., Ambrosio, L. & Netti, P. A. (2008) PCL microspheres based functional scaffolds by bottom-up approach with predefined microstructural properties and release profiles. *Biomaterials*, 29(36), 4800-4807.

Lutolf, M. P. & Hubbell, J. A. (2005) Synthetic biomaterials as instructive extracellular microenvironments for morphogenesis in tissue engineering. *Nature Biotechnology*, 23(1), 47-55.

Lutolf, M. P., Lauer-Fields, J. L., Schmoekel, H. G., Metters, A. T., Weber, F. E., Fields, G. B. & Hubbell, J. A. (2003) Synthetic matrix metalloproteinase-sensitive hydrogels for the conduction of tissue regeneration: Engineering cell-invasion characteristics. *Proceedings of the National Academy of Sciences of the United States of America*, 100(9), 5413-5418.

Luu, Y. K., Capilla, E., Rosen, C. J., Gilsanz, V., Pessin, J. E., Judex, S. & Rubin, C. T. (2009) Mechanical Stimulation of Mesenchymal Stem Cell Proliferation and Differentiation Promotes Osteogenesis While Preventing Dietary-Induced Obesity. *Journal of Bone and Mineral Research*, 24(1), 50-61.

Mabey, T. & Honsawek, S. (2015) Role of Vitamin D in Osteoarthritis: Molecular, Cellular, and Clinical Perspectives. *International Journal of Endocrinology*, 14.

Mackay, A. M., Beck, S. C., Murphy, J. M., Barry, F. P., Chichester, C. O. & Pittenger, M. F. (1998) Chondrogenic differentiation of cultured human mesenchymal stem cells from marrow. *Tissue Engineering*, 4(4), 415-428.

Madsen, D. H., Jurgensen, H. J., Ingvarsen, S., Melander, M. C., Albrechtsen, R., Hald, A., Holmbeck, K., Bugge, T. H., Behrendt, N. & Engelholm, L. H. (2013) Differential Actions of the Endocytic Collagen Receptor uPARAP/Endo180 and the Collagenase MMP-2 in Bone Homeostasis. *Plos One*, 8(8).

Magalhaes, J., Lebourg, M., Deplaine, H., Ribelles, J. L. G. & Blanco, F. J. (2015) Effect of the Physicochemical Properties of Pure or Chitosan-Coated Poly(L-Lactic Acid)Scaffolds on the Chondrogenic Differentiation of Mesenchymal Stem Cells from Osteoarthritic Patients. *Tissue Engineering Part A*, 21(3-4), 716-728.

Magalhaes, J., Roman, J. S., Crawford, A., Hatton, P. V., Sousa, R. A. & Reis, R. L. (2008) Engineering cartilage like tissue using polymeric systems derived from 2-ethyl-2-pyrrolidone-methacrylate combined with hyaluronic acid. *Tissue Engineering Part A*, 14(5), 729-729.

Mahmoudifar, N. & Doran, P. M. (2012) Chondrogenesis and cartilage tissue engineering: the longer road to technology development. *Trends in Biotechnology*, 30(3), 166-176.

Maidhof, R., Marsano, A., Lee, E. J. & Vunjak-Novakovic, G. (2010) Perfusion Seeding of Channeled Elastomeric Scaffolds with Myocytes and Endothelial Cells for Cardiac Tissue Engineering. *Biotechnology Progress*, 26(2), 565-572.

Majeska, R. J. & Wuthier, R. E. (1975) Studies on matrix vesicles isolated from chick epiphyseal cartilage - association of pyrophosphatase and atpase activities with alkaline-phosphatase. *Biochimica Et Biophysica Acta*, 391(1), 51-60.

Malafaya, P. B. & Reis, R. L. (2009) Bilayered chitosan-based scaffolds for osteochondral tissue engineering: Influence of hydroxyapatite on in vitro cytotoxicity and dynamic bioactivity studies in a specific double-chamber bioreactor. *Acta Biomaterialia*, 5(2), 644-660.

Malafaya, P. B., Silva, G. A. & Reis, R. L. (2007) Natural-origin polymers as carriers and scaffolds for biomolecules and cell delivery in tissue engineering applications. *Advanced Drug Delivery Reviews*, 59(4-5), 207-233.

Mann, C. J. & Weiner, H. (1999) Differences in the roles of conserved glutamic acid residues in the active site of human class 3 and class 2 aldehyde dehydrogenases. *Protein Science*, 8(10), 1922-1929.

Mannello, F. & Tonti, G. A. (2007) Concise review: No breakthroughs for human mesenchymal and embryonic stem cell culture: Conditioned medium, feeder layer, or feeder-free; Medium with fetal calf serum, human serum, or enriched plasma; Serum-free, serum replacement nonconditioned medium, or ad hoc formula? All that glitters is not gold! *Stem Cells*, 25(7), 1603-1609.

Mansour, J. (2013) *Biomechanics of cartilage*, 66-79.

Marklein, R. A. & Burdick, J. A. (2010) Controlling Stem Cell Fate with Material Design. *Advanced Materials*, 22(2), 175-189.

Marotti, G., Remaggi, F. & Zaffe, D. (1985) Quantitative investigation on osteocyte canaliculi in human compact and spongy bone. *Bone*, 6(5), 335-337.

Marshall, D., Johnell, O. & Wedel, H. (1996) Meta-analysis of how well measures of bone mineral density predict occurrence of osteoporotic fractures. *British Medical Journal*, 312(7041), 1254-1259.

Martin, I., Miot, S., Barbero, A., Jakob, M. & Wendt, D. (2007) Osteochondral tissue engineering. *Journal of Biomechanics*, 40(4), 750-765.

Martin, I., Vunjak-Novakovic, G., Yang, J., Langer, R. & Freed, L. E. (1999) Mammalian chondrocytes expanded in the presence of fibroblast growth factor 2 maintain the ability to differentiate and regenerate three-dimensional cartilaginous tissue. *Experimental Cell Research*, 253(2), 681-688.

Martin, I., Wendt, D. & Heberer, M. (2004) The role of bioreactors in tissue engineering. *Trends in Biotechnology*, 22(2), 80-86.

Martin, Y. & Vermette, P. (2005) Bioreactors for tissue mass culture: Design, characterization, and recent advances. *Biomaterials*, 26(35), 7481-7503.

Martins, A. M., Alves, C. M., Reis, R. L., Mikos, A. G. & Kasper, F. K. (2009) Toward Osteogenic Differentiation of Marrow Stromal Cells and In Vitro Production of Mineralized Extracellular Matrix onto Natural Scaffolds. *Biological Interactions on Materials Surfaces: Understanding and Controlling Protein, Cell, and Tissue Responses*, 263-281.

Mastrogiacomo, M., Derubeis, A. R. & Cancedda, R. (2005) Bone and cartilage formation by skeletal muscle derived cells. *Journal of Cellular Physiology*, 204(2), 594-603.

Mathieu, L. M., Mueller, T. L., Bourban, P. E., Pioletti, D. P., Muller, R. & Manson, J. A. E. (2006) Architecture and properties of anisotropic polymer composite scaffolds for bone tissue engineering. *Biomaterials*, 27(6), 905-916.

Mazzoleni, G., Di Lorenzo, D. & Steimberg, N. (2009) Modelling tissues in 3D: the next future of pharmaco-toxicology and food research? *Genes and Nutrition*, 4(1), 13-22.

McHugh, K. J., Tao, S. L. & Saint-Geniez, M. (2013) A novel porous scaffold fabrication technique for epithelial and endothelial tissue engineering. *Journal of Materials Science-Materials in Medicine*, 24(7), 1659-1670.

Meirelles, L. D. S., Chagastelles, P. C. & Nardi, N. B. (2006) Mesenchymal stem cells reside in virtually all post-natal organs and tissues. *Journal of Cell Science*, 119(11), 2204-2213.

Mendler, M., Eichbender, S. G., Vaughan, L., Winterhalter, K. H. & Bruckner, P. (1989) Cartilage contains mixed fibrils of collagen type-II, type-IX, and type-XI. *Journal of Cell Biology*, 108(1), 191-197.

Merry, K., Dodds, R., Littlewood, A. & Gowen, M. (1993) Expression of osteopontin messenger-rna by osteoclasts and osteoblasts in modeling adult human bone. *Journal of Cell Science*, 104, 1013-1020.

Meuleman, N., Tondreau, T., Delforge, A., Dejeneffe, M., Massy, M., Libertalis, M., Bron, D. & Lagneaux, L. (2006) Human marrow mesenchymal stem cell culture: serum-free medium allows better expansion than classical alpha-MEM medium. *European Journal of Haematology*, 76(4), 309-316.

Mi, F. L., Tan, Y. C., Liang, H. C., Huang, R. N. & Sung, H. W. (2001) In vitro evaluation of a chitosan membrane cross-linked with genipin. *Journal of Biomaterials Science-Polymer Edition*, 12(8), 835-850.

Mikos, A. G., Herring, S. W., Ochareon, P., Elisseeff, J., Lu, H. H., Kandel, R., Schoen, F. J., Toner, M., Mooney, D., Atala, A., Van Dyke, M. E., Kaplan, D. & Vunjak-Novakovic, G. (2006) Engineering complex tissues. *Tissue Engineering*, 12(12), 3307-3339.

Misra, M., Miller, K. K., Almazan, C., Ramaswamy, K., Lapcharoensap, W., Worley, M., Neubauer, G., Herzog, D. B. & Klibanski, A. (2004) Alterations in cortisol secretory dynamics in adolescent girls with anorexia nervosa and effects on bone metabolism. *Journal of Clinical Endocrinology & Metabolism*, 89(10), 4972-4980.

Mizuno, N., Shiba, H., Ozeki, Y., Mouri, Y., Niitani, M., Inui, T., Hayashi, H., Suzuki, K., Tanaka, S., Kawaguchi, H. & Kurihara, H. (2006) Human autologous serum obtained using a completely closed bag system as a substitute for foetal calf serum in human mesenchymal stem cell cultures. *Cell Biology International*, 30(6), 521-524.

Modl, J. M., Sether, L. A., Haughton, V. M. & Kneeland, J. B. (1991) Articular-cartilage - correlation of histologic zones with signal intensity at mr imaging. *Radiology*, 181(3), 853-855.

Monteiro, O. A. C. & Airoldi, C. (1999) Some studies of crosslinking chitosan-glutaraldehyde interaction in a homogeneous system. *International Journal of Biological Macromolecules*, 26(2-3), 119-128.

Moon, G. Y., Lee, S. S., Lee, K. Y., Kim, S. H. & Song, K. H. (2008) Behavior of hydrogen evolution of aqueous sodium borohydride solutions. *Journal of Industrial and Engineering Chemistry*, 14(1), 94-99.

Moran, C. J., Withers, D. P., Kurzweil, P. R. & Verdonk, P. C. (2015) Clinical Application of Scaffolds for Partial Meniscus Replacement. *Sports Medicine and Arthroscopy Review*, 23(3), 156-161.

Moreau, J. L. & Xu, H. H. K. (2009) Mesenchymal stem cell proliferation and differentiation on an injectable calcium phosphate - Chitosan composite scaffold. *Biomaterials*, 30(14), 2675-2682.

Morinobu, M., Ishijima, M., Rittling, S. R., Tsuji, K., Yamamoto, H., Nifuji, A., Denhardt, D. T. & Noda, M. (2003) Osteopontin expression in osteoblasts and osteocytes during bone formation under mechanical stress in the calvarial suture in vivo. *Journal of Bone and Mineral Research*, 18(9), 1706-1715.

Morrison, J. B. (1970) Mechanics of knee joint in relation to normal walking. *Journal of Biomechanics*, 3(1), 51-&.

Morrison, N. A., Qi, J. C., Tokita, A., Kelly, P. J., Crofts, L., Nguyen, T. V., Sambrook, P. N. & Eisman, J. A. (1994) Prediction of bone-density from vitamin-d receptor alleles. *Nature*, 367(6460), 284-287.

Morrison, S. J. & Scadden, D. T. (2014) The bone marrow niche for haematopoietic stem cells. *Nature*, 505(7483), 327-334.

Mosher, C. Z., Spalazzi, J. P. & Lu, H. H. (2015) Stratified scaffold design for engineering composite tissues. *Methods*, 84, 99-102.

Mow, V. C., Holmes, M. H. & Lai, W. M. (1984) Fluid transport and mechanical-properties of articular-cartilage - a review. *Journal of Biomechanics*, 17(5), 377-394.

Mow, V. C., Ratcliffe, A. & Poole, A. R. (1992) Cartilage and diarthrodial joints as paradigms for hierarchical materials and structures. *Biomaterials*, 13(2), 67-97.

Muir, H. (1958) Nature of the link between protein and carbohydrate of a chondroitin sulphate complex from hyaline cartilage. *Biochemical Journal*, 69, 195-204.

Mukherjee, N. & Wayne, J. S. (1998) Load sharing between solid and fluid phases in articular cartilage: I - Experimental determination of in situ mechanical conditions in a porcine knee. *Journal of Biomechanical Engineering-Transactions of the Asme*, 120(5), 614-619.

Mundy, G. R., Shapiro, J. L., Bandelin, J. G., Canalis, E. M. & Raisz, L. G. (1976) Direct stimulation of bone-resorption by thyroid-hormones. *Journal of Clinical Investigation*, 58(3), 529-534.

Munoz, N., Kim, J., Liu, Y. J., Logan, T. M. & Ma, T. (2014) Gas chromatography-mass spectrometry analysis of human mesenchymal stem cell metabolism during proliferation and osteogenic differentiation under different oxygen tensions. *Journal of Biotechnology*, 169, 95-102.

Muzzarelli, R. A. A. (2009a) Chitins and chitosans for the repair of wounded skin, nerve, cartilage and bone. *Carbohydrate Polymers*, 76(2), 167-182.

Muzzarelli, R. A. A. (2009b) Genipin-crosslinked chitosan hydrogels as biomedical and pharmaceutical aids. *Carbohydrate Polymers*, 77(1), 1-9.

Muzzarelli, R. A. A. (2011) Chitosan composites with inorganics, morphogenetic proteins and stem cells, for bone regeneration. *Carbohydrate Polymers*, 83(4), 1433-1445.

Muzzarelli, R. A. A., Greco, F., Busilacchi, A., Sollazzo, V. & Gigante, A. (2012) Chitosan, hyaluronan and chondroitin sulfate in tissue engineering for cartilage regeneration: A review. *Carbohydrate Polymers*, 89(3), 723-739.

Newman, A. P. (1998) Articular cartilage repair. *American Journal of Sports Medicine*, 26(2), 309-324.

Noback, C. R. & Robertson, G. G. (1951) Sequences of appearance of ossification centers in the human skeleton during the 1st 5 prenatal months. *American Journal of Anatomy*, 89(1), 1-28.

O'Brien, F. J., Harley, B. A., Yannas, I. V. & Gibson, L. (2004) Influence of freezing rate on pore structure in freeze-dried collagen-GAG scaffolds. *Biomaterials*, 25(6), 1077-1086.

O'Brien, F. J., Harley, B. A., Yannas, I. V. & Gibson, L. J. (2005) The effect of pore size on cell adhesion in collagen-GAG scaffolds. *Biomaterials*, 26(4), 433-441.

O'Brien, J., Wilson, I., Orton, T. & Pognan, F. (2000) Investigation of the Alamar Blue (resazurin) fluorescent dye for the assessment of mammalian cell cytotoxicity. *European Journal of Biochemistry*, 267(17), 5421-5426.

O'Brien, K. O., Abrams, S. A., Liang, L. K., Ellis, K. J. & Gagel, R. F. (1998) Bone turnover response to changes in calcium intake is altered in girls and adult women in families with histories of osteoporosis. *Journal of Bone and Mineral Research*, 13(3), 491-499.

Oldershaw, R. A. & Hardingham, T. E. (2010) Notch signaling during chondrogenesis of human bone marrow stem cells. *Bone*, 46(2), 286-293.

Oliveira, J. M., Rodrigues, M. T., Silva, S. S., Malafaya, P. B., Gomes, M. E., Viegas, C. A., Dias, I. R., Azevedo, J. T., Mano, J. F. & Reis, R. L. (2006) Novel hydroxyapatite/chitosan bilayered scaffold for osteochondral tissue-engineering applications: Scaffold design and its performance when seeded with goat bone marrow stromal cells. *Biomaterials*, 27(36), 6123-6137.

Oliveira, J. T., Crawford, A., Mundy, J. M., Moreira, A. R., Gomes, M. E., Hatton, P. V. & Reis, R. L. (2007) A cartilage tissue engineering approach combining starch-polycaprolactone fibre mesh scaffolds with bovine articular chondrocytes. *Journal of Materials Science-Materials in Medicine*, 18(2), 295-302.

Otto, F., Thornell, A. P., Crompton, T., Denzel, A., Gilmour, K. C., Rosewell, I. R., Stamp, G. W. H., Beddington, R. S. P., Mundlos, S., Olsen, B. R., Selby, P. B. & Owen, M. J. (1997) Cbfa1, a candidate gene for cleidocranial dysplasia syndrome, is essential for osteoblast differentiation and bone development. *Cell*, 89(5), 765-771.

Owen, T. A., Aronow, M., Shalhoub, V., Barone, L. M., Wilming, L., Tassinari, M. S., Kennedy, M. B., Pockwinse, S., Lian, J. B. & Stein, G. S. (1990) Progressive development of the rat osteoblast phenotype invitro - reciprocal relationships in expression of genes associated with osteoblast proliferation and differentiation during formation of the bone extracellular-matrix. *Journal of Cellular Physiology*, 143(3), 420-430.

Ozer, A. (2007) Removal of Pb(II) ions from aqueous solutions by sulphuric acid-treated wheat bran. *Journal of Hazardous Materials*, 141(3), 753-761.

Page-McCaw, A., Ewald, A. J. & Werb, Z. (2007) Matrix metalloproteinases and the regulation of tissue remodelling. *Nature Reviews Molecular Cell Biology*, 8(3), 221-233.

Paley, D. (1990) Problems, obstacles, and complications of limb lengthening by the ilizarov technique. *Clinical Orthopaedics and Related Research*(250), 81-104.

Pangburn, S. H., Trescony, P. V. & Heller, J. (1982) Lysozyme degradation of partially deacetylated chitin, its films and hydrogels. *Biomaterials*, 3(2), 105-108.

Pankhurst, Q. A., Connolly, J., Jones, S. K. & Dobson, J. (2003) Applications of magnetic nanoparticles in biomedicine. *Journal of Physics D-Applied Physics*, 36(13), R167-R181.

Pattappa, G., Heywood, H. K., De Bruijn, J. D. & Lee, D. A. (2011) The Metabolism of Human Mesenchymal Stem Cells During Proliferation and Differentiation. *Journal of Cellular Physiology*, 226(10), 2562-2570.

Pei, Y., Fan, J.-j., Zhang, X.-q., Zhang, Z.-y. & Yu, M. (2014) Repairing the Osteochondral Defect in Goat with the Tissue-Engineered Osteochondral Graft Preconstructed in a Double-Chamber Stirring Bioreactor. *Biomed Research International*.

Peppas, N. A., Hilt, J. Z., Khademhosseini, A. & Langer, R. (2006) Hydrogels in biology and medicine: From molecular principles to bionanotechnology. *Advanced Materials*, 18(11), 1345-1360.

Perez-Ilzarbe, M., Diez-Campelo, M., Aranda, P., Tabera, S., Lopez, T., del Canizo, C., Merino, J., Moreno, C., Andreu, E. J., Prosper, F. & Antonio Perez-Simon, J. (2009) Comparison of ex vivo expansion culture conditions of mesenchymal stem cells for human cell therapy. *Transfusion*, 49(9), 1901-1910.

Perez-Simon, J. A., Lopez-Villar, O., Andreu, E. J., Rifon, J., Muntion, S., Diez Campelo, M., Sanchez-Guijo, F. M., Martinez, C., Valcarcel, D. & del Canizo, C. (2011) Mesenchymal stem cells expanded in vitro with human serum for the treatment of acute and chronic graft-versus-host disease: results of a phase I/II clinical trial. *Haematologica-the Hematology Journal*, 96(7), 1072-1076.

Peterson, L., Minas, T., Brittberg, M., Nilsson, A., Sjogren-Jansson, E. & Lindahl, A. (2000) Two- to 9-year outcome after autologous chondrocyte transplantation of the knee. *Clinical Orthopaedics and Related Research*(374), 212-234.

Petrochenko, P. E., Torgersen, J., Gruber, P., Hicks, L. A., Zheng, J. W., Kumar, G., Narayan, R. J., Goering, P. L., Liska, R., Stampfl, J. & Ovsianikov, A. (2015) Laser 3D Printing with Sub-Microscale Resolution of Porous Elastomeric Scaffolds for Supporting Human Bone Stem Cells. *Advanced Healthcare Materials*, 4(5), 739-747.

Pierschbacher, M. D. & Ruoslahti, E. (1984) Cell attachment activity of fibronectin can be duplicated by small synthetic fragments of the molecule. *Nature*, 309(5963), 30-33.

Pillai, C. K. S., Paul, W. & Sharma, C. P. (2009) Chitin and chitosan polymers: Chemistry, solubility and fiber formation. *Progress in Polymer Science*, 34(7), 641-678.

Pisciotta, A., Riccio, M., Carnevale, G., Beretti, F., Gibellini, L., Maraldi, T., Cavallini, G. M., Ferrari, A., Bruzzesi, G. & De Pol, A. (2012) Human Serum Promotes Osteogenic Differentiation of Human Dental Pulp Stem Cells In Vitro and In Vivo. *Plos One*, 7(11).

Pittenger, M. F., Mackay, A. M., Beck, S. C., Jaiswal, R. K., Douglas, R., Mosca, J. D., Moorman, M. A., Simonetti, D. W., Craig, S. & Marshak, D. R. (1999) Multilineage potential of adult human mesenchymal stem cells. *Science*, 284(5411), 143-147.

Pochampally, R. R., Smith, J. R., Ylostalo, J. & Prockop, D. J. (2004) Serum deprivation of human marrow stromal cells (hMSCs) selects for a subpopulation of early progenitor cells with enhanced expression of OCT-4 and other embryonic genes. *Blood*, 103(5), 1647-1652.

Poon, L., Wilson, L. D. & Headley, J. V. (2014) Chitosan-glutaraldehyde copolymers and their sorption properties. *Carbohydrate Polymers*, 109, 92-101.

Pound, J. C., Green, D. W., Roach, H. I., Mann, S. & Oreffo, R. O. C. (2007) An ex vivo model for chondrogenesis and osteogenesis. *Biomaterials*, 28(18), 2839-2849.

Pugnaloni, A., Solmi, R., Muzzarelli, R., Emanuelli, M., Moroni, F., Gazzanelli, G., Baldassarre, V. & Biagini, G. (1988) Chitosan biochemical structure and biomorphology. *Bollettino Societa Italiana Biologia Sperimentale*, 64(2), 101-108.

Rashidi, H., Strohbuecker, S., Jackson, L., Kalra, S., Blake, A. J., France, L., Tufarelli, C. & Sottile, V. (2012) Differences in the Pattern and Regulation of Mineral Deposition in Human Cell Lines of Osteogenic and Non-Osteogenic Origin. *Cells Tissues Organs*, 195(6), 484-494.

Ren, D. W., Yi, H. F., Wang, W. & Ma, X. J. (2005) The enzymatic degradation and swelling properties of chitosan matrices with different degrees of N-acetylation. *Carbohydrate Research*, 340(15), 2403-2410.

Reves, B. T., Jennings, J. A., Bumgardner, J. D. & Haggard, W. O. (2012) Preparation and functional assessment of composite chitosan-nano-hydroxyapatite scaffolds for bone regeneration. *Journal of functional biomaterials*, 3(1), 114-30.

Rho, J. Y., Ashman, R. B. & Turner, C. H. (1993) Youngs modulus of trabecular and cortical bone material - ultrasonic and microtensile measurements. *Journal of Biomechanics*, 26(2), 111-119.

Rho, J. Y., Tsui, T. Y. & Pharr, G. M. (1997) Elastic properties of human cortical and trabecular lamellar bone measured by nanoindentation. *Biomaterials*, 18(20), 1325-1330.

Richardson, S. M., Hughes, N., Hunt, J. A., Freemont, A. J. & Hoyland, J. A. (2008) Human mesenchymal stem cell differentiation to NP-like cells in chitosan-glycerophosphate hydrogels. *Biomaterials*, 29(1), 85-93.

Rinaudo, M. (2006) Chitin and chitosan: Properties and applications. *Progress in Polymer Science*, 31(7), 603-632.

Roach, H. I. (1999) Association of matrix acid and alkaline phosphatases with mineralization of cartilage and endochondral bone. *Histochemical Journal*, 31(1), 53-61.

Rodrigues, M. T., Lee, S. J., Gomes, M. E., Reis, R. L., Atala, A. & Yoo, J. J. (2012) Bilayered constructs aimed at osteochondral strategies: The influence of medium supplements in the osteogenic and chondrogenic differentiation of amniotic fluid-derived stem cells. *Acta Biomaterialia*, 8(7), 2795-2806.

Sahota, O., Mundey, M. K., San, P., Godber, I. M., Lawson, N. & Hosking, D. J. (2004) The relationship between vitamin D and parathyroid hormone: calcium homeostasis, bone turnover, and bone mineral density in postmenopausal women with established osteoporosis. *Bone*, 35(1), 312-319.

Saini, S. & Wick, T. M. (2004) Effect of low oxygen tension on tissue-engineered cartilage construct development in the concentric cylinder bioreactor. *Tissue Engineering*, 10(5-6), 825-832.

Santos, S. C. R., Vilar, V. J. P. & Boaventura, R. A. R. (2008) Waste metal hydroxide sludge as adsorbent for a reactive dye. *Journal of Hazardous Materials*, 153(3), 999-1008.

Sayers, A., Lawlor, D. A., Sattar, N. & Tobias, J. H. (2012) The association between insulin levels and cortical bone: Findings from a cross-sectional analysis of pQCT parameters in adolescents. *Journal of Bone and Mineral Research*, 27(3), 610-618.

Schaefer, D., Martin, I., Shastri, P., Padera, R. F., Langer, R., Freed, L. E. & Vunjak-Novakovic, G. (2000) In vitro generation of osteochondral composites. *Biomaterials*, 21(24), 2599-2606.

Schallmoser, K., Bartmann, C., Rohde, E., Bork, S., Guelly, C., Obenauf, A. C., Reinisch, A., Horn, P., Ho, A. D., Strunk, D. & Wagner, W. (2010) Replicative senescence-associated gene expression changes in mesenchymal stromal cells are similar under different culture conditions. *Haematologica-the Hematology Journal*, 95(6), 867-874.

Schumacher, B. L., Block, J. A., Schmid, T. M., Aydelotte, M. B. & Kuettner, K. E. (1994) A novel proteoglycan synthesized and secreted by chondrocytes of the superficial zone of articular-cartilage. *Archives of Biochemistry and Biophysics*, 311(1), 144-152.

Schwarz, R. P., Goodwin, T. J. & Wolf, D. A. (1992) Cell culture for three-dimensional modeling in rotating-wall vessels: an application of simulated microgravity. *Journal of tissue culture methods : Tissue Culture Association manual of cell, tissue, and organ culture procedures*, 14(2), 51-7.

Sekiya, I., Larson, B. L., Smith, J. R., Pochampally, R., Cui, J. G. & Prockop, D. J. (2002) Expansion of human adult stem cells from bone marrow stroma: Conditions that maximize the yields of early progenitors and evaluate their quality. *Stem Cells*, 20(6), 530-541.

Sendemir-Urkmez, A. & Jamison, R. D. (2007) The addition of biphasic calcium phosphate to porous chitosan scaffolds enhances bone tissue development in vitro. *Journal of Biomedical Materials Research Part A*, 81A(3), 624-633.

Shahdadfar, A., Fronsdal, K., Haug, T., Reinholt, F. P. & Brinchmann, J. E. (2005) In vitro expansion of human mesenchymal stem cells: Choice of serum is a determinant of cell proliferation, differentiation, gene expression, and transcriptome stability. *Stem Cells*, 23(9), 1357-1366.

Shapiro, F., Koide, S. & Glimcher, M. J. (1993) Cell origin and differentiation in the repair of full-thickness defects of articular-cartilage. *Journal of Bone and Joint Surgery-American Volume*, 75A(4), 532-553.

Shapiro, I. M., Landis, W. J. & Risbud, M. V. (2015) Matrix vesicles: Are they anchored exosomes? *Bone*, 79, 29-36.

Shapiro, R. & Heaney, R. P. (2003) Co-dependence of calcium and phosphorus for growth and bone development under conditions of varying deficiency. *Bone*, 32(5), 532-540.

Shi, C. M., Zhu, Y., Ran, X. Z., Wang, M., Su, Y. P. & Cheng, T. M. (2006) Therapeutic potential of chitosan and its derivatives in regenerative medicine. *Journal of Surgical Research*, 133(2), 185-192.

Shin, H., Jo, S. & Mikos, A. G. (2003) Biomimetic materials for tissue engineering. *Biomaterials*, 24(24), 4353-4364.

Sikavitsas, V. I., Bancroft, G. N. & Mikos, A. G. (2002) Formation of three-dimensional cell/polymer constructs for bone tissue engineering in a spinner flask and a rotating wall vessel bioreactor. *Journal of Biomedical Materials Research*, 62(1), 136-148.

Silva, M. M. C. G., Cyster, L. A., Barry, J. J. A., Yang, X. B., Oreffo, R. O. C., Grant, D. M., Scotchford, C. A., Howdle, S. M., Shakesheff, K. M. & Rose, F. R. A. J. (2006) The effect of anisotropic architecture on cell and tissue infiltration into tissue engineering scaffolds. *Biomaterials*, 27(35), 5909-5917.

Silva, S. S., Motta, A., Rodrigues, M. T., Pinheiro, A. F. M., Gomes, M. E., Mano, J. F., Reis, R. L. & Migliaresi, C. (2008) Novel Genipin-Cross-Linked Chitosan/Silk Fibroin Sponges for Cartilage Engineering Strategies. *Biomacromolecules*, 9(10), 2764-2774.

Smith, I. O., Liu, X. H., Smith, L. A. & Ma, P. X. (2009) Nanostructured polymer scaffolds for tissue engineering and regenerative medicine. *Wiley Interdisciplinary Reviews-Nanomedicine and Nanobiotechnology*, 1(2), 226-236.

Smith, M. D., Barbenel, J. C., Courtney, J. M. & Grant, M. H. (1992) Novel quantitative methods for the determination of biomaterial cytotoxicity. *International Journal of Artificial Organs*, 15(3), 191-194.

Sobral, J. M., Caridade, S. G., Sousa, R. A., Mano, J. F. & Reis, R. L. (2011) Three-dimensional plotted scaffolds with controlled pore size gradients: Effect of scaffold geometry on mechanical performance and cell seeding efficiency. *Acta Biomaterialia*, 7(3), 1009-1018.

Solmesky, L., Lefler, S., Jacob-Hirsch, J., Bulvik, S., Rechavi, G. & Weil, M. (2010) Serum Free Cultured Bone Marrow Mesenchymal Stem Cells as a Platform to Characterize the Effects of Specific Molecules. *Plos One*, 5(9).

Sottile, V., Halleux, C., Bassilana, F., Keller, H. & Seuwen, K. (2002) Stem cell characteristics of human trabecular bone-derived cells. *Bone*, 30(5), 699-704.

Staal, A., Geertsma-Kleinekoort, W. M. C., Van den Bemd, G., Buurman, C. J., Birkenhager, J. C., Pols, H. A. P. & Van Leeuwen, J. (1998) Regulation of osteocalcin production and bone resorption by 1,25-dihydroxyvitamin D-3 in mouse long bones: Interaction with the bone-derived growth factors TGF-beta and IGF-I. *Journal of Bone and Mineral Research*, 13(1), 36-43.

Steadman, J. R., Briggs, K. K., Rodrigo, J. J., Kocher, M. S., Gill, T. J. & Rodkey, W. G. (2003) Outcomes of microfracture for traumatic chondral defects of the knee: Average 11-year follow-up. *Arthroscopy-the Journal of Arthroscopic and Related Surgery*, 19(5), 477-484.

Steele, J. A. M., McCullen, S. D., Callanan, A., Autefage, H., Accardi, M. A., Dini, D. & Stevens, M. M. (2014) Combinatorial scaffold morphologies for zonal articular cartilage engineering. *Acta Biomaterialia*, 10(5), 2065-2075.

Straffelini, G., Fontanari, V. & Molinari, A. (1999) True and apparent Young's modulus in ferrous porous alloys. *Materials Science and Engineering a-Structural Materials Properties Microstructure and Processing*, 260(1-2), 197-202.

Stute, N., Holtz, K., Bubenheim, M., Lange, C., Blake, F. & Zander, A. R. (2004) Autologous serum for isolation and expansion of human mesenchymal stem cells for clinical use. *Experimental Hematology*, 32(12).

Su, X., Sun, K., Cui, F. Z. & Landis, W. J. (2003) Organization of apatite crystals in human woven bone. *Bone*, 32(2), 150-162.

Sugiki, T., Uyama, T., Toyoda, M., Morioka, H., Kume, S., Miyado, K., Matsumoto, K., Saito, H., Tsumaki, N., Takahashi, Y., Toyama, Y. & Umezawa, A. (2007) Hyaline cartilage formation and enchondral ossification modeled with KUM5 and OP9 chondroblasts. *Journal of Cellular Biochemistry*, 100(5), 1240-1254.

Sumner, D. R. (2015) Long-term implant fixation and stress-shielding in total hip replacement. *Journal of Biomechanics*, 48(5), 797-800.

Sun, H. B. (2010) Mechanical loading, cartilage degradation, and arthritis. *Molecular and Integrative Physiology of the Musculoskeletal System*, 1211, 37-50.

Sung, H. W., Huang, R. N., Huang, L. L. H. & Tsai, C. C. (1999) In vitro evaluation of cytotoxicity of a naturally occurring cross-linking reagent for biological tissue fixation. *Journal of Biomaterials Science-Polymer Edition*, 10(1), 63-78.

Swieszkowski, W., Tuan, B. H. S., Kurzydlowski, K. J. & Hutmacher, D. W. (2007) Repair and regeneration of osteochondral defects in the articular joints. *Biomolecular Engineering*, 24(5), 489-495.

Tai, H., Mather, M. L., Howard, D., Wang, W., White, L. J., Crowe, J. A., Morgan, S. P., Chandra, A., Williams, D. J., Howdle, S. M. & Shakesheff, K. M. (2007) Control of pore size and structure of tissue engineering scaffolds produced by supercritical fluid processing. *European Cells & Materials*, 14, 64-76.

Tallheden, T., van der Lee, J., Brantsing, C., Mansson, J. E., Sjogren-Jansson, E. & Lindahl, A. (2005) Human serum for culture of articular chondrocytes. *Cell Transplantation*, 14(7), 469-479.

Tampieri, A., Sprio, S., Sandri, M. & Valentini, F. (2011) Mimicking natural bio-mineralization processes: A new tool for osteochondral scaffold development. *Trends in Biotechnology*, 29(10), 526-535.

Taniyama, T., Masaoka, T., Yamada, T., Wei, X., Yasuda, H., Yoshii, T., Kozaka, Y., Takayama, T., Hirano, M., Okawa, A. & Sotome, S. (2015) Repair of Osteochondral Defects in a Rabbit Model Using a Porous Hydroxyapatite Collagen Composite Impregnated With Bone Morphogenetic Protein-2. *Artificial Organs*, 39(6), 529-535.

Tataria, M., Quarto, N., Longaker, M. T. & Sylvester, K. G. (2006) Absence of the p53 tumor suppressor gene promotes osteogenesis in mesenchymal stem cells. *Journal of Pediatric Surgery*, 41(4), 624-632.

Tateishi, K., Ando, W., Higuchi, C., Hart, D. A., Hashimoto, J., Nakata, K., Yoshikawa, H. & Nakamura, N. (2008) Comparison of human serum with fetal bovine serum for expansion and differentiation of human synovial MSC: Potential feasibility for clinical applications. *Cell Transplantation*, 17(5), 549-557.

Tavassol.M & Crosby, W. H. (1968) transplantation of marrow to extramedullary sites. *Science*, 161(3836), 54-&.

Temenoff, J. S. & Mikos, A. G. (2000) Review: tissue engineering for regeneration of articular cartilage. *Biomaterials*, 21(5), 431-440.

Templeton, D. M. (1988) The basis and applicability of the dimethylmethylene blue binding assay for sulfated glycosaminoglycans. *Connective Tissue Research*, 17(1), 23-32.

Thein-Han, W. W., Kitiyanant, Y. & Misra, R. D. K. (2008) Chitosan as scaffold matrix for tissue engineering. *Materials Science and Technology*, 24(9), 1062-1075.

Thompson, A. M. & Stockwell, R. A. (1983) An ultrastructural-study of the marginal transitional zone in the rabbit knee-joint. *Journal of Anatomy*, 136(JUN), 701-713.

Tomihata, K. & Ikada, Y. (1997) In vitro and in vivo degradation of films of chitin and its deacetylated derivatives. *Biomaterials*, 18(7), 567-575.

Tonti, G. A. & Mannello, F. (2008) From bone marrow to therapeutic applications: different behaviour and genetic/epigenetic stability during mesenchymal stem cell expansion in autologous and foetal bovine sera? *International Journal of Developmental Biology*, 52(8), 1023-1032.

Torzilli, P. A., Grigiene, R., Borrelli, J. & Helfet, D. L. (1999) Effect of impact load on articular cartilage: Cell metabolism and viability, and matrix water content. *Journal of Biomechanical Engineering-Transactions of the Asme*, 121(5), 433-441.

Trebec, D. P., Chandra, D., Gramoun, A., Li, K., Heersche, J. N. M. & Manolson, M. F. (2007) Increased expression of activating factors in large osteoclasts could explain their excessive activity in osteolytic diseases. *Journal of Cellular Biochemistry*, 101(1), 205-220.

Tuan, R. S., Chen, A. F. & Klatt, B. A. (2013) Cartilage Regeneration. *Journal of the American Academy of Orthopaedic Surgeons*, 21(5), 303-311.

Tunesi, M., Bossio, C., Tonna, N., Della Valle, C., Bianco, F., Chiesa, R. & Giordano, C. (2013) Mesenchymal stem cell differentiation on electrochemically modified titanium: an optimized approach for biomedical applications. *Journal of applied biomaterials & functional materials*, 11(1), e9-e17.

Turner, C. H., Forwood, M. R., Rho, J. Y. & Yoshikawa, T. (1994) Mechanical loading thresholds for lamellar and woven bone-formation. *Journal of Bone and Mineral Research*, 9(1), 87-97.

Unsworth, B. R. & Lelkes, P. I. (1998) Growing tissues in microgravity. *Nature Medicine*, 4(8), 901-907.

Urist, M. R. (1965) Bone - formation by autoinduction. *Science*, 150(3698), 893-&.

van Beuningen, H. M., Glansbeek, H. L., van der Kraan, P. M. & van den Berg, W. B. (1998) Differential effects of local application of BMP-2 or TGF-beta 1 on both articular cartilage composition and osteophyte formation. *Osteoarthritis and Cartilage*, 6(5), 306-317.

Vanderrest, M. & Garrone, R. (1991) Collagen family of proteins. *Faseb Journal*, 5(13), 2814-2823.

Vater, C., Kasten, P. & Stiehler, M. (2011) Culture media for the differentiation of mesenchymal stromal cells. *Acta Biomaterialia*, 7(2), 463-477.

Vetsch, J. R., Paulsen, S. J., Mueller, R. & Hofmann, S. (2015) Effect of fetal bovine serum on mineralization in silk fibroin scaffolds. *Acta Biomaterialia*, 13, 277-285.

Vinatier, C., Mrugala, D., Jorgensen, C., Guicheux, J. & Noel, D. (2009) Cartilage engineering: a crucial combination of cells, biomaterials and biofactors. *Trends in Biotechnology*, 27(5), 307-314.

Vondermark, K., Gauss, V., Vondermark, H. & Muller, P. (1977) Relationship between cell-shape and type of collagen synthesized as chondrocytes lose their cartilage phenotype in culture. *Nature*, 267(5611), 531-532.

Vunjak-Novakovic, G., Obradovic, B., Martin, I., Bursac, P. M., Langer, R. & Freed, L. E. (1998) Dynamic cell seeding of polymer scaffolds for cartilage tissue engineering. *Biotechnology Progress*, 14(2), 193-202.

Wakitani, S., Goto, T., Pineda, S. J., Young, R. G., Mansour, J. M., Caplan, A. I. & Goldberg, V. M. (1994) Mesenchymal cell-based repair of large, full-thickness defects of articular-cartilage. *Journal of Bone and Joint Surgery-American Volume*, 76A(4), 579-592.

Wang, L. M. & Stegemann, J. P. (2010) Thermogelling chitosan and collagen composite hydrogels initiated with beta-glycerophosphate for bone tissue engineering. *Biomaterials*, 31(14), 3976-3985.

Wang, L. M. & Stegemann, J. P. (2011) Glyoxal crosslinking of cell-seeded chitosan/collagen hydrogels for bone regeneration. *Acta Biomaterialia*, 7(6), 2410-2417.

Wang, N., Butler, J. P. & Ingber, D. E. (1993) Mechanotransduction across the cell-surface and through the cytoskeleton. *Science*, 260(5111), 1124-1127.

Wei, W., Wang, L.-Y., Yuan, L., Wei, Q., Yang, X.-D., Su, Z.-G. & Ma, G.-H. (2007) Preparation and application of novel microspheres possessing autofluorescent properties. *Advanced Functional Materials*, 17(16), 3153-3158.

Weil, B. R., Abarbanell, A. M., Herrmann, J. L., Wang, Y. & Meldrum, D. R. (2009) High glucose concentration in cell culture medium does not acutely affect human mesenchymal stem cell growth factor production or proliferation. *American Journal of Physiology-Regulatory Integrative and Comparative Physiology*, 296(6), R1735-R1743.

Weinreb, M., Shinar, D. & Rodan, G. A. (1990) Different pattern of alkaline-phosphatase, osteopontin, and osteocalcin expression in developing rat bone visualized by insitu hybridization. *Journal of Bone and Mineral Research*, 5(8), 831-842.

Wendt, D., Marsano, A., Jakob, M., Heberer, M. & Martin, I. (2003) Oscillating perfusion of cell suspensions through three-dimensional scaffolds enhances cell seeding efficiency and uniformity. *Biotechnology and Bioengineering*, 84(2), 205-214.

Wenger, M. P. E., Bozec, L., Horton, M. A. & Mesquida, P. (2007) Mechanical properties of collagen fibrils. *Biophysical Journal*, 93(4), 1255-1263.

Williams, R. M., Zipfel, W. R. & Webb, W. W. (2005) Interpreting second-harmonic generation images of collagen I fibrils. *Biophysical Journal*, 88(2), 1377-1386.

Worch, K. P., Pacifici, M., Polson, A. M. & Kirsch, T. (1998) Role of annexin II and V in matrix vesicle-mediated biomineralization. *Journal of Dental Research*, 77, 927-927.

Xia, W. Y., Liu, W., Cui, L., Liu, Y. C., Zhong, W., Liu, D. L., Wu, J. J., Chua, K. H. & Cao, Y. L. (2004) Tissue engineering of cartilage with the use of chitosan-gelatin complex scaffolds. *Journal of Biomedical Materials Research Part B-Applied Biomaterials*, 71B(2), 373-380.

Yan, L.-P., Wang, Y.-J., Ren, L., Wu, G., Caridade, S. G., Fan, J.-B., Wang, L.-Y., Ji, P.-H., Oliveira, J. M., Oliveira, J. T., Mano, J. F. & Reis, R. L. (2010) Genipin-cross-linked collagen/chitosan biomimetic scaffolds for articular cartilage tissue engineering applications. *Journal of Biomedical Materials Research Part A*, 95A(2), 465-475.

Yang, Q., Chen, L., Shen, X. & Tan, Z. (2006) Preparation of polycaprolactone tissue engineering scaffolds by improved solvent casting/particulate leaching method. *Journal of Macromolecular Science Part B-Physics*, 45(6), 1171-1181.

Yokoi, H., Aratake, T., Nishio, S., Hirose, J., Hayashi, S. & Takasaki, Y. (1998) Chitosan production from Shochu distillery wastewater by funguses. *Journal of Fermentation and Bioengineering*, 85(2), 246-249.

Yoo, J. U., Barthel, T. S., Nishimura, K., Solchaga, L., Caplan, A. I., Goldberg, V. M. & Johnstone, B. (1998) The chondrogenic potential of human bone-marrow-derived mesenchymal progenitor cells. *Journal of Bone and Joint Surgery-American Volume*, 80A(12), 1745-1757.

Yoshimura, H., Muneta, T., Nimura, A., Yokoyama, A., Koga, H. & Sekiya, I. (2007) Comparison of rat mesenchymal stem cells derived from bone marrow, synovium, periosteum, adipose tissue, and muscle. *Cell and Tissue Research*, 327(3), 449-462.

Zhang, S. Q., Xiao, Z. S., Luo, J. M., He, N., Mahlios, J. & Quarles, L. D. (2009) Dose-Dependent Effects of Runx2 on Bone Development. *Journal of Bone and Mineral Research*, 24(11), 1889-1904.

Zhang, Y., Ni, M., Zhang, M. Q. & Ratner, B. (2003) Calcium phosphate-chitosan composite scaffolds for bone tissue engineering. *Tissue Engineering*, 9(2), 337-345.

Zhang, Y. & Zhang, M. Q. (2002) Calcium phosphate/chitosan composite scaffolds for controlled in vitro antibiotic drug release. *Journal of Biomedical Materials Research*, 62(3), 378-386.

Zhang, Z.-Z., Jiang, D., Wang, S.-J., Qi, Y.-S., Zhang, J.-Y. & Yu, J.-K. (2015) Potential of Centrifugal Seeding Method in Improving Cells Distribution and Proliferation on Demineralized Cancellous Bone Scaffolds for Tissue-Engineered Meniscus. *Acs Applied Materials & Interfaces*, 7(28), 15294-15302.

Zhao, L., Li, G., Chan, K. M., Wang, Y. & Tang, P. F. (2009) Comparison of Multipotent Differentiation Potentials of Murine Primary Bone Marrow Stromal Cells and Mesenchymal Stem Cell Line C3H10T1/2. *Calcified Tissue International*, 84(1), 56-64.

Zhao, Y., Park, R.-D. & Muzzarelli, R. A. A. (2010) Chitin Deacetylases: Properties and Applications. *Marine Drugs*, 8(1), 24-46.

Zhou, B., Tsaknakis, G., Coldwell, K. E., Khoo, C. P., Roubelakis, M. G., Chang, C. H., Pepperell, E. & Watt, S. M. (2012) A novel function for the haemopoietic supportive murine bone marrow MS-5 mesenchymal stromal cell line in promoting human vasculogenesis and angiogenesis. *British Journal of Haematology*, 157(3), 299-311.

Zhu, S.-J., Choi, B.-H., Huh, J.-Y., Jung, J.-H., Kim, B.-Y. & Lee, S.-H. (2006) A comparative qualitative histological analysis of tissue-engineered bone using bone marrow mesenchymal stem cells, alveolar bone cells, and periosteal cells. *Oral surgery, oral medicine, oral pathology, oral radiology, and endodontics*, 101(2), 164-9.

Zuk, P. A., Zhu, M., Mizuno, H., Huang, J., Futrell, J. W., Katz, A. J., Benhaim, P., Lorenz, H. P. & Hedrick, M. H. (2001) Multilineage cells from human adipose tissue: Implications for cell-based therapies. *Tissue Engineering*, 7(2), 211-228.

Websites:

http://classes.midlandstech.edu/carterp/Courses/bio210/chap06/lecture1.html *Accessed on 27.9.2015.*

http://histonano.com/books/Junqueira's%20Basic%20Histology%20PDF%20WHOLE%20BOK/8.%20Bone.htm *Accessed on 27.9.2015.*

https://mix.msfc.nasa.gov/IMAGES/HIGH/0101761.jpg *Accessed on 27.9.2015.*

www.sigmaaldrich.com/materialsscience/biomaterials/tutorial.html *Accessed on 27.9.2015.*

Appendices

1. PicoGreen™ DNA Assay

The bacteriophage lambda DNA (100 µg/mL) standard provided with the Thermo Fisher Quant-iT PicoGreen® kit was diluted 50X in TE buffer to make a 2 µg/ mL working solution. Aliquots were transferred to sterile vials and stored at -20 °C. A high range standard curve was created by diluting the 2 µg/ mL DNA stock solution according to Table A1. 1 ml of the aqueous working solution of Quant-iTTM PicoGreen® reagent was added and the mixture was incubated for 2 to 5 minutes at room temperature, protected from light. The fluorescence was then measured at excitation 480 nm and emission 520 nm, to create a DNA standard curve (Figure A1).

Volume of TE (µl)	Volume of 50 ng/ ml DNA (µl)	Final DNA Concentration
0	1000	1 µg/ ml
900	100	100 ng/ ml
990	10	10 ng/ ml
999	1	1 ng/ ml
1000	0	BLANK

Table A1 Preparation of high-range DNA standard curved for the PicoGreen™ DNA assay.

2. RT-PCR Primers

Osteocalcin (OC)

Forward primer: CATGAGAGCCCTCACACTCC

Reverse primer: CAGCAGAGCGACACCCTAGACC

Product size: 319bp

Osteopontin (OP)

Forward Primer: GACCTGACATCCAGTACCC

Reverse Primer: GTTTCAGCACTCTGGTCATC

Product size: 184bp

RUNX2

Forward Primer: CCAGATGGGACTGTGGTTACC

Reverse Primer: ACTTGGTGCAGAGTTCAGGG

Product size: 395bp